



විදුලිබල හා පුනර්ජනනීය බලශක්ති අමාත්‍යාංශය  
மின்சக்தி மற்றும் மீள்சக்தி அமைச்சு  
Ministry of Power & Renewable Energy



ශ්‍රී ලංකා සුතිත බලශක්ති අධිකාරිය  
இலங்கை நிலைபெறுதகு சக்தி அதிகாரசபை  
Sri Lanka Sustainable Energy Authority

# National Energy Symposium 2017





# **National Energy Symposium**

## **2017**

19<sup>th</sup> and 20<sup>th</sup> November 2017

BMICH, Colombo 07, Sri Lanka

Organized by



**Sri Lanka Sustainable Energy Authority**  
**Ministry of Power and Renewable Energy**



## TECHNICAL COMMITTEE

M. G. A. Goonetilleke  
Harsha Wickramasinghe  
Vimal Nadeera  
Chamila Jayasekera  
Athula Jayathunga  
K. Sanath Kithsiri

## CONFERENCE SUPPORT

P.P.K. Wijethunga	Hashanthi Thotagamuwa
Ravini Karunarathne	Sandasara Subhashni
Poornima Kalhari	Dulanjalee Niralgama
Apsara Katugaha	Lalika Limali
Anoja Thilakarathne	Mandula Sugathapala
Punya Samarasinghe	Pasan Sugathapala
Sunimal Perera	Bhagya Withanage
Amanda Gimhani	Thilina Pigera

# Table of Contents

Research Title	Page No.
Cloud Motion Tracking for Short-Term PV Prediction	1
Determining the Regulating Reserve Requirement with the Integration of Variable Renewable Energy Sources to the Sri Lankan Power System	9
Future Energy Mix for Sri Lankan Electricity Sector in the Perspective of National Energy Security	24
Techno Economic Feasibility of Solar PV with Battery Energy Storage for Domestic Sector and EV Charging	37
Energy Efficient Utilisation of Solar PV through a DC MicroGrid	45
Smart Distribution Transformer for Frequency Support	56
Proposal of a Novel Method to Determine the Required Storage for Photovoltaic Systems to Create Virtual inertia	65
Design of Domestic Solar Thermal System for a Five Member Family in Kandy, Sri Lanka	73
An Investigation of a Supercapacitor-based Lightning Energy Harvesting Technique	82
Ocean Wave Energy Mapping for South Western Coast of Sri Lanka	89
Rainfall Variation on Hydro Power Generation in the Victoria Reservoir	98
The Development of Marine Renewable Energy in Sri Lanka	108
Development of a Small Scale Sea Wave Energy Converter System to Generate Electricity	119

---

A Correlation Analysis of Factors Influencing Cooling Energy Demand of Condominiums in Sri Lanka	126
Design of a Control System to Optimize Power Consumption in Air Conditioners to Satisfy Human Thermal Comfort	138
Thermal Performance Analysis of Walls for Designing Green Buildings	147
Introduce 12V/ 24V Direct Current for Lighting Buildings to Save Energy and Reduce Electronic Waste	158
Investigation of Energy Efficiency Improvement by Replacement of Standard Efficiency Motors with Premium Efficiency Motors in Tea Withering Troughs	164
Development of Energy Saving Charcoal Based Evaporative Cooling System for Preservation of Perishable	175
Criticality of Building Morphology on End Use Energy Demand: Evidence based assessment of urban office stock in Colombo Metropolitan Region	185
Numerical Modelling of Thermally Thick Biomass Particle Pyrolysis	199
Eulerian-Lagrangian Approach for Modeling of Biomass Fluidized Bed Combustion	209
Assessment of performance and development of biomass fired cabinet dryers for improved energy efficiency	214

---



### **Message from the Minister of Power and Renewable Energy**

Environmental sustainability is being highly focused at international level. Under the global climate obligations, for which Sri Lanka is a signatory to, many countries have declared their contributions to the global sustainable energy agenda, by way of taking initiatives to cut down greenhouse gas emissions. Sri Lanka has agreed through its Nationally Determined Contributions (NDCs), the country's commitment towards this global endeavour. Energy sector is the key area that has been earmarked to make a high international image through its positive contributions towards global climate obligations.

In the country's pathways in the area of environmental benign technologies and systems, both the consumption aspect as well as the generation aspect can make great contributions. In this context, there is a pivotal role to play by academia, researches, industrialists, policy makers and all others who are in the entire value chain in the use of energy. Therein, the role of researchers and innovators by way of involving in R&D as well as in innovations is of utmost significance in popularizing environment benign energy technologies. I expect there will be valuable research outcomes contributing towards the national energy programmes and sustainable energy interventions presently under way, through Vidulka 2017 Energy Symposium.

I wish success of the programme and also the continuity of the research activities presented in this forum.

**Hon. Ranjith Siyambalapitiya**  
**Minister of Power and Renewable Energy**



### **Message from the Deputy Minister of Power and Renewable Energy**

Energy has become one of the prime factors in the current socio-economic move at global level. Frequent fluctuations in fuel oil prices are creating a massive impact on the countries devoid of indigenous energy resources. As Sri Lanka is incurring a huge amount of foreign expenditure for meeting the energy needs, it has a direct impact on the country's economy as well as on energy security. So our broad scope is to achieve self-sufficiency in energy, in an appropriate manner.

Long-term programmes are being implemented with the objective of harnessing renewable energy to the maximum feasible potential, improving energy efficiency in all the sectors, minimizing energy losses in generation, distribution and the usage of energy, and also creating mass awareness on the sustainable use of energy.

National Energy Symposium and the National Innovation Forum on Biomass Energy in parallel to Vidulka Exhibition are commendable efforts of Sustainable Energy Authority in the area of energy based research. The dialog among academia, professionals, researchers, industrialists and also policy makers created through this forum will provide valuable outcomes towards the development of the sector. I take this opportunity to wish all the best to the proceedings of this important event.

**Hon. Ajith P. Perera**

**Deputy Minister of Power and Renewable Energy**



## **Message from the Secretary of the Ministry of Power and Renewable Energy**

Sri Lanka is inherited with a tremendous potential of renewable energy resources, which will be an asset to the country in meeting the future energy needs. We are on the target of achieving self-sufficiency in energy in 2050. Solar, wind, biomass and hydro are the proven resources in this context. Hydro power has already contributed to generate power with the least cost to the economy. Our programmes have been studied and replicated in many countries in the region as well as in other parts of the world. Through proper initiatives, we will be able to go a long way in other renewable energy sources, such as solar and wind. In these programmes and also in promoting energy conservation, capacity development among engineers and technocrats and also creating a wide dialogue among professionals will be very important.

Vidulka Energy Symposium has created a remarkable image within the universities and other research organizations, as a premier forum to discuss energy related research, innovations, project designs, new concepts, simulations, etc. I hope Vidulka 2017 will give high impetus in context of drawing higher attention that we have given to the sustainable energy programmes in the country.

I wish Vidulka a success, and I expect the professionals in the field will further contribute to realize outcomes of the researches being presented towards betterment of the country.

**Dr. B. M. S. Batagoda**  
**Secretary**  
**Ministry of Power and Renewable Energy**





## **Message from Chairman of the Sri Lanka Sustainable Energy Authority**

In a situation where depletion of energy resources is being felt at global level, it is essential that measures are taken to have a steady and affordable supply of energy, and in order to ensure that we need to address the issue both in short term basis and long term basis.

In this context, Sustainable Energy Authority has a vast role to play in its thrust areas of renewable energy development and energy conservation & management. These interventions will extensively provide opportunities for upkeep of environmental conservation as sustainable energy interventions encompass a vast spectrum of environment benign technologies. Thus our intention is to create an energy conscious nation, and the Vidulka Exhibition and Symposium are conducted in line with this. I think it will be useful to discuss about the current developments in the energy sector and also to draw attention of the professionals in the sector to resolve pertinent issues therein. I'm of the view that it is a key national requirement at present.

I take this opportunity to thank all researchers, other stakeholders and also the staff of the Sustainable Energy Authority who made these programmes a reality.

**Keerthie Wickramaratne**  
**Chairman**  
**Sri Lanka Sustainable Energy Authority**

# Cloud Motion Tracking for Short-Term PV Prediction

D. M. L. H. Dissawa<sup>#1</sup>, M. P. B. Ekanayake<sup>#2</sup>,  
G. M. R. I. Godaliyadda<sup>#3</sup>, J. B. Ekanayake<sup>#4</sup>, A. P. Agalgaonkar<sup>\*5</sup>

*# Department of Electrical and Electronic Engineering, Faculty of Engineering,  
University of Peradeniya, Sri Lanka*

<sup>1</sup> lasanthikadissawa@yahoo.com

<sup>2</sup> mpb.ekanayake@ee.pdn.ac.lk

<sup>3</sup> roshangodd@ee.pdn.ac.lk

<sup>4</sup> ekanayakej@cardiff.ac.uk

*\* School of Electrical, Computer and Telecommunications Engineering, University of  
Wollongong, Australia*

<sup>5</sup> ashish@uow.edu

## Abstract

The contribution of solar Photovoltaic (PV) power generation to the power system has seen a significant growth in recent years. Though PV has many advantages, due to its variability and uncertainty, the increased penetration of installed PV systems leads to power system operational issues.

The main factor affecting the PV output is solar irradiance. It follows predictable and seasonal patterns. However, the amount of solar radiation that reaches the ground will vary with the local weather conditions, especially due to the intermittency of cloud cover. In order to mitigate the effect of variability and intermittency of PV generation, several mitigation strategies are introduced and solar radiation forecasting is the major tool to address these problems.

A technique for cloud motion estimation for short-term Irradiance prediction using ground-based sky images was introduced. A sequence of whole sky images is processed to identify cloud motion vectors. A Cross-correlation based cloud boundary tracking method was utilized to track the individual cloud's feature point movements from one image frame to the next image frame. Then according to the cloud movement, irradiance drop and subsequent PV fluctuations were predicted.

**Keywords:** Cloud tracking; fast cross-correlation; Irradiance forecast

## Introduction

Power generation using solar photovoltaic (PV) has seen a rapid growth in recent years since it has many advantages such as low environmental impact and zero fuel costs compared with the conventional energy sources.

The output power of a PV panel depends on the solar irradiance, the ambient temperature and on the characteristics of the PV module. The main factor that affects PV output is solar irradiance [1]. The solar irradiance follows a predictable and seasonal pattern. However, the amount of solar irradiation that reaches the ground will vary with the local weather conditions, especially due to the intermittency of cloud cover. In other words, mainly the amount of solar irradiation that reaches the ground depends on how much of the sun covered by the clouds. When clouds covered the sun, usually the ground surface irradiance drops due to attenuation of direct component.

The intermittency nature of the PV output creates problems related to power system operation, power quality and power system stability. Because of the PV variability, power generation through solar PV is considered as a non-dispatchable generation option. The variability of PV occurs at multiple time scales, from seconds to minutes to hours even to days. The impact of variability increases with the increasing share of PV power plants in the power system [2], [3].

There are several mitigation strategies to reduce the effect of variability and intermittency of PV generation. These include forecasting methods, maintaining flexible generation or load, connecting storages like battery banks,

introducing operational practices such as fast scheduling and dispatch etc. [2], [3]. From these strategies, solar power forecasting is the major tool to address the problems related to the high share of variable solar generation within the electricity grid. An accurate prediction can limit the curtailment of generation and reduce reserve capacity. It is the cost-effective way to handle this problem.

The models used for forecast solar PV power depends on the desired time scale of the forecast. References [2] and [3] introduced three forecasting horizons related to the power system operations (intra-hour, intra-day and day ahead). There are several methods in the literature to forecast the PV production. According to [4], Numerical Weather Prediction Models (NWP) can give accurate predictions in the range of 6 hours to several days. Whereas in a time horizon smaller than 6 hours, satellite data based models typically outperform NWP models. Using satellite images the cloud velocity can be extracted for prediction. Due to time and space availability, satellite images based PV prediction models can be used for the temporal range from 30 minutes up to 6 hours [4].

For the intra-hour range prediction, cloud information from ground-based sky images [5]–[9], or time series models which based on historical data [10]–[11] are employed. These methods derive irradiance forecasts with much higher spatial and temporal resolution compared with the satellite image-based forecasts.

Irradiance forecast based on ground-based images is first introduced by [5]. It used the cross-correlation of cloud

patches to find cloud moving velocity. Reference [7] proposed cloud tracking and forecasting method based on the Lucas-Kanade optical flow algorithm. This method basically predicts the trajectory of selected feature points in the image frames. Using the cloud path, it determines the time duration for clouds to reach a known area in the image. The considered sky images were captured from a narrow field of view, approximately 60 degrees in horizontal and vertical directions. Therefore the captured area of the sky is small. They proposed a whole sky imagery system is better for large forecasting intervals.

Reference [6] also introduced an intra-hour irradiance prediction method based on cloud movement prediction. In order to estimate cloud movements, an optical flow algorithm was utilised. A feature point based optical flow algorithm was implemented. The feature points were defined on the edges or well-defined lines in the given binary image which was created by applying a threshold to the red to blue ratio image. The tracking method used is based on a feature point searching algorithm.

A method for cloud motion and stability estimation using ground-based sky images was introduced in [8]. To find the sub-pixel accuracy of cloud motion for every pixel, a Variational Optical Flow (VOF) technique was used. At the initial stage, the images were processed to remove the fisheye distortion. Cloud stability was quantified using point trajectory length which was obtained by developing an optical flow tracker.

As previously mentioned, fast dispatch with accurate PV power forecasting can reduce the effects of PV variability. For fast dispatch, short-term forecast (intra-

day) is necessary and the resolution of prediction with respect to time obtained by the NWP models or satellite data based models is not enough. Further, the smart inverters on the distribution system will enable PV variability analysis of short time scale [12], [13]. Furthermore, short-term forecast is critical for micro-grids, because large ramp events may occur due to PV fluctuations. Therefore sky image based Short term PV fluctuation prediction method was introduced.

## Material and Methods

This research is based on a 60 kW rooftop PV system installed at the Department of Electrical and Electronics Engineering, University of Peradeniya, Sri Lanka. The PV system together with a weather station has the ability to store PV power data and weather conditions such as irradiance, ambient temperature, wind speed, etc.

Since the methodology is fully based on image processing techniques, the sky images are the most dominant input information. For this, the ground-based sky images were taken from a fish-eye lens camera with a resolution of 1024x768 pixels. The camera is fixed near to the PV panels. The images were captured at every 10 seconds and were stored in JPEG format. The camera is connected to a computer and it is programmed using Matlab.

### I. Proposed method for cloud movement tracking

To predict the cumulus cloud motion on a sunny day individual clouds need to be identified separately. Most previous research [5]-[7], the individual cloud movement was not considered

separately and the mean cloud feature point moving velocity was applied to all the clouds and predict the PV/irradiance drop. This may create some errors. In this research, individual cloud boundary segment's movement was tracked and according to each cloud movement, the irradiance drop was predicted.

The main image processing techniques incorporated in the cloud movement tracking and cloud motion estimation is presented under this section.

#### A. Masking and cloud detection

In order to segment the image into sky and cloud, it is necessary to identify the regions of sky, cloud and sun from the rest of the scene. Therefore a mask was created considering foreground objects as shown in Figure 1. For the foreground estimation, a simple color threshold algorithm was used. Then, the foreground mask was applied to the raw image.

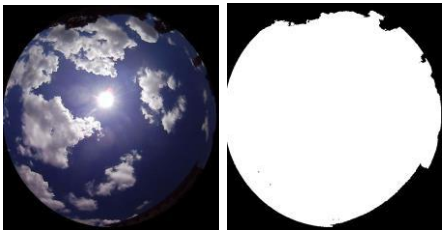


Figure 1: Raw image and Image mask

After that, to segment the cloudy area in the image, the image blue component and the red component difference was found and (B-R) image was constructed. From that image, cloudy regions and the blue sky regions were separately identified. Therefore, by applying a threshold to the (R-B) component binary cloud image was obtained. White and blue regions of the true colour image were separately identified as shown in Figure 2.

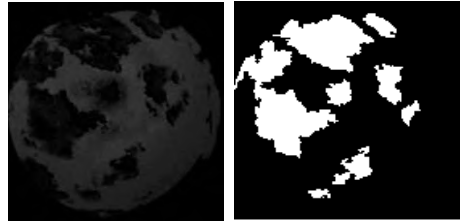


Figure 2: B-R image and Binary image obtained from (B-R) image

To separately identify white patches in Figure 2, `bwconncomp()` function in MATLAB was applied to the binary image. The `bwconncomp()` function gives the connected components found in the binary image.

As in Figure 2, the sun was also seen as a cloud. To separate the sun from clouds, the sun's location was mapped on to the image [14]. Then the white patch related to the sun's image coordinate was removed and the other white regions are considered as clouds. Figure 3 shows the sun's location on the image and the separately identified clouds.

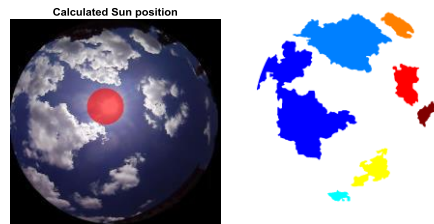


Figure 3: The sun location and Cloud segmented image

#### B. Cross-Correlation based cloud movement tracking

Our next target is to find each cloud moving velocity. For that, each cloud boundary segment correspondents of each frame were found using fast cross-correlation algorithm [15]. Clouds have no fixed boundaries. Boundaries may change from time to time. Therefore

cloud boundary feature point tracking is not an accurate method to find the correspondence between each frame, though some research ([8],[9]) are carried out based on the assumption that the cloud boundaries are not much varying from one frame to next frame for a considerable amount of time. Therefore, instead of tracking cloud feature points such as corner points and edges, here the cloud boundary segments were tracked.

Initially, the areas related to the cloud in the first image frame are separately identified. Then boundary points around the clouds were selected according to the cloud size as shown in Figure 4. Then a block of pixels around a cloud boundary point in the first image frame was correlated with the next image frame within a search distance. Then the location of the highest correlation was identified and the region belongs to that location was considered as the corresponding cloud boundary in that image frame. Figure 5 shows the first image frame, template image around a boundary point, correlation output and the template image found in the next image frame.

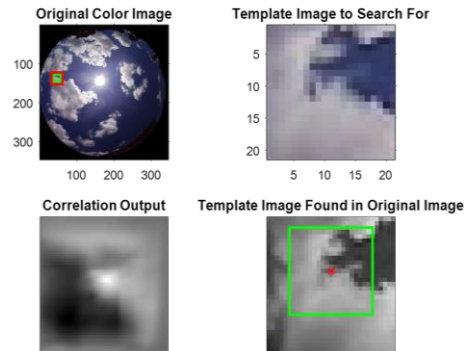


Figure 5: Original colour image, template image, correlation output and the template image found in the next image



Figure 6: Feature points in the first image (Red) corresponding feature points in next image (Green)

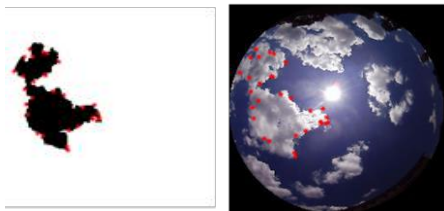


Figure 4: Selected boundary points around a cloud

Figure 6 shows the initial ( $t= T$ ) boundary point locations in red color and the corresponding boundary points found in the next image frame ( $t=T+10$  sec) in green color.

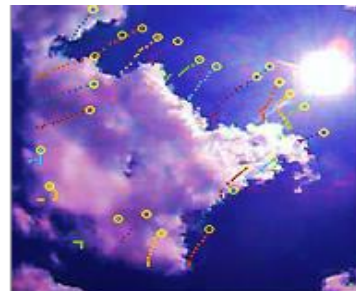


Figure 7: Feature point trajectories

To find the cloud moving velocity, for each boundary point, the corresponding locations were found in 6 consecutive image frames (image frames captured within one minute). All the boundary point locations were plotted on the 6th image frame as shown in Figure 7. Using the frame rate and feature point coordinate history, for each feature

point, the point average moving velocity and acceleration were found.

## II. PV drop prediction

For one iteration six consecutive image frames were selected. The initial binary image in the image sequence was classified according to the percentage of white pixels in the image. The categories are clear sky (<10% white pixels), overcast (>60 % white pixels) or partially cloudy (10% - 60 % white pixels). For miniatures-ahead predictions, if the current image is categorized as a clear sky, then it was assumed that PV will not drop over the time interval of interest. On the other hand, if the current image is categorized as overcast, then it was assumed that PV will drop over the time interval of interest. If the initial image is classified into partially cloudy condition, then the cloud motion tracking by cross-correlation is used to predict future cloud location. Then according to the future cloud locations, PV drop was predicted.

To find the PV power drop occurrence time, the clouds moving in the direction of the sun were selected considering each cloud's resultant boundary point moving velocity. If the resultant velocity is directed to the sun's location, it is taken as a cloud moving in the direction of the sun. After identifying the clouds which are moving in the direction of the sun, the points which moved towards the sun's position were selected. Using the selected boundary points moving velocities, accelerations and the distance between the boundary point and the sun's location, the time taken by each feature points to reach the sun area were calculated. Then accordingly, the PV drop occurring time duration was identified.

## Results

For a moderately cloudy day, PV drop was predicted. Figure 8 shows PV variation on 5<sup>th</sup> July 2017 with the predicted PV drop. Here, the irradiance drop was predicted 2 minutes before the

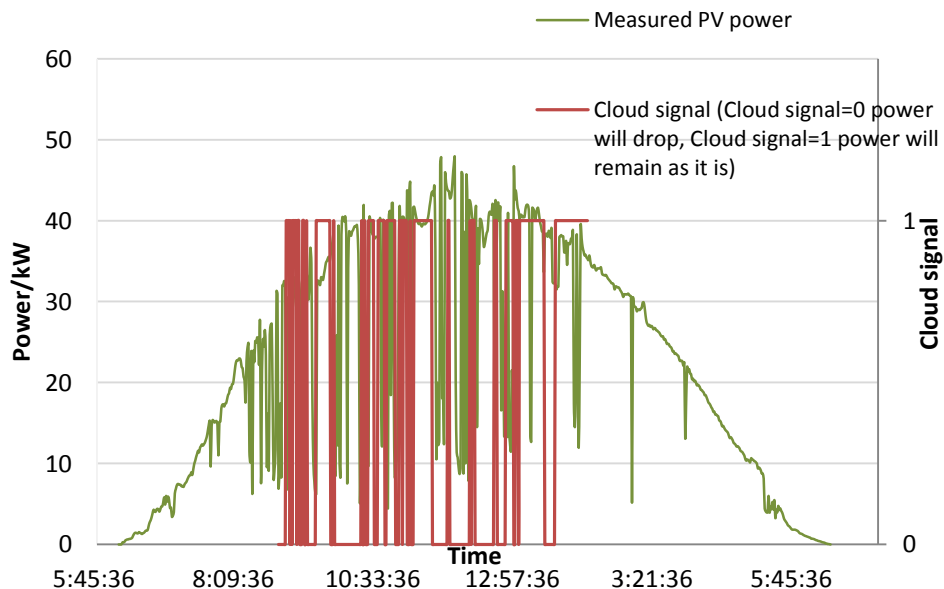


Figure 8: Measured PV power on 2 minute PV drop prediction

real time. The cloud signal “1” shows no PV drop occurs on the other hand cloud signal “0 “ shows there is a PV drop.

## Conclusions

A method for intra-hour irradiance PV drop forecasting by cloud boundary tracking based on fast cross-correlation technique was introduced. The method was implemented using ground-based sky images. To capture the sky images a fish-eye lens camera was used. Instead of tracking the cloud corner points, the proposed method considers cloud boundary segments (the area around a boundary point) to find the cloud moving velocity. Using the proposed technique, the duration at which the irradiance drop was successfully predicted 2 min before the real time.

## Future Work

This method will be developed using sky image properties to generate an accurate PV forecast.

## Acknowledgements

The authors would like to acknowledge the financial support provided by Sri Lanka Sustainable Energy Authority to carry out this work. Further, Asian Development Bank is acknowledged for the PV system supplied to the University of Peradeniya.

## References

- [1] G. M. Masters, Renewable and Efficient Electric Power Systems. John Wiley & Sons, 2013.
- [2] L. Bird, M. Milligan, and D. Lew, “Integrating variable renewable energy: Challenges and solutions,”

National Renewable Energy Laboratory, 2013.

- [3] V. Kostylev, A. Pavlovski, and others, “Solar power forecasting performance—towards industry standards,” in 1<sup>st</sup> International Workshop on the Integration of Solar Power into Power Systems, Aarhus, Denmark, 2011.
- [4] H. M. Diagne, P. Lauret, and M. David, “Solar irradiation forecasting: state-of-the-art and proposition for future developments for small-scale insular grids,” in WREF 2012-World Renewable Energy Forum, 2012.
- [5] C. W. Chow et al., “Intra-hour forecasting with a total sky imager at the UC San Diego solar energy testbed,” *Solar Energy*, vol. 85, no. 11, pp. 2881–2893, Nov. 2011.
- [6] M. Cervantes, H. Krishnaswami, W. Richardson, and R. Vega, “Utilization of Low Cost, Sky-Imaging Technology for Irradiance Forecasting of Distributed Solar Generation,” 2016, pp. 142–146.
- [7] P. Wood-Bradley, J. Zapata, J. Pye, and others, “Cloud tracking with optical flow for short-term solar forecasting,” *Solar Thermal Group, Australian National University, Canberra, Australia*, 2012.
- [8] C. W. Chow, S. Belongie, and J. Kleissl, “Cloud motion and stability estimation for intra-hour solar forecasting,” *Solar Energy*, vol. 115, pp. 645–655, May 2015.
- [9] C.-L. Fu and H.-Y. Cheng, “Predicting solar irradiance with all-sky image features via regression,” *Solar Energy*, vol. 97, pp. 537–550, Nov. 2013.
- [10] P. F. Alvanitopoulos, I. Andreadis, N. Georgoulas, M. Zervakis, and N. Nikolaidis, “Solar radiation prediction model based on Empirical Mode Decomposition,” in *Imaging*



- Systems and Techniques (IST), 2014 IEEE International Conference on, 2014, pp. 161–166.
- [11] N. Zhang and P. K. Behera, "Solar radiation prediction based on recurrent neural networks trained by Levenberg-Marquardt backpropagation learning algorithm," in 2012 IEEE PES Innovative Smart Grid Technologies (ISGT), 2012, pp. 1–7.
- [12] H. G. C. P. Dinesh, P. H. Perera, G. M. R. I. Godaliyadda, M. P. B. Ekanayake, and J. B. Ekanayake, "Individual power profile estimation of residential appliances using low frequency smart meter data," in 2015 IEEE 10<sup>th</sup> International Conference on Industrial and Information Systems (ICIIS), 2015, pp. 140–145.
- [13] H. G. C. P. Dinesh, P. H. Perera, G. M. R. I. Godaliyadda, M. P. B. Ekanayake, and J. B. Ekanayake, "Residential appliance monitoring based on low frequency smart meter measurements," in 2015 IEEE International Conference on Smart Grid Communications (SmartGridComm), 2015, pp. 878–884.
- [14] D. M. L. H. Dissawa, M. P. B. Ekanayake, G. M. R. I. Godaliyadda, J. B. Ekanayake, and A. P. Agalgaonkar "Cloud Motion Tracking for Short-Term on Site Cloud Coverage Prediction," In 2017 International Conference on Advances in ICT for Emerging Regions (ICTer), 2017, pp.332-337.
- [15] J. P. Lewis, "Fast Normalized Cross-Correlation.", Vision Interface, 1995.

# Determining the Regulating Reserve Requirement with the Integration of Variable Renewable Energy Sources to the Sri Lankan Power System

Randika Wijekoon<sup>1</sup>, Prof. Janaka Ekanayake<sup>2</sup>

<sup>1</sup>*Transmission and Generation Planning Branch, Ceylon Electricity Board,*

<sup>2</sup>*Faculty of Engineering, University of Peradeniya,*

<sup>1</sup>randika.wijekoon@ceb.lk

<sup>2</sup>jbe@ee.pdn.ac.lk

## Abstract

At present nearly 45% of country's electricity demand is met by renewable energy sources, and the renewable energy based power generation is increasingly gaining attention with the technological advances and global climatic concerns. Sri Lanka, being a country with rich potentials, has an ambitious program on developing indigenous renewable energy sources. The integration of large amounts of variable renewable energy (VRE) forms such as wind power and solar power poses various technical and economic challenges and requires special integration measures for power system operation. One measure of increasing the system flexibility is maintaining increased levels of regulating reserves. Quantifying the extent of incremental reserve requirement is vital for integrating VRE at technically and economically optimum levels. This paper, as a future oriented work, focuses on estimating the regulating reserve requirement for catering the system load and subsequently quantifying the incremental regulating reserve requirement for variable renewable energy integration.

**Key words:** Variable Renewable Energy, Operational flexibility, Regulating reserve

## Introduction

### Background

Sri Lanka being an island has an isolated power system and it was recognized as a 100% renewable system until mid-nineties owing to the major hydro resource development. With the growing demand, it has now evolved to a system with a mix of both renewable and thermal generation sources and the size of the existing generating system is 4,018 MW as in 2016. This includes 1,903MW (47%) of renewable energy sources and 2,115MW (53%) of thermal energy sources.

Country's future electricity demand which has been growing at an average annual rate of around 6% during the past 20 years [1], is expected to be met by both thermal and indigenous renewable energy sources. The progress of the total renewable and thermal installed capacity and the peak demand variation of the country over the last 30 years are shown in Figure 1.

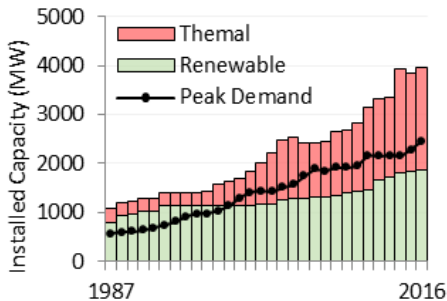


Figure 1: Peak Demand and Installed Capacity of past 30 years

Sri Lanka, together with other countries, has expressed its national obligation towards mitigating the global climate change impacts to the United Nations Framework Convention on Climate Change (UNFCCC). Even though the greenhouse gas (GHG) emission of the

country is as small as 0.05% of the global total [2], Sri Lanka has an ambitious program towards reducing the overall GHG emissions. Electricity sector has a major role in this obligation and the development of Indigenous renewable energy development is a key area for decarbonizing the sector. Since the major hydro resources have been harnessed to a greater extent, wind and solar potentials of the country has gained much attention as the next leading form of indigenous resource.

Integrating more wind and solar photovoltaic resources into a power system poses several technical challenges depending on the characteristics of both the system and the resources. Wind and Solar PV sources which are inherently intermittent and uncertain can be challenging for reliable system operation. Further the dynamic characteristics of such resources can influence the stability of the power system.

On the other hand, the scale, strength and the flexibility of the power systems can mainly govern its capability to accommodate Variable Renewable Energy (VRE) sources. Integrating VRE sources beyond such limits requires special measure to increase the system's operational flexibility and the strength. To identify the integration limits of the high level of VRE requires careful and comprehensive analysis in different time scales and the main challenges are as shown in Table 1 [3].

Table 1: VRE Integration Challenges

Time Scale	Area of Challenge
Seconds	Stability challenges
Minutes to Days	Balancing challenges
Months to years	Adequacy challenges

Intermittency of wind and solar PV resources affect in the minutes to days in time scale and the seasonality of such VRE sources occur in the month time scale. Therefore maintaining extra operating reserves in different time scales provides relief particularly for the operational challenges. In maintaining the normal operating reserves levels, different systems adopt different techniques together with the past operational experience. However with increased penetration level of VRE, estimating extra reserve levels at different time scales is crucial and requires system specific studies in detail. Many of the VRE integration studies carried out in the recent past for various systems all over the world therefore contained a considerable amount of work on addressing these issues.

In Sri Lankan context, with its ambitious program on VRE integration, addressing incremental reserve requirement is timely and necessary. Ceylon Electricity Board conducts a comprehensive renewable energy integration study and has addressed this topic to a certain degree. In-depth analysis on system specific reserve requirements can further strengthen the VRE integration possibilities.

This paper focuses on three main topics in estimating the operation reserves. Initially it establishes the basic understating on operating reserve classifications which are often misinterpreted due to different terminology adopted by different systems. Then the paper describes the influence of VRE on different reserve classes and places attention on methodology and the estimation of the

regulating reserve. Subsequent sections cover the estimation of regulating reserve required for load variability the determination of additional operating reserve required for future VRE integration.

### **Operating Reserve classification and International Practices**

Operating reserves are maintained in power systems to support the supply demand balance in different time scales. North America Electric Reliability Corporation (NERC) defines the operating reserves as *“The capability above firm system demand required to provide for regulation, load-forecasting error, equipment forced and scheduled outages and local area protection. Operating Reserve consists of both Spinning Reserve and Non-spinning Reserve”* [4]. Even though there is a common objective for maintaining reserves for any power system, there are significant inconsistencies in defining, classifying and specifying operating reserve types in different systems. The operating reserves can be categorized based on their response speed, duration, the direction of use, frequency of use and the purpose of use.

Given the wide variation in definitions and naming conventions of operating reserves and the increased attention especially due to the VRE growth, clear distinction between different reserve types is crucial for in-depth analysis. The recent work has classified different reserve types to improve the understanding with distinction [5]-[8]. Its simplified illustration is in Figure 2.

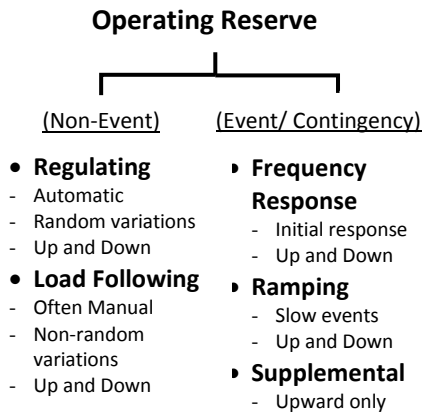


*Figure 2: Operating Reserve Classification based on the purpose of use*

Generally, the system operator holds reserves to maintain the active power balance under normal operation to cater random variations that occur continuously. The minor variations of the supply and demand occur in the system are first responded by the frequency response (inertial response) and then by the regulating reserves (load frequency control). Correcting the current imbalance and its response is faster than the economic dispatch adjustment. Load following reserve (Balancing Reserves) corrects the anticipated imbalance and its response is slower than the dispatch optimization. Frequency response (Governor Response) reserve provides the initial response following a major disturbance correcting the instantaneous imbalances arise from more infrequent and severe events whereas the ramping reserves are used to correct the non-instantaneous or the slower component of the same. Supplemental reserves are

reserves that are activated at last to restore other type of reserves again to ensure that the system's preparedness for another event. Regulating and frequency response reserves which are faster need to be synchronized to the system as spinning reserve. Load following, ramping and supplemental reserves which have slower response can be a mix of spinning and non-spinning reserve [7].

Many European systems have classified operating reserves as Primary, Secondary and Tertiary. Their objectives, the general deployment time frame and the relation to the above mentioned operating categories are shown in Table 2.

Magnitude and the time scales of each of these reserves are system specific and dependant on the system characteristics such as size of the system, strength of the system, availability of interconnections, VRE penetrations and their performance. Developed systems in European and North American regions, requires reserve services to be estimated and specified in detail to maintain reliability standards. In certain systems instead of direct specifications, control performance standards are enforced on frequency quality so that balancing authority or the Transmission System Operator (TSO) decides on the required reserves levels. Some operating reserve classes are mandatory while some reserve services are market driven [6]-[8].

Table 2: Operating Reserve Classification based on the type of control

Primary	Secondary	Tertiary
To stabilize the frequency	To restore the frequency	To restore Primary and Secondary Reserves
Seconds to 10-15 minutes	10-15 Minutes to 60 minutes	60 minutes-4 hours
Mainly the frequency response reserve	Mainly the Regulating Reserve	Mainly the load following and Supplemental reserve

### Operating Reserve and VRE

Required operating reserves depend on the characteristics of the system and adopted reliability criteria in operation. However it is widely agreed that intermittency and the uncertainty of VRE sources such as wind and solar PV, likely to increase the requirement for operating reserves. However it is also observed that assessment of required levels and classes of operating reserves is a difficult task. Understanding the influence of VRE on different reserve types is therefore important and the literature from recent past provides useful insight to the problem [7], [8], [9]. Table 3 briefly summarises the influence of VRE in different classes of operating reserve discussed above.

Table 3: Influence of VRE in different classes of reserves

<b>Frequency Response Reserve</b>	Solar PV and wind plants do not provide inertial response. Thus more VRE necessitates more frequency response reserves.
<b>Regulating Reserves</b>	Solar PV and wind plants output variations are observed in regulating time frame. Therefore VRE is more likely

	to affect the regulating reserve requirement.
<b>Load Following Reserves</b>	Since the long-term forecasts for solar and wind is not perfectly accurate, additional load following reserves likely to be required for VRE.
<b>Event/Contingency Reserve</b>	Wind and solar variations are not as instantaneous as contingency events. Therefore contingency reserves are not likely to be affected and to be verified by detail analysis.
<b>Ramping Reserves</b>	Past studies has concluded that wind has unpredictable, severe non-instantaneous events that affect ramping reserves. Effect of solar on ramping reserves is being researched.

Estimating incremental reserves has been given major attention in the wind and solar integration studies conducted in the recent past. It can be observed that estimating regulating type of reserve has gained much focus followed by the load following type of reserves in most of these integration studies [7]. Accordingly at this stage, the work presented in this paper focuses on estimating the additional regulating reserve required for both load and VRE variability.

### Reserve Estimation Methodology

Estimating the incremental regulating reserve services due to VRE requires the analysis of both load and VRE characteristics. Initially, it is essential to assess the regulating reserve required for load variability alone and that establishes the basic regulating reserve levels needed for the normal system operation. Further analysis on extra regulating reserves for

VRE can then be estimated and compared with those results. Therefore the first part of this study heavily focuses on the characteristics of the load profile from 2018 to 2027 and key findings are then presented.

Subsequently the characteristics of wind and solar generation profiles are examined in terms of variability in the regulating time frame. Wind and solar PV resources were modelled and generation profiles were obtained using the System Advisory Model developed by National Renewable Energy Laboratory, USA. Ultimately different VRE penetration scenarios were developed and total variability characteristics were examined in order to investigate the impact of VRE penetration on regulating reserve levels. Figure 3 illustrates the outline of the methodology describe above.

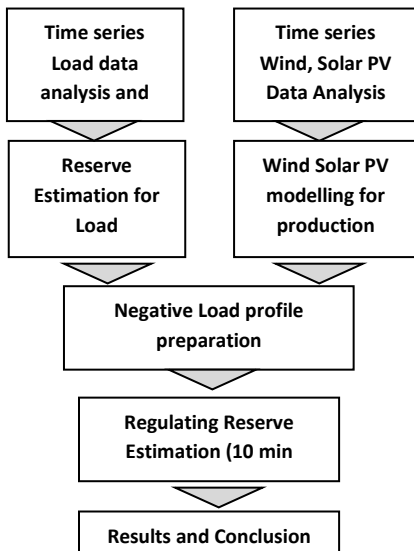


Figure 3: Study methodology

Methodologies used for regulating reserve estimation have been discussed in the literature and various concepts have been proposed in various occasions. Much attention was placed on this topic

in the recent past especially owing to the wind and solar integration studies conducted around the world. These methodologies range from simple traditional methods to sophisticated novel methodologies and have continuously evolved as each study learns from previous studies. In broad classification there are two main approaches for the regulating reserve estimation and they are mainly deterministic and probabilistic methods. In deterministic approach which is simple and traditional, derives a fixed percentage of reserve based on the largest event in the required time frame. However this approach does not consider the probability of occurrence of other smaller events, and the dependence between events thus often overestimates the reserve requirement [05]. Diverging from the traditional methods probabilistic methods were then gained attention and it uses the statistical approach in determining certain operating reserve requirement. Probabilistic approach can be adopted when the time series data is available for load/VRE and can be relatively complex, data intensive exercise. In this method either the standard deviation of variations or the exceedance level can be applied. The work presented in this paper examines the applicability of probabilistic methods for regulating reserves estimation and finally recommends and continues with the exceedance level approach.

As explained earlier in this paper the focus is on estimating the regulating reserve requirement that can cover the random variation. When the time series data is available, such variation can be obtained by taking the difference between consecutive data points in the considered time scale. In the probabilistic method, this variability information is

statistically analysed and a reserve level is set so that an intended amount of variations are covered by reserves. In the standard deviation method which is also known as *n-sigma* method, multiples of standard deviations are taken as the reserve level. In many integration studies, three times the standard deviation (*3-sigma*) is adopted to theoretically cover 99.7% of the variations [10]. However that is based on the assumption that the variability information follows a normal Gaussian distribution. Certain detailed studies have also paid attention on estimating correct number of sigma in this regard. However stronger conclusion can be made for different system if such data is analysed in detail to determine the reserve level. Improving from the *n-sigma* method, exceedance level method first defines the expected confidence level at which reserves should cover the variations and then determined the exact reserve levels. Instead of applying a number of sigmas to a data set, using exceedance level can yield more accurate results since various load and VRE variability characteristics can represent various probability distributions. The work presented in this paper considered the confidence level of 99.7% for exceedance level method since the same level of confidence is expected by many other studies through the *n-sigma* method.

### Regulation Requirement for Load

First the actual time series data of the total demand of Sri Lankan system for past four years (2013-2016) were analysed in detail to examine variability characteristics and the appropriateness of 3-sigma method and the exceedance level

method. Time series data available in 30 minute resolution was interpolated to generate time series data in 10 minute resolution based on the assumption that the total system is large enough to approximate the linearity between smaller time intervals. Figure 4 illustrates the duration curve of 10 minute variability characteristics of past four years. No significant year to year variation is observed from the results. Severe downward variation in the figure corresponds to the major outages occurred in the past four years.

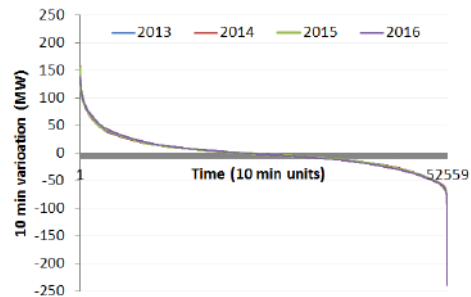


Figure 4: Duration curves of the variability

In order to verify the validity of 3-sigma and exceedance level methods on actual data either end of above duration curves were closely examined for all four years. For simplicity illustration only for the year 2016 is given in the figure 5 and figure 6. Figure 5 focuses on the largest upward variations and the figure 6 focuses on the same for the downward direction. It is seen that in normal (Non-Event) operation largest upward variations arise due to the load rise in morning and evening peaks. Largest negative variations are from the major plant and line outages (Events) and the rest is from load variations.



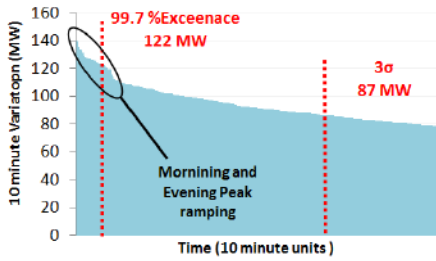


Figure 5: Largest upward load variation

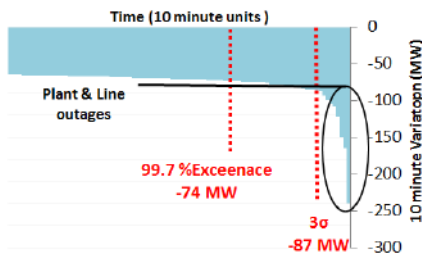


Figure 6: Largest downward load variation

Key observation from all four years results is that for upward reserves 3 sigma method does not cover steep variations arising from morning and evening peaks but the exceedance level with 99.7% confidence level (99.85<sup>th</sup> percentile) covers majority of the upward variation. However for downward variations reserves 3-sigma method covers nearly all of the non-event variation with a confidence level greater than 99.7%. This asymmetry is clearly seen through the histogram in Figure 7 and the boxplot shown in Figure 8.

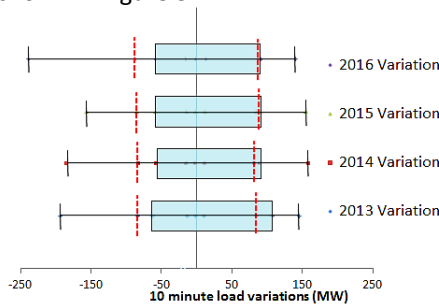


Figure 7: Boxplot of load variability information of four years

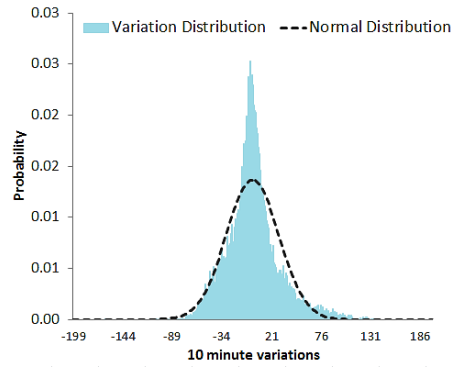


Figure 8: Probability distribution of 10min load variation of 2016 and its normal distribution

Figure 8 illustrates the normal distribution corresponds to the variability data set of 2016 in dash line and it does not fit into the actual characteristics of the data. It reveals that the actual load data variations can deviate from the Gaussian distribution which is commonly assumed in the 3-sigma method. Gaussianity or the randomness of load variation characteristics can vary from system to system since many other factors can drive the load variations patterns. Therefore examining its behaviour is useful while making assumptions on normality. In this analysis load variability in the regulating time scale (10 min) was found to be best represented by the Laplace distribution and it is illustrated in Figure 9.

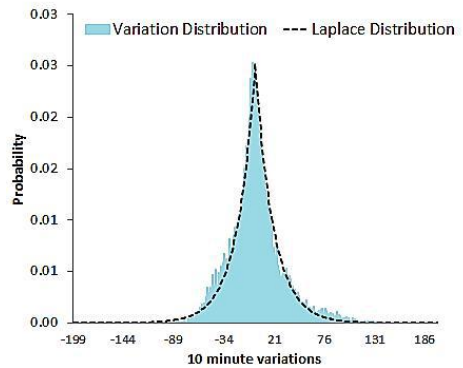


Figure 9: Probability distribution of 10min load variation of 2016 and its Laplace distribution

In conclusion 3-sigma method is not sufficient to cover the upward variations and more than adequate to cover downward variation. Hence exceedance level based percentiles yield more meaningful results on regulating reserve needs.

Next part of this exercise focus on estimating the regulating reserve requirement for future load with the similar analysis for the next 10 years. Therefore future demand data was derived taking 2016 as the base year. Time series load data for 10 years were prepared using a special algorithm developed by the author of this paper. The resulting times series load data of the algorithm matches the long term energy and peak forecasts, load factor forecasts, off-peak and daytime load growth forecasts of a given year. The target values for this analysis are according to the forecasts of the Long-Term Generation Expansion Plan 2018-2037 prepared by Ceylon Electricity Board. The sample from the derived load data in Figure 10 shows the expected evolution of the daily load profile in next 10 years.

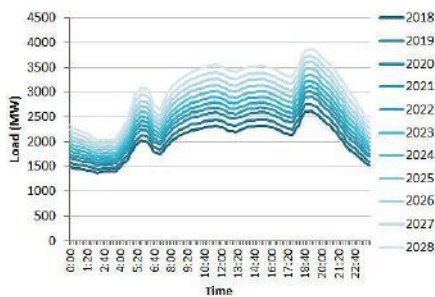


Figure 10: Derived 10 min load data for future years

As recommended earlier in this paper the exceedance level method was applied to derived time series load data variations to determine the require regulating reserve levels. Table 4 presents the final results obtained on regulating reserve requirement for load estimated using both 3 sigma and exceedance level methods.

The standard deviation ( $\sigma$ ) of the variation data lies in the range of 1.1-1.2% of the peak demand. However, using  $3\sigma$  under-estimates the upward regulating reserve requirements over-estimates the downward regulating reserve requirements of the load. It is observed that the present downward regulating reserve requirement of 78 MW increases by 27 MW in 10 years period and 125 MW of upward regulating reserve in 2017 increases by 16 MW in 10 years at 99.7% exceedance level.

In the system planning phase it is very useful to understand the relationship between the percentage of regulating reserve requirement and the system peak load. The Mid-West Independent System Operator (MISO) has developed a characteristics curve which has been referred by several system planning related studies. Finally a similar characteristic curve which is specific to the Sri Lankan system was developed based on the results of this work as this can be a useful tool assisting the system planning work. Figure 11 reveals the said relationship between the peak and the regulating reserve.

Table 4: Regulating reserve for load (MW)

Peak Load	Std Dev- $\sigma$ (MW)		Regulating Reserve		
	(%)		Exceedance (99.7%)		
			$n\sigma$	3 $\sigma$	(Up)
2013	2164	28 1.3	84	74	123
2014	2152	27 1.3	82	71	114
2015	2283	28 1.2	85	77	118
2016	2453	29 1.2	87	74	122
2017	2585	30 1.2	91	78	125
2018	2738	32 1.2	96	82	130
2019	2903	34 1.2	101	86	134
2020	3077	35 1.2	106	90	136
2021	3209	37 1.2	111	96	134
2022	3346	38 1.1	114	95	132
2023	3491	39 1.1	118	98	132
2024	3643	41 1.1	123	102	135
2025	3804	43 1.1	128	105	136
2026	3972	44 1.1	133	110	140
2027	4149	45 1.1	136	114	141

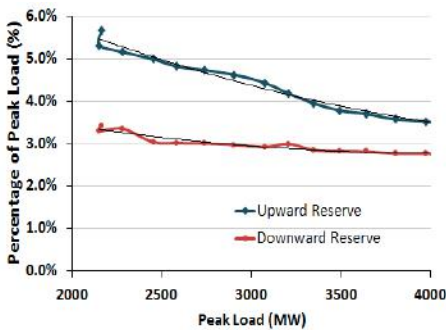


Figure 11: Relationship between Peak load and regulating reserve requirement

### Incremental Regulating Reserve Requirement with VRE Integration

Variability of wind and solar PV resources is higher than the load variability especially in the regulating (10 min) time frame as concluded by the literature as well as from the actual data [11], [12]. Generation profiles for five wind regimes around the country and two solar PV regimes have been considered in this work. Figure 12 shows the normalized variability of load, wind and solar PV. This reveals that the load variations are

relatively lower than the wind and solar PV variation in 10 minute scale.

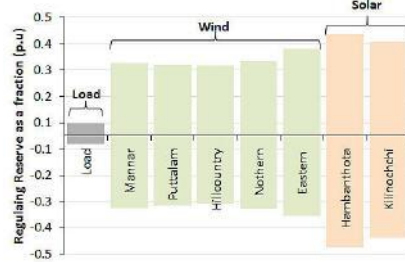


Figure 12: Normalized variability levels of load, wind and solar

When power system is operated to maintain the active power balance, it is the “load - VRE” or the “negative load” that has to be catered by the conventional fleet of power plants [13]. Therefore the ultimate time series data of the negative load data is analysed to determine the regulating reserve requirement.

In order to analyse the influence of wind and solar PV on reserves, several VRE integration scenarios were developed. The first three scenarios assume that the future development of renewables is from solar only. Next three scenarios consider development of wind only and the last three scenarios assumes equal development of wind and solar PV at different penetration levels.

Table 5: Scenarios considered for the period 2018-2037

Scenario	Description
A	5% -Solar Future development is solar only /From 5-15% energy share
B	10% -Solar
C	15% -Solar
D	5% -Wind Future development is wind only /From 5-15% energy share
E	10% -Wind
F	15% -Wind
G	10% -Mixed Equal development of Wind and solar, 10-15% energy share
H	15% -Mixed
I	20% - Mixed

Figure 13 shows the cumulative VRE capacities assumed in each scenario and the corresponding energy shares.

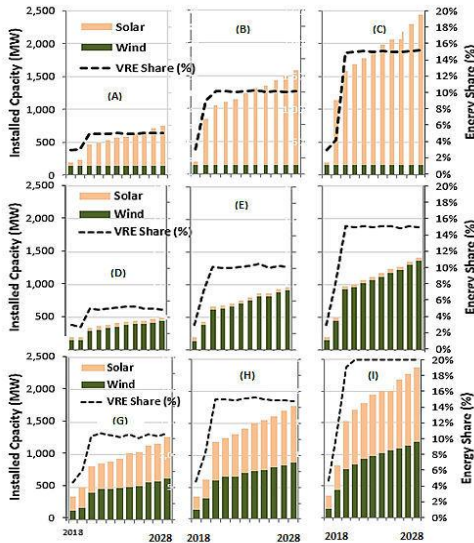


Figure 13: VRE capacity projection of the scenario analysis

After preparing the negative load profiles in 10 min time scale for each scenario statistical analysis were carried out and the regulating reserve level were determined based on the 99.7% exceedance level. The result of the first three scenarios (A, B, C) in which capacity is dominated by solar PV is shown in a single graph (Figure 14). It exhibits an increasing trend for additional regulating reserve requirement.

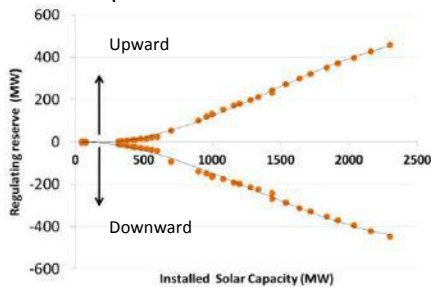


Figure 14: Additional regulating reserve capacity vs solar PV capacity

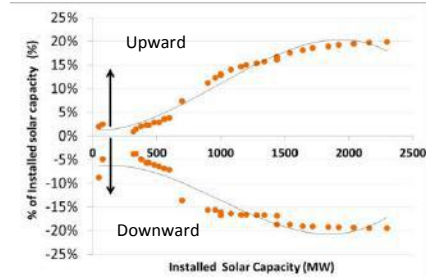


Figure 15: Additional regulating reserve percentage vs solar installed capacity

Figure 15 shows the additional regulating reserve requirement as a percentage of solar PV capacity. The key observation is that the additional reserve requirement is not a constant function with solar installed capacity but it increases as the penetration level rises. Regulating reserve requirement is in the range of 10-20% if the capacity is between 1,000 MW and 2,500 MW.

Figure 16 illustrates the additional regulating reserve requirement for wind dominated scenarios (D, E, F). It is observed that the regulating reserve requirement is comparatively lower than the solar dominant scenarios. These are partly due to the inherent resource characteristics and partly due to the availability of five regimes for wind as opposed to two regimes for solar.

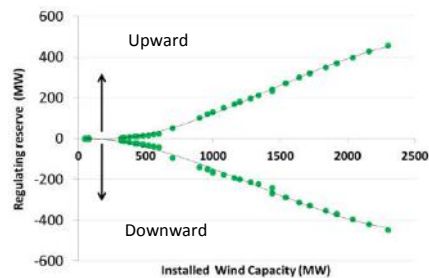


Figure 16: Additional regulating reserve capacity vs wind capacity

Wind integration requires 2-8% of wind capacity as additional regulating reserve requirement and the relationship is not linear as the penetration level increase. Since both solar and wind does not exhibit a constant relationship for reserve requirement, accurate estimation of reserves is possible only with the negative load approach for a given VRE integration scenario.

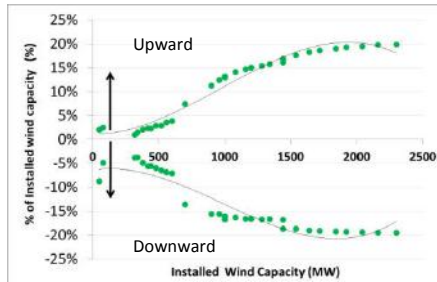


Figure 17: Additional regulating reserve percentage vs wind installed capacity

Three key scenarios, namely G, H, and I assumes the equal development of solar and wind to achieve and maintain 10%, 15% and 20% energy shares for a 10 year period. Application of the exceedance level method through the negative load approach yields ultimate results on the regulating reserve requirement of such a VRE integration program.

Results illustrated in Figure 18 and Table 6 reveal the magnitude of regulating reserve requirement in each scenario. Yellow colour indicates the reserve required to cater the load variability estimated in the previous section of this paper. Other three scenarios requires progressively higher amount of regulating reserves.

The final results can be presented as a percentage of peak load as it is commonly used in the current context. According to Figure 19 upward and downward regulating reserve for load variability ranges from 2.8-4.7% during the study period. Beyond 2020 scaling up the VRE energy share from 10% to 20% increases the total regulating reserve requirement from 4.4% to 7.3% on average. Table 7 provides the results on upward and downward total regulating reserve percentages.

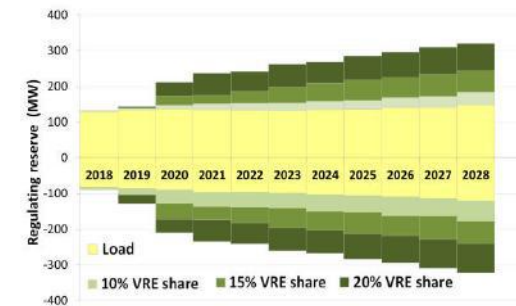


Figure 18: Total Regulating Reserve Requirement for mixed wind and solar development

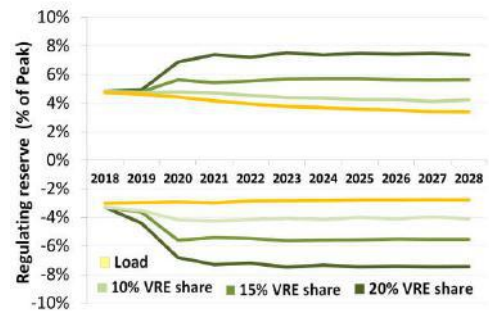


Figure 19: Regulating Reserve Requirement for VRE penetration levels as a percentage of the Peak load

Table 6: Total Regulating Reserve Requirement (MW) 2020-2028

	2018	2019	2020	2021	2022	2023	2024	2025	2026	2027	2028
<b>Total VRE</b>	354	499	824	874	899	939	1034	1044	1149	1174	1274
<b>Upward</b>	133	138	147	151	152	153	159	161	169	172	183
<b>Downward</b>	-90	-102	-128	-137	-139	-142	-151	-152	-163	-164	-178
<b>Total VRE</b>	354	624	1205	1265	1325	1415	1495	1545	1605	1685	1765
<b>Upward</b>	133	139	174	175	186	199	209	218	224	234	244
<b>Downward</b>	-90	-105	-172	-173	-183	-197	-204	-212	-219	-229	-240
<b>Total VRE</b>	354	829	1525	1705	1805	1935	1995	2095	2175	2275	2375
<b>Upward</b>	133	143	211	237	241	263	268	285	295	310	320
<b>Downward</b>	-90	-128	-209	-234	-241	-261	-267	-284	-295	-310	-322

Table 7: Total Regulating Reserve Requirement as a percentage of the load (MW)

	Load		10% Share		15% Share		20% Share	
	Up	Down	Up	Down	Up	Down	Up	Down
<b>2018</b>	4.7	3.0	4.8	3.3	4.8	3.3	4.8	3.3
<b>2019</b>	4.6	3.0	4.7	3.5	4.8	3.6	4.9	4.4
<b>2020</b>	4.4	2.9	4.8	4.1	5.7	5.6	6.9	6.8
<b>2021</b>	4.2	3.0	4.7	4.3	5.4	5.4	7.4	7.3
<b>2022</b>	4.0	2.8	4.5	4.1	5.6	5.5	7.2	7.2
<b>2023</b>	3.8	2.8	4.4	4.1	5.7	5.6	7.5	7.5
<b>2024</b>	3.7	2.8	4.4	4.1	5.7	5.6	7.4	7.3
<b>2025</b>	3.6	2.8	4.2	4.0	5.7	5.6	7.5	7.5
<b>2026</b>	3.5	2.8	4.3	4.1	5.6	5.5	7.4	7.4
<b>2027</b>	3.4	2.7	4.1	4.0	5.6	5.5	7.5	-7.5
<b>2028</b>	3.4	2.8	4.2	4.1	5.6	5.5	7.4	-7.4

## Conclusion

This paper focused on estimating the regulating reserve requirement for load variability and additional reserve needs for VRE integration.

It was observed that the country's Load profile has its own variability characteristics driven by consumption patterns that can be best represented by the Laplace distribution instead of the commonly assumed normal distribution. Therefore the paper investigated the validity of two reserve estimation methods (*n-sigma* and *Exceedance level*)

Results of the VRE integration scenario analysis shows that the additional reserve requirement of VRE is not a constant

and found that applying exceedance level method yields more accurate results. The load variability is different for upward and downward directions and hence reserves need to be separately estimated. One key outcome of this study is the development of a characteristic curve of the regulating reserve needs vs peak load for the Sri Lankan system. That can be effectively used as a planning tool to enhance the long term planning process.

Results revealed that the relative variability of wind in regulating time frame is higher than the load variation and lower than that of solar.

function of solar or wind capacity. Consequently it increases as the penetration level rises. Therefore this

paper recommends the scenario based approach for reserve estimation future planning exercises.

It was found that upward and downward regulating reserve for load variability ranges from 3.4-4.7% (Upward) and 2.8-3.0% (Downward) during the period 2018-2028. Scaling up of VRE energy share from 10% to 20% after 2020 increases the total regulating reserve requirement from 5.6% to 7.4% at the end of the period. Ultimate Results are compiled in a look-up table to assist the system planning process. It is also emphasized that with higher penetration of VRE, providing both upward and downward reserves become necessary in the future.

After quantifying the total regulating reserves requirement, system operational strategies should be devised to provide the reserve services at an optimum manner.

### Acknowledgement

The authors wish to acknowledge the support extended by the Generation Planning Unit of Ceylon Electricity Board for providing necessary information, tools and valuable inputs to conduct this research work.

### References

1. Long Term Generation Expansion plan, Ceylon Electricity Board, 2018-2037, April 2017.

2. IEA, "Key CO<sub>2</sub> Emission Trends," *IEA - Int. Energy Agency*, 2016.
3. H. Chandler, A. Tuohy, and R. Chandra, *Harnessing Variable Renewables - A Guide to the Balancing Challenge*. 2011
4. NERC, "Reliability Standards for the Bulk Electric Systems of North America," NERC Reliability Standard., 2012.
5. H. Holttinen *et al.*, "Methodologies to Determine Operating Reserves due to Increased Wind Power," vol. 3, 2013.
6. Y. G. Rebours, D. S. Kirschen, M. Trotignon, and S. Rossignol, "A Survey of Frequency and Voltage Control Ancillary Service; Part I: Technical Features," *IEEE Trans. Power Syst.*, vol. 22, 2007.
7. M. Milligan *et al.*, "Operating Reserves and Wind Power Integration : An International Comparison Preprint," October 2010.
8. E. Ela, M. Milligan, and B. Kirby, "Operating Reserves and Variable Generation" 2011.
9. NREL, "Impacts of Solar Power on Operating Reserve Requirements," 2012.
10. H. Holttinen *et al.*, "Methodologies to Determine Operating Reserves due to Increased Wind Power," vol. 3, no. 4, pp. 713–723, 2013.
11. B. Parsons and E. Ela, "Impacts of Large Amounts of Wind Power on Design and Operation of Power Systems ; Results of IEA Collaboration," 2008.

12. Holttinen, H., Milligan, M., Kirby, B., Acker, (2008). Using Standard Deviation as a Measure of Increased Operational Reserve Requirement for Wind Power. Wind Engineering.
13. Ela, E., Kirby, B., Lannoye, E., Milligan, M., Flynn, D., Zavadil, B., & O'Malley, M. (2010). Evolution of operating reserve determination in wind power integration studies. IEEE PES General Meeting, PES 2010.



# Future Energy Mix for Sri Lankan Electricity Sector in the Perspective of National Energy Security

Kaushalya, K.H.A <sup>1</sup>, Hapuarachchi, D.C<sup>2</sup>, Samarasekara, M.B.S <sup>3</sup>

*Generation Planning Unit, Transmission & Generation Planning Branch, Ceylon Electricity Board, Sri Lanka*

<sup>1</sup> asith.kaushalya@ceb.lk  
<sup>2</sup> diyasha.hapuarachchi@ceb.lk  
<sup>3</sup> cegp.tr@ceb.lk

## Abstract

International Energy Agency defines energy security as “uninterrupted availability of energy sources at an affordable price” and further connects long-term energy security with timely investments to supply energy in line with economic developments and sustainable environmental needs. The purpose of this paper is to analyze the draft Long Term Generation Expansion Plan (LTGEP) 2018-2037 prepared by Ceylon Electricity Board (CEB) from the perspective of national energy security [1]. CEB has developed a Base Case in draft LTGEP 2018-2037 with an energy mix mainly consisting of Coal and Natural Gas based thermal generation and renewable energy technologies. This base case was selected from a set of scenarios developed considering factors such as fuel diversification, fuel price trends, climate change perspectives etc. With the Decision on LTGEP 2018-2037, Public Utilities Commission of Sri Lanka (PUCSL) has proposed a revised plan with only natural gas based thermal power plants and renewable energy technologies as future major power plant additions [2]. This study analyzes the Base Case Plan of draft LTGEP 2018-2037 with certain comparisons from Revised Plan considering impact to the future energy security giving due consideration to the fuel price uncertainties, reliability of supply, adhering to least cost principles, sustainable development perspective, externality costs, environmental impacts, land usage regarding power plant development and comparisons with the energy mix of other countries.

**Keywords** : national energy security, long term generation planning, energy mix, fuel diversity, externality costs

## Introduction

National energy security is becoming an increasingly important factor in the energy domain. According to the International Energy Agency (IEA) energy security refers to the “uninterrupted availability of energy sources at an affordable price” and further states that the long term energy security mainly deals with timely investments to supply energy in line with economic developments and sustainable environmental needs.

National Energy Policy and Strategies of Sri Lanka under Gazette No. 1553/10 on 10th June 2008 have considered “Ensuring Energy Security” as an energy policy element [3]. Further the updated National Energy Policy and Strategies of Sri Lanka also identifies “Assuring Energy Security” as the first pillar out of ten and strategies to implement this in electricity sector define as follows[4];

- Diversity in energy resources used in electricity generation will be ensured subject to economic, environmental, technological and operational requirements.
- Global diversification of energy sources will be pursued to safeguard supply chain against external geo-political uncertainties.
- Ensure the adequacy and reliability of transmission and distribution infrastructure in both electricity and fuel supply networks to meet any future contingencies.
- Regular risk assessments will be conducted to identify and mitigate possible internal, external contingencies that

could critically affect the performance of the energy sector.

- Indigenous energy resources will be explored and strategically developed by making necessary upstream investments at appropriate times, giving due consideration to future trends in energy supply and use.
- The national requirements of electricity will be met with proven generation technologies and fuel sources.
- Maintenance of strategic fuel reserves in strategic locations in the country will be made mandatory for all key players in electricity and petroleum industries.
- Viable cross-border electricity transfer and cooperation with countries in the region will be encouraged.

Electricity is one of the three main energy supply sources in Sri Lanka and directly related to the socio economic development of the country. Therefore, it is important to develop and maintain an efficient, coordinated and economical electricity supply with sufficient amount of electricity to satisfy the demand. Through the Long Term Generation Expansion Plan (LTGEP), CEB methodologically plans its power plant developments in order to provide reliable, quality electricity to the entire nation at affordable prices. The outline of the Generation Planning Study Process is shown in Figure 1.

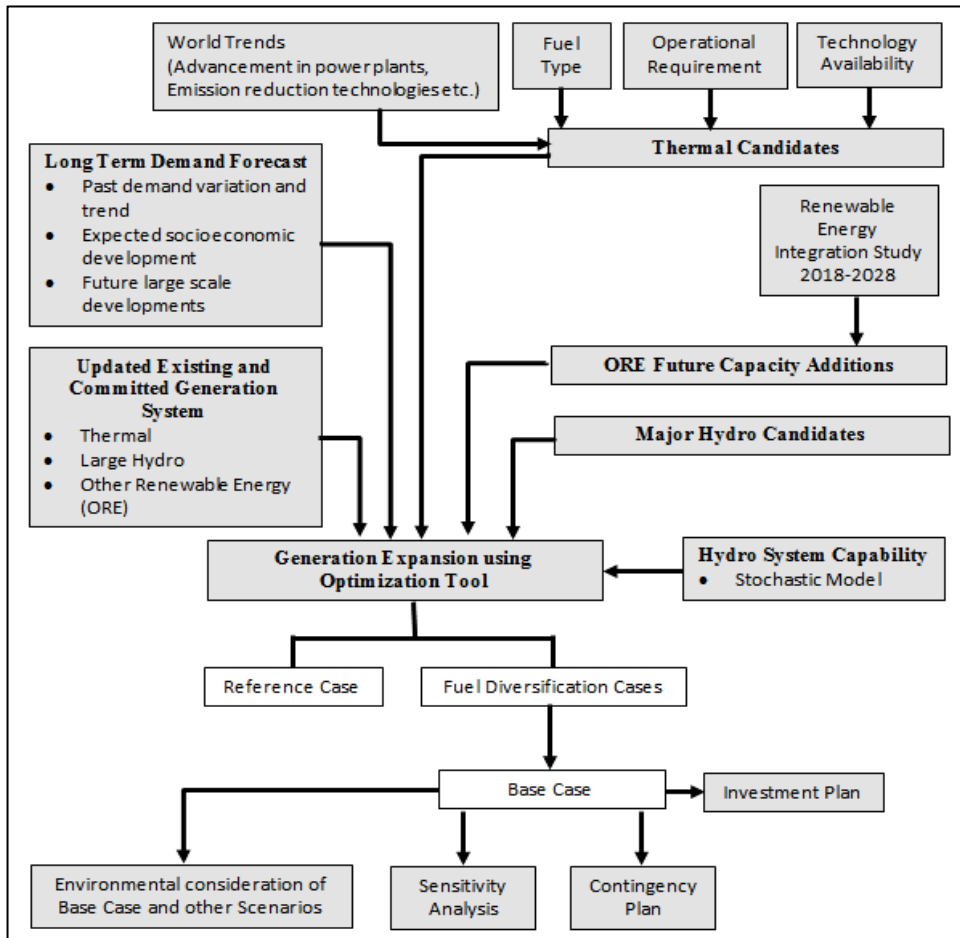


Figure 1: Long Term Generation Planning Study Process

By following the above study process, CEB has developed the Base Case in draft LTGEP 2018-2037 with an energy mix mainly consisting of Coal and Natural Gas based thermal generation and renewable energy technologies. This base case was selected from a set of scenarios developed by giving due consideration to the fuel diversification, past fuel price variation, future fuel price forecast, implementation of power plants, proposed government development, impact to the unit

generation cost and climate change perspectives with environment.

CEB has submitted the draft LTGEP 2018-2037 for the approval of PUCSL and with the decision on LTGEP 2018-2037, PUCSL has proposed a plan with all future thermal additions by natural gas based thermal power plants.

Figure 2 & 3 illustrates the capacity and energy mix of CEB Base Case and PUCSL Revised Case in 2037.

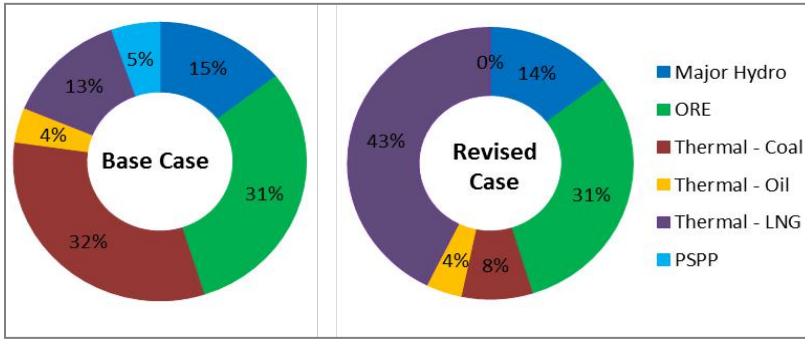


Figure 2: Capacity Share comparison in 2037

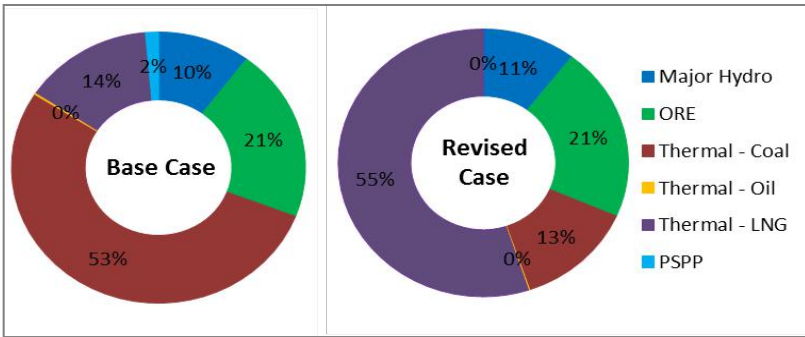


Figure 3: Energy Share comparison in 2037

## Methodology

In LTGEP planning process, operating information and system limitations on the existing generating plants, details and costs of candidate thermal and hydro plants were used on optimization tools and a series of simulations were conducted to derive the feasible optimum generation expansion sequence from several scenarios for the 20 year planning horizon. Focal considerations such as fuel price uncertainties, reliability of supply, adhering to least cost principles, externality costs, environmental impacts, land usage regarding power plant development and comparisons with the energy mix of other countries were chosen and analyzed the Base Case Plan of draft LTGEP 2018-2037 and PUCSL

revised plan considering impact to the future electricity sector energy security.

## Analysis

### Fuel Price Uncertainty

#### Past and Future Fuel Price Variation

In the Long Term Generation Planning Process, it is necessary to consider appropriate prices for fuel which will be best representative of the future price variations.

CEB has considered the **past two year average fuel prices** for the draft LTGEP 2018-2037 and conducted sensitivity analysis to check the robustness of the plan against the fuel price variation. PUCSL has considered past one year average fuel prices for their proposed plan.

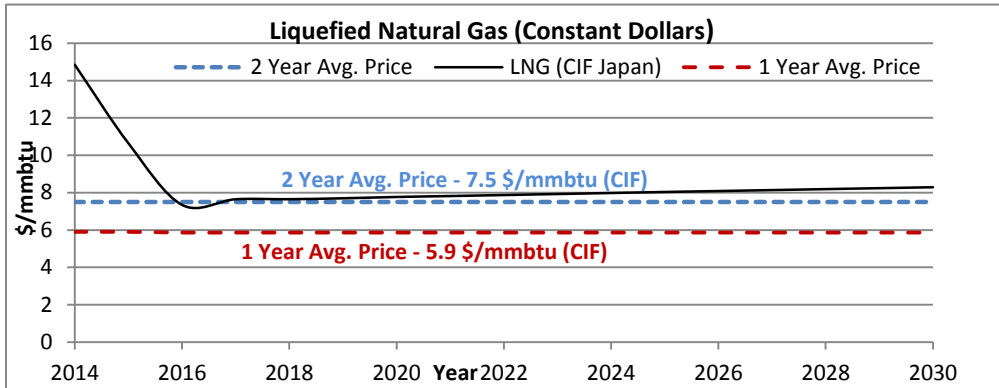


Figure 4: Liquefied Natural Gas price variation in Constant Dollar Term

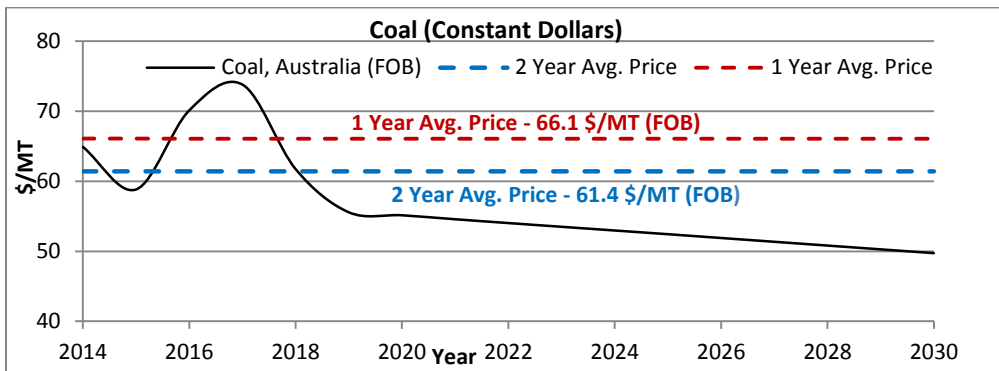


Figure 5: Coal price variation in Constant Dollar Term

In long term generation planning process, constant dollar terms are used and figure 4 & 5 show the comparison between the 1 year and 2 year average fuel prices with World Bank Projections [5].

When considering the LNG past prices as shown in Figure 4, 2016 shows an exceptionally lower value in the recent past and it can be seen an increasing trend beyond 2017. Therefore it is not appropriate to consider 2016, 1 year average price for long term planning since it represents an exceptional value with lowest figure. However, 2015 and

2016, 2 year average fuel price is in line with LNG price forecast.

Figure 5 shows a downward trend in Coal prices from 2014 to 2015 and an upward trend beyond 2015. According to the past price variations, 2016 was an exceptional year for higher Coal prices and predictions show a price peaking in 2017 and gradually reduce afterwards. Accordingly, the consideration of 2016 1 year average fuel price for the long term planning is biased towards the peak value with rapid growth for Coal price. However, 2015 and 2016, 2 year average prices has a better representative of the price variations in the recent past and

also in the view of the preparation of this bi annual expansion plan which requires a prudent price point applicable to a 20 year time horizon.

Based on the above, it can be concluded that the 2 year average fuel prices provide better representation than 1 year average fuel prices for Coal and LNG.

### Impact for Specific Cost with Fuel Price Variation

As per the fuel prices (LNG & Coal) considered for the LTGEP, resultant specific costs of major candidate power plants at 80% plant factor is shown in Table 1. Accordingly, with 2016, 1 year and 2016, fourth quarter average fuel prices also Coal power plants show lower cost than LNG power plants.

Table 1: Specific Cost at 80% Plant Factor

	2 Year Avg. Fuel Prices	1 Year Avg. Fuel Prices	4 <sup>th</sup> Quarter Avg. Fuel Prices
LNG Prices (USD/mmbtu)	10	8.36	9.09
150 MW CCY – NG (USCts/kWh)	9.39	8.38	8.91
300 MW CCY – NG (USCts/kWh)	9.37	<b>8.20</b>	8.72
Coal Prices (USD/MT)	69.7	80.9	110.5
300 MW Coal (USCts/kWh)	6.70	<b>7.12</b>	8.25
600 MW Coal (USCts/kWh)	6.77	7.16	8.20

Therefore it can be concluded that, the 300MW & 600MW Coal power plant shows lower operating cost than 150MW & 300MW LNG Combined Cycle power plant for a wide range of fuel price variation.

### Reliability of Power Supply

System Reliability is an integral aspect of an energy system with respect to meeting consumer expectations of reliability as a fundamental delivery requirement for electric utilities and it is broadly defined through metrics describing power availability or outage duration, frequency, and extent. In Sri Lankan Context, system reliability level is indicated mainly by two aspects which are Loss of Load Probability and Reserve Margin.

### Loss of Load Probability (LOLP)

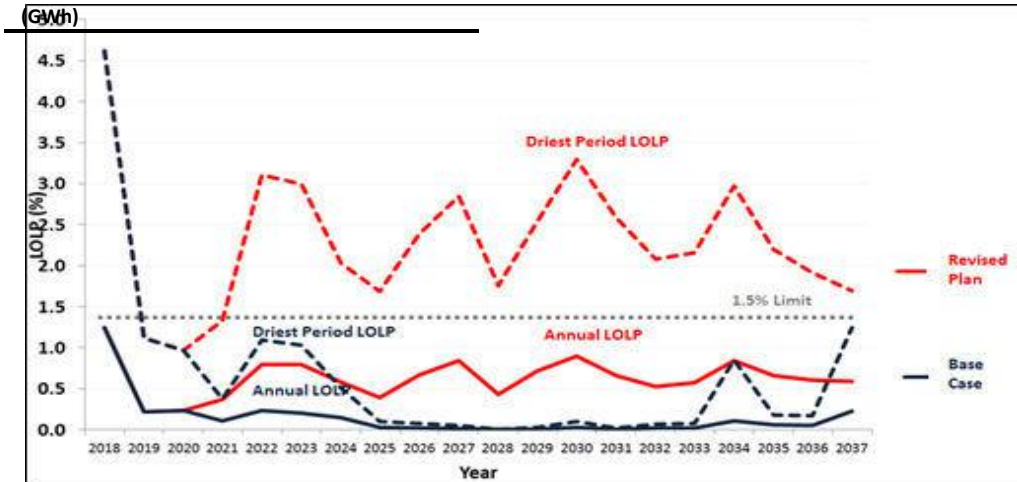
The index Loss of Load Probability - LOLP (%) is a projected value of amount of time, in the long run, the load of a power system is expected to be higher than the capacity of the available generating resources. As per the Grid Code, the maximum value for annual LOLP should be 1.5%. In the base case plan developed by CEB for the Draft LTGEP 2018-2037, the LOLP values have been kept within the limit throughout the planning horizon in the weighted average hydro condition as well as in the driest hydro condition considering the hydro generation statistics of the recent years.

Annual generation figure from major hydro power plants for the last 5 years is shown in Table 2.

Table 2: Annual Hydro Generation 2012-2016 [6]

Year	2012	2013	2014	2015	2016
Major Hydro Generation (GWh)	2727	6010	3652	4924	3498

This aspect has not been considered in the revised plan where the LOLP of the driest hydro condition violates the stipulated upper limit (as shown in Figure 6) which compromises the reliability of the system.



It is evident from the figures in Table 2 that in 3 years out of 5, hydro generation from major plants have been below 3,700GWh which could be considered as dry to very dry hydro condition based on the generation data of past 30 years.

Therefore in the generation expansion studies, maintaining the system reliability even at the dry hydro conditions was analyzed in detail and it led to keeping the LOLP value below 1.5% even at the driest hydro condition in the base case for the planning horizon. This has been carried out as a prudent practice giving due consideration to the possible outages of thermal power plants at the dry hydro conditions which has occurred in past power crisis situations.

**Reserve Margin**

Reserve Margin is the difference between available capacity and peak demand which reinforces the system to maintain a reliable operation while meeting unexpected generation outages and unforeseen changes in demand. With regard to the Reserve Margin, the prudent practice which is adopted in the LTGEP 2018-2037 is to calculate the reserve margin at the critical month of the year, with the consideration of the possible dry hydro conditions. Accordingly, in the CEB Base case plan, reserve margin is kept above 2.5% throughout the planning period as per the grid code which is shown in Figure 7.

Figure 6: LOLP Variations of CEB Base Case and PUCSL Case

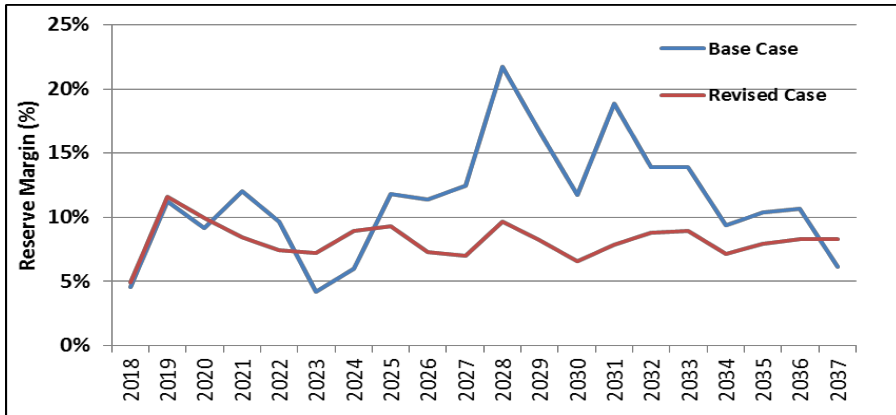


Figure 7: Reserve Margin Variations of CEB Base Case and PUCSL Case

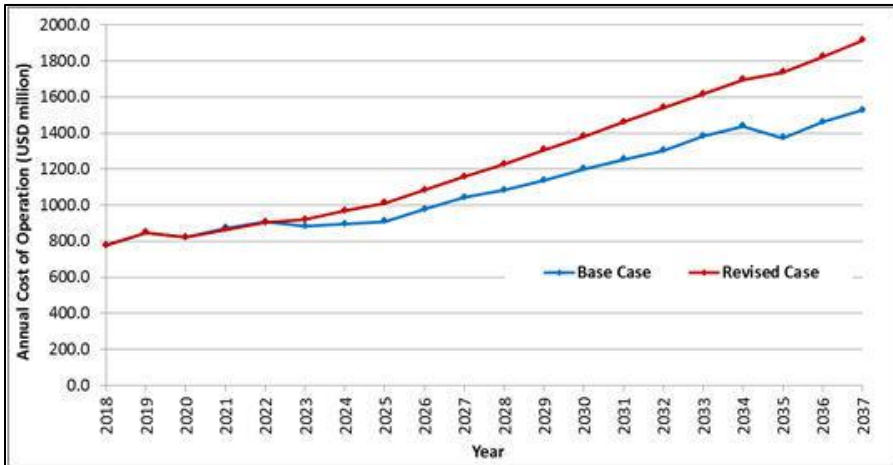


Figure 8: Annual Operational Cost 2018-2037

### Adhering to Least Cost Principles

It is important to supply electricity to the people with an affordable price. To supply the future electricity demand with lowest possible cost, it is important to select correct fuel options and technologies to optimize the whole electricity generation system.

Annual operational cost is an important factor in determining total generation

cost of the system. Figure 8 shows the annual operational cost of Base case and Revised case for 1 year average fuel prices.

Accordingly, Base case shows lower operational cost than Revised case resulting lower generation cost over the planning horizon.



Investment cost directly relates with planned power plant developments and need to consider the scarcity of lands especially in the urban areas, when development of power plants. LNG power plants are planned to develop with in urban areas due to the environment friendliness than other large scale thermal power plants. CEB planned to develop 300MW LNG power plants than 150MW LNG units by considering economical use of lands within highly scarce areas and the efficient use of the power plants.

Impacts on society and environment arising due to electricity sector developments should be given due consideration. Therefore, introduction of high efficient Coal power plants with emission control technologies and penetration of indigenous resources has been considered in the CEB planning process. Table 3 shows the emission standards issued by Central Environmental Authority (CEA) for Coal power plants and the specification of the 300MW candidate Coal power plant used in LTGEP 2018-2037 Base case [7].

Table 3: CEA Regulation and Stack Emission of Proposed 300MW Coal Candidate

Pollutant	CEA Standard for Coal >=50MW	300 MW Coal Power Plant
Nitrogen Oxides	650 mg/Nm3	400 mg/Nm3 (without SCR)
Sulphur Dioxide	850 mg/Nm3	100 mg/Nm3
Suspended Particulate	150 mg/Nm3	20 mg/Nm3

To maintain within the specified standards, CEB has considered high efficient Coal power plants with emission

control technologies which will cause higher investment cost than conventional power plants which is shown in the Table 4.

Table 4: Comparison of Coal Power Plant Capital Costs

	Conventional Coal PP300MW	High Efficient Coal PP300MW	Super Critical Coal PP600MW
<b>Pure Capital Cost (USD/kW)</b>	1,367.6	1,786.2	1,916.8

**Promotion of Other Renewable Energy (ORE)**

Coal and Petroleum products which are used in the present electricity sector to generate the electricity are non-indigenous resources of energy and totally depend on import. So utilizing the indigenous energy resources which are readily available in the country is important in considering both fuel diversification and maximum use of available resources.

Hydro is the main indigenous resource in the country at present and it is almost completely harvested. CEB expect to increase ORE (Wind, Solar, Biomass and Mini Hydro) contribution in future where at present ORE generation is 11% of total energy generation in Sri Lanka. The study "Integration of Renewable Based Generation in to Sri Lankan Grid 2017-2028" [8] was carried out by CEB with the objective of assessing the technical, operational, economic aspects and to determine the optimum level of renewable energy based generation to the grid in future. Figure 9 illustrates the future penetration of Wind, Solar, Biomass and Mini Hydro technologies to the system.

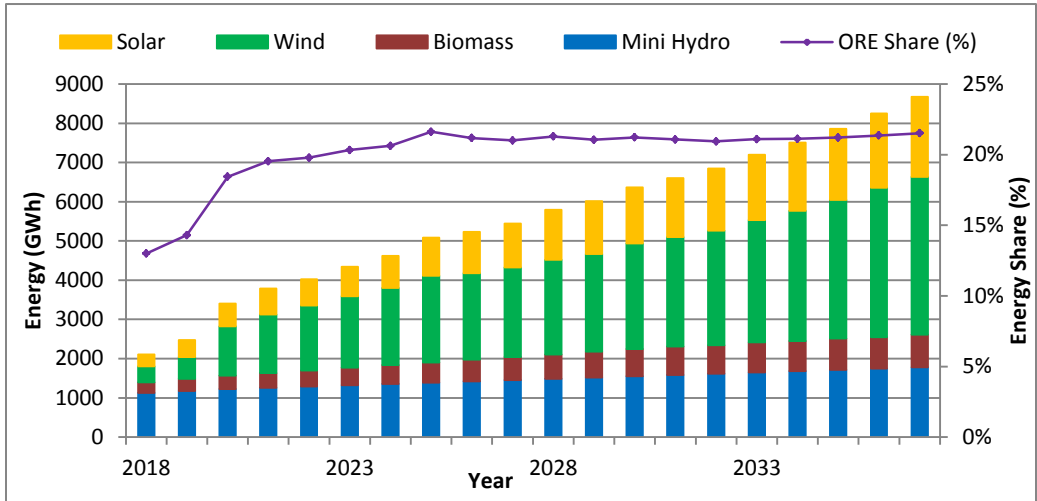


Figure 9: Proposed ORE Capacity Addition 2018 –2037

Therefore, integration of ORE capacity 3,454MW and 8,670GWh generation in to the system by 2037 will enhance the national energy security by reducing dependency of imported petroleum resources and also the carbon emissions in electricity generation.

**Externalities**

The externality cost of power generation could be mainly categorized in local context and global context. Local externalities include environmental and health damages from local pollutants (SO<sub>2</sub>, NO<sub>x</sub>) , wastes, occupational health, risk of accidents, noise and other social impacts. Global externality is greenhouse gas emissions contributing to climate change.

**Local Externalities**

Local Externalities encompasses both the environmental and social impacts of the power generation to the local population. The emission of air pollutants such as SO<sub>2</sub>, NO<sub>x</sub> and issues associated with thermal discharges of

power plants mainly contributes to the environmental impacts of the power generation. Social impacts of power generation include effects on lifestyle of the local population, possible losses of crops, etc.

The Base Case plan of draft LTGEP 2018-2037 contains 2700 MW of Coal based power plants and 1500 MW NG based combined cycle power plants while the Reference case(Case with the minimum cost) consists of same capacity of NG based combined cycle power plants and 3600 MW Coal based power plants.

In comparison, the capacity and energy contribution from 2897 MW of ORE plants in the Base Case plan has replaced 900 MW of additional Coal based power plants in the Reference case. This high level of ORE additions has directly resulted in decreasing the environmental impacts of the plan by significantly reducing the air pollutants and other thermal discharges which would have emitted from the thermal power plants.

Also, ORE integration has contributed in introducing positive social and economic

impacts such as Local employment and other economic benefits, lower currency risk in indigenous technologies, Pertinent cost reduction trends in some ORE technologies, Use of indigenous resources that improve energy security etc.

It is also noted that environmental impacts of the power plants are evaluated in detail at the Environmental Impact Assessment (EIA) of a project and at that point maximum possible mitigation measures would be imposed to reduce the environmental and social impacts of the certain project.

**Global Externalities**

When climate change impacts are considered, Base Case plan of LTGEP 2018-2037 has proposed High Efficient Coal Plants and Super Critical Coal Plants to be added to the system in future years. The Table 5 shows a comparison of these power plant technologies with the conventional coal power plants.

*Table 5: Comparison of Coal Power Plant Technologies*

	Conventional Coal PP	High Efficient Coal PP	Super Critical Coal PP
<b>Unit Capacity (MW)</b>	300	300	600
<b>Full Load Efficiency (%)</b>	33.3	38.4	41.3

It is evident that High Efficient Coal Plants and Super Critical Coal Plants operate at higher efficiency levels than conventional Coal plants, thus maintaining lower emissions during operation. These plants also employ more advanced emission reduction

techniques which allow them to achieve lesser emission levels.

Moreover, total CO<sub>2</sub> Emissions (Million tons) from Electricity Generation projections based on 2014 actuals and the CEB Base case plan are shown in the Table 6 and it is observed that CO<sub>2</sub> Emissions from Electricity Generation are far below even the present level of other countries(India - 2020, USA - 5176 , Switzerland – 38) [9] in year 2037 as well.

*Table 6: Total Annual CO<sub>2</sub> Emissions based on 2014 Actuals and Base Case Projections*

Year	2014	2025	2030	2037
<b>Total Annual CO<sub>2</sub> Emissions in Base Case (Million tons)</b>	6.79	6.41	11.33	19.25

**Externality Costs**

When externality costs are considered, it is established that these costs are a function of income level and population density, typically expressed as per capita GDP and specifications of power plant technologies. Therefore externality costs calculated in a certain country cannot be directly used for evaluation purposes in another country.

This proves that best representative values for externality costs should be determined for the local context through a proper and independent study before incorporating in the long term planning.

Also it should be noted that the concept of externality cost should be utilized to

promote indigenous energy resources in power generation which in turn improves the energy security aspect of the power sector. It could be observed that Base Case plan of LTGEP 2018-2037 has integrated the optimum amount of ORE to the system fulfilling this purpose.

Moreover the Base Case plan has included maximum possible cost implication of externalities to the proposed power plant developments by replacing conventional coal technologies with high efficient coal plants and introducing NG based combined cycle power plants with relatively lower emissions.

### Comparison with the Energy Mixes of Other Countries

CEB base case has considered a mix of NG and coal based thermal plants, major hydro power plants, pumped hydro power plant, wind, solar, mini hydro, biomass based renewable energy plants which ensure energy security and robustness in fuel price fluctuations.

If a case is proposed restricting all the major future thermal plant additions to be fueled by NG or Coal, it could be detrimental in the perspective of energy security. This is mainly due to the fact that the cost of the plan is highly susceptible to the price variations of fuels.

This fact could be further strengthened by analysis of the future energy mixes of different Countries based on their present policies presented in Table 7 which shows a balanced energy mix of different fuels including coal, NG, renewables etc.

Table 7: Comparison of 2014 and future projected energy mix of selected countries [10]

Country	Year	LNG	Coal	Nuclear	Renewable	Other
USA	2014	27%	40%	19%	13%	1%
	2040	34%	25%	16%	24%	0%
China	2014	2%	73%	2%	23%	0%
	2040	7%	58%	9%	26%	0%
EU	2014	14%	27%	28%	29%	2%
	2040	28%	13%	17%	43%	0%
Japan	2014	41%	34%	0%	13%	11%
	2040	27%	31%	16%	27%	1%
Russia	2014	50%	15%	17%	17%	1%
	2040	45%	14%	20%	21%	0%
Non OECD Asia	2014	8%	67%	3%	19%	2%
	2040	11%	58%	6%	23%	1%
India	2014	5%	75%	3%	15%	2%
	2040	10%	65%	4%	20%	1%
Malaysia	2015	40%	43%	0%	16%	1%
	2025	28%	52%	0%	9%	11%
Vietnam	2015	30%	34%	0%	34%	2%
	2030	17%	53%	6%	23%	1%

It could be clearly observed that all these countries have proposed to maintain balanced energy mixes throughout their planning horizon with the consideration of all the available fuels and technologies which would directly enhance the energy security of the respective countries.

## Conclusion

This study was developed mainly on the analysis of the Base Case of draft LTGEP 2018-2037 in the perspective of energy security and the factors used in the determination of the salient points in the base case plan which addresses the concept of energy security of the Sri Lankan power sector. For the comparison purposes, the revised plan proposed by PUCSL was also taken into consideration.

For a country like Sri Lanka in which power generation is currently based on a mix of imported fossil fuels and local indigenous resources, energy security should be maintained primarily by increasing the fuel diversity, increasing reliability of energy resources, increasing utilization of indigenous resources such as renewable energy sources and especially Local Natural Gas for which provisions are made in the Base Case plan for effective utilization.

As a comparison, a case which has restricted all the major future thermal plant additions to be fueled by a single fuel could be detrimental in the perspective of energy security. This is mainly due to the fact that the cost of the plan is highly susceptible to the price variations of fuels. In contrast a case which has considered a mix of different fuel based thermal plants which ensure energy security and robustness in fuel price fluctuations.

As per the list of factors discussed in this paper, Base Case Plan of LTGEP 2018-2037 has been prepared with careful consideration of the energy security in power sector under the uncertainty of fuel prices, power supply reliability, least

cost principles, promotion of ORE by focusing sustainable development, externality costs and energy mixes of other countries. Therefore it could be concluded that the Base Case plan has proposed an energy mix for the planning horizon which would be capable of preserving the energy security of the country.

## References

- [1] Generation Planning Unit, Ceylon Electricity Board. Long Term Generation Expansion Plan 2018-2037 (Draft).
- [2] Public Utilities Commission of Sri Lanka, Decision on Least Cost Long Term Generation Expansion Plan 2018-2037
- [3] National Energy Policy and Strategies of Sri Lanka, June 2008.
- [4] National Energy Policy and Strategies of Sri Lanka, Version 6.3, February 2017
- [5] Commodity Markets, January 2017 Forecast, World Bank. Available: <http://www.worldbank.org/en/research/commodity-markets#3>
- [6] Statistical Unit, Ceylon Electricity Board. Statistical Digests 2012-2016
- [7] Central Environmental Authority. Interim Source Emission Regulations (Draft).
- [8] Transmission and Generation Planning Branch, Ceylon Electricity Board. Integration of Renewable Based Generation in to Sri Lankan Grid 2017 - 2028.
- [9] International Energy Agency, CO<sub>2</sub> Emissions from Fuel Combustion, 2014 Edition
- [10] International Energy Agency, World Energy Outlook, 2016 Edition

# Techno Economic Feasibility of Solar PV with Battery Energy Storage for Domestic Sector and EV Charging

Asanka S. Rodrigo<sup>1</sup>, Mevan N. Pathiratne<sup>2</sup>, Cheon-Kee Jeong<sup>3</sup>,  
and Gi Jeung Um<sup>4</sup>

<sup>1</sup>*Department of Electrical Engineering, University of Moratuwa, Sir Lanka*  
<sup>1</sup>asankar@uom.lk

<sup>2</sup>*Ceylon Electricity Board, Colombo 01, Sri Lanka*  
<sup>2</sup>mevnil\_601@yahoo.com

<sup>3</sup>*DIK CO., LTD., South Korea*  
<sup>3</sup>jck3261@naver.com

<sup>4</sup>*Korea Research Institute on Climate Change, South Korea*  
<sup>4</sup>gijeungum@gmail.com

## Abstract

As emphasis on renewable energy increases harnessing the maximum solar energy potential has become imperative. However, the effective use of its potential is restricted by certain factors. The inherent feature of intermittency causes variations in power and voltage while the dependency on time of generation during day time limits its actual requirement. A night time peak as in Sri Lanka demands a cost effective renewable solution. Battery Energy Storage systems provide an integral solution for both these limitations. A case is studied and presented on implementing a PV combined battery energy storage system on domestic consumers and EV Charging centers with two investment scenarios. The Levelized Cost of Energy (LCOE) of Photovoltaic and Battery Energy Storage System (PVBESS) reduces with increasing system capacity and a 5 kW domestic PVBESS configuration shall have a LCOE of LKR 42.14 on a combined consumer utility investment plan. It is presented that under a peak energy system based on gas turbines could be replaced by a combined investment of consumer and utility on battery energy storage with both parties gaining equal benefit. Furthermore, it is found that the implementation of such scheme is heavily dependent on the peak power energy mix and hence extensive commitment on implementing a PVBESS solution could lead to a loss to the utility, if the share of gas turbines energy during the peak hours is less than 80%.

**Keywords** : Battery Energy Storage System, PV systems, Peak Power, Levelized Cost of Energy

## Introduction

Earlier PV systems were mainly installed in off grid rural areas. However recently it has been a popular choice even in urban areas to be installed in parallel with grid connected supply. Most rooftops provide an ideal location for residential, commercial and industrial electricity consumers to install PV panels. The growth of Photovoltaic systems has risen rapidly over the past decade and subsequently costs have decreased immensely. The economics of PV systems is now on the verge of reaching grid parity in many countries. Sri Lanka also moving towards more and more solar roof top systems. Under the present Ministry of Power and Renewable Energy (MOPRE) targets, it is expected to introduce 200 MW of solar PV to the grid in 2020 through the “Battle for Solar” Programme. It is expected to deliver about 1,869 MWh under the “Battle for solar” Programme in a day on 2020, which shall yield the opportunity to provide 1,495 MWh of energy considering the 20% energy loss [1].

However, the main issue with the solar energy is that it produces energy only during the day time. The effective operation of the solar panel can be classified during the period from morning 6am to evening 6 pm. However, in Sri Lanka, the maximum demand occurs during the night time from the period around 6.30 pm to 9.30 pm.

Battery energy storage systems are increasingly being used to help integrate solar power into the grid. These systems are capable of absorbing and delivering both real and reactive power with sub-second response times. With these capabilities, battery energy storage systems can mitigate issues with solar power generation such as ramp rate, frequency, and voltage issues. Beyond these applications focusing on system stability, energy storage control systems can also be integrated with energy markets to make the solar resource more economical [2]. Furthermore, when the grid parity is considered for estimating the levelized cost of energy (LCOE) of solar PV, it is comparable with grid electrical prices of conventional technologies and thus it is considered as the industry target for cost-effectiveness.

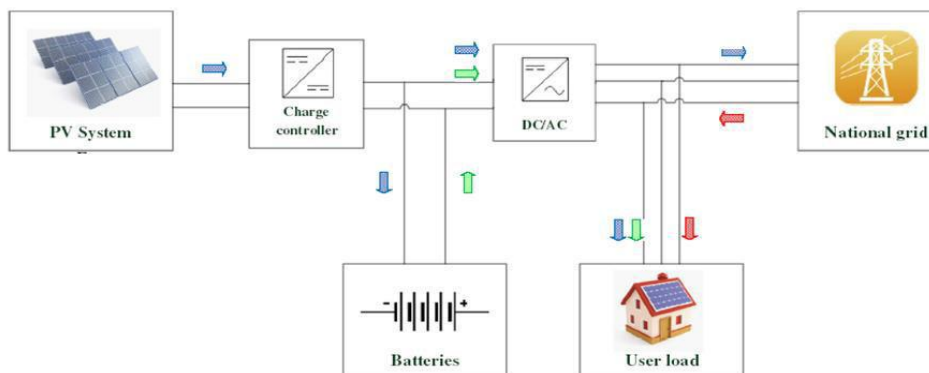


Figure 1: Illustration of PVBESS

## Photovoltaic and Battery Energy Storage System (PVBESS)

The Figure 1 illustrates a PVBESS, which includes PV System, Charger control, Inverter system and a Battery storage system.

### PV panels

PV panels are the main equipment of the configuration which converts solar irradiance to electric power. The study conducted by National Renewable Energy Laboratory of Colorado gives a comprehensive analysis on the available solar irradiance potential in Sri Lanka [3]. Accordingly;

Solar Irradiance Index Energy per day,  
 $E_{PV}$  (kWh/per day);

$$E_{PV} = D_T \times E_{IPV}$$

Where,

Energy produced by the PV panel per day =  $E_{PV}$  (kWh/perday)

PV panel degradation on year T  
 =  $D_T$  (%)

The Efficiency of PV panels do not remain constant throughout the lifetime of the panel. The performance of Solar PV degrades annually. Usually it is an accepted norm by each supplier in which they give a guarantee in which the PV panel will have 90% of the original output in 10 years and 80 % of the original output in 25 years of operation. That is the estimated degradation of 10% in 10 years & 20% in 25 years [4].

### Inverter

The inverter used to convert the solar panel produced energy may be a uni-directional or bi-directional unit depending on the purpose of the application. Since the viability of charging the battery bank through grid energy has not been considered as economically feasible yet an uni-

directional inverter is considered sufficient for a PVBESS installation.

### Charge Controller

A charge controller is required to ensure that the batteries do not overcharge or discharge beyond the certain level as accepted. The State of Charge (SOC) is the inverse of depth of discharge (DOD) which provides the figure of the available capacity of a battery. The charge controller shall function as follows.

During Daytime of solar power Generation ( $E_{pv} > 0$  &  $06.30 H < T < 18.30$ )

*If  $SOC \geq SOC_{(max)}$*

*Stop charging the battery and supply the energy to the household*

*Else if  $SOC_{(max)} > SOC > SOC_{(max DOD)}$*

*Charge the battery*

*Else if  $SOC < SOC_{(max DOD)}$*

*Charge the battery*

During the peak energy time (  $18.30 H < T < 21.30$  )

*If  $SOC > SOC_{(max DOD)}$*

*Discharge the battery*

*If  $SOC < SOC_{(max DOD)}$*

*Stop discharging the battery*

### Battery

There are various types of batteries available in the market today. Usually different types of batteries have unique advantages to suit for their applications. Unlike the usual car batteries, the renewable energy storing batteries must be selected to have large number of deep cycle discharges.

effectively the total energy shall be estimated based on as an ideal battery which shall be the product of unit voltage and current capacity.

Energy stored in the battery per day  
 =  $E_{BS}$  (kWh/per day)



Energy discharged by the battery per day  
 =  $E_{BD}$  (kWh/per day)  
 Capacity to store Energy per day  
 =  $C_{BS}$  (kWh/per day)  
 Depth of Discharge  
 = DOD (%)  
 Charging Efficiency  
 =  $\eta_c$  (%)  
 Discharging Efficiency  
 =  $\eta_d$  (%)

$$E_{PV} = E_{IPV} \cdot D$$

$$E_{BS} = E_{PV} \cdot \eta_c$$

$$C_{BS} = E_{BS} \cdot (DOD) = E_{PV} \cdot \eta_c \cdot (DOD)$$

$$E_{BD} = E_{BS} \cdot \eta_d = E_{PV} \cdot \eta_c \cdot \eta_d$$

The Depth of Discharge (DOD) has a huge impact on the battery lifetime. If the battery bank operates at a higher DOD the lifetime of a battery bank will be lesser. All reputed battery manufactures supply the DOD vs. Lifecycle graph on their manufacturing sheet. The battery lifecycle graph provided by Weida on VRLA batteries is utilized for this research [5].

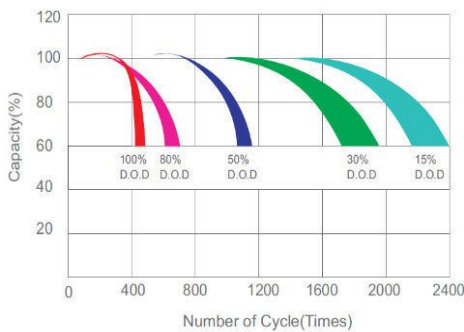


Figure 2: Life Cycle Characteristics of a Battery [5]

### Economics of PVBESS

The Levelized cost of Electricity (LCOE) is a measurement of the net present value of the unit cost of electricity over the operating lifetime of the asset. The LCOE can be calculated through the following formula.

$$LCOE = \frac{NPV \text{ of Total Cost}}{NPV \text{ of Total Energy Produced}}$$

The following price configuration is utilized as per the availed data from Solar Panel suppliers as at year 2016.

Table 1: Cost for different PV configurations

PV Configuration	kW	PV panel (Rs.)	Inverter (Rs.)	Charge Controller (Rs.)	Installation (Rs.)
1		112000	75000	16000	34000
1.5		165000	80000	16000	34000
2		221000	102000	24000	34000
3		330000	148000	34000	64000
4		435000	195000	40000	64000
5		535000	220000	77750	64000

The present market, the price of a 12 V 200 Ah battery is around as Rs. 35000 and thus the battery capacities required for different configurations for 1 kW to 5 kW were calculated illustrated below.

*Table 2: Cost for different BES configurations*

<b>PVBESS Configuration</b>	<b>Batter Energy Storage Cost (Rs.)</b>
1 kW	78750
1.5 kW	110250
2 kW	149625
3 kW	220500
4 kW	299250
5 kW	370125

It is assumed that the Operation and maintenance cost is taken as Rs. 2000 per year.

Based on above cost components, the LCOE for different grid connected PV system capacities were evaluated for 1 kW to 5 kW and summarized below.

*Table 3: LCOE for different PV configurations*

<b>PV System Capacity</b>	<b>LCOE (Rs./kWh)</b>
1 kW	16.42
1.5 kW	13.32
2 kW	12.63
3 kW	12.53
4 kW	12.00
5 kW	11.22

In order to identify the best combination which results in the least cost for lifetime operation the LCOE under different depth of discharge (DOD) were

calculated. In this calculation, the discount factor of 10% was used and the associated lifetime was taken as 25 years of operation of the solar panel.

*Table 4: Variation of LCOE for different DODs for different PV configurations*

<b>Solar PV + BESS</b>	<b>LCOE (Rs./kWh)</b>			
	<b>30%</b>	<b>50%</b>	<b>80%</b>	<b>100%</b>
	<b>DOD</b>	<b>DOD</b>	<b>DOD</b>	<b>DOD</b>
1 kW	59.51	55.36	53.59	56.41
1.5 kW	55.06	50.67	48.64	50.81
2 kW	53.75	49.44	47.33	49.40
3 kW	53.33	48.83	46.72	48.75
4 kW	52.36	48.09	45.85	47.61
5 kW	51.80	47.36	44.28	47.04

Accordingly, the LCOE is significantly affected by the DOD. Under all PVBESS configurations, the 30% DOD indicates a higher LCOE. This means investing in large capacity of battery banks to increase the lifecycles is not beneficial. The 50% & 100 % DOD percentages have resulted in a comparatively less LCOE while the most optimum least cost configuration has been seen when utilizing an 80% DOD. Even though investing on exact capacity shall limit its lifetime a balance in lifetime and initial cost is achieved by operating it at a level of 80% DOD. Therefore, the most feasible configuration is a 5 kW PVBESS configuration at 80% DOD.

### Capital Investment

Following two capital investment scenarios are considered and analyzed in this paper;

- Consumer capital investment Scenario

- Consumer + Utility capital investment scenario

**Consumer capital investment Scenario**

In this scenario, the consumer will purchase the PV panel system, inverter and the battery storage system and will own the complete system. The consumer has the responsibility of maintaining and replacing the battery energy storage systems periodically at the end of the life cycles.

The cumulative net present value of costs distribution depicts the lifetime investment costs of the PVBESS system. Therefore,

$$\text{Annual Cost} = \text{Investment cost on PV} + \text{Inverter} + \text{Battery} + \text{Charge Controller} + \text{O\&M cost} + \text{Installation cost}$$

Therefore, the Cumulative Net Present value of costs (CNPV) can be calculated as;

$$CNPV = \sum_{t=0}^{25} \frac{C_{pv}^t + C_{inv}^t + C_{cc}^t + C_{BESS}^t + C_{OM}^t + C_{OI}^t}{(1+d)^t}$$

Where,

- Investment cost on PV panels =  $C_{pv}$
- Inverter cost =  $C_{inv}$
- BESS cost =  $C_{BESS}$
- Charge Controller cost =  $C_{cc}$
- Operation & Maintenance cost =  $C_{OM}$
- Installation cost =  $C_{OI}$
- Discount factor =  $d$

The CNPV of PVBESS cost over the lifespan of 25 years of different system configurations operating on DOD level of

80% is calculated as per the above formula and illustrated in the Figure 3.

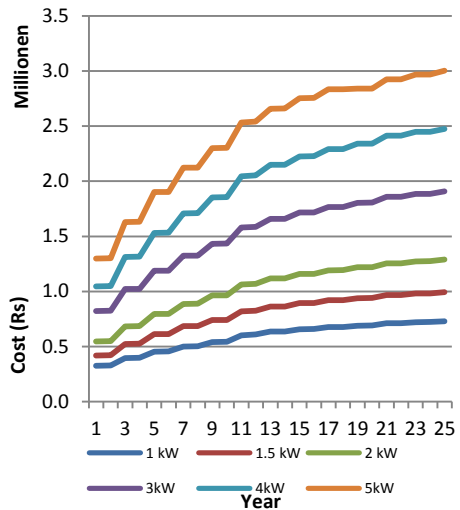


Figure 3: Net Present value of costs

In order to justify the investment, the consumer must be provided a tariff satisfactory to recover the costs and gain financial benefit. Here, the CNPV value of Avoided Cost Distribution for the utility with the CNPV of System cost distribution of the consumer were considered. In order to equalize the advantage of implementing the proposed system, it is suggested to split the savings 50:50 between the consumer and the utility.

It is identified that the only viable tariff rates which are capable of recovering the PVBESS lifetime cost were starting at a very high value of Rs.48/kWh. The degree of variation is also limited as such a higher rate above Rs.52/kWh shall incur a loss to the utility through the lifetime operation of the power plant. Thus the rates from 48 to 51 were checked with the economic parameters of internal rate of return (IRR), payback period, consumer's Net present value of

profit and Utility Net present Value of profit at end of the lifespan of 25 years.

It is found that the 1 kW PVBESS configuration does not become viable at any tariff rate thus proving ineffective and unviable. The 1.5 kW & 2 kW PVBESS configuration only receives payback at a rate higher than Rs.50/kWh but that also is after more than 15 years. For PVBESS above 3 kW all the validated rates give marginal benefit with minimum payback in 11 years. The most compatible with the plotted 50:50 Balance margin curve is PVBESS systems above 3 kW at a rate of Rs.50/kWh.

### **Consumer + Utility capital investment scenario**

In this scenario the consumer will invest in PV panel system and inverter systems. However, the Utility will invest for the battery storage systems. This means the under 80% DOD of BESS the utility will have to invest on replacement of batteries every 2 years.

It is found that the flat rate tariff margins which fit in the profitable margin for both the utility and the consumer are from Rs. 20-24/kWh. As earlier in the consumer investment only scenario the 1 kW PVBESS configuration does not payback during its lifetime. The 1.5 kW PVBESS configuration only gives a marginal benefit.

It is observed a minimum of 8 years payback period is incurred for the consumer in all configurations. On the other hand, even with utility investments on battery storage the return on investment for the utility is acceptable.

### **Conclusions**

The Solar Energy has great potential to supply energy for increasing demand but its full potential is not yet harnessed. The domestic and commercial consumers of electricity are allowed several schemes where they can generate and provide energy to the utility from Solar PV panels for energy credit or revenue. This study gives an understanding on the maximum limit possible for a tariff corresponding to a PVBESS integration which has to be reviewed dynamically depending on the scheduled peak energy sources dispatching order.

The introductions of PVBESS to the consumer side where they are given incentive to produce store and provide energy during the peak hours of demand were analyzed. The Levelized cost of Energy for PVBESS systems are nearly four times higher than the existing PV only grid connected systems.

It is seen that the consumer only investment scenario has very limited margin of flexibility for variation in tariff to gain benefit for both the consumer and the utility. The PVBESS configurations under 2 kW do not payback and systems also require a flat rate tariff above Rs. 50/kwh for consumer profitability. The flat rate Rs.50/kWh achieves equal profitability for consumer and utility but the payback period for the consumer is high.

## References

- [1] Sri Lanka Sustainable Energy Authority, "The Battle for Solar Energy", [http://www.energy.gov.lk/surya\\_bala\\_s\\_agramaya/index.php](http://www.energy.gov.lk/surya_bala_s_agramaya/index.php)
- [2] C.A. Hill, M.C Such, D. Chen, J. Gonzalez, and W.M Grady, 'Battery Energy Storage for Enabling Integration of Distributed Solar Power Generation', IEEE TRANSACTIONS ON SMART GRID, VOL. 3, NO. 2,850-857, 2012
- [3] D. Renné, R. George, B. Marion and D. Heimiller, 'Solar Resource Assessment for Sri Lanka and Maldives', National Renewable Energy Laboratory, 2003.
- [4] D. C. Jordan, S. R. Kurtz , "Photovoltaic Degradation Rates—an Analytical Review" , Progress in Photovoltaics: Research and Applications Volume 21, Issue 1 , 12–29 , January 2013.
- [5] Weida battery life cycle curve datasheet HXG12-200

# Energy Efficient Utilisation of Solar PV through a DC MicroGrid

Ashan Imantha M.H. Bandara<sup>1</sup>, Prabath J. Binduhewa<sup>2</sup> and Janaka B. Ekanayake<sup>3</sup>

*Department of Electrical and Electronics Engineering, Faculty of Engineering,  
University of Peradeniya, Sri Lanka*

<sup>1</sup> ashanimhb31@gmail.com

<sup>2</sup> prabhath@ee.pdn.ac.lk

<sup>3</sup> jbe@ee.pdn.ac.lk

## Abstract

Adaptation of renewable energy sources, especially Photovoltaic (PV) system, to generate electricity is becoming popular in the world. Among the various technologies, MicroGrid arises as an attractive solution for integrating the renewable energy sources. Even though AC MicroGrids is attractive with present AC network, DC MicroGrids open an efficient platform to integrate sources having natural DC power output. In this study, a DC MicroGrid architecture for commercial buildings with rooftop Photovoltaic was proposed. The proposed architecture is equipped with utility connection and energy storage units in the form of battery and supercapacitor. Power electronic converters are used to integrate different sources and loads. In order to ensure efficient operation, a central controller which can optimise the use of different energy sources and loads is essential. Therefore, an Energy Management System (EMS) was developed to utilize energy distribution within the MicroGrid more efficiently by optimizing power usage and cost associated with the DC MicroGrid. Simulation studies were carried out in PSCAD/EMTDC to investigate the operation of the DC MicroGrid under various operating conditions. Performance of each power converter modules and energy utilization according to EMS are presented in this paper.

**Keywords :** MicroGrid, Solar PV, Renewable Energy, DC MicroGrid, EMS

## Introduction

Demand for electricity increases exponentially in recent years. Currently fossil fuels and coal are used as major conventional energy source to generate electricity. However, the moderate depletion of the fossil fuel reserves due to the excessive usage leads to growing concerns about the security of electricity supply. As a result of burning fossil fuels overly cause more carbon emission which raises alarms about global warming. Thus warranting the security of future energy supply while minimizing the impacts on environment becomes a challenging task. Thus most of the researchers focused towards the utilization of Renewable Energy Sources (RES) such as wind, solar photovoltaic (PV), geothermal and wave energy to generate electricity. But the environmental dependency of RES introduces challenges on the stable operation of the utility networks. Also with current AC networks, RES are interfaced through one or more power conversion stages which reduce the overall efficiency of energy extraction from RES to load.

MicroGrid is a small power system which has its own local generation, energy storages and loads. With the plug and play capability within the MicroGrid, RES can be connected or disconnected seamlessly without changing the structure of the MicroGrid. Due to the unpredictability of RES plug and play capability becomes an attractive feature when connecting RES to the MicroGrid [1]. Moreover MicroGrid can be operated in grid connected mode or autonomously (islanded mode) [2]. During the islanded mode operation in the absence of utility support, in order to maintain the inertia an energy storage is essential for a MicroGrid.

Though AC MicroGrids are widely studied and implemented in the world DC MicroGrid emerges in the recent studies [1]–[3]. Absence of frequency and reactive power makes operation of the dc MicroGrid more easy compare to the ac MicroGrids. On the other hand, in ac-dc power converters are higher compare to the dc-dc power converters. Further dc MicroGrid enables to connect RES and energy storages mostly with dc-dc converters which enhances the overall efficiency of energy utilization compare to ac MicroGrid. Since most of the modern loads are internally dc operated through a dc MicroGrid the preliminary ac-dc conversion stages of loads can be eliminated [4]–[7].

The distribution voltage of a dc MicroGrid be determined by its application. Typically for 24V or 48V selected to domestic or small scale applications. On the other hand, 380V selected for commercial or large scale applications. Distribution is done as either two wire transmission or three wire transmission. Advantage of three wire transmission is the availability of the zero potential pole [6], [8],[9].

Maintaining the power flow while keeping energy balance within the MicroGrid is a challenging task. Hence it is essential to have a good energy management scheme to achieve successful operation [5]. In [10], an ac MicroGrid with EMS was studied. The six operating modes were defined and logic based selection was done to select most appropriate operating condition to schedule the utility power exchange, ESS and renewable energy sources (RES). It uses grid voltage and frequency to define different operating modes. In [11], an EMS application on dc MicroGrid established in an office building was

studied. They used power balance as the decision making variable and tried to optimize the carbon emission through intelligent energy management of the dc MicroGrid. A dc MicroGrid with supervisory control was presented in [12]. In this study, a separate block was implemented as supervisory subsystem which contains four layers. The topmost layer is used to coordinate with user as human machine interface. Then the next three layers together formulated the EMS. The prediction layer used metadata to predict the load and source profiles. Then the energy management layer defined the schedule and operating layer send the commands according to the schedule given by energy management layer. The operating layer again developed as a logic based system.

This paper presents the design and of a dc MicroGrid with and energy management system (EMS). The paper consists of four sections including the introduction. Methodology section presents the design procedure of the proposed dc MicroGrid and its EMS. Case Study section includes the detailed methodology followed for the simulation study carried out in PSCAD/EMTDC software platform. Results, Conclusions and acknowledgements presented in following sections.

## **Methodology**

### **DC MicroGrid topology**

The proposed dc MicroGrid topology consists of four sources and two distribution feeders as shown in Figure 1. These sources and load feeders are integrated to a common dc bus through various power converters. The dc bus voltage of the dc MicroGrid was selected

as 380V. Specifications and other details of the power converters are presented in Table 1. In both grid connected and islanded mode Energy Management System (EMS) of the dc MicroGrid schedules the available sources to achieve reliable operation.

### **Grid connected mode operation**

In grid connected mode, the Converter-A was set to control the dc-link voltage. So it will exchange power between ac utility and dc MicroGrid by keeping constant dc-link voltage. Converter-B was scheduled to operate in the maximum power point tracking mode. So it captures available maximum PV power and supplied to the dc MicroGrid. The Converter-C and Converter-D are operated in power reference mode where battery storage is charged or discharged to deliver long term energy requirement. On the other hand, super capacitor is scheduled to meet rapid power transients. All the power converters are scheduled to minimize the operational cost and aging of energy storage units.

### **Islanded mode operation**

Key concern in Islanded mode operation is make sure to keep MicroGrid operating as maximum as possible. In this mode battery interfacing converter (Converter-C) was allocated to control the dc-link. PV interfacing converter (Converter-B) usually operated in MPPT mode. However, the charge of the storage units are at the maximum level then PV is curtailed to match the supply and demand. On the other hand, if there is not enough charge to deliver critical loads during islanded mode operations the non-critical loads are disconnected to secure the supply.



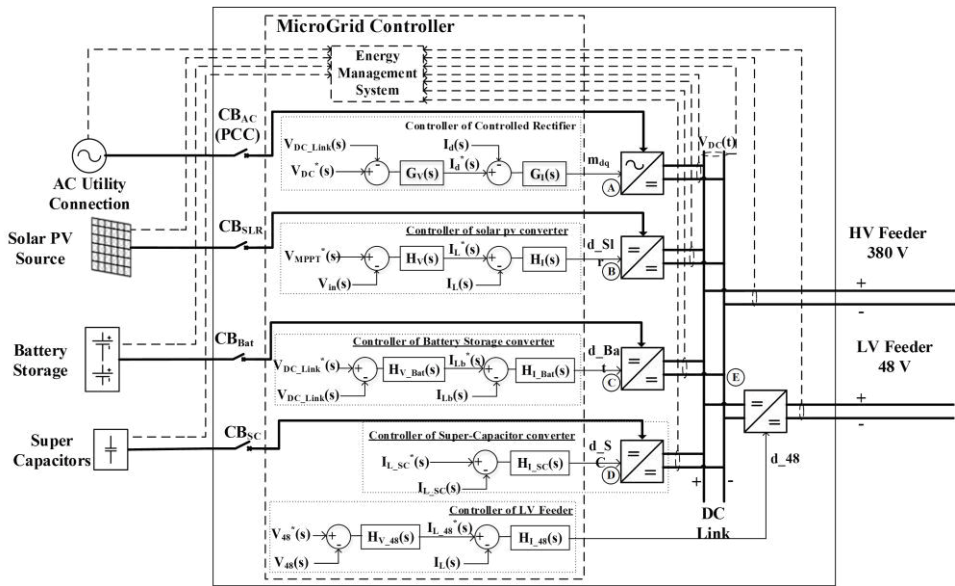


Figure 1: Proposed Topology of the DC MicroGrid

Table 1 Specifications of the Converters.

Converter	Type	Ratings	Purpose	Operation
A	Bi-directional Controlled Rectifier	3 kW	Interfacing converter for ac utility	<ul style="list-style-type: none"> <li>Control the DC Link voltage</li> </ul>
B	DC-DC Step-up (Boost) Converter	2 kW	Interfacing PV source	<ul style="list-style-type: none"> <li>Maximum Power point tracking</li> </ul>
C	Dc-dc Isolated Bi-directional Converter	3 kW	Battery storage Interface	<ul style="list-style-type: none"> <li>Power reference mode</li> <li>DC Link voltage control</li> </ul>
D	DC-DC Isolated Bi-directional Converter	1 kW	Super Capacitor Interface	<ul style="list-style-type: none"> <li>Power reference control to maintain dc link stability.</li> </ul>
F	DC-DC Isolated Step-down Converter	1.5 kW	Low voltage load feeder	<ul style="list-style-type: none"> <li>Output voltage control</li> </ul>
G	Direct Interface	1.5 kW	High voltage load feeder	<ul style="list-style-type: none"> <li>Supply high power loads.</li> </ul>

## Energy management system

The main objective of the EMS is to schedule every energy source while minimizing the overall operational cost. This can be done in several ways. The common practice is to run the optimization algorithm in predefined time intervals separately and deliver the dispatch schedule at the beginning of the next time period. However, this may be prone to prediction errors. Therefore, an EMS was developed using a rule based system. The main objective of the EMS is

to schedule every energy source while minimizing the overall operational cost. This can be done in several ways. The common practice is to run the optimization algorithm in predefined time intervals separately and deliver the dispatch schedule at the beginning of the next time period. However, this may be prone to prediction errors. Therefore in this paper, an EMS was developed using a rule based system and the constraints are developed to optimize the overall operation.

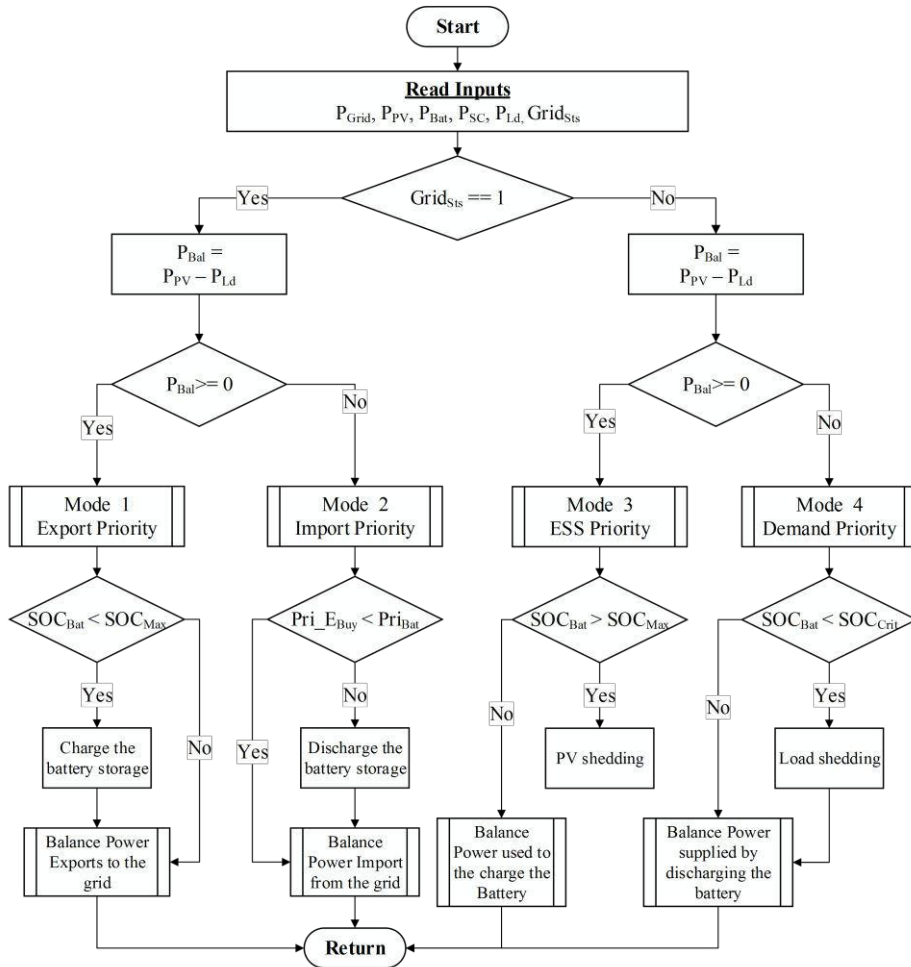


Figure 2: Block Diagram of the EMS

The proposed EMS is presented in Figure 2. First EMS reads current power generation from controlled rectifier ( $P_{Grid}$ ), solar PV ( $P_{PV}$ ), battery storage ( $P_{Bat}$ ), super-capacitor ( $P_{SC}$ ), and demand ( $P_{Ld}$ ). After processing available data, schedule is dispatched with power references to next time period.

There are four operating modes in the proposed EMS. And these modes are selected according to the status of the grid ( $Grid_{Sts}$ ) and Power balance ( $P_{Bal}$ ). The  $Grid_{Sts}$  parameter is evaluated as given in Eq. 1

$$Grid_{Sts} = \begin{cases} 1 \\ 0 \end{cases} \quad \text{Eq. 1}$$

where the grid availability is denoted by logic '1' and islanded mode is denoted by logic '0'.

Similarly power balance is calculated using Eq. 2

$$P_{Bal} = P_{PV} - P_{Ld} \quad \text{Eq. 2}$$

where  $P_{PV}$  is the available solar PV power and  $P_{Ld}$  is the demand.

Four combinations of  $Grid_{Sts}$  and  $P_{Bal}$  is used to select the operating mode and of the EMS MicroGrid. The selection of combinations are given in the Table 2.

### Export priority mode

As presented in Figure 2, if the  $P_{PV}$  is more than the demand EMS has two choices. Either to charge the energy storage or export additional power to the ac utility. The exported power ( $Rf_{Grid}$ ) is calculated as given in Eq. 3

Eq. 3.

$$Rf_{Grid} = P_{Bal} - Rf_{Bat} \quad \text{Eq. 3}$$

The  $Rf_{Bat}$  is the charging power set to battery interfacing converter.

### Import priority mode

When the demand is higher than the PV generation EMS has to select least expensive source to supply the demand. Thus EMS compares the ac utility energy prices and battery unit generation cost ( $C_{Bat}$ ) which is calculated using Eq. 4.

$$C_{Bat} = \frac{\text{Replacement Cost}}{C_r DOD_r (0.9 L_r - 0.1)} \quad \text{Eq. 4}$$

where  $C_r$  is the rated capacity (kWh),  $DOD_r$  is the rated depth of discharge (%) and  $L_r$  is the number of life cycles for the battery storage [13].

If the battery energy cost is cheaper EMS schedules the battery storage to supply the demand. Power balance is as same as in Eq. 3.

### Energy storage (ESS) priority mode

EMS moves to this mode during islanded operation when there is excess PV. The major focus on this mode is to avoid the excessive charging of energy storage units. Thus the EMS compares the state-of-charge of the battery ( $SOC_{Bat}$ ) against the maximum limit ( $SOC_{Max}$ ). If the  $SOC_{Bat}$  is higher than the limit PV is curtailed to avoid over charge and set a power reference to the converter.

The PV power reference was generated as given in Eq. 5

$$Rf_{PV} = P_{Bat} + P_{Ld} \quad \text{Eq. 5}$$

where  $P_{Bat}$  is the output power from battery storage and  $P_{Ld}$  is the demand.

Table 2: Operating Modes of the EMS

Grid Status	Power Balance	Operating Mode
1	>0	Export Priority
1	>0	Import Priority
0	<0	Energy Storage Priority
0	<0	Demand Priority

### Demand Priority Mode

Once the demand is more than PV generation in islanded mode it is essential to secure the supply for critical loads while safeguarding the energy storage units. Thus EMS switches to the demand priority mode.

Primarily battery storage is discharged to deliver required demand till it reaches to its critical level ( $SOCC_{crit}$ ). When the critical level is met, non-critical loads are disconnected in order to maintain the supply for critical loads. The reference power for the loads ( $Rf_{Ld}$ ) is set by using the Eq. 6.

$$Rf_{Ld} = P_{Bat} + P_{PV} \quad \text{Eq. 6}$$

### Case Study

Proposed topology and the EMS presented in Figure 1 and Figure 2 were modeled in PSCAD/EMTDC software package to evaluate the performance of the proposed dc MicroGrid. After that a case studies were conducted to monitor the performance of the dc MicroGrid under different situations.

The load profile for the case study was generated using field measurements taken at the Electronics Laboratory, of the Department of Electrical and Electronic Engineering, University of

Peradeniya. The occupancy of the lab is as followed.

- At 07:30 h – Lab is opened for student and staff
- 09:00 h – 12:00 h – Morning lab classes
- 12:00 h – 14:00 h – Lunch time and day time idle usage of the lab
- 14:00 h – 17:00 h – Evening lab classes
- 17:00 h – 07:30 h (Following Day) – night time Idle usage

Then a time-of-use (TOU) tariff model was adopted as ac utility energy import price. This model was derived using Ceylon Electricity Board TOU tariff scheme. The corresponding data is presented in Table 3.

Battery storage was modeled using data sheet of the Smart Battery SB 100 battery. The  $C_{Bat}$  was calculated as Rs. 27.43/=.

Next the PV profile was generated from the irradiance data measured at the weather station of the rooftop PV plant located in the Department of Electrical and Electronic Engineering, University of Peradeniya. PV-UJ225GA6 manufactured by Mitsubishi Electric was used to model the PV source. For PV generation it was assumed that the sunrise at 06.00 h and sunset at 18.00 h.

Two grid failures were introduced at 8.36 h (restored at 09.12 h) and 11.12 h (restored at 13.18 h) to observe the transition between grid-connected and islanded mode operations.

In the simulation it was assumed that 0.25 sec is equals to 15 min in real time. Thus simulation was carried out for 24 sec period which equals to 24 h in real time.

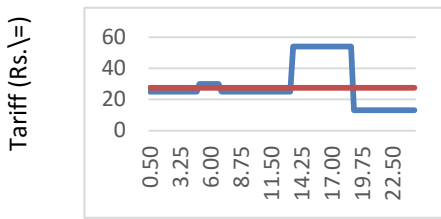
Table 3: Time of Use ac utility tariff

Time (h)	Tariff (Rs./=)
6.00 – 10.30	25.00
10.30 – 12.30	30.00
12.30 – 19.00	25.00
19.00 – 22.00	54.00
22.00 – 6.00 (Next day)	13.00

Results

Figure 3 shows the resulted power profiles of the dc MicroGrid for case study. Figure 3 (a), (b) and (c) present the variation of utility tariff, PV generation and total demand of the MicroGrid.

According to the EMS outputs MicroGrid controller schedules the battery



a. Variation of utility tariff (Blue – Utility Price, Red -  $C_{Bat}$ )



b. Variation of solar PV output power



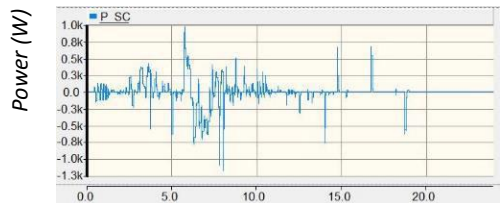
c. Variation of Load



d. Variation of power supplied from controlled rectifier



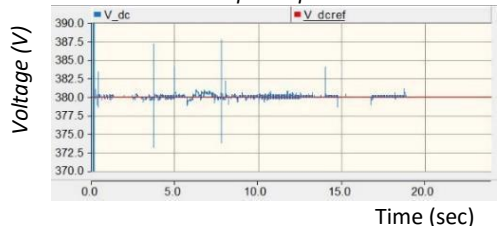
e. Variation of power supplied from battery storage



f. Variation of power supplied from super-capacitor



g. Variation of SOC of the Battery



h. Variation of dc link voltage

Figure 3: Observations for Case Study

interface converter, controlled rectifier and super-capacitor converter. Power supplied from the controlled rectifier, battery storage and super-capacitor are given in Figure 3 (d), (e) and (f). The positive power flow indicates power supplied to the dc MicroGrid by each converter.

Also the Variation of the SOC of the battery storage and the variation of the dc link voltage are presented in Figure 3 (g) and (h) respectively.

By comparing Figure 3 (a), (b) and (c) from 0.5 sec to 5 sec (6.00 h to 10.30 h) it is visible that the demand is more than the PV. Therefore EMS moves to Export priority mode and controlled rectifier is set to export excess power to ac utility.

Due to the grid failure at 3.1 sec (8.36 h) protection system of the MicroGrid disconnected the dc MicroGrid from utility connection and EMS operation switches to islanded operation. Because of PV generation is larger than demand EMS moves to demand priority mode and set battery interface converter to discharging mode. After the grid is restored at 3.7 sec (09:12 h) EMS moves Import priority mode under grid connected operation. From 5 sec to 6.75 sec (10:30 h – 12:15 h) the utility tariff increased more than the battery energy cost. Therefore the battery converter activates and supply majority of required power demand. This variation is visible in Figure 3 (d) and (e)

Conversely another grid failure occurred during this period at 5.7 sec (11.12 h). Therefore again another transition between at EMS modes occurred from grid connected to islanded operation. After 6.75 sec (12:15 h) solar PV generation increases more than the

demand. Hence EMS moves to ESS priority mode and set the battery storage into charging mode. When the grid is restored at 7.8 sec (13.18 h) EMS moves to grid connected operation and switches to import priority mode because PV is more than the demand. Hence the battery interface converter is set to charging mode. However demand increase more than PV after 8.5 sec (14.00 h) and ac utility price is cheaper compare to battery storage cost. Thus battery converter is put into idle and the utility interface converter and the PV converter supplied the demand.

At 13.50 sec (19.00 h) utility tariff increases more than battery unit. Hence the MicroGrid controller sets the controlled rectifier to export power. Moreover EMS schedules the battery interface converter to discharge the battery and support the utility grid during its peak demand. After battery reached to its minimum SOC level this operation stopped at 14.75 sec (20.30 h) and controlled rectifier import power from the ac utility to supply the base load. At 17 sec (22:15 h) the imported power increased because EMS scheduled the battery converter to charge the battery to ready for the next day. This can be observed by comparing Figure 3 (d), (e) and (g).

The super-capacitor is utilized to supply the power deficit and absorb excess by looking at the variation of the dc link voltage. At every instance, it charge and discharge by supplying required power difference. This variation is presented in Figure 3 (f). Moreover the stresses on the converter controls the dc link voltage is reduced. And the dc link voltage become more stable. Variation of dc link voltage is presented in Figure 3 (h).

## Conclusions

The overall energy management of the MicroGrid was successfully implemented with the EMS. With the proposed EMS scheme the system was capable of handling the power sharing according to the demand and generation within the dc MicroGrid. The MicroGrid controller ensured the safe operation of the MicroGrid according to the dispatch schedules provided by the EMS.

Operation of the MicroGrid under all four modes of the EMS was studied. When there is excess power, MicroGrid operator has the opportunity to utilize its energy storage within the MicroGrid or export it to the utility. On the other hand when there is power shortage MicroGrid controller import power from the ac utility to keep the power balance in more cost effective manner. Transition of the controls between grid connection and islanding operations and power sharing between each converter and loads was done seamlessly. Further MicroGrid controllers handle the power set points according to the schedule dispatched by the EMS. The super-capacitor interface converter operation helps to minimize the dc link ripple. Also during islanding, it provides the inertia support to the MicroGrid to avoid the collapse.

## Acknowledgements

Authors would like to acknowledge Sustainable Energy Authority of Sri Lanka and providing financial support for this project.

## Reference

- [1] R. H. Lasseter, "MicroGrids," in 2002 IEEE Power Engineering Society Winter Meeting. Conference Proceedings (Cat. No.02CH37309), 2002, vol. 1, pp. 305–308 vol.1.
- [2] T. Dragičević, X. Lu, J. C. Vasquez, and J. M. Guerrero, "DC Microgrids—Part II: A Review of Power Architectures, Applications, and Standardization Issues," IEEE Trans. Power Electron., vol. 31, pp. 3528–3549, May 2016.
- [3] P. . Loh, D. Li, Y. K. Chai, and F. Blaabjerg, "Hybrid AC-DC Microgrids with Energy Storages and Progressive Energy Flow Tuning," IEEE Trans. Power Electron., vol. 28, no. 4, pp. 1533–1543, 2013.
- [4] D. Cheng, L. Xu, and L. Yao, "DC Voltage variation based Autonomous Control of DC Microgrids," IEEE Trans. Power Deliv., vol. 28, no. 2, pp. 637–648, 2013.
- [5] L. Che and M. Shahidehpour, "DC Microgrids: Economic Operation and Enhancement of Resilience by Hierarchical Control," IEEE Trans. Smart Grid, vol. 5, no. 5, pp. 2517–2526, Sep. 2014.
- [6] A. T. Ghareeb, A. A. Mohamed, and O. A. Mohammed, "DC microgrids and distribution systems: An overview," IEEE Power & Energy Society General Meeting, 2013, pp. 1–5.
- [7] J. M. Guerrero, J. C. Vasquez, J. Matas, L. G. de Vicuna, and M. Castilla, "Hierarchical Control of Droop-Controlled AC and DC Microgrids—A General Approach Toward Standardization," IEEE Trans. Ind. Electron., vol. 58, no. 1, pp. 158–172, Jan. 2011.

- [8] D. Ricchiuto, R. A. Mastromauro, M. Liserre, I. Trintis, and S. Munk-Nielsen, "Overview of multi-DC-bus solutions for DC microgrids," in 2013 4th IEEE International Symposium on Power Electronics for Distributed Generation Systems (PEDG), 2013, pp. 1–8.
- [9] D. J. Becker and B. J. Sonnenberg, "DC microgrids in buildings and data centers," in 2011 IEEE 33rd International Telecommunications Energy Conference (INTELEC), 2011, pp. 1–7.
- [10] N. Korada and M. K. Mishra, "Grid Adaptive Power Management Strategy for an Integrated Microgrid With Hybrid Energy Storage," *IEEE Trans. Ind. Electron.*, vol. 64, no. 4, pp. 2884–2892, Apr. 2017.
- [11] K. Shimomachi, R. Hara, H. Kita, M. Noritake, H. Hoshi, and K. Hirose, "Development of energy management system for DC microgrid for office building:-Day Ahead operation scheduling considering weather scenarios-," in 2014 Power Systems Computation Conference, 2014, pp. 1–6.
- [12] B. Wang, M. Sechilariu, and F. Locment, "Intelligent DC microgrid with smart grid communications: Control strategy consideration and design," *IEEE Power & Energy Society General Meeting*, 2013
- [13] T. A. Nguyen and M. L. Crow, "Stochastic Optimization of Renewable-Based Microgrid Operation Incorporating Battery Operating Cost," *IEEE Trans. Power Syst.*, vol. 31, no. 3, pp. 2289–2296, May 2016.



# Smart Distribution Transformer for Frequency Support

R. R. L. L. Wijayaratne <sup>#1</sup>, P. J. Binduhewa <sup>\*2</sup>, S. G. Abeyratne <sup>\*3</sup> J. B. Ekanayake <sup>\*4</sup>, M. J. M. N. Marikkar <sup>#5</sup>, D. A. J. Nanayakkara <sup>#6</sup>

<sup>#</sup> *LTL Transformers (Pvt) Ltd*  
*Sri Lanka*

<sup>1</sup> lochana.wijayaratne@ltl.lk  
<sup>5</sup> marikkar@ltl.lk  
<sup>6</sup> dammika@ltl.lk

<sup>\*</sup> *Department of Electrical and Electronic Engineering*  
*University of Peradeniya, Peradeniya, Sri Lanka*

<sup>2</sup> prabhathb@ee.pdn.ac.lk  
<sup>3</sup> sunil@ee.pdn.ac.lk  
<sup>4</sup> jbe@ee.pdn.ac.lk

## Abstract

Distribution transformer is one of the major equipment in the distribution network which provides the final voltage transformation. As per the standards, voltage in the distribution lines should be maintained within  $\pm 6\%$  of rated voltage whereas the grid frequency should be maintained within  $\pm 1\%$  of rated frequency. However with the integration of renewable energy sources and loads such as electric vehicles, it has become a challenge to maintain both voltage and frequency within statutory limits with the conventional approaches. As a result, utilities are trying to introduce expensive grid reinforcement measures. In order to address the above issues, an electronically controlled transformer embedded with active voltage regulation and demand management mechanism is investigated. The demand management method is based on the Conservation Voltage Reduction (CVR). A single busbar model available in the literature was modified to match with the Sri Lankan power system. Then it was further modified to integrate the effect of CVR enabled loads. Different case studies were conducted based on a real time frequency response curve to analyze the effectiveness of adding CVR. The results showed that the stability of the system was improved when renewable energy systems were integrated into the network.

**Keywords:** Conservation voltage reduction; Active Voltage Regulation; Demand side management; Transformer; Serial Injection

## Introduction

CVR is a concept which is practiced by many utilities to reduce electrical demand and/or energy consumption over time. It is a derivative of the voltage reduction that has been a long term practice to reduce the load under emergency situations [1], [2]. It works on the principle that the customer end point voltages are kept more towards the lower half of the acceptable voltage range (i.e. 216 V to 230 V) without harming customer appliances [3]. References [4], [5] and [6] present a real time analysis done to investigate the effectiveness of CVR on energy consumption tested for different feeders. Further the results obtained in [5] shows that CVR is much more effective than other conventional demand side management measures in reducing the system peak load.

In this paper, the single busbar model explained in reference [7] was modified to match with the Sri Lankan power system and it was further modified to integrate the effect of CVR enabled loads. To analyze the effectiveness of adding CVR to the system, two different case studies were conducted based on a real time frequency event obtained from Ceylon Electricity Board (CEB). As explained before CVR is a derivative of voltage reduction. Basically for constant impedance and constant current loads their power consumption reduces with the reduction of voltage. Among these two types of loads, constant impedance loads have a large contribution for CVR as the power drawn decreases with the voltage squared [3]. Therefore the effect of CVR was calculated giving priority to constant impedance loads.

## Simulation Study

### Single Busbar model

In order to implement the single busbar model, a frequency event occurred in Sri Lanka on 02/09/2015 at 15.49 hrs was considered. This was caused by a sudden tripping of generator at Lakvijaya power station. The corresponding frequency response curve is shown in Fig 2. As per the response, generator supplying 210 MW to the system with the total load of 1,422 MW has suddenly stopped thus causing sudden frequency reduction. With the help of under frequency load shedding at 48.75 Hz and 48.5 Hz and from secondary frequency responses, the system has regained the frequency within 30 minutes. First the single busbar model [7] shown in Fig. 1 was tuned to match with the above mentioned frequency response.

The main parameters of the single busbar model were calculated using the data obtained from CEB corresponding to the frequency event and given in Table 1.

*Table 1 : Model Parameters*

Parameter	Value
Heq	5
G	4.1
D	1%

### CEB load shedding criteria

The present load shedding criteria used by the CEB is given in Table 2. As it demonstrates, these are designed in different stages to minimize the possible frequency overshoot and inconvenience to the public.

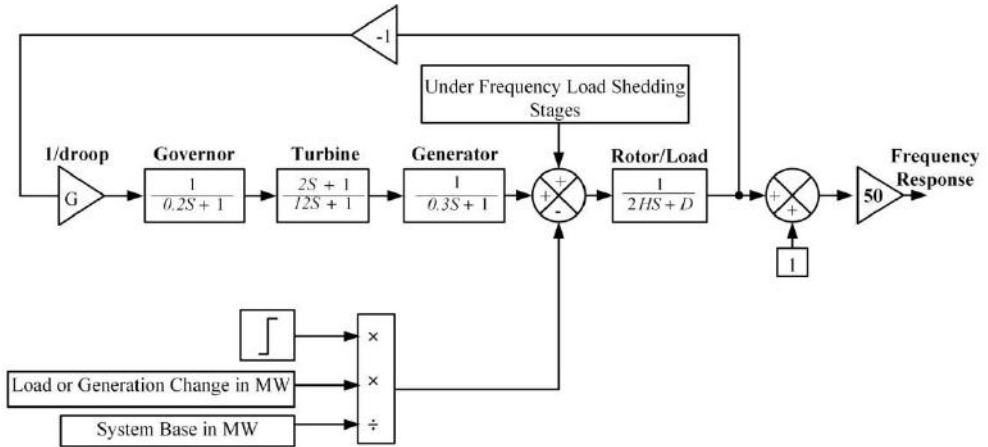


Figure 1: Single busbar model integrated with CEB under frequency load shedding scheme

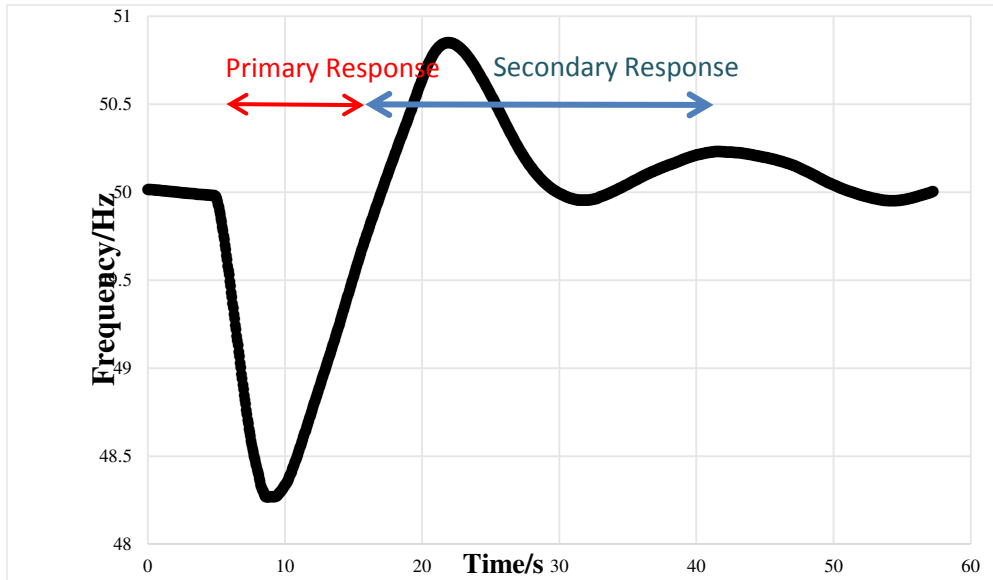


Figure 2: Frequency Response corresponding to the incident on 09/02/2015 with primary and secondary response

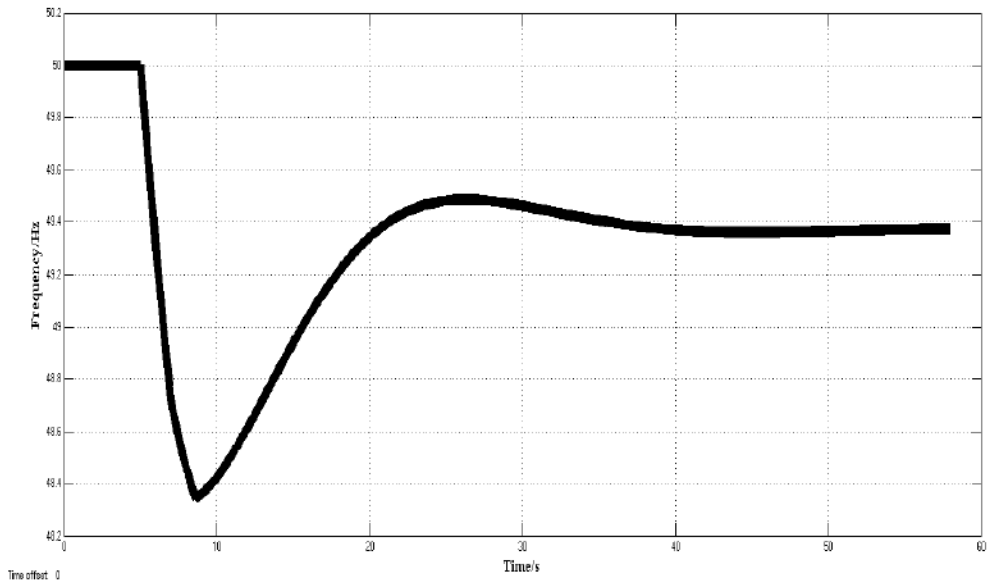


Figure 3: Frequency response of the modified model with two stage UFLS

Table 2 : CEB Load shedding criteria

Frequency State	Time Delay and % of load to be shed
$f \geq 48.75$ Hz	No load shed
$f < 48.75$ Hz	Stage I: 7.5% of load 100 ms time delay
$f < 48.5$ Hz	Step II: 7.5% of load 500 ms time delay
$f < 48.25$ Hz	Step III: 11% of load 500 ms time delay
$f < 48$ Hz	Step IV: 11% of load 500 ms time delay
$f < 47.5$ Hz	Step V: 5.5% load instantaneous
$f < 49$ Hz	4.5% +13.5% of load, 100 ms time delay

### Model Validation

Fig. 2 and Fig. 3 show the actual frequency response curve and the frequency response obtained from the Simulink® single busbar model. The primary response which occurs from 0 to 15s is marked in the actual response. This portion is compared with the simulated result. This is because only the primary response is implemented in the Simulink® model.

According to the frequency response curve in Fig. 2, the generator tripped at 5.25s and the lowest frequency point occurred at 8.15s. Similarly in the simulation model, a sudden reduction of 210 MW was considered at 5.25 s and UFLS I and II were applied for 48.75 Hz and 48.5 Hz. A comparison of the obtained responses from 0-15 s is given in Table 3.

Table 3 : Summarized results for frequency responses given in Fig. 2 and 3

	<b>Actual frequency response in Fig. 2</b>	<b>Simulation generated frequency response in Fig. 3</b>
<b>Time to <math>f_{min}</math></b>	8.85 s	8.6 s
<b><math>f_{min}</math></b>	48.27	48.34 Hz
<b>df/dt</b>	-0.468	-0.469
<b>UFLS Stages</b>	I and II	I and II(4.5% and 4%)

By observing the values given in Table 3, it can be seen that both responses have almost equal values for  $f_{min}$ , time for  $f_{min}$  and df/dt. This validated the Simulink® model developed. Therefore the simulation model shown in Fig 1 was used for further studies to analyze the CVR effect on the power system.

### Effect of CVR during Frequency Excursion

#### Case Study 1: CVR and No load Shedding

In this case load shedding schemes were removed from the system such that only the effect of CVR is taken into account. The CVR effect is considered for system frequencies from just below 50 Hz to 47.5 Hz. Therefore the maximum frequency deviation with respect to the nominal system frequency is 2.5 Hz. The maximum possible reduction in load due to CVR is calculated as follows:

Power reduction due to CVR;

$$= \left( \begin{matrix} \text{CVR contributed} \\ \text{load \%} \end{matrix} \right) * \left( \begin{matrix} \text{Total} \\ \text{Load} \end{matrix} \right) * \left( \begin{matrix} \text{Percentage of power reduction} \\ \text{due to customer end point voltage} \\ \text{lowered by 6\%} \\ \text{from nominal value} \end{matrix} \right)$$

Percentage of power reduction due to lowering the customer end point voltage

$$= \frac{\left( \begin{matrix} \text{Initial} \\ \text{Power} \\ \text{Consumption} \end{matrix} \right) - \left( \begin{matrix} \text{Later Power} \\ \text{Consumption} \\ \text{with CVR} \end{matrix} \right)}{\left( \begin{matrix} \text{Initial} \\ \text{Power} \\ \text{Consumption} \end{matrix} \right)} \times 100\%$$

$$= \frac{\left( \frac{V^2}{R} \right) - \left( \frac{(V * 0.94)^2}{R} \right)}{\left( \frac{V^2}{R} \right)} \times 100\%$$

$$= 11.64\%$$

Therefore the CVR gain was chosen as 0.1164/2.5. Fig. 4 shows the single busbar model integrated with CVR without load shedding scheme. Frequency responses for five different CVR contributed loads were considered. Black colored frequency response in Fig. 5 demonstrates an incident without both CVR and UFLS. Other responses are for different CVR contributed loads. The results are summarized in Table 4.

By observing the frequency response curve given in Fig. 5, with minimum CVR contributions (20%), the system has regained from the under frequency within less than 15 minutes. And the obtained minimum system frequency is 47.75 Hz. Similarly when there are 100% of CVR loads, the system frequency does not decrease beyond 48.5 Hz. Therefore these results show that the responses with CVR contribution have much better performance compared to the system without CVR.

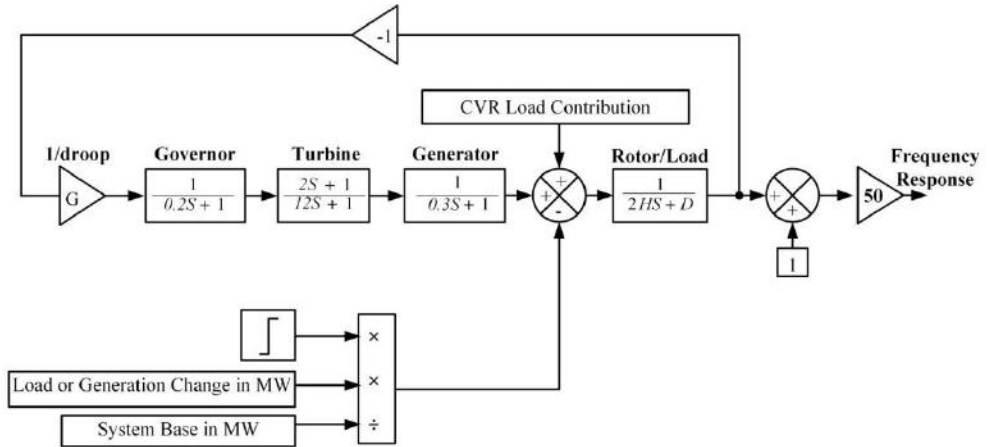


Figure 4: Single busbar model with CVR

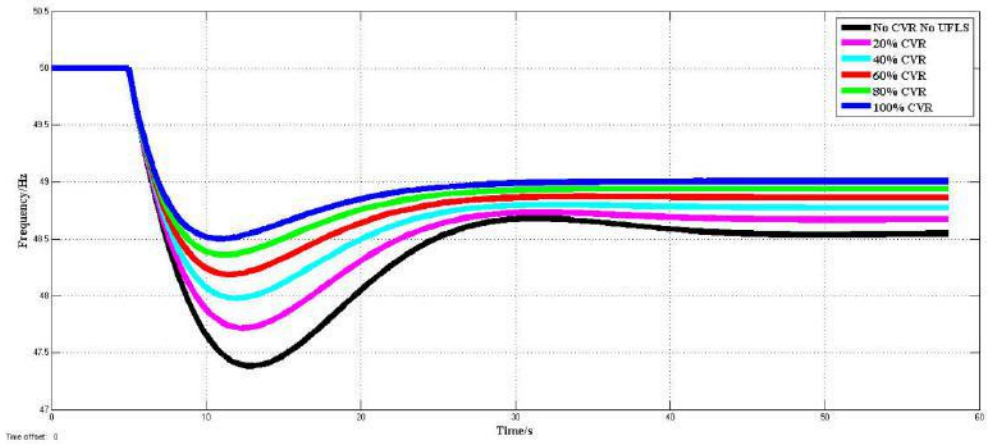


Figure 5: Frequency responses for different CVR load contributions

Table 4: Summarized results for the case study with CVR

CVR contributed loads/%	df/dt	f <sub>min</sub>
0	-0.590	47.37
20	-0.517	47.75
40	-0.449	48.13
60	-0.39	48.29
80	-0.339	48.5
100	-0.294	48.62

### Case Study 2: CVR and Under Frequency Load Shedding

In this case both load shedding scheme and CVR contribution were considered. But compared to the previous case study CVR effect was considered for system frequencies from just below 50 Hz to 48.75 Hz. The lower frequency limit was chosen by considering the fact that the load shedding starts at this point. Therefore the CVR load contribution changes thus the CVR gain block was modified as (0.1164/1.25). So the maximum power reduction due to CVR takes place at 48.75 Hz. Fig. 6 shows the single busbar model integrated with CVR and load shedding. The frequency responses obtained for five

different CVR contributed loads were plotted and given in Fig. 7.

By observing the frequency response given in Fig. 7, the results are summarized in Table 5. The black coloured frequency response curve represents the incident with UFLS and without CVR. And all the other cases were created such that they have both UFLS and CVR contribution.

Table 5 : Summarized results for the case study with CVR

CVR %	df/dt	f <sub>min</sub> /Hz	UFLS schemes with load shed %
0	-0.490	48.30	I & II (4.5% & 2.5%)
20	-0.468	48.42	I & II (4.5% & 2.5%)
40	-0.451	48.44	I & II (4.5% & 2.5%)
60	-0.426	48.46	I & II (4.5% & 2.5%)
80	-0.239	48.8	Not applied
100	-0.194	48.95	Not applied

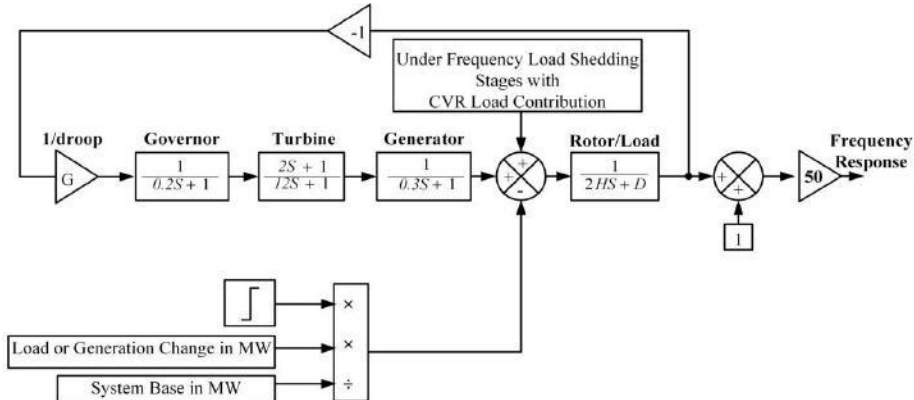


Figure 6: Simulink® modelled single busbar model with CVR and UFLS

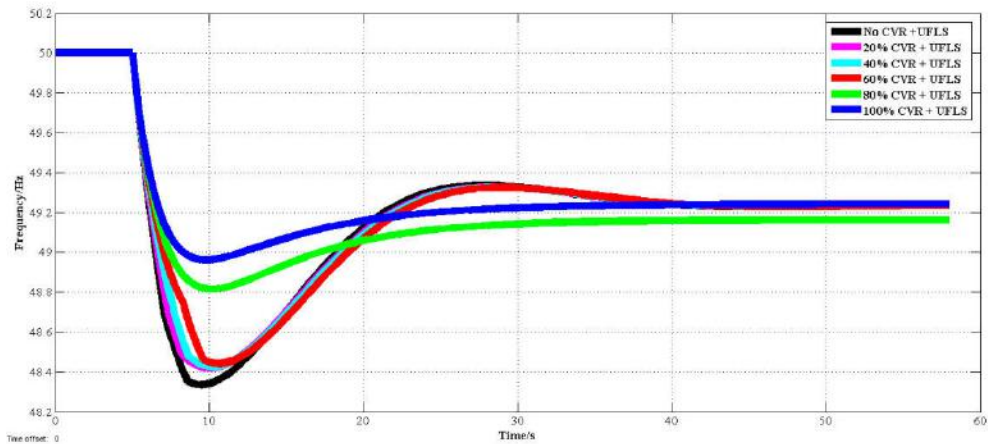


Figure 7: Frequency responses for different CVR contributions and UFLS

## Conclusions

By comparing the results obtained for case studies 1 with 2, it is clear that when CVR is used with load shedding it gives better frequency regulation after a frequency event. Also compared to the base case, UFLS stage two has been reduced by 1.5% (from 4% to 2.5%) which is an indication of improved system availability.

Therefore it is clear that if this concept is properly implemented in the distribution transformer, it will help to add more renewable energy sources to the power system.

## Acknowledgements

The authors would like to acknowledge the financial support provided by the International Research Center (InRC) of University of Peradeniya and the financial and technical contribution of the LTL Transformers (Pvt) Ltd, Sri Lanka.

## References

- [1] B. R. Scalley and D. G. Kasten, "The Effects of Distribution Voltage Reduction on Power and Energy Consumption," *IEEE Trans. Educ.*, vol. 24, no. 3, pp. 210–216, Aug. 1981.
- [2] "Evaluation of Conservation Voltage Reduction (CVR) on a National Level | <http://cleanenergysolutions.org>." [Online]. Available: <https://cleanenergysolutions.org/content/evaluation-conservation-voltage-reduction-cvr-national-level>. [Accessed: 24-May-2014].
- [3] R. W. Uluski, "VVC in the Smart Grid era," in *2010 IEEE Power and Energy Society General Meeting*, 2010, pp. 1–7.
- [4] D. Kirshner, "Implementation of conservation voltage reduction at Commonwealth Edison," *IEEE Trans. Power Syst.*, vol. 5, no. 4, pp. 1178–1182, Nov. 1990.
- [5] J. G. De Steese, J. E. Englin, and R. D. Sands, "Conservation Voltage Reduction Potential In The Pacific Northwest," in *Energy Conversion*



- Engineering Conference, 1990. IECEC-90. Proceedings of the 25th Intersociety, 1990, vol. 4, pp. 43–47.*
- [6] B. W. Kennedy and R. H. Fletcher, “Conservation voltage reduction (CVR) at Snohomish County PUD,” *IEEE Trans. Power Syst.*, vol. 6, no. 3, pp. 986–998, Aug. 1991.
- [7] Thomas Bopp, “Technical and commercial integration of distributed and renewable energy sources into existing electricity networks,” PhD Thesis, The University of Manchester, 2006.

# Proposal of a Novel Method to Determine the Required Storage for Photovoltaic Systems to Create Virtual inertia

B.Mayanthi Wathsala P. Gunarathna , I.A. Premaratne

*Department of Electrical and Computer Engineering, the Open University of Sri Lanka  
Nawala, Nugegoda, Sri Lanka*

<sup>1</sup> mwathsala2@gmail.com

<sup>2</sup> iapre@ou.ac.lk

## Abstract

Photovoltaic power generating systems are now becoming a popular method in harvesting renewable energy. Unlike rotating machines, photovoltaic generation does not have stored kinetic energy and thereby provides no inertia which is essential to maintain the stability of power systems. With increasing number of photovoltaic generators, maintaining the stability of power system becomes difficult. As a solution, storage can be used to discharge power during unstable period and thereby create virtual inertia. The determination of the optimum storage that is sufficient to create virtual inertia for a distribution area which has installed large number of photovoltaic systems, is important in such cases. This research proposes a novel method to calculate the capacity of battery or a combination of battery and super capacitor system, required to maintain a virtual inertia. This paper reviews existing methods on improvement of virtual inertia by using different methods such as DC-link capacitors and installing traditional generators parallel to photovoltaic generators to build up inertia. The maximum deviations in output power of photovoltaic over irradiation are considered by analyzing solar irradiation pattern in Sri Lanka. Storage devices and photovoltaic systems are dynamically modeled for a transient analysis using software. With the verification of results, the optimum capacity of storage can be calculated using the proposed function.

**Keywords:** Photovoltaic system, virtual inertia, storage devices, irradiation, Temperature

## Introduction

The concept of generating power using renewable sources, especially solar is more famous among people because of the very first impression of using solar cells is more advantageous for consumers. That means solar power is a renewable source, especially as it is free of charge, no cost of maintenance, the amount of generated power from home is enough to doing general things and extra power can be sold to service provider. As the construction cost is a bit high for a normal family, banks provide loan facilities to set up solar power at homes. Because of the inertia constant of renewable sources is not in sufficient value, generating power using renewable source is not profitable from the utility point of view. Therefore gas turbine should be in standby mode to improve system stability.

The inertia constant (H) of the synchronous machines does not widely vary from machine to machine which is occurred with stored kinetic energy on rotor blades relating to speed of the rotor. The kinetic energy is absorbed into grid or discharged from grid by synchronous machines when the frequency fluctuates. And also the frequency of the grid can be instantly changed by the lower system inertia. Therefore, there should be sufficient inertia to control frequency. When consider solar or wind, there are no stored kinetic energy hence there is no any initial response related to frequency and it can be directly affected to power system stability.

## Material and Methods

### Existing systems

There are few existing systems used in all over the globe to provide virtual inertia constant to the system. However, this technology is not yet practiced in Sri Lanka since this is the beginning of generating electricity by using solar energy than in the past. The virtual inertia can be provided by using the DC-Link capacitors [1] which should be large enough to cover large disturbance that may occur on the grid, installing traditional generators parallel to photovoltaic generators to build up inertia. There are few small diesel generators in Kelanittissa power plant which can be used for this purpose but this method is not cost effective and the virtual inertia emulation through storage [2].

### Theoretical background

#### Inertia constant (H)

The system inertia is one of the vital system parameters upon which the synchronized operation of current day power system is based. The inertia constant of the rotating machine can be defined as the time (seconds) taken to change current rotating speed of machine or in other words, the time taken to release stored kinetic energy in rotating mass. It can be fined by using second order swing equation as below. According to the equation (1), the inertia constant is directly proportional to the system frequency. [3]

$$\frac{GH}{\pi f} \times \frac{d^2\delta}{dt^2} = P_m - P_e \quad MW \dots (1)$$

Where,

G = the MVA rating of the machine (MVA)

- H = the inertia constant (S)
- F = frequency (Hz)
- $P_m$  = mechanical power (W)
- $P_e$  = electrical power (W)

Inertia constant can also be defined as below (equation 2), the kinetic energy per apparent power unit.

$$H = \frac{\text{stored kinetic energy at synchronus speed}}{\text{machine rating in MVA}} \dots\dots (2)$$

Provide the quality supply is the responsibility of the utility. Therefore the system stability always should be maintained. The system instability can be occurred due to imbalances between generation and demand. If the generated power is higher than the demand, the frequency is increased than 50 Hz. The frequency is decreased than 50 Hz when the generated power is lower than demand. The frequency stability issues are normally occurred with inadequacies in equipment responses, poor coordination of control and protection equipment or insufficient generation reserve.

**Storage**

According to the Brian Silveti report [4], there are few fundamental characteristics of energy storage technologies when addressing electric grid problems without considering their cost. Frist one is how quickly the storage device can respond to a grid disturbance. Other one is how long the device continues to discharge at a particular level of power (kW).

There are only two types of storages that can be used to fulfill these project objectives which are battery energy storage and supper capacitor energy

storage since other types of storages such as pump hydro energy storage, compressed air storage [5], [6] cannot be installed everywhere. It should have large area and suitable environmental factors to install such a plant. Compared to them, battery and super capacitor type energy storages have the facility to install anywhere. It can be expensive but it has considerable efficiency, charge discharge rate and capacity of storage. Actually capacity of super capacitor is lower than battery energy storage but has higher charge discharge rate.

Super capacitor is also called as electrochemical Double-layer capacitor or ultra-capacitor which can store energy and release electrical energy which is similar with electrochemical cell. It requires short charging time and it can deliver high power density but lower energy density than electrochemical cell. The life cycle is unlimited and operating temperature range is very wide. [7]

**Photovoltaic cell**

The panel of photovoltaic is designed to following circuit by using the equations mentioned under the equivalent circuited. [8]

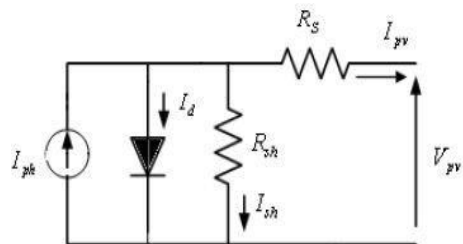


Figure 1: Equivalent circuit for a PV panel

Where;

- $I_{pv}$  = current flow through the output (A)
- $I_{ph}$  = light current (photon current source) (A)

- $I_d$  = current flow through diode (reverse saturation current) (A)
- $I_{sh}$  = current flow through the shunt resistor ( $R_{sh}$ ) (A)
- $R_s$  = series resistance ( $\Omega$ )
- $R_{sh}$  = shunt resistance ( $\Omega$ )
- $V_{pv}$  = output voltage (V)

By using Kirchoff's current law,

$$I_{pv} = I_{ph} - I_d - I_{sh} \quad \dots\dots\dots(3)$$

Diode current is ( $I_d$ );

$$I_d = I_r \left( e^{\frac{q(V_{pv} + R_s I_{pv})}{kA(T_r - T)}} \right) \times \left( \frac{T}{T_r} \right)^3 \quad \dots\dots (4)$$

$$I_r = \frac{I_s}{\left[ e^{\frac{qV_{oc}}{kN_s A T_r - 1}} \right]} \quad \dots\dots (5)$$

$$I_{ph} = \left[ I_s + (K_i \times (T_r - T)) \right] \times \frac{S}{1000} \quad \dots\dots(6)$$

$$I_{sh} = \frac{V_{pv} + I_{pv} R_s}{R_{sh}} \quad \dots\dots (7)$$

From substitute above four equations to

$$I_{pv};$$

$$I_{pv} = N_p I_{ph} - N_p I_d \left( e^{\frac{q(V_{pv} + R_s I_{pv})}{kA T}} - 1 \right) - \frac{V_{pv} + I_{pv} R_s}{R_{sh}} \quad \dots\dots(8)$$

**Detailed explanation of the proposed System**

The actual output of this project will be a function which can use to calculate sufficient capacity of storage, required to maintain a virtual inertia.

The irradiation, atmospheric temperature, number of panels and its specifications for a system, number of investors and its efficiency, and storage

efficiency are the variables that use in this function. The total output of the panel is depended on irradiation and temperature. But most responsible factor is the irradiation. The function can be evaluated by using simulation.

When modeled photovoltaic array, the specification of the panel for 320W is used and solar irradiation and temperature variation during day are collected from department of metrology. By using minimum and maximum temperature during a day, few days were selected and output of the panel was simulated and outputs were observed with varying some parameters.

When calculate total storage, maximum power output of the panels should be considered at highest irradiation because of it is the largest difficulty that can be occurred with the failure of the generating solar power. Also maximum inefficiency of the storage and maximum inefficiency of inverter will be used for function.

**Function**

The design of the overall system will be a function for total storage (Z) as below;

$$Z = \left[ [(I_{mpp} \times V_{mpp}) \times N_p \times \eta_{I(u)}] \times (2 - \eta_{I(s)}) \times (2 - \eta_s) \right] \times H \quad \dots\dots (9)$$

Where;

$$I_{mpp} = \frac{G}{1000} \times [Isc(STC) + \Delta Isc(25 - T) \times Isc(STC)]$$

$$V_{mpp} = Voc(STC) + [\Delta Voc(25 - T)] \times Voc(STC)$$

- H = Inertia (s)
- $N_p$  = number of panels
- $\eta_{I(u)}$  = inverter efficiency of unit

$\eta_{I(s)}$  = inverter efficiency of storage  
 $\eta_s$  = efficiency of storage  
 $I_{mpp}$  = output current at maximum power point (A)  
 $V_{mpp}$  = voltage at maximum power point (V)  
 $G$  = irradiation ( $W/m^2$ )  
 $T$  = Temperature ( $^{\circ}C$ )

Therefore inputs or variables of proposed function will be;

- Number of panel ( $N_p$ )
- Number of investors and its efficiency

This function can be used to calculate total storage that needs to recover the output of AC power that releases to the system.

But this overall system can be completed with panels which has different specifications. That means panel capacities can be change from unit to

When consider invertors that connected to overall system, inverter near the storage ( $\eta_{I(s)}$ ) should be considering separately due to its inefficiency also should add to capacity of the total storage. Inverter efficiency ( $\eta_{I(u)}$ ) near the PV panel is only considered to get real value of AC supply to the system.

- Efficiency of storage ( $\eta_s$ )
- Irradiation ( $G$ )
- Temperature ( $T$ )

units (domestic units). At this condition above mentioned equation (9) should be modified as below (equation 10)

$$Z = \sum_{i=0}^{\infty} [(I_{mpp} \times V_{mpp}) \times N_p \times \eta_{I(u)}]_i [(2 - \eta_{I(s)}) \times (2 - \eta_s)] H \dots (10)$$

Where;  $i$ =number of units ( $i=1, 2, 3\dots$ )

$$Z = \sum_{i=0}^{\infty} [(I_{mpp} \times V_{mpp}) \times N_p \times \eta_{I(u)}]_i [(2 - \eta_{I(s)}) \times (2 - \eta_s)] H$$

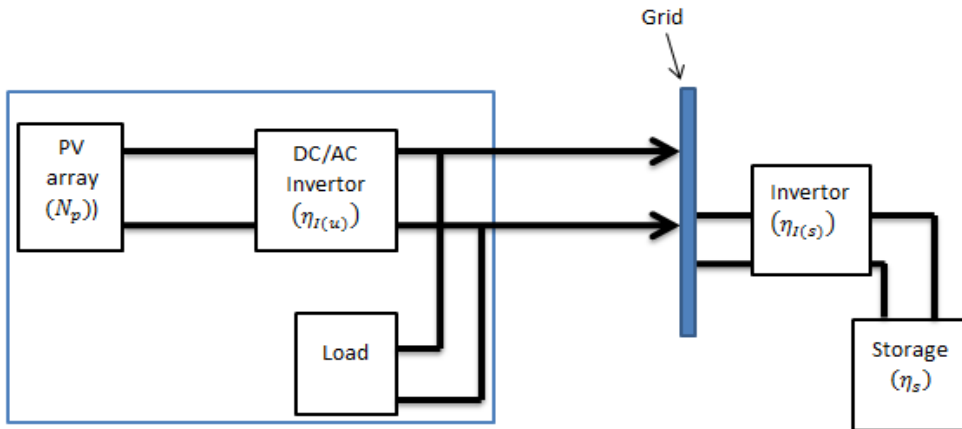


Figure 2: Block diagram for sample system

## Results

According to analysis of data collected from Department of Meteorology, maximum irradiation does not always appear with the maximum temperature. Moreover, at normal weather conditions considerable amount of irradiation can be received during eight hours per day.

The variation of irradiation is highly affected to output current and temperature is not much affected to output current by comparing irradiation. But output voltage is varied with temperature which is not depended on irradiation.

### Solar panel specifications;

- Open circuit voltage (Voc) : 45.8V
- Short circuit current (Ish) : 9.10A
- Voltage at Pmax (Vmp) : 37.1V
- Current at Pmax (Imp) : 8.63A
- Maximum power (Pmax) : 320W

Variation of current, voltage and power with irradiancies of 1,000 W/m<sup>2</sup> at constant temperature (25°C) is shown on figure 3. This is simulated to get proper idea of behaves of series resistance (R<sub>s</sub>) and with proper value of R<sub>s</sub>, panel output is nearly equal with panel specification. According to panel specifications, current at maximum power point (Imp<sub>pp</sub>) should be equal to 8.63A and voltage at the maximum power point is equal to 37.1V at the standard test conditions.

Variation of current, voltage and output power with variation of Irradiation and Temperature is shown on below

attached figure (figure 3) which was obtained from simulation.

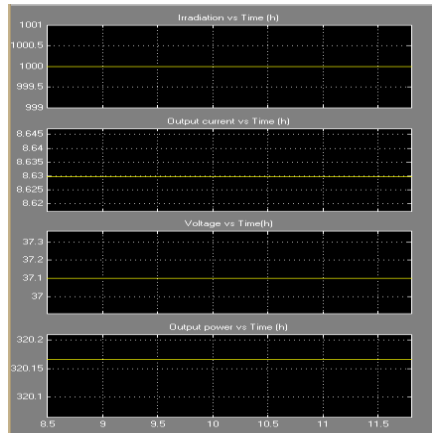


Figure 3: Simulation result for a 320W PV panel at standard condition

Table 1: Irradiation and Temperature variation for 28/04/2016

Time	Irradiation (MJ/m <sup>2</sup> )	Temperature (°C)
5-6	-	26.9
6-7	0.25	27.2
7-8	1.08	29.3
8-9	1.8	31.1
9-10	2.63	32.6
10-11	2.56	33
11-12	2.59	32.7
12-13	3.55	33.2
13-14	3.25	33.1
14-15	2.67	33.1
15-16	2	32.9
16-17	1.23	32.5
17-18	0.35	31
18-19	0.02	29.9
19-20	-	29.5

According to manual calculation of  $(V_{oc})_{mpp}$ , it is varied around 37 and 38V. Therefore variation of  $V_o$  is consider as between 35 to 39.5V. Data obtained on 28/04/2016 were considered.

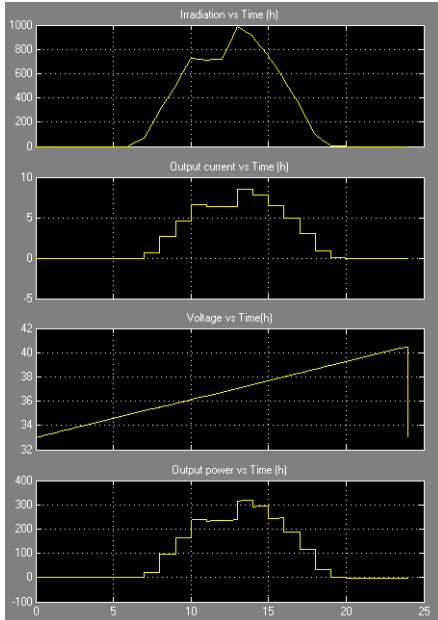


Figure 4: Simulation result for a 320W PV panel with Irradiation and Temperature variation

The direct drop of the output power of panel with inputs can be identified from above attached simulation results. Considering maximum power output of the day, the required total storage can be calculated as below by using proposed function with 90% of efficiency of invertors (near storage and unit), 95% of storage efficiency and 4s of inertia. The variation of storage with respect to temperature and irradiation are attached below. When input temperature variation to the function, average temperature was used. This graph was plotted using proposed equation with irradiation and temperature data at 28/04/2016.

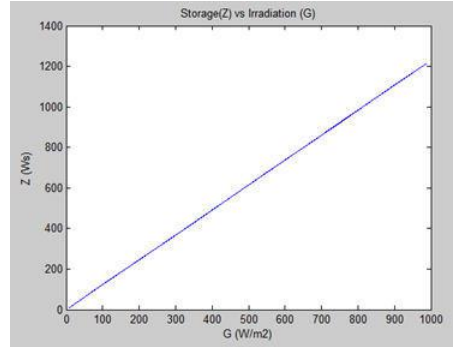


Figure 5: The storage requirement over variation of Irradiation

According to figure 5, the total storage requirement is highly varied with respect to variation of Irradiation.

## Discussions

When calculate total storage for system it is done at the start. The existing capacities of solar panel at the start can be changed on owner's opinion. The number of solar panels installed in household will be increased or decreased by owners without informing. When collect data from the Department of Meteorology, there is facility to get minimum and maximum of temperature and irradiation, daily variation of temperature and irradiation. Sometimes it does not have record irradiation values due to auto rejection from meters which not in permissible range. Irradiation can be changed highly and it is the value that cannot be guessed.

## Conclusions

This paper presents a function to calculate total storage by considering system which is completed with units within different parameters of panel specifications to reduce impact of the system instability. When disturbances



occur with generation of electricity, storage can be used to discharge power to fulfilled collapse power till absorbed power from utility grid during very short periods. It will be nearly 4s (4s is inertia constant (H) for Sri Lanka) for maximum power discharged. If collapse power is lower than maximum power of panels which used to calculate, storage time will be increased than 4s. According to the proposed function inertia constant can be varied as need when calculate total storage required.

### **Future Works**

The first phase of this research is to identify the function to calculate the storage. The next phase will be to implementation and testing. Therefore it should have simulated with photovoltaic model to verify total storage calculated by proposed function and also controlling algorithm for storage have to designed.

### **Acknowledgements**

I thank Open University of Sri Lanka and National Energy Symposium in Sri Lanka for giving me a great opportunity to publish a research paper.

I am highly grateful to the Department of Meteorology for giving me relevant data to do this research.

### **References**

- [1] W. Eberhard, S.Y. Ron, 2016. Virtual inertia with PV inverters using DC-link capacitors.
- [2] X. Wang, M. Yue, M.Eduard, 2014. PV generation enhancement with a virtual inertia emulator to provide inertial response to the grid.
- [3] D.P. Kothari and I.J. Nagrath 2003, Modern Power System Analysis
- [4] Brain Silveti, P.E., 2011. , Energy Storage and Variable Renewable Energy Sources.
- [5] J.I.S. Martin, I. Zamora, J.J.S. Martin, V. Aperribay, P. Eguia, 2011. Energy Storage Technologies for Electric Applications
- [6] D.Connolly, 2007. An investigation into the energy storage technologies available, for the integration of alternative generation techniques.
- [7] A.M.Mahmudi,2014,Battery/Superca pacitor combinations for Supplying vehical electrical and Electronic load.
- [8] M. Azzouzi, D. Popescu, and M. Bouchahdane, 2016. Modeling of Electrical Characteristics of Photovoltaic Cell.

# Design of Domestic Solar Thermal System for a Five Member Family in Kandy, Sri Lanka

I. W. Kularathne<sup>1</sup> & Macedon MOLDOVAN<sup>2</sup>

<sup>1</sup> *Department of Mechanical Engineering, Faculty of Engineering, University of Peradeniya,  
Sri Lanka*

<sup>2</sup> *Department of Product Design, Mechatronics and Environment, Faculty of Product Design  
and Environment, Transilvania University of Brasov, Romania*

<sup>1</sup> iwk@pdn.ac.lk

<sup>2</sup> macedon.moldovan@unitbv.ro

## Abstract

The present project was carried out to design a solar thermal system to fulfil the domestic hot water requirement for a family of five members in Kandy, Sri Lanka considering required hot water temperature as 55°C. The design was carried out considering both annual optimum tilt angle and also monthly optimum tilt angle to observe the effect on the solar fraction. It was observed that higher solar fractions of 84% and 87% could be achieved considering annual and monthly optimum tilt angles. According to the results, annual average domestic hot water requirement could be largely covered by one solar collector for a family of five members in Kandy.

**Keywords :** Solar energy, solar thermal system design, domestic hot water, Kandy in Sri Lanka, optimum tilt angle

## Introduction

Sri Lanka is located near the equator and as a result it receives an impressive solar energy. Sri Lanka does not experience a considerable seasonal variation in solar radiation over the island, though significant differentiation could be observed between the lowlands and mountainous regions [1]. According to solar radiation data about two thirds of the land area in the low country receives a radiation of 4-5.5 kWh/m<sup>2</sup> per day, whilst hill country receives a lower radiation of 2-3.5 kWh/m<sup>2</sup> per day [2]. But only 3% of the energy demand in the country is fulfilled by renewable energy including solar energy by 2015 [3].

Solar energy has been utilized by Sri Lankans from the earliest times for conventional applications such as drying of crops, clothes, etc., and it has remained as a non-commercial energy resource. Apart from conventional solar energy usage, presently usage of solar thermal technologies contribute significantly in many applications such as hot water production, space heating and cooling, industrial processes, etc.

In the hill country area of Sri Lanka, domestic solar thermal systems are extensively used to fulfil their domestic hot water requirement due to relatively cold climate. Also according to solar radiation data, solar radiation varies considerably depending on the place. Therefore it is important to design solar thermal systems for different locations in Sri Lanka and to estimate solar fractions to study the practicability. The present study was carried out to estimate solar fraction at Kandy to fulfil the domestic hot water requirement.

## Materials and methods

The design requirements are tabulated in Table 1 while main characteristics of the solar collector are tabulated in Table 2. The available solar energy data such as: global solar energy in horizontal plane ( $E_{Gh}$ ), global solar energy in the solar collector plane ( $E_{Gn}$ ), diffuse solar energy in the horizontal plane ( $E_{Dh}$ ) and outdoor air temperature ( $T_a$ ), etc. were obtained from Meteonorm software [4] considering the latitude, the tilt and azimuth angles of the roof. The monthly available solar energy and outdoor air temperature are presented in Table 3 for Kandy.

Using the latitude of Kandy and the day no. as 15<sup>th</sup> for each month, all the angles necessary to estimate solar radiation data were computed using fundamental equations [6]. By using these angles, turbidity factor and cloud crossing factor that have already been determined experimentally for Kandy [5], and the solar constant, monthly received global solar irradiance ( $G_n$ ) and then monthly average solar received irradiance data ( $G_{nm}$ ) were calculated. The data obtained for the month of June is given in Tables 4 and 5. Further on, the received global solar energy ( $E_{Gn}$ ) for each month of the year was calculated and, based on, the useful thermal energy output according with an average efficiency of the solar thermal collector (using equation 2), necessary to evaluate the monthly solar fraction in covering the thermal energy demand to heat the domestic hot water calculated using equation 1 (Table 6). By averaging the monthly solar fraction over the year, the solar fraction was obtained. Similarly, the solar fraction was obtained considering the monthly optimum tilt angle and then compared.

Table 1: Data for dimensioning a domestic hot water system for Kandy [6],[7]

Description	Notation	Value
Domestic residential hot water usage / [l/person/day]	q	50
No. of persons in a family / [person]	$n_u$	5
Targeted solar fraction / [%]	f	50
Latitude at Kandy / [°]	-	07° 18' N
Longitude / [°]	-	80° 43' E
Density of water / [Kg/m <sup>3</sup> ]	$\rho$	1000
Specific heat capacity of water/ [J/Kg·K]	c	4186
Optimum tilt angle based on Meteorom data / [°]	-	8°
Temperature of hot water / [°C]	$t_{hw}$	55
Temperature of cold water / [°C]	$t_{cw}$	27
Energy demand per day / [kWh/day]	$E_{day}$	8.14
Mean temperature of the solar collector [°C]	$t_m$	$(55+27)/2=44$

Table 2: Data of the solar collector [7]

Description	Notation	Value
Absorption surface of a solar thermal collector / [m <sup>2</sup> ]	$S_a$	2.32
Nominal yield of the solar thermal collector	$\eta_o$	0.776
Heat loss coefficient / [W/(m <sup>2</sup> K)]	$K_1$	3.92
Heat loss coefficient / [W/(m <sup>2</sup> K <sup>2</sup> )]	$K_2$	0.0165

Table 3: Available solar energy and outdoor air temperature in Kandy, Sri Lanka [1]

Month	EGh [kWh/m <sup>2</sup> ]	EGn [kWh/m <sup>2</sup> ]	Edh [kWh/m <sup>2</sup> ]	EBn [kWh/m <sup>2</sup> ]	Ta [°C]	Td [°C]	EF [m/s]
January	142	150	67	118	23.8	18.8	4
February	151	158	59	136	24.3	19.1	3.1
March	183	186	73	157	25.0	20.7	2.5
April	174	171	69	145	25.1	21.5	2.3
May	162	156	69	135	26.0	22.2	3.7
June	145	138	74	106	25.3	21.8	4.3
July	146	141	83	88	25.0	21.3	4.3
August	152	148	90	86	25.0	21.2	4.4
September	153	153	72	116	24.9	21.1	3.7
October	153	157	84	101	24.4	21.2	2.8
November	145	152	64	120	23.7	20.4	2.5
December	133	141	58	113	23.6	19.5	3.5
<b>Total Year</b>	<b>1841</b>	<b>1852</b>	<b>862</b>	<b>1421</b>	<b>24.7</b>	<b>20.7</b>	<b>3.4</b>

## Equations

Daily energy demand to heat the domestic hot water

$$E_{\text{day}} = \beta = [n_u \times q \times \rho \times c \times (t_{\text{hw}} - t_{\text{cw}})] / 3,600,000 \text{ [kWh/day]} \quad (\text{Eq. 1})$$

Mean efficiency of the solar thermal collector

$$\eta_m = \eta_o - K_1 [(t_m - t_a) / G_m] - K_2 [(t_m - t_a)^2 / G] \quad (\text{Eq. 2})$$

## Results and Discussion

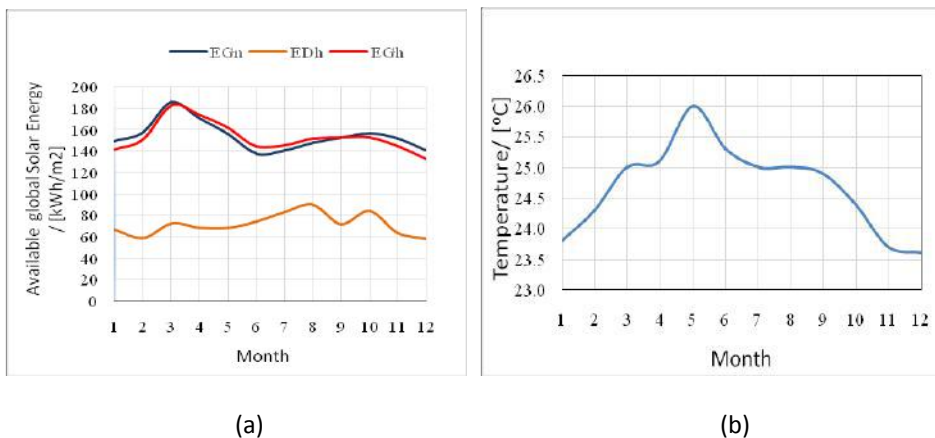


Figure 1: Available solar energy (a) and outdoor air temperature (b) in Kandy Sri Lanka

Considering the available solar energy data from Meteonorm for Kandy in Table 3, the graphs of available global solar energy in the horizontal plane (EGh), and In the solar collector plane (EGn), and diffuse solar energy (EDh) along with the variation of outdoor temperature are plotted in Figure 1.

According to the Figure 1, it is visible that Kandy has a considerably high and relatively constant solar radiation throughout the year. This type of solar radiation is quite useful in solar design due to the fact that additional storage devices are not necessary to store the thermal energy. There is a relatively constant outdoor air temperature in

Kandy. This also is an additional advantage considering heat losses and also less overheating of the solar collector.

The variation of the solar angles with solar time and also the variation of the available solar irradiance with time are shown in Figure 2. Considering the graphs, there is a considerable high direct and global solar irradiance between 8.00 a.m. to 4.00 p.m. of the day. According to table 5, there is a considerable high global solar radiation received in in the solar collector plane on 15<sup>th</sup> of June starting from 7:00 a.m. with 473 W/m<sup>2</sup> and then increasing up to 1090 W/m<sup>2</sup> at noon and again

decreasing up to 481 W/m<sup>2</sup> at 17:00. Thus, when considering variation throughout the day, there are many hours for harnessing a high amount of solar radiation during a day. This kind of solar irradiance is quite important and highly efficient in solar systems.

solar collector based on annual optimum tilt angle solar fraction varies from 71% to 100% with one collector that means the required amount of energy (solar fraction more than 60%) could be obtained using one collector during any month of the year.

Considering Table 6 and Figure 3 monthly variation of solar thermal system parameters made of one thermal

Also, an average solar fraction of 84% could be obtained with one collector for 5 member family in Kandy.

Table 4: The angles necessary to estimate the available and received solar radiation, for June 15

1-Jan	Day no.	Turbidity factor	Diffuse factor	Cloud crossing factor	Solar time	Hour angle	Declination	Sun elevation angle	Sun azimuth angle	Incidence angle
day	n	Tl	CD	Fcc	ts	ω	□	α	ψ	γ
-	-	-	-	-	h	°	°	°	°	°
15-Jun	166	4.4	0.55	1	4	120	23.35	-23.95	119.55	117.69
15-Jun	166	4.4	0.55	1	5	105	23.35	-10.73	115.50	104.08
15-Jun	166	4.4	0.55	1	6	90	23.35	2.84	113.19	90.33
15-Jun	166	4.4	0.55	1	7	75	23.35	16.58	112.30	76.59
15-Jun	166	4.4	0.55	1	8	60	23.35	30.33	112.91	63.04
15-Jun	166	4.4	0.55	1	9	45	23.35	43.92	115.68	49.95
15-Jun	166	4.4	0.55	1	10	30	23.35	56.97	122.63	37.88
15-Jun	166	4.4	0.55	1	11	15	23.35	68.34	139.93	28.23
15-Jun	166	4.4	0.55	1	12	0	23.35	73.83	0.00	8.17
15-Jun	166	4.4	0.55	1	13	-15	23.35	68.34	-139.93	28.23
15-Jun	166	4.4	0.55	1	14	-30	23.35	56.97	-122.63	37.88
15-Jun	166	4.4	0.55	1	15	-45	23.35	43.92	-115.68	49.95
15-Jun	166	4.4	0.55	1	16	-60	23.35	30.33	-112.91	63.04
15-Jun	166	4.4	0.55	1	17	-75	23.35	16.58	-112.30	76.59
15-Jun	166	4.4	0.55	1	18	-90	23.35	2.84	-113.19	90.33
15-Jun	166	4.4	0.55	1	19	-105	23.35	-10.73	-115.50	104.08
15-Jun	166	4.4	0.55	1	20	-120	23.35	-23.95	-119.55	117.69

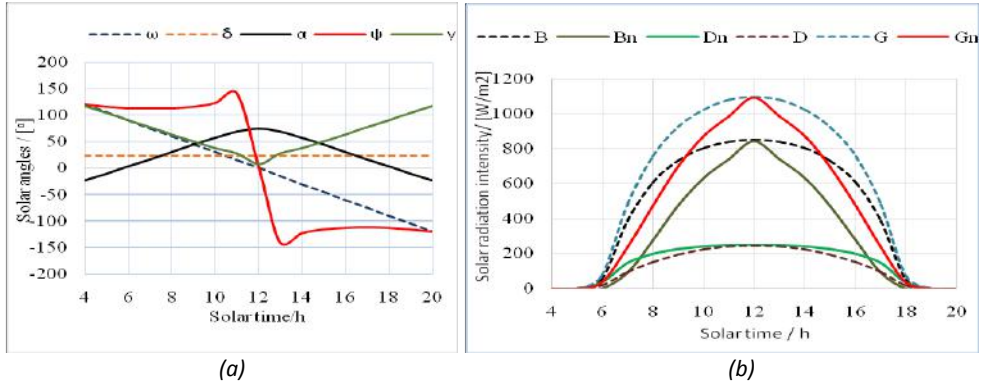


Figure 2: The variation of solar angles (a) and solar radiation intensity (b) with time

Table 5: The solar irradiance available and received by a solar thermal collector disposed in the roof plane with  $\alpha_n = 8^\circ$  and  $\psi_n = 0^\circ$ , under clear sky conditions, for June 15

Solar time	Extra terrestrial solar irradiance	Direct solar irradiance	Received direct solar irradiance	Diffuse horizontal solar irradiance	Received diffuse solar irradiance	Diffuse solar irradiance	Global solar radiance	Available global solar irradiance	Monthly average global solar irradiance
ts	B0	B	Bn	Dh	Dn	D	G	Gn	Gn
h	W/m2	W/m2	W/m2	W/m2	W/m2	W/m2	W/m2	W/m2	W/m2
4	1324	0	0	0	0	0	0	0	0
5	1324	0	0	0	0	0	0	0	0
6	1324	53	0	35	34	18	71	34	34
7	1324	388	90	147	146	94	482	236	236
8	1324	607	275	199	198	150	757	473	473
9	1324	732	471	226	225	191	923	696	696
10	1324	802	633	241	239	221	1023	873	873
11	1324	839	739	248	247	239	1078	986	986
12	1324	850	841	250	249	245	1095	1090	1090
13	1324	839	739	248	247	239	1078	986	986
14	1324	802	633	241	239	221	1023	873	873
15	1324	732	471	226	225	191	923	696	696
16	1324	607	275	199	198	150	757	473	473
17	1324	388	90	147	146	94	482	236	236
18	1324	53	0	35	34	18	71	34	34
19	1324	0	0	0	0	0	0	0	0
20	1324	0	0	0	0	0	0	0	0
<b>22,506</b>	<b>7,690</b>	<b>5,257</b>	<b>2,441</b>	<b>2,429</b>	<b>2,074</b>	<b>9,764</b>	<b>7,686</b>	<b>452</b>	

Table 6: Solar fraction evaluation for one solar collector (based on annual optimum tilt angle)

Month	No. of days per month	Required thermal energy to heat hot water	Global solar energy on the collector plane	Average exterior temperature	Average intensity of global solar radiation in the collector plane	Average solar collector efficiency STC	Thermal energy produced by SST	Usable thermal energy produced by SST	Auxiliary thermal energy produced by back-up source	Solar fraction
	N days	$E_{demand}$ kWh	$E_{Gn}$ kWh/m <sup>2</sup>	$T_a$ °C	$G_{nm}$ W/m <sup>2</sup>	$\eta_m$	Esst kWh	$E_{usst}$ kWh	$E_{auxiliary}$ kWh	f %
Jan	31	252	150	23.8	431	0.61	197	197	55	78
Feb	28	228	158	24.3	472	0.63	215	215	13	94
Mar	31	252	186	25.0	473	0.63	255	252	0	100
Apr	30	244	171	25.1	477	0.64	235	235	9	96
May	31	252	156	26.0	477	0.64	218	218	35	86
Jun	30	244	138	25.3	452	0.63	188	188	56	77
Jul	31	252	141	25.0	460	0.63	192	192	60	76
Aug	31	252	148	25.0	460	0.63	202	202	50	80
Sep	30	244	153	24.9	456	0.63	208	208	36	85
Oct	31	252	157	24.4	453	0.62	211	211	41	84
Nov	30	244	152	23.7	424	0.60	199	199	45	81
Dec	31	252	141	23.6	393	0.59	180	180	73	71
<b>Total</b>	<b>365</b>	<b>2,971</b>	<b>1,852</b>		<b>5,428</b>		<b>2,501</b>	<b>2,498</b>	<b>473</b>	<b>84</b>

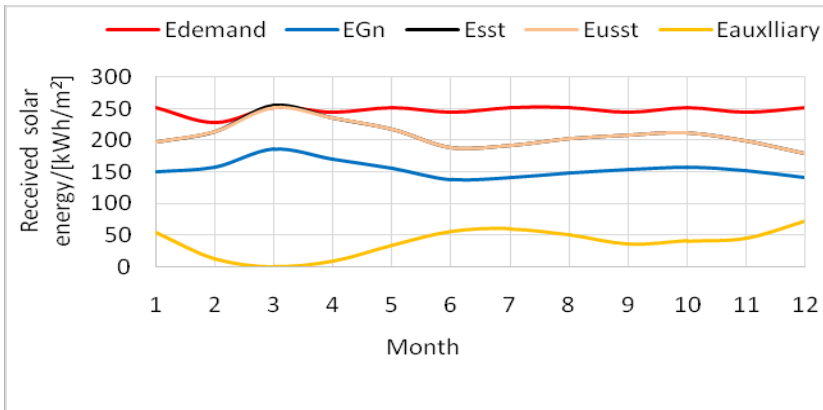


Figure 3: Monthly variation of solar thermal system parameters made of one thermal solar collector (based on annual optimum tilt angle)



Table 7: Solar fraction evaluation for one solar collector (based on yearly optimum tilt angle and monthly optimum tilt angle)

Month	Yearly optimum tilt angle			Monthly optimum tilt angle		
	Tilt angle	Received solar energy on collector plane	Solar fraction	Tilt angle	Received solar energy on collector plane	Solar fraction
	$\chi$ °	EGn kWh/m <sup>2</sup>	f %	$\chi$ °	EGn kWh/m <sup>2</sup>	f %
January	8	150	78	35	161	84
February	8	158	94	25	164	98
March	8	186	100	15	186	100
April	8	171	96	0	174	98
May	8	156	86	0	161	89
June	8	138	77	0	144	80
July	8	141	76	0	146	79
August	8	148	80	0	151	82
September	8	153	85	10	153	85
October	8	157	84	20	159	85
November	8	152	81	30	161	86
December	8	141	71	35	154	78
<b>Total</b>		<b>1851</b>	<b>84</b>		<b>1914</b>	<b>87</b>

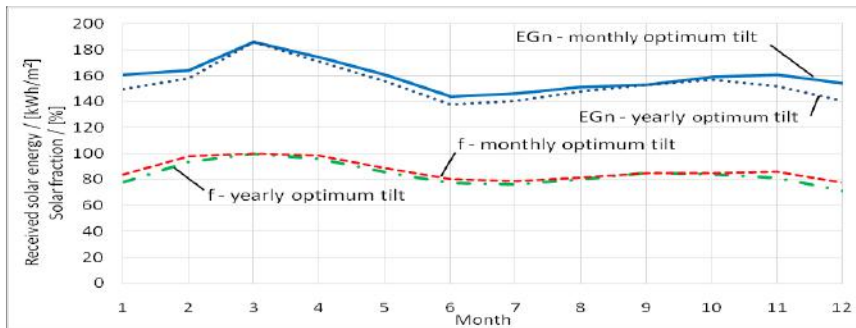


Figure 4: Variation of received solar energy and solar fraction based on yearly and monthly optimum tilt angle

Similarly based on monthly optimum tilt angle, solar thermal system parameters given in Table 7 and Figure 4 could be obtained. Accordingly received solar energy on the collector plane has been increased and the total solar energy received per year has been increased by 63 kWh/m<sup>2</sup>. Also the solar fraction has been varied from 78% to 100% with one collector and average solar fraction has been increased from 84% up to 87%.

## Conclusion

It could be concluded that the required hot water for domestic usage for a family of five members in Kandy, Sri Lanka, could be fulfilled with a solar fraction of 84% using one solar collector with absorption surface area of 2.32 m<sup>2</sup> by placing it at an annual optimum tilt angle,  $\alpha_n = 8^\circ$ , and at an azimuth angle,  $\psi_n = 0^\circ$ . This solar fraction can be increased up to 87% by monthly adjusting the position of the solar collector according to the monthly

values obtained for the optimum tilt angle.

Considering the difficulty to change the solar collector to optimum angle on monthly basis, this increment in the solar fraction is impracticable and also due to availability of a high solar fraction with annual optimum tilt angle.

## References

- [1] "Meteonorm: Irradiation data for every place on Earth" 20 March. 2017, [www.meteonorm.com/](http://www.meteonorm.com/).
- [2] Perera J. A. S., Solar energy in Sri Lanka, The official e-newsletter of the Institution of the Engineers Sri Lanka, Issue 14, 2013
- [3] Sayanthan S. Kannan N., Renewable energy resource of Sri Lanka: A review, International Journal of Environmental & Agriculture Research (IJOEAR), ISSN:2454-1850, Vol-3, Issue-4, April- 2017, pp. 80-85
- [4] *Sri Lanka Sustainable Energy Authority*, 22 March. 2017, [www.energy.gov.lk/](http://www.energy.gov.lk/).
- [5] *Sri Lanka Latitude and Longitude Map*, 22 March. 2017, [www.mapsofworld.com/lat\\_long/sri-lanka-lat-long.html](http://www.mapsofworld.com/lat_long/sri-lanka-lat-long.html).
- [6] Vătăşescu M., Burduhos B., Moldovan M., Articulated systems for solar orientation, Transilvania University Publishing House of Braşov, 2011
- [7] *Viessmann Werke GmbH & Co. KG*, 23 March. 2017, [www.viessmann.com/](http://www.viessmann.com/)

# An Investigation of a Supercapacitor-based Lightning Energy Harvesting Technique

T.C.P.K. Wickramasinghe<sup>1</sup>, K.H.S.N. Viduranga<sup>2</sup>

*Department of Electrical and Computer Engineering,  
The Open University of Sri Lanka  
Nawala, Nugegoda, Sri Lanka  
tcwic@ou.ac.lk  
shalithnishan@gmail.com*

## Abstract

This paper presents a lightning energy harvesting technique that can store energy in a supercapacitor (SC) bank. Lightning is the natural phenomenal renewable energy source, which generates a large amount of electrical energy within a short duration. A single lightning flash discharges about few  $10^9$  to  $10^{10}$  of joules and can last from tens to few hundreds of microseconds. Due to the large amount of energy discharges from a lightning strike, it is difficult to harvest energy via direct flashes, as it can damage the storage. The proposed system acquires only a fraction of energy cause by lightning in 11kV/33kV voltage power lines close to a service entrance of a power system. Further, the design consists of a fast responding metal oxide-based surge arrester, connected in parallel with the SC bank to provide protection to the storage. A high density SC bank with 5.8 F, 160 V can store 74 kJ in a volume of  $0.007 \text{ m}^3$  with weight of 5.2 kg. In complete isolation, the stored energy in SC bank can energize DC-loads at the service entrance. This technique reduces the AC-DC power conversion requirement for low voltage DC-loads such as 24/48V battery backup.

**Keywords:** harvesting lightning energy, supercapacitors, surge protection

## Introduction

Nature offers many different kinds of renewable resources, some yet to be discovered. Lightning is a natural phenomenon that can discharge large amount of energy in billion joules from a single strike, but very limited research has been conducted on harnessing lightning energy. Currently published research on lightning energy harvesting systems (LEHSs) are based on attracting direct strikes via lightning rods and they present only a very limited information about system reliability[1]-[3]. These techniques incur high costs of implementation and protection. Due to complexity of some LEHS designs, experiments have not been conducted even at proof-of-concept prototype level.

This paper investigates about a novel LEHS applicable to a service entrance of 13kV/33kV transmission line. Further, a fast responding protection technique is proposed for reliability of the storage device. A simplified topology of the proposed LEHS is shown in Fig.1(a). The system is divided into three functions; (i) to obtain a part of energy generated by lightning in a power line, (ii) to store energy in supercapacitor bank, and, (iii) to protection of supercapacitors from overvoltage.

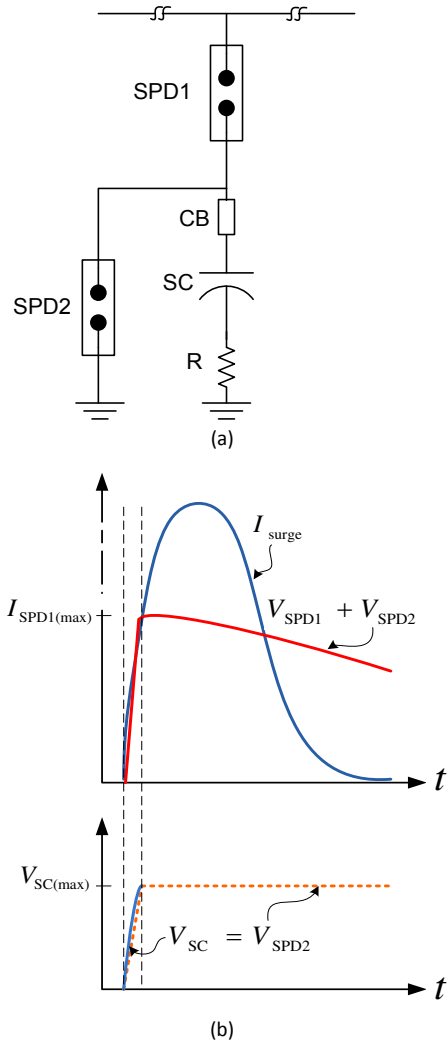


Figure 1: A simplified topology of the lightning energy harvesting system(a) basic topology, (b) typical characteristics of SC and SPDs at SPD operation region

## Proposed system

There are two surge protection devices (SPD) connected in series. The SPD connects to the power line (SPD1) suppresses surge generated in the line while SPD2 clips at the defined maximum voltage of SC bank (thereby providing overvoltage protection). Figure 1(b) illustrates the typical characteristics of SC-bank and the SPDs at operation region. To address the unbalanced grounding issues a low valued resistor (R) is used at the ground terminal. The circuit breaking system (CB) isolates a charged SC from the LEHS to power a DC-load. Figure 2 illustrates the proposed system apply in a three-phase line.

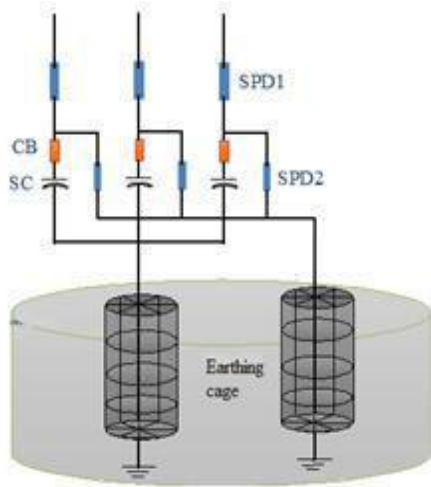


Figure 2: Proposed system for three-phase high voltage line

## Applicable location

In general, SPDs are utilized according to IEEE C62.41 location categories. They are, (i) category A: long-branch circuits, indoor receptacle, (ii) category B: major feeders, short-branch circuits, indoor service panels, and (iii) category C: outdoor overhead lines, service

entrance. The proposed LEHS considers the category C location and it is based on the levels of surge protection as recommended by IEEE [4].

Figure 3 shows the location of LEHS in 11kV/33kV three-phase connection. The existing location consists of drop-down lift-on (DDLO) fuses, surge arrestors and a power transformer. DDLO fuses provide overcurrent protection while SPDs protect system from overvoltage generated by lighting and other artificial surges. In general, SPDs discharge current to ground via a copper rod which connects to an earthing cage. The proposed LEHS can be applied between the DDLO fuses and the ground as illustrated in Fig. 3.

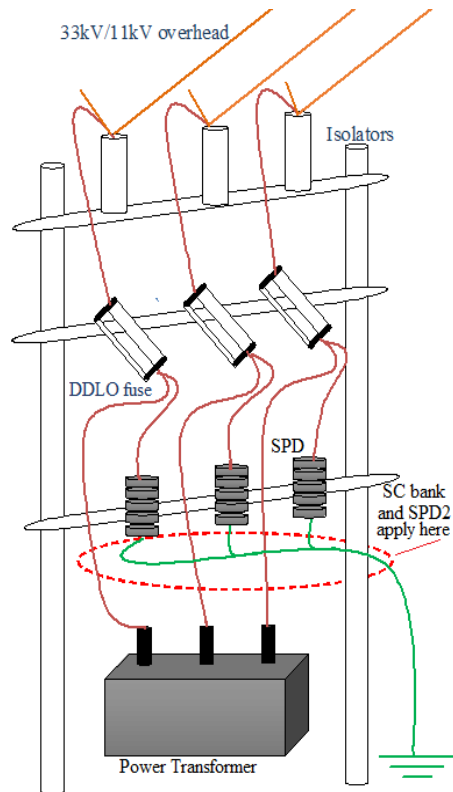


Figure 3: A possible location of application with existing protection mechanisms

A separate earthing-cage is required for SC storage to maintain a balance ground as illustrated in Fig.2. The resistance in series path of SC is significant with time expose to high voltage and current. MOV-based SPD2 can be designed to operate at a lower resistance and at low voltages to protect the storage.

## Methodology

To verify SPDs technical requirements, a conceptual design of LEHS is developed and simulated the transient response using software system. The protection mechanism for the LEHS can be verified by comparing the simulation results and results of appropriate experiments.

IEC 61000-4 and IEC60099-4 standards provides the basis for the design of AC power line transient SPDs.

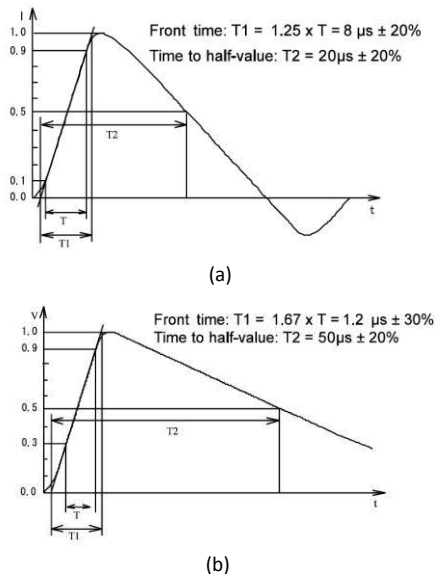


Figure 4: Surge waveforms: (a) 8/20  $\mu$ s short-circuit current (b) 1.2/50  $\mu$ s open-circuit voltage

Large signal analysis is useful to predict the nonlinear behaviour of SPDs in transient conditions. The transient is

defined in terms of a surge generator producing a given waveform and having specified open circuit voltage and source impedance. According to the IEC 61000-4 standards, a combination wave consisting of two waveforms, which are shown in Figure 4. They are the 1.2/50 $\mu$ s open-circuit voltage waveform and the 8/20 $\mu$ s short-circuit current waveform. Their rise times and half-amplitude duration, define these impulse waveforms. Above two waveforms are considered in finding parameters for SPD2.

## Results and Discussions

The proposed LEHS is possible due to farad-order capacitance with milliohm series resistance in SCs provide an extremely small time constant ( $\tau = RC$ ) that can withstand short duration surges with energy values specified in IEEE C62-XX series, IEC 61400 and similar standards.

Surge endurance testing preformed on three different commercial brands of SC families has been considered for the design [5]. The results obtained for open-circuit surge voltages up to 6.6kV indicate following: i) thin profile SCs under 0.5F/2.5V do not get destroyed by a single voltage surge; ii) most SC families over 0.5-F/2.5V value can withstand over 100 repeated surges; and iii) much larger tank-type SCs do not get destroyed by less than 500 repeated surges [6]. With the above figures, it can be predicted that the high-voltage, tank-type SCs will withstand for higher voltage and current surges.

This project considers a Maxwell SC module of 5.8F/160V. Table 1 presents few important electrical properties of the SC module. A first-order circuit model of SC was considered for the

simulation. The four parameters in the circuit illustrates in Fig.5 are capacitance C, series resistor R<sub>s</sub>, a parallel resistor R<sub>p</sub>, and a series inductor L. In a practical SC, R<sub>p</sub> is much higher than R<sub>s</sub>, and can be negligible particularly in high-power applications.

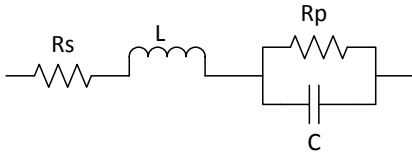


Figure 5: First order SC model

Tank-type modules are collection of many individual cells. The total capacitance of a SC bank with *n* number cells in series is;

$$C_{cell} = C_0 + kV_c \quad (1)$$

$$C_{bank} = \left(\frac{1}{n}\right) * C_{cell} \quad (2)$$

$$= \left(\frac{1}{n}\right) * (C_0 + kV_c)$$

The maximum peak current of the SC for 1 second is given by

$$I_{peak} = \frac{\left[\frac{1}{2}CV\right]}{C * R + 1} \quad (3)$$

Where,

- $I_{peak}$  = Current (A)
- $R$  =Equivalent series resistance( $\Omega$ )
- $C$  = Capacitance (F)
- $V$  = Voltage (V)

For a period of 1s, the SC module (5.8F/160V) can absorb 200A theoretically.

Table1: SC specifications: Maxwell  
BMOD0006 E160 B02

Parameters	Units	Values
<b>Rated capacitance</b>	F	5.8
<b>Maximum ESR<sub>CD</sub>, initial</b>	m $\Omega$	240
<b>Rated voltage</b>	V	160
<b>Max. peak current (1 second)</b>	A	200
<b>Leakage current at 250, maximum</b>	mA	25

In order to protect loads by direct or nearby strokes and to reduce the failure rate, metal-oxide arresters (MO SPD) install in distribution/transmission lines.

Endurance against surge in gapless metal-oxide type surge arresters utilized in the Ceylon Electricity Board in 33kV lines are studied for the design. In simulation of SPDs, the model proposed by the IEEE Working Group 3.4.11 is selected (in Fig. 6). This model consists of a non-linear resistance  $A_0$  and  $A_1$ , separated by a R-L filter.

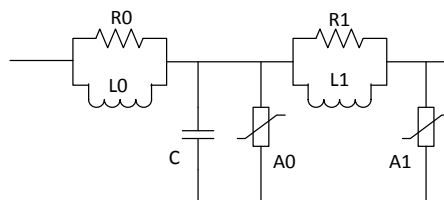


Figure 6: Simplified arrester model

For slow front surges, the filter impedance is low and the nonlinear resistances are in parallel. For fast front surges filter impedance becomes high, and the current flows through the nonlinear resistance  $A_0$ .

Calculated values for SPD2 according to 160V arrester the proposed LEHS is given in Table 2.

$$d = 0.362 \text{ m}$$

$$n = 1$$

Table 2: Calculated parameter values of the surge arrester

Parameter		
<b>L1</b>	$(15d)/n \mu\text{H}$	5.43 $\mu\text{H}$
<b>R1</b>	$(65d)/n \Omega$	23.53 $\Omega$
<b>Lo</b>	$(0.2d)/n \mu\text{H}$	0.0724 $\mu\text{H}$
<b>Ro</b>	$(100d)/n \Omega$	36.2 $\Omega$
<b>C</b>	$(100n)/d \text{ pF}$	276.24 pF

The lightning energy absorbed by arresters is given by

$$E = \int_0^t v(t)i(t) dt \quad (4)$$

Where,

$v(t)$  = SPD residual voltage (kV)

$i(t)$  =discharge current via SPD(kA)

With the availability of wide-bandgap semiconductors operate above 500 °C, high temperature power electronic components have become possible [7]. In general, they have high limits of thermal runaway at low breakdown voltages. This is an advantage for designing a low voltage MO-based SPDs for protection of SC.

## Conclusions

A conceptual topology of a lightning energy harvesting system was presented along with the components and their electrical parameters. The research is still needed to take advantage of experimental-based results to prove the feasibility of the concept.

## Future Works

The research is ongoing to test the proof-of-concept prototype of the protection mechanism of SC. Experiment results are required to compare with simulation results and the mathematical model. SC bank with five series 48V SC-modules in series (formed a 240V SC bank with F) can be used for sensible conditions.

## References

- [1] Farizz MB, Herman JM, et al. A new source of renewable energy from lightning stroke: a small scale system. IEEE Power Electron. conf. 2010, pp 1490-3.
- [2] Malavika S, Vishal S. Harnessing electrical energy from lightning, Int. Jnl. App. or Innovation in Engineering Management. 2013; 9: 23-7.
- [3] Helman DS. Catching lightning for alternative energy. Renewable energy, 36(5), 1311-4.
- [4] "Approved Draft Revision to Recommended Practice for Powering and Grounding Electronic Equipment. (Color Book Series - Emerald Book),"IEEE Std P1100/D2, 2005.



[5] Madawala UK, Thrimawithana D, Kularatna N. An ICT-supercapacitor hybrid system for surge-free power transfer. IEEE Trans. on Industrial Electron. 2007;54: 3287.

[6] Kularatna N, Fernando J, Pandey A, James S. Surge capability testing of

supercapacitor families using a lightning surge simulator, IEEE Trans. on Industrial Electron. 2011;58: 4942.

[7] Battay C, Planson D, et al. State of art high temperature power electronics. Material Science and Engineering. 2011; 176:283-8.

# Ocean Wave Energy Mapping for South Western Coast of Sri Lanka

R.N. Chamara<sup>1</sup> and H.P.V.Vithana<sup>2</sup>

<sup>1,2</sup> *Faculty of Engineering, University of Ruhuna, Hapugala, Galle*

## Abstract

Ocean wave energy is one of the untapped renewable energy sources that has a significant potential to be developed in Sri Lanka. Wave energy is environmentally friendly source as it does not generate solid, liquid waste and or gaseous harmful products. Determination of wave energy content at various locations is particularly useful for commercial developers of wave power. This research establishes an assessment of wave climate in south western Sri Lanka and quantifies wave energy/power both spatially and temporally. Buoy measured wave height data and satellite altimeter wave height data were used for the analysis of long term wave climate. A wave propagation model was developed using DELFT 3D modelling system to obtain spatial variation of significant wave height and hence, wave power per metre of wave crest (W/m) around the south western coast.

**Keywords :** Ocean, wave energy, Sri Lanka

## Introduction

While wind and solar have been the leading sources of renewable energy up to now, ocean waves are increasingly being recognised as a viable source of power for coastal regions [1]. Being an island surrounded by the ocean, Sri Lanka offers ideal conditions to develop this abundant energy source.

When considering the wave climate in Sri Lanka, south west coastline is very important as the region is affected by both monsoons - south west monsoon predominantly and north east monsoon to a lesser extent. The wave climate off the southern coast of Sri Lanka is characterised by long period swell waves and local wind generated sea waves. The swell waves are those waves generated in the southern Indian Ocean and have propagated out of the generation zones. These waves approach from a more or less southerly direction in deep water [2], [3]. This paper describes the analysis and results of a wave energy mapping study for the south western coast of Sri Lanka. The most violent sea conditions are observed during south west monsoon (May to September) during which both sea and swell waves occur at maximum strength. In order to estimate long-term wave energy climate and available power in south western coast of Sri Lanka, it is necessary to find the significant wave height ( $H_s$ ) variation, both spatially and temporally. The objective of this ongoing study is to identify the high wave energy zones having potential for commercial scale wave power generation.

## Methodology

### Measured Wave Data

Directional wave measurements have been carried out on the south west coastal ocean in Sri Lanka by the Coast Conservation Department from February 1989 to September 1992. A pitch and roll buoy was deployed off Galle harbour at a depth of 70 m [2]. The sea climate in this region is characterized by a bimodal spectra with an all year rather strong long period swell wave component and a sea wave component [2], [3]. Both wave systems have different deep water wave directions. For statistical analysis sea waves were separated from swell waves. The data set obtained from the Coast Conservation Department of Sri Lanka was used for the present wave energy mapping study. The significant wave height ( $H_s$  or  $H_{m0}$ ), Zero-crossing period  $T_z$ , mean period  $T_m$ , and peak period  $T_p$ , were defined by the following equations.

$$H_s = 4\sqrt{m_0} \quad (\text{Eq.1})$$

$H_s$  = Significant Wave height (m)  
 $m_0$  = Initial spectral moment ( $m^2$ )

$$T_z = \sqrt{\frac{m_0}{m_2}} \quad (\text{Eq.2})$$

$T_z$  = Zero crossing wave period (s)  
 $m_2$  = Second spectral moment ( $m^2s^{-2}$ )

$$T_m = \frac{m_0}{m_1} \quad (\text{Eq.3})$$

$T_m$  = Mean wave period  
 $m_1$  = first spectral moment ( $m^2s^{-1}$ )

$$T_p = 1/f_p \quad (\text{Eq.4})$$

$T_p$  = Peak wave period (s)  
 $f_p$  = peak frequency (Hz)

$m_n$  ( $n=0,1,2$ ) is the spectral moments of spectral density [1].

The wave power in deep water is expressed by equation (5). With ( $\rho$ ) sea water density ( $1025 \text{ kgm}^{-3}$ ) and wave energy period,  $T_E$  is defined by  $m_{-1}/m_0$  [2]. The power per unit width of wave crest,  $P$ , is given by equation (5) and can be simplified into equation (6),

$$P = \frac{\rho g^2}{64\pi} H_s^2 T_E \quad (\text{Eq.5})$$

$P$  = Power per unit width of wave crest ( $\text{Wm}^{-1}$ )

$\rho$  = Sea water density ( $\text{kgm}^{-3}$ )

$T_E$  = Wave energy time period (s)

$$P = 0.49 H_s^2 T_E \quad (\text{Eq.6})$$

In order to determine the wave energy period,  $T_E$  from limited datasets it has been a common practice to employ fixed conversion factors based on a theoretical spectral shape, such as Bretschneider or JONSWAP, which is deemed to be representative of the dominant wave conditions. The main challenge in this study was lack of measured wave data. Measured data offshore of Galle [2] did not contain the original raw wave data but it consisted of calculated significant wave heights. Therefore, construction of monthly wave energy spectra was not possible to calculate monthly  $T_E$  values. However, the report [2] provided a wave energy spectrum for the whole measurement period [see Figure 1]. This was fitted to JONSWAP spectrum and it was found that JONSWAP spectrum fits reasonably well to the measured wave energy spectrum when peak shape factor is equal to 2.36.

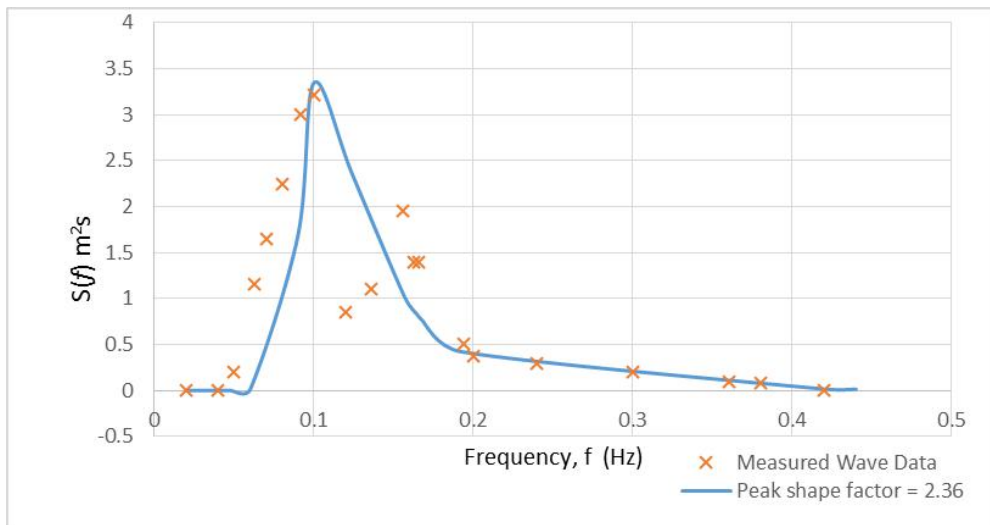


Figure 1: Comparison of measured and JONSWAP Wave Spectra

Cahill and Lewis [1], [4] calculated wave energy period ( $T_E$ ) for different types of spectra on the basis of field measurements and found that the wave energy period varies with peak shape factor. Table 1 shows different wave period ratios for different peak shape factors in the JONSWAP spectrum.

The corresponding wave period ratio ( $T_E/T_Z$ ) for the energy spectrum for the present study is 1.2. Also noteworthy is the wave period ratio for the Bretschneider spectrum which is 1.206.

*Table 1: Wave period ratio for JONSWAP spectra [1,4]*

<b>Peak shape factor</b>	<b>Wave Period Ratio, <math>T_E/T_Z</math></b>
1	1.22
2	1.2
3.3	1.18
5	1.16
7	1.14
10	1.12

## 2.2 Ocean wave model

In this study ocean wave model was developed using DELFT 3D modelling system with measured wave data and bathymetry data (Figure 2) being used as

boundaries. Mean monthly significant wave height was used as the boundary condition (i.e.,  $H_s=1.91\text{m}$ , peak wave period,  $T_p = 10.7$  sec, mean wave direction = 215 deg/N). Figures 3 and 4 show the spatial distribution of wave heights obtained from the model simulation.

Due to lack of buoy measured wave data satellite data were used for model calibration and validation. Satellite wave data covering a period of fifteen years were downloaded from the TOPEX altimeter data record of NASA. These data were measured twice per day by satellite altimeters. The satellite wave height data and buoy measured wave height data for the same location for the same time period were compared as shown in Figures 5(a,b). For this analysis Root Mean square error was 0.02 m and  $R^2=0.85$ . According to the results of the comparison satellite data can be applied for the model calibration and validation purposes with sufficient accuracy in the absence of buoy measured wave data. Figure 5(a) shows the monthly mean significant wave height variation (1989-1992) for buoy measured wave data and satellite altimeter measured wave data. Then Figure 5(b) shows the deviation of same data with  $y = x$  line.

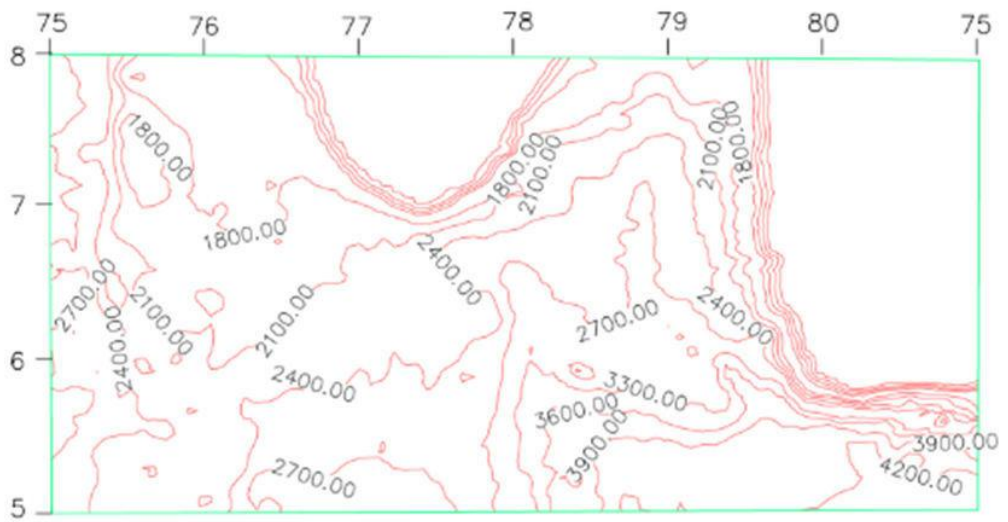


Figure 2: water depth variation in south western coast

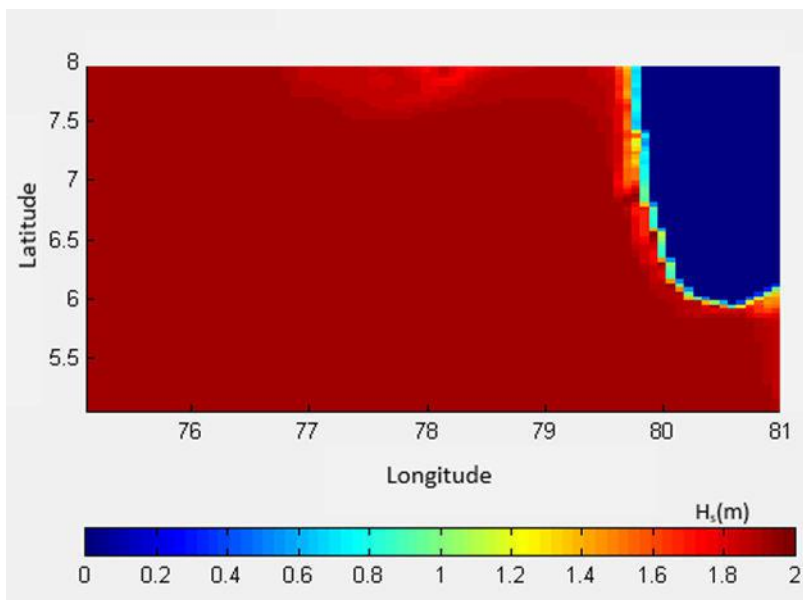


Figure 3: Spatial variation of mean monthly significant wave height,  $H_s$  (m)

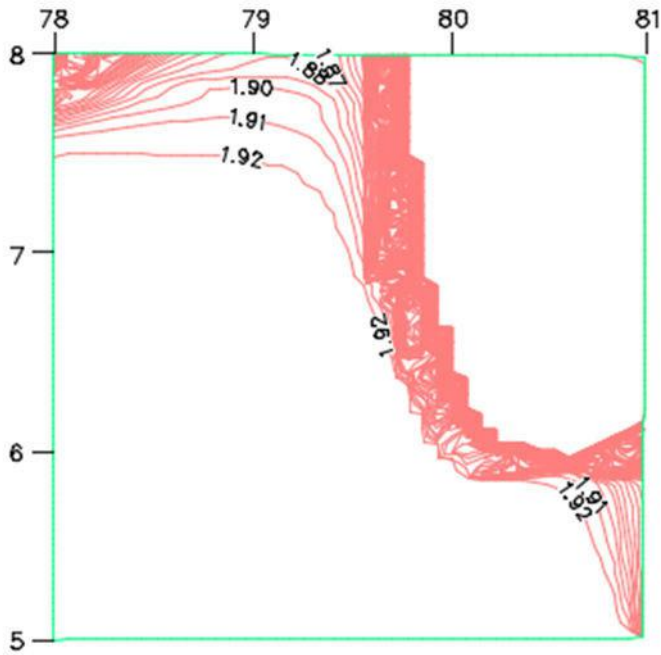


Figure 4: Mean monthly significant wave height,  $H_s$  (m) contours for September

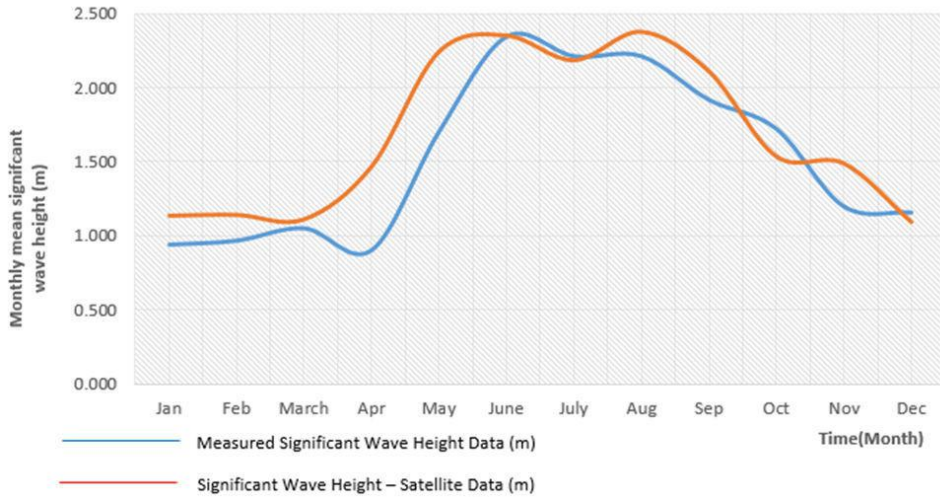


Figure 5(a): Comparison of measured significant wave height data with satellite data

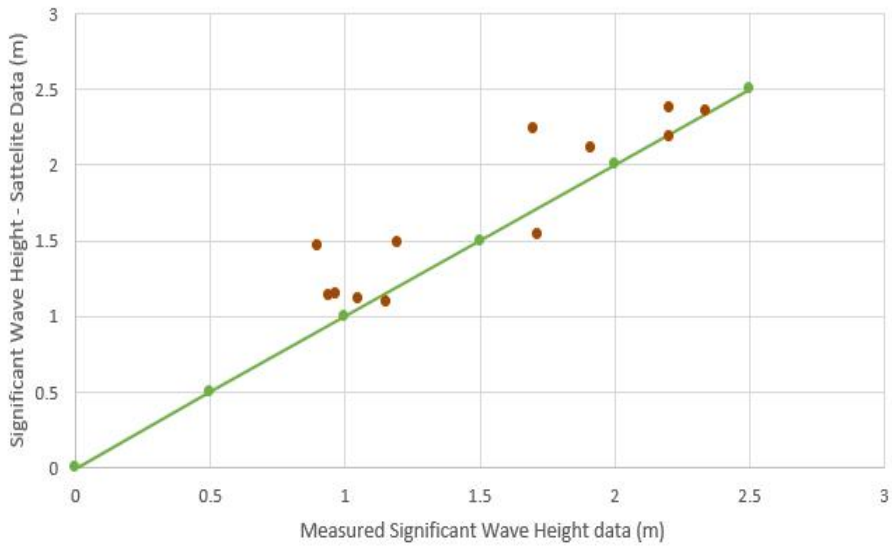


Figure 5(b): Comparison of measured significant wave height data with satellite data

## Results and Discussion

The Figure 6 shows contours of wave power per metre wave crest (W/m) in the south western coast of Sri Lanka for the month of September. It shows that wave power is generally uniform for the selected domain. However, wave power

content will need to be calculated for the entire year to compare suitability of several potential sites. The research is ongoing to include other parts of the Sri Lanka's coast.



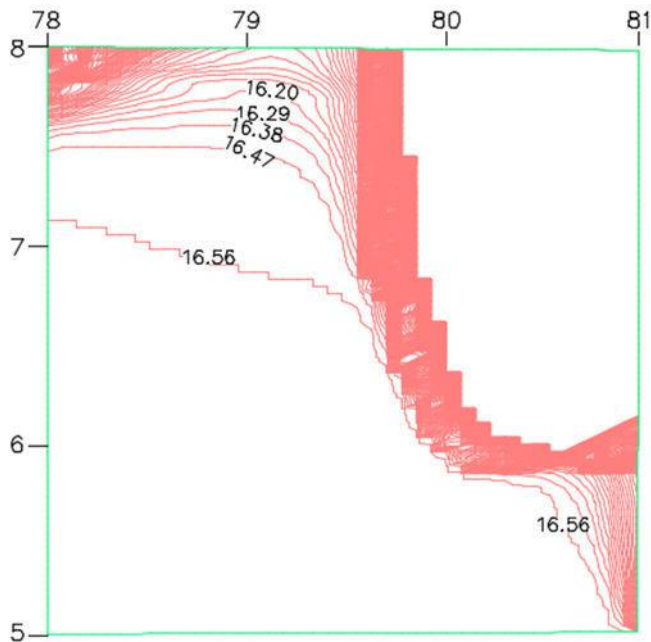


Figure 6: Wave power per metre wave crest (W/m) for September

## Recommendations

There is a severe lack of measured wave data to be used for wave energy resource assessment. Present research was hampered by a lack of high resolution accurate bathymetry data and measured wind/wave data. Non-availability of high resolution bathymetry data resulted in poor details in model results near the coast. Therefore, long term wind/wave measurement around the island is a timely necessity if Sri Lanka is to develop its coastal wind/wave energy resource. Therefore, it is recommended to deploy met-ocean stations around the island for this purpose.

## Acknowledgements

The authors express their appreciation to the Coast Conservation and Coastal Resource Management Department for their assistance in securing wave data. Authors also wish to thank Marine Geoscience Data System (<http://www.marine-geo.org/about/overview.php>) for allowing the use of bathymetry data.

## References

- [1 ] Cahill, B. G., and T. Lewis, Wave energy resource characterization of the Atlantic Marine Energy Test Site, *Int. J. Mar. Energy*, 2013: 1, pp 3–15.
- [2] Scheffer, H-J., Fernando, K.R.M.D. and Fittschen, T., Directional wave climate

study south west coast of Sri Lanka, Sri Lankan – German Cooperation, CCD-GTZ Coast Conservation project, 1994.

[3] Ranasinghe, D. P. L. & Gunaratne, P. P., Assessment of nearshore wave climate in southern coast of Sri Lanka, Annual

Research Journal of SLSAJ: 2011: 11, pp. 43-51.

[4] Cahill, B.G., and Lewis, T., Wave period ratios and the calculation of wave power, Proceedings of the 2nd Marine Energy Technology Symposium, Mets2014, Seattle, WA, USA, April 15-18, 2014.

# Rainfall Variation on Hydro Power Generation in the Victoria Reservoir

W.M.T.T.K. Samarakoon<sup>1</sup>, K.W.G.Rekha Nianthi<sup>2</sup>

*Department of Geography, University of Peradeniya, Sri Lanka*  
<sup>1</sup>Thilochanasamarakoon92@gmail.com  
<sup>2</sup>rekhanianthi@yahoo.com

## Abstract

The main objective of this study was to examine the rainfall variation on hydropower generation (HPG) in the Victoria Reservoir (VR). Rainfall, active energy generation and reservoir water level data (1996-2015) have been used for trends and correlation analyses. A questionnaire survey was conducted to find out the management issues on hydropower generation from working engineers and management officers. This study found that the hydropower generation primarily depends on the variation of seasonal rainfall. VR water level mainly depends on Southwest and Northeast Monsoon rainfall. The total active energy generation in VR has been changing. Seasonal rainfall and active energy generation (GWh) had a positive correlation (0.7). Hydropower generation and VR water level (m) had a positive correlation (0.7). Energy generation and water consumption volume (mcm) of Victoria reservoir had a positive correlation (0.9). Annual average rainfall of monthly rainfall and the annual average water level had a positive correlation (0.5). The trend of energy generation ( $R^2=0.03$ ), water level ( $R^2=0.18$ ) and water consumption ( $R^2=0.37$ ) have fluctuation pattern. This reservoir water level can be changed with water release of Polgolla barrier and rainfall in the Victoria catchment. Therefore, a clear trend cannot be identified in the energy generation in VR. Nawalapitiya, Peradeniya and Victoria showed increasing (Positive) trend pattern but the trend is not significant. Teldeniya, Deltota and Kundasale have shown a decreasing (Negative) trends but not significant. Engineers have suggested, building mini hydro power stations are more important in the country. They expect to start the second stage of the VR development project. It will mobilize a large amount of rainwater for hydropower generation in the country. However, the long-term accessibility of rainfall data and other relevant data are required for further analysis.

**Keywords:** hydro power, generation, rainfall, reservoir, correlation, trend

## Introduction

Many countries are using rivers and waterfalls for generating hydroelectricity in fulfilling their energy needs and Sri Lanka is also identified as one such country. Victoria reservoir is one of the most important reservoirs for Hydro Power Generate (HPG) in Sri Lanka. Victoria catchment area is 1,869 km<sup>2</sup> and surface area is 23 km<sup>2</sup>. The total capacity of the reservoir is 722,000,000 m<sup>3</sup> and active capacity is 689,000,000 m<sup>3</sup> [1]. The Victoria power station has three turbines. The nearly half a kilometer long Victoria Dam is playing a significant role on the national grid adding power generated by three turbines. The installed capacity is 210 MW and annual average power generation is 780 GWh. This power station generates high-level power capacity more than other reservoirs. The total amounts of the seasonal rainfall and HPG have a close relationship. However, the power generating process depends on reservoir water and reservoir water depends on rainfall. Sri Lanka faces an increasing demand for electricity. This has grown gradually over time due to the increase of average per capita electricity consumption. As a solution to this, Sri Lanka has taken a policy decision to move towards thermal and coal for electricity generation.

Sri Lanka HPG capacity has been changing with the variation of seasonal rainfall. Sri Lanka has four major climatic seasons. These are First Inter-Monsoon (FIM) from March to April, South West Monsoon (SWM) from May to September, Second Inter-Monsoon (SIM) from October to November and North East Monsoon (NEM) from December to February. Monsoonal, Convective and Orographic rainfall account for a major

share of the annual rainfall in Sri Lanka. The mean annual rainfall varies from 900 mm in the driest parts (south-eastern and north-western) to over 5,000 mm in the wettest parts (western slopes of the Central Highland). The mean annual temperature in Sri Lanka has homogeneous temperatures in the lowlands and decreasing towards the highlands. The coldest month with respect to mean monthly temperature is generally identified as January, and the warmest months are identified as April and August [2].

Sri Lanka has three hydroelectric complexes i.e. Laxapana, Mahaweli and Samanala. Sri Lankan Government is planning to establish new projects to increase the HPG. Victoria is most importance hydropower reservoirs of the Upper Mahaweli Catchment. The Victoria reservoir has the steepest gradient and the largest capacity at full supply level. The rainwater is high in Victoria from May to August [3]. Continuous rainfall will enable the reservoir water levels to spill soon and the decreased rainfall has severely reduced HPG. While in fewer rainfall years, the country is forced to rely heavily on thermal power generation. According to the research, the receding water levels in hydropower reservoirs have dropped HPG down to 1.6% and the thermal power generation has increased up to 82.5% [4]. During early May in 2012 due to the heavy rainfall, the generation of hydropower electricity increased up to 23% but it has declined again when dry weather condition in the same year. The total active storage in the hydropower reservoirs has come down to 25% and water level in the hydropower reservoirs have gone down due to the prevailed dry condition in the same year. As a result, the active storage

level has dropped nearly to 20% in the Victoria reservoir, 30% in the Kotmale reservoir and 31% in the Randenigala reservoir [5].

A key factor that controls the output of a hydropower plant is the availability of water which depends on the rainfall in Victoria catchment area. There would be a close correlation between the rainfall and the generation outputs [6]. Diversion of water for irrigation could also reduce the generation output. Sri Lanka's HPG has been increased significantly following heavy rains in the catchment areas of the reservoirs. Normally, before rain begins the HPG get down about to 20% but with the good rainfall and torrential rains it can raise up to 85% in Victoria, Castlereagh 92%, Maussakale 62%, and Kotmale 85%. In parallel to the dramatic increase in HPG the thermal generation had been reduced up to about 40%. Sri Lanka's climate has been changing. Variability of SWM, NEM and convectional rain are noticed. These changes will have direct impacts on water availability for HPG.

Stream-flow and pool elevation are related to Geological factors. Operation and management factors are directly linked to turbine efficiency because turbines have played a major role in HPG. Deforestation, improper land use practices and siltation can be considered as some other factors. Deforestation in upper catchment causes heavy soil erosion and causes siltation in the catchment areas. As a result significantly reducing their water capacity and decreasing in HPG [7]. Both the bed and suspension load downstream and large amounts are deposited in the multipurpose reservoirs leading to a reduction of their storage capacity and as a result, decrease the HPG. There has

been a slight decline in hydropower consumption in the country since 1995. Most probably due to the decrease of power generated caused by the reduction of storage capacities in reservoirs [8]. Deforestation may lead to electricity shortages in tropical rainforest region that rely heavily impacts on hydropower. The wider deforestation can reduce overall rainfall and therefore HPG might be able to decrease. The prevailing climatic conditions and topography of the land have created excellent conditions that are well situated for the HPG in Sri Lanka. Rainfall is an important factor of climate. Inter Tropical Convergence Zone (ITCZ) is moving above the equator and Sri Lanka makes an important role in the variability of seasonal rainfall and has a significant relationship with HPG. The Central Highland topography is another most important feature of rainfall distribution in Sri Lanka. Central Highland controls the rainfall in its windward and leeward side. As a result, the western part of the Central Highland gets higher rainfall than the eastern part of Central Highland during the SWM. Therefore, Orographic rainfall also plays an important role for HPG.

Seasonal variability of rainfall is noticed in Sri Lanka. As a result, the Sri Lankan Government suggests power cut program especially during the dry season covering all islands. People are engaging with electricity for their day to day; domestic, industries, factories, office activities and etc. On the other hand, HPG is directly linked to the economy of the country. Due to rainfall variability and with the dry spells the HPG also fluctuate and it may influence the economic activities. For example, availability and low cost of electricity supply is a vital factor in manufacturing

industry. Therefore it is necessary to find the relationship between rainfall and electricity generation especially with changes in seasonal rainfall. The primary objective of this study was to examine the relationship between seasonal rainfall variations and HPG in Victoria reservoir. This study also examined the relationship between reservoir water level and power generation. Existing management issues of the Victoria reservoir also taken into consideration.

Victoria reservoir located at elevation 340 m to 440 m and the upstream dam site is 1338 km<sup>2</sup>. This power station is generating high-level power capacity of more than other hydropower reservoirs in the country. This power station started on 14<sup>th</sup> April in 1985.

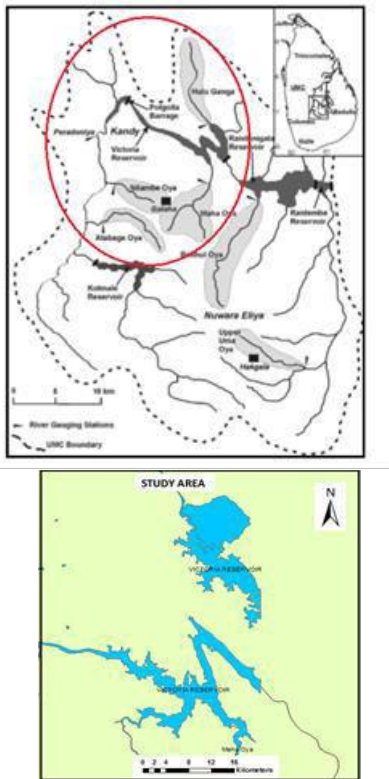


Figure 1: Victoria reservoir and catchment area

## Material and Methods

Both quantitative and qualitative data have been used for this study. This research mainly depends on secondary data such as; rainfall, HPG and reservoir water level. These data have been collected from the Victoria power station and Natural Resources Management Centre (NRMC). Monthly operational report of Victoria power station, related research papers, books, newspaper articles, and websites are also used to gather information. Primary data collection has been done through an interview and questionnaire survey especially to identify the management issues of Victoria power station. Working engineers and management officers of Victoria power station have been interviewed to capture the management issues.

Data on rainfall, reservoir water level, Hydro Power Generation have been collected. Rainfall data were collected from 06 weather stations of Victoria catchment from 1996 to 2015. These stations are Nawalapitiya, Peradeniya, Delthota, Kundasale, Teldeniya, and Victoria (Adhikarigama). Data is not available some stations in some years but taken the average values where applicable. Rainwater of these stations is drained to the Victoria reservoir. Due to the difficulties of free rainfall data/purchasing system in Sri Lanka, it is unable to get long-term records for this type of important research.

Ms-Excel Software was used for the data analysis. Arc GIS software used to create study area map. Linear regression trend and correlation analysis were used where necessary for data analysis. A positive correlation indicates the extent to which those variables increase or

decrease in parallel, a negative correlation indicates the extent to which one variable increases as the other decreases i.e. Correlation,  $r$ , is limited to  $-1 \leq r \leq 1$  (For positive association,  $r > 0$ ; and for a negative association  $r < 0$ ). Following equation is used for calculation of correlation.

$$r = \frac{\sum(x-\bar{x})(y-\bar{y})}{\sqrt{[\sum(x-\bar{x})^2 \sum(y-\bar{y})^2]}}$$

Least squares regression analysis has been engaged for trend analysis with algebraic line expression, with the regression line is written as: Here,  $b_0$  is the y-intercept and  $b_1$  is the slope of the regression line.

$$\hat{y} = b_0 + b_1x$$

## Results and Discussions

### Monthly, annually and seasonal rainfall variation of the Victoria Catchment

Victoria catchment receives well total annual rainfall than other reservoirs of Mahaweli complex. Victoria reservoir catchment is distributed of both wet and intermediate zones in the Kandy district. As a result, Victoria reservoir has been received rainfall from both South West Monsoon and North East Monsoon.

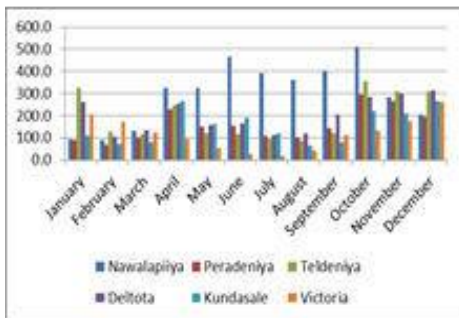


Figure 2: Monthly average rainfall variation of the selected 6 stations of Victoria reservoir catchment

Figure 2 showed the monthly average rainfall of selected 06 stations. Nawalapitiya gives high rainfall from May to September including April. Highest rainfall gives from October and second from June. When considering the total rainfall from all the station high amount is contributes in months of October and November because Second Inter Monsoon in Sri Lanka receives rainfall from depressions originated in the Bay of Bengal.

Table 1: Observed total annual average rainfall at selected Meteorological stations in Victoria Catchment

Rainfall station and data period	Rainfall (mm)
Nawalapitiya (1995-2015)	3,586
Peradeniya (1995-2015)	1,899
Teldeniya (2011-2015)	2,265
Deltota (1995-2004)	2,412
Kundasale (2005-2015)	1,769
Victoria (1996-2015)	1,312

Table 01 show that the total annual average rainfall is higher in Nawalapitiya station and lower in Victoria rainfall station. In percentage 27% rainfall is from Nawalapitiya, 10% from Victoria, 14% from Peradeniya, 17% from Teldeniya 18% from Deltota and 13% from Kundasale.

Seasonal rainfall is very important for agriculture and hydropower generation in the country and therefore climatic seasons primarily depend on seasonal rainfall.

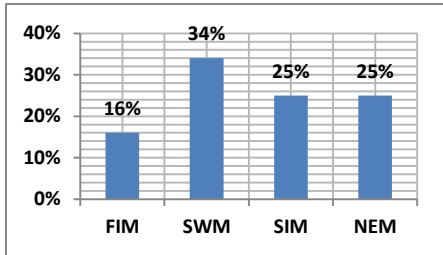
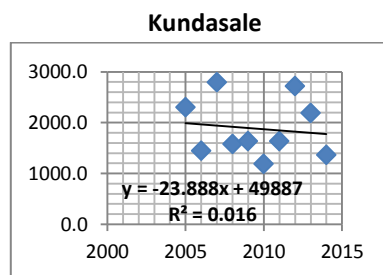
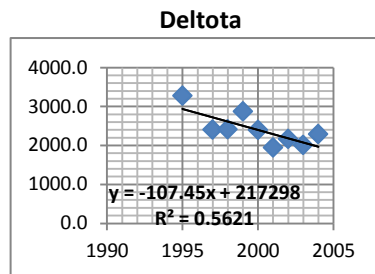
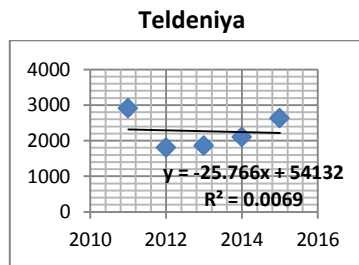
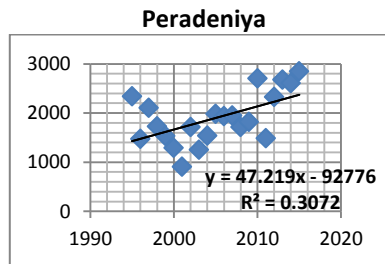
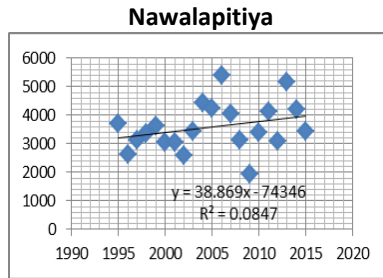


Figure 3: Seasonal average rainfall variation of the selected 06 stations of Victoria reservoir catchment

Figure 3 shows the seasonal rainfall variation of Victoria reservoir catchment under the NEM, SWM, FIM and SIM. North East Monsoon is distributed from December to February. Generally, NEM is receiving high rainfall for the Eastern part of the Central Highland. However Victoria reservoir is situated between wet and intermediate zone, as a result, this reservoir has received rainfall from all the seasons but mostly from SWM. It was 34% (742 mm), SIM (25%: 541 mm) and NEM and FIM show similar percentage as 25%. FIM was 16% (341 mm) and has contributed less amount of rainfall compared to other seasons in the Victoria catchment.

**Trend of mean total annual rainfall in Victoria catchment**

Linear trend (mm/year) in monthly average rainfall at different Meteorological stations in Victoria catchment is shown in the figure 4. The value in the formula represents the slope or trend (a). The positive sign (+) indicates a positive trend and the negative sign indicates a negative trend.





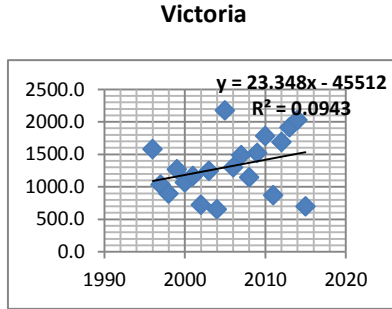


Figure 4: Trend of annual mean of monthly mean rainfall in victoria catchment in different time scale

The trends of annual mean rainfall over different years were obtained using linear regression best fit lines. The linear regression trends with their linear regression equations and coefficient of determination for selected years are represented in figure 4 (for all the selected rainfall stations).

This figure shows the trend of rainfall pattern at selected stations of Victoria catchment. The selected rainfall stations showed a linear trend pattern in different time period. Nawalapitiya, Peradeniya and Victoria showed increasing (Positive) trend pattern but the trend is not significant. Teldeniya, Deltota and Kundasale have shown a decreasing (Negative) trends but not significant.

**Relationship between rainfall and HPG**

Rainfall and HPG have a close relationship because hydropower primarily depends on water resources. Most of the hydropower reservoirs fulfill their water needs by rainfall. Sri Lanka has a good rainfall pattern in all over the year. As result in Sri Lanka’s HPG is mainly depends on rainwater. Sri Lanka electricity primarily depends on thermal

heat and hydropower. Hydropower electricity supply more than 20% energy needs in Sri Lanka. Victoria Power station is an important hydropower generation reservoir in the upper Mahaweli catchment. It is supplying energy to the national grid than other hydropower stations. Total HPG is oscillating between 289 to 1,186 GWh annually from 1996 to 2015. Figure 5 shows that during the study period, from 2000 to 2005 were continuously recorded as below the average of energy generation in the Victoria power station. Power was decreased by (-297 GWh) in 2005. During this period Sri Lanka had been faced long-term dry spells with drought period.

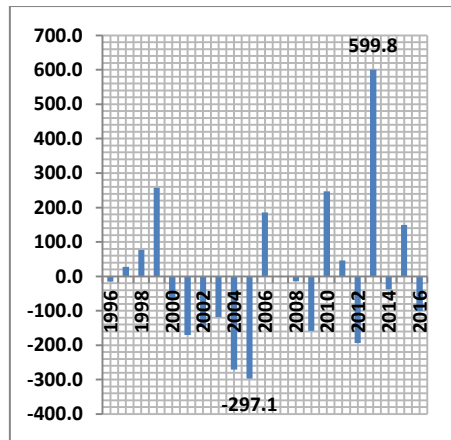


Figure 5: Deviation of total active energy generation in victoria power station (GWh)

With the low amount of rainfall, hydropower generation was rapidly decreased. In 2001 it was decreased by -170.6 and 2009 by -157.9. Year 2013 was a very important year at the Victoria power station. In this year Victoria has been generated maximum hydro energy than other years during the study period. The value was 1,186 GWh and it was about 600 GWh above the average. Further, in 1998, 1999, 2006, 2010 and 2015 generated above the average. In 1999 total power generation was nearly

844 GWh, in 2010: 833 and 2013: 1,186. After year 2013 had been received a low amount of rainfall in the catchment area. As result, Sri Lanka faced again dry seasons in 2014. As a result, HPG was decreasing during the period.

Apart from the less rainfall, the other main reason of decreasing HPG during the dry seasons is, the energy production was controlled by the power station management board. Even though when drought continues as long months, the authority tries to supply their products to the national grid. The best example is 2004 and 2005. As a solution for the dry periods, they were reducing their production but engage with another source of power generation. They were generated maximum energy from coal or thermal heat during the drought period.

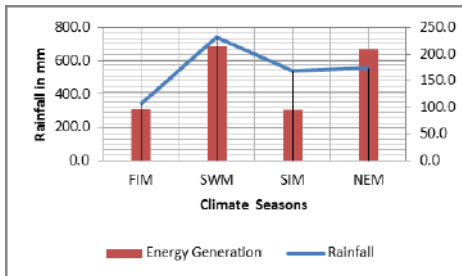


Figure 6: Seasonal variation between rainfall and power generation in Victoria.

Energy generation is changing the amount of seasonal total average rainfall. Figure 6 shows their relationship. From SWM and NEM rainfall and power generation has a positive relationship. Power generation is higher in SWM and NEM. The SWM is very important in Sri Lanka because a large amount of rainfall receive from this monsoon in the western part of the Central Highland.

### Management issues of Victoria Power station

Victoria reservoir belongs to the Mahaweli Authority (MA) and Victoria power station is belongs to the Ceylon Electricity Board (CEB). Therefore both institutions shared the management process of the Victoria. As a result, some management issues have been created among institutions. Institution management regulations are a different one to another. MA has allotted for Victoria reservoir. But CEB has not allayed about. The major task of CEB is to generate hydropower using reservoir water. After discussing between CEB and MA they release reservoir water for power generation. CEB should discuss with MA and should get the permission to release water to Randenigala reservoir after power generation. They released the amount of water after approved by MA. CEB has not had the responsibility about water management activities in Victoria reservoir since CEB haven't acquirement about this reservoir. Mahaweli Authority is continuing management part of Victoria reservoir. But CEB uses reservoir water for their energy generation; they aren't subscribing management water at Victoria and it now is a problematic issue. Victoria power station generates energy only for daily national consumption. Then they aren't trying to maximize energy generation in daily. From 1996 to 2016 period Victoria power station has generated average maximum energy only one time. In 2013, it was 1,186 GWh. It is controlled by the Center of the electricity system. However, CEB is carrying out some program for to minimize power cuts and give the quality service for customers. Normally CEB carries out active maintenance of the station with a

regular timetable and checked the quality of equipment in power stations from time to time. They also have the security system of the transmission network, update system, clearance system to the dangerous buildings and other physical barriers close to the energy transmission and distribution network.

## Conclusion

This research examined the impact of seasonal rainfall variation and relationship between rainfall and HPG at Victoria. Victoria is the largest hydropower reservoir in the upper Mahaweli catchment. It is distributed between wet zone and a small patch of the intermediate zone in Kandy District. From SWM, NIM, FIM and SIM rainfall received Victoria catchment in all over the year. As a result, Victoria reservoir obtains the water from all seasonal rainfall. Then an HPG is changing with the amount of rainfall and water level of the reservoir. HPG has a positive correlation with rainfall and reservoir water level and positive correlation between reservoir water level and HPG. The study revealed that seasonal rainfall has varied at Victoria catchment and it is affecting some fluctuated with time to time. As well as HPG is changing with reservoir water level at Victoria. From this study is introducing some recommendation for increase HPG is Sri Lanka. Especially today, most of the countries are using hydropower as renewable energy. Engineers have suggested that it is necessary to start the second stage of the Victoria development program. Definitely, it will mobilize the large amount of rainwater HPG as well as support for the cultivation purposes. To build mini hydro power stations gets maximum efficiency from

rainwater in Sri Lanka is also one of the suggestions. Many of tributaries and rivers are supplying water from Victoria reservoir. CEB has no active program for control sedimentation in the major reservoir. It is carried out by Mahaweli Authority. But nowadays Victoria reservoir is affected by siltation. The siltation is very dangerous problems for the hydro reservoir in the Upper Mahaweli catchment.

## Recommendation

In order to increase the power generation, it is necessary to control the siltation and remove the excess siltation from the Victoria reservoir. It will support to increase electricity supply of the Sri Lanka. Relevant authorities should take immediate implementation program for remove the silt from the Victoria. It is necessary to start the second stage of the Victoria development program it will mobilize the large amount of rainwater for HPG. The build of mini hydro power generation stations will get maximum efficiency from rainwater in Sri Lanka.

## References

- [1] (<http://wikipedia.org/victoria-dam> Mahaweli Authority of Sri Lanka)
- [2] Rekha Nianthi, K.W.G. (2012). Climatological Research in Sri Lanka, Godage International Publication, S. Godage and Brothers (Pvt) Ltd, ISBN: 978-955-30-2975.
- [3] Silva, E. A. S. (2000). Hydraulic changes of three reservoirs (Minneriya, Udawalawe and Victoria) in Sri Lanka. Kandy: Institute of Fundamental Studies

- [4] Sanderatne, N. (2014). Drought could impact adversely on economic performance, Sunday Times (<http://www.sundaytimes.lk/140309/columns/drought-could-impact-adversely-on-economic-performance-88254.html>).
- [5] Bandara, H, (2012). CEB losses rise with drop in reservoir levels: Thermal power replaces hydropower as south-west monsoon fails to deliver, Sunday-Times, [http://www.sundaytimes.lk/120617/News/nws\\_15.html](http://www.sundaytimes.lk/120617/News/nws_15.html).
- [6] Rathnasiri, J, (2016). Electricity traffic increases improve efficiency and cut losses first, National Academy of Science.
- [7] Rodrigo, C. A. S., (2014). Drained out or new potential: Hydro power and Sri Lanka's energy challenge. The island.
- [8] Hewawasam, T, (2009). Effect of land use in the upper Mahawali catchment area on erosion, land slide and siltation in the hydro power reservoirs in Sri Lanka. Sri Lanka: National Science Foundation.

# The Development of Marine Renewable Energy in Sri Lanka

Matt Folley<sup>1</sup>, Prasanna Gunawardane<sup>2</sup>

*Department of Mechanical Engineering  
University of Peradeniya, Sri Lanka*

<sup>1</sup>m.folley@qub.ac.uk  
<sup>2</sup>sdgspg@pdn.ac.lk

## Abstract

Sri Lanka, along with all other developing nations, needs to increase the amount of power that it generates whilst limiting any increase in greenhouse gases to satisfy the Paris Climate Accord. This agreement requires increasing the amount of power generated using renewable energy resources, which includes marine renewable energy. As a highly-populated island nation that has a significant tourism industry, there is a limit to land-based development of wind and solar energy due to various factors such as visual intrusion and land availability. Consequently, although wind and solar energy may be able to make a significant contribution, alone they are unlikely to be able to meet the future required supply of renewable energy. Unfortunately, marine renewable energy is still at the pre-commercial stage, which means that it could not immediately contribute to the Sri Lankan energy supply and further development is required. However, this presents an opportunity for Sri Lanka to create a pre-eminent research and development centre for marine renewable energy technologies in the region, particularly as no centre of this kind currently exists. This paper proposes a range of support mechanisms and activities that would be required for Sri Lanka to grasp this opportunity and the associated potential benefits that would be accrued if this were achieved.

**Keywords :** research, marine, wave, policy, renewable, investment

## Introduction

It is almost universally recognised that climate change is being to have a large impact on the world, associated with increased extreme weather events and changes in weather patterns. Moreover, it is also recognised that the generation of energy through the burning of fossil fuels is a major contributor to climate change and that there is a need for more non-fossil fuel energy sources of energy to be developed to limit future changes to the climate. Although nuclear power is proposed as a potential solution, the vast majority of fossil fuel energy is expected to be replaced by renewable sources of energy such as wind, solar, geothermal, wave and tidal energy.

For any country the challenge of moving from a fossil fuel based economy to one based on renewable energy is enormous. This challenge is amplified for countries, like Sri Lanka, whose demand for energy is continuing to grow as the standard of living increases for the general population. That is, not only does the energy generated from fossil fuel power plants have to be replaced, but additional power plants are also required to meet the increasing demands. Despite this challenge, the Sri Lankan government has shown itself to be fully committed to renewable energy with the pledge made at the 22<sup>nd</sup> UNFCCC Conference of Parties in Marrakech, Morocco, as part of the Climate Vulnerable Forum, to use only renewable energy for electricity generation by 2050 [1].

The scale of the task facing Sri Lanka should not be under-estimated. In a report funded by the Asian Development Bank (ADB) it is estimated that the installed electricity generating capacity

will increase from 3.7 GW to 34 GW by 2050, and that this will require an investment of US\$54-US\$56 billion [2]. The report sets out an ambitious development programme so that by 2050 Sri Lanka will have installed 15 GW of wind turbines and 16 GW of solar panels, the balance being made up of hydropower plants and other renewable energy sources. The potential for marine renewable energy is not included, but it is recognised that it “there is a need to conduct detailed assessments to explore their feasibility and viability in Sri Lanka” [2].

Although the ADB presents a potential scenario for Sri Lanka to become 100% renewable by 2050, it also identifies a number of challenges that must be overcome for this to be realised. One of the challenges identified is the need to install ancillary equipment to manage the inherent variability of supply from renewable energy. In addition, it may be expected that environmental considerations linked to the tourism industry is an additional challenge. The deployment of wind turbines in the UK, USA and Europe has attracted a large amount of opposition due to the visual intrusion [3]. Modern wind turbines may have a height to the nacelle of more 100 metres and can be seen from a large distance, especially as an ideal location for wind turbine deployment is high ground. The importance of tourism to the Sri Lankan economy means that this additional challenge must be considered and may significantly reduce the number of wind turbines that can be installed and thus limit the potential contribution from wind power. Similar objections have also been made to solar farms, which although at ground level must cover a very large area to generate significant amounts of energy and in

sensitive areas this could be problematic. This issue of visual intrusion could put a serious hole into the proposed energy development plan for Sri Lanka. Marine renewable energy, specifically wave and tidal energy, has the potential to help overcome these two challenges.

The challenge associated with the variability of supply can be met as the difference in the seasonal/daily load profile of marine renewable energy when compared to wind and solar power means that total variability of the supply is likely to be reduced. The extent to which the variability is reduced will depend on the characteristics of the generating plants, their location and the climatic variation. Thus, determining the reduction in variability will require detailed modelling, but any reduction in the estimated US\$5 billion [2] required for load balancing must be considered as beneficial.

The challenge associated with the visual intrusion of wind turbines may mean that although Sri Lanka is estimated to have the technical potential to install 24 GW of wind turbines [2], this does not mean that 15 GW can be installed without upsetting the tourism industry. In contrast, marine renewable energy converters typically extend only a few metres above the mean water surface level and many concepts are fully submerged. Consequently, the visual impact and thus environmental objections to marine renewable energy plant are likely to be significantly reduced.

Located in the Indian Ocean, at the southern tip of India, Sri Lanka has a reasonable wave energy resource that is greatest along the southern coastline. The average wave power density along

this coast is estimated to be approximately 15 kW/m [4], which is considered suitable for the deployment of wave energy converters. A detailed study of the tides and marine currents around Sri Lanka has not been undertaken, but initial expectations are that tidal energy is limited as velocities over 1.5 m/s are typically required [5]. The Sri Lanka wave resource in particular has attracted a number of international companies who have expressed an interest in developing wave energy in Sri Lanka [6, 7]; however, to date, no prototype marine energy converter has been deployed in Sri Lanka.

The above indicates that marine renewable energy could make a significant contribution to the target of 100% renewable energy by 2050, but little progress is currently being made. To understand why marine renewable energy technologies are not being developed and/or deployed in Sri Lanka this paper first considers the current status of marine renewable energy development from a global perspective. Then, the barriers to the development of marine renewable energy are then considered before the presentation of a road-map for the development of marine renewable energy in Sri Lanka.

### **Status of Marine Renewable Energy Development**

Based on the number of companies that are developing marine renewable energy technologies it could be inferred that the industry is in very good health. This is supported by reports produced by the European Union [8] and the US Department of Energy [9] that estimate that marine renewable energy is expected to make a significant contribution to the energy market

sometime in the period 2020 – 2050. However, a careful analysis of these companies and reports shows that marine renewable energy is currently in the pre-commercial stage. This means that it is not possible to buy a marine renewable energy technology in the same way you would for a wind turbine or solar panel. This does not mean that the technology is necessarily any less commercial-viable, but that the investment and development work required to achieve commercial-viability has not yet been made.

To understand this current status of marine renewable energy it is necessary to look at how it first came to prominence during the oil crisis of the 1970s. At this time there was a large fear in Europe, and the UK in particular, that the lights would go out and there was a need to reduce dependence on imported oil. This meant that the first prototypes of wave energy converters were ambitiously large and expensive. Although the focus of marine renewable energy has shifted since the 1970s from fuel independence to combating climate change, the focus on utility-scale prototypes remained.

Developing a completely novel concept from the drawing-board to full-scale prototype is extremely expensive and risky. An example is the Pelamis wave energy converter that had spent an estimated US\$100 million on deploying three different prototypes before going into receivership. Aquamarine Power Ltd spent a similar amount of money on two prototypes before encountering the same fate as Pelamis. However, the moral of this story is not that wave energy is not commercially viable, but that developing a novel concept at such a large-scale is not sensible. It is

equivalent to the Wright brothers deciding to build a transatlantic passenger liner rather than a single-seater plane that could at first only fly a few kilometres. Similarly, giant 5 MW wind turbines were not developed in isolation, but only after the gradual understanding developed from smaller turbines.

There is now a growing recognition within the marine renewable energy industry that the first devices will need to be smaller and thus suitable for niche markets [10]. Such markets could be isolated communities or islands, anywhere where the cost of energy is high and marine renewable energy exists. This is not to lose sight of the bigger prize, the utility-scale converters, but it is recognition that it is necessary to start small and get bigger. However, it may be expected that whoever is able to develop the first small-scale technologies will be in an ideal situation to exploit the opportunities when the utility-scale technologies become viable. Moreover, these opportunities will not only exist for the technology developer, but also for all of the associated companies that may have been responsible for Operations and Maintenance, mooring line design and deployment or a myriad of other activities that are required when developing a novel technology.

This brings us to the current situation in marine renewable energy development. The large investments required for the development and deployment of a utility-scale technology have been frightened off by the high-profile “failures” of Wavegen Ltd, Pelamis Power Ltd and Aquamarine Power Ltd. Consequently, companies looking to develop their technology are starting to focus on smaller scale technologies



suitable for niche markets. Unfortunately, the European, Japan and USA government strategies are still focused on utility-scale technologies, leaving the companies to search elsewhere for development opportunities. At the same time, other countries are doing very little to develop marine renewable energy technology, typically hoping to simply buy a commercial product that has been developed in elsewhere. This means that Sri Lanka could grab this opportunity to attract these companies to develop their technologies in Sri Lanka, in a mutually beneficial arrangement. However, to attract these companies, the barriers to development (as seen by a commercial company) must first be understood. This is the subject of the next section.

### **Barriers to Marine Renewable Energy Development**

The barriers to marine renewable energy in Sri Lanka can be separated into two basic types. There are barriers to the pre-commercial development of marine renewable energy technologies and barriers to the commercial development of marine renewable energy technologies. Any company that is interested in investing to Sri Lanka will be concerned about both of these barriers, but it is likely that because marine renewable energy is currently in the pre-commercial phase of development it is the barriers to pre-commercial development that are most relevant to the company.

Almost all companies that are known to be developing marine renewable energy technologies are small or medium-sized enterprises (SMEs). This means that both financial and human resources are typically very limited. Thus, although a

company may have sufficient resources to develop their technology, they often struggle to have sufficient resources to develop a project. In this case, a project is the planning and implementation of the deployment and operation of a marine renewable energy converter. During the commercial phase of a technology the project costs (both in terms of financial and human resources) are often only a small proportion of the total costs. This is because the technology is well-proven and the processes for obtaining consent and operating the plant are well refined and highly efficient. Conversely, during the pre-commercial phase of development the project costs can be the dominant costs as the consenting and operational processes is generally poorly understood and defined the regulators leading to the requirement for multiple iterations. Alternatively, the lack of understanding can lead to overly-cautious and highly demanding consenting and operational processes. In either case the effect is to dramatically increase the expense and time required for the project, dramatically increasing costs.

A significant proportion of a project's cost for the marine renewable energy industry is the cost of producing a sufficiently high-quality set of resource data, which tells the company what power may be generated and the largest waves to expect. For other renewable energy sources (wind and solar) adequate data already exists at little or no cost to enable project planning. Unfortunately, this is not the case for marine renewable energy. Moreover, the cost of collection/ generation of data to assess the marine renewable energy resource is significantly higher than for the wind or solar resource as both the equipment and deployment of the

required instrumentation are more costly. This often means that a company will limit its search for suitable deployment locations to those locations where high-quality marine renewable energy resource data already exists.

Another important project cost in the pre-commercial phase is associated with obtaining the required permissions for deployment and connection to the grid (if appropriate). It is not uncommon for it to be required to obtain permission from more than a dozen governmental or semi-governmental institutions for a single deployment. For each of these institutions to fulfil their role they will rightly request information from the company deploying the marine renewable energy technology. This may not only be a time-consuming process, possibly lasting a number of years, but also potentially costly where additional information needs to be generated such as would be required to produce an Environmental Impact Assessment. The limited funding available to most marine renewable energy technology developers means that they are adverse to entering a process that may result in a significant delay to their deployment, together with the risk that any one of the institutions could stop the deployment result in the loss of both the time and money invested into the project. Consequently, most marine renewable energy companies will be drawn to locations where there is the least risk of delays in obtaining permission to deploy and obviously where the costs are known and reasonable.

A further project cost is the production of a suitable supply chain for the particular marine renewable energy technology being deployed. Producing a supply chain means the identification of

a set of companies that stock (or can produce) the required parts and/or have the skills required for the construction, operation and maintenance of the technology. This supply chain can generally be separated into two distinct elements, an international supply chain and a local supply chain. A marine renewable energy company will typically already have a well-developed international supply chain, which includes highly-specialised components that may have been developed in collaboration with the marine renewable energy company. Ideally, the local supply chain will provide the rest. The locality of the suppliers will have an impact on both time and cost, with the more local companies expected to be both more responsive and cheaper. However, it is critical for the marine renewable energy company to be confident that the components and/or services supplied are of a high-quality so as not to put the success of the project at risk. The process of producing a high-quality supply chain can be very time-consuming, especially for the local supply chain, as assessing the quality of a supply company can be a slow process (especially in a foreign country). As a consequence it is common for marine renewable energy companies to use well-known and reputable international companies for their supply chain, knowing that they are paying significantly more than required to obtain a certain degree of confidence.

The largest barrier to deployment of a renewable energy technology is often considered to be the price that will be paid for the energy generated. A variety of mechanisms exist for supporting renewable energy such as feed-in tariffs and carbon credits, which are effectively designed to increase the amount that is

paid for the renewable energy generated. However, whilst this may be relevant for a commercial renewable energy technology it is not generally a direct issue for a technology in the pre-commercial phase. This is because the income generated by the sale of electricity is typically only a small proportion of the total project costs and so the price does not significantly affect the project economics. Nevertheless, the existence of an attractive feed-in tariff or generous carbon credits can have an indirect impact on the project as it provides a clear demonstration of government support for the industry. Without clear government support it can be difficult for a marine renewable energy company to attract investors as there is a perceived risk that the project will not be completed due to some intransigence that could be overcome with government support. Thus, marine renewable energy companies will generally be attracted to deployments where there are good pricing support mechanisms, but not directly because of the actual support mechanism, but because of the perceived support for the nascent industry.

### **Sri Lankan Marine Renewable Energy Road-map**

It is important to recognize, that with respect to attracting marine renewable energy developers to Sri Lanka, the competition is global. That is, a marine renewable energy developer will go to whatever country in the world that best satisfies its requirements. A number of countries, including UK, USA, Ireland, Spain, France, Portugal, have developed policies to attract marine renewable energy developers with the creation of test centres and support services [11-17]. Significantly, none of these

countries are in Asia and equally importantly they remain focused on utility-scale technology development. This presents to Sri Lanka (and indeed all countries in Asia) with the opportunity to become the regional leader for the industry and the focus of marine renewable energy development in the region. However, this will not happen without Sri Lanka making a clear commitment to the industry and demonstrating that commitment internationally.

Sri Lanka can make a clear commitment to marine renewable energy by engaging in a 5-year development plan. Sensibly this plan needs to be structured to overcome the barriers to the development of marine renewable energy in Sri Lanka that were identified in the previous section. It is good to note that a start in this direction has already been made by the Sri Lankan Sustainable Energy Authority commissioning a wave energy resource assessment for Sri Lanka. Moreover, the proposed assessment is planned to be to international standards by following the IEC's (International Electro-technical Commission's) Technical Specification for Wave Energy Resource Assessment and Characterisation [18]. When completed this will provide wave energy technology developers with the data required to design their technologies as well as calculate their economic viability. Another indication of Sri Lanka's interest in marine renewable energy is the recent formation of the Marine Renewable Energy Association of Sri Lanka (MREASL). This association currently only consists of interested academics, but provides the platform for a broader association that includes industry and governmental organizations. With this membership the association would be

able to play an important role in providing a clear line of communication to support development of the marine renewable energy industry in Sri Lanka. It would also demonstrate to the international community that Sri Lanka is putting together a structure to support marine renewable energy development.

Although the commissioning of a wave energy resource assessment of Sri Lanka and the creation of MREASL are both encouraging, they are unlikely to be sufficient to overcome the barriers to the development of marine renewable energy in Sri Lanka. This will require the additional of three further support structures; policy support, creation of a marine renewable energy R&D facility and investment in human resources.

It is important to generate confidence in any investor in marine renewable energy that the government supports the industry through appropriate policy statements. These could include a specific feed-in tariff for marine renewable energy and duty exemption for the import of components used in the development of marine renewable energy technologies. In many ways the significance of any policy is more in the perceived support that it gives to the industry (thus generating confidence) than in the size of actual financial impact, which could be quite small.

The creation of a marine renewable energy research, development and test centre in Sri Lanka would have a considerable impact on the potential for the development of marine renewable energy in Sri Lanka. This could be achieved by reducing some of the most significant barriers to development. Specifically, a marine renewable test site could be pre-permitted for the

deployment of marine renewable energy converters. This would mean that developers would not have the uncertainty of obtaining permissions from a wide range of institutions, which would save them time, money and reduce risk. A marine renewable energy test site could also work to identify suitable local contractors and work with the developers in identifying a suitable local supply chain. Finally, additional infra-structure could be made available, such as office and workshop space that can all help to smooth the process of testing a marine renewable energy converter.

The final support structure required is the development of human resources in Sri Lanka. This would be through the provision of training courses and research programmes in the field of marine renewable energy. The training courses would mean that relevant people in institutions, industry and academia would understand the requirements of the nascent industry and be able to propose relevant solutions. An intensive 5-day course on wave energy is already proposed to be run in early 2018; similar courses should be planned on a regular basis to ensure Sri Lankan researchers, academics and companies are kept up-to-date. It is proposed that a small research programme is also started to investigate aspects of the marine renewable energy sector that are particularly relevant to Sri Lanka.

A detailed estimate of costs for the creation of a marine renewable energy test site and research programme is beyond the scope of this paper. However, some minimal indicative costs can be produced, which are detailed in Table 1 below. Depending on the site

and the facilities to be provided by the centre there may be additional costs associated with land purchase, cable installation, additional infrastructure, etc.

Table 1: Indicative costs

Item	Cost (LKR)
Instrumentation	5,000,000
Test Centre Director	1,800,000 / Yr
Technical Assistant	1,200,000 / Yr
Overheads	500,000 / Yr
Researchers (3)	2,200,000 / Yr
Equipment	500,000 / Yr
Travel	1,500,000 / Yr

Income from the marine renewable energy centre can be separated into two basic types; direct income and indirect income. The direct income will come from the hire fees charged to developers whilst their technologies are deployed at the test site. A variety of possible charging arrangements are possible, but it would seem that a reasonable fee would be LKR 10 million per year. This compares favourably with the cost of a berth at the European Marine Energy Centre, which charges the equivalent of LKR 50 million per year.

A marine renewable energy prototype typically costs in the region of LKR 100 – 500 Million and during development it would be expected to spend about 10 – 20% of this amount annually on operations, re-fits, maintenance, etc. The marine renewable energy test centre would be in an ideal position to provide some of these services, with an assumption of 10% of the annual prototype costs going to the test centre this would equate to an additional income of LKR 2.5 Million per prototype. This would result in a total direct income of LKR 7.5 Million per occupied berth.

Figure 1 shows the income and expenditure for the marine test centre for the first five years of its operation. The income is based on no berths being occupied for the first two years, one berth being occupied in the third year, two berths in the fourth year and three berths in the fifth year onwards. It can be seen that the income exceeds the expenditure even with only one berth filled and the net balance of the test centre (whose costs include the researchers) is positive after five years.

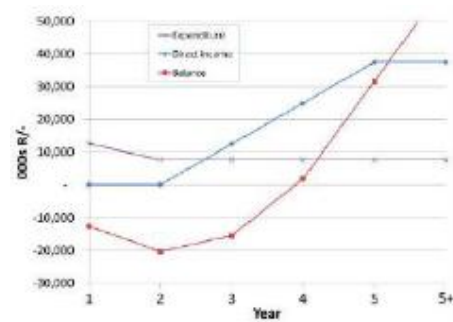


Figure 1: Balance for the test centre for 5 years

The indirect income from the test centre would be via the additional work generated for the local industry. Although it will be expected that the more specialised tasks will be done by external companies, there is still likely to be significant work in tender vessel operation, fabrication and fitting of non-specialised replacement parts, etc. If 50% of the annual prototype costs were to go to Sri Lankan businesses this would result in an annual boost to the economy of LKR 12.5 Million per occupied berth.

The final and potentially most significant impact that the development of a marine renewable energy in Sri Lanka is the creation of an industry that will be able to supply the international markets for marine renewable energy when this develops. The global marine renewable energy market is predicted to reach

US\$100 Billion by 2050. Even if Sri Lanka were able to capture only 1% of the market this would equate to more than 1% of the Sri Lanka total GDP. A more successful degree of market penetration could put the marine renewable energy at a similar significance to the national economy as rubber. This is a significant potential return for a very modest initial investment.

## Conclusions

The need for an increase in the amount of energy generated in Sri Lanka from renewable sources is generally accepted. This will not only help Sri Lanka to satisfy its commitments in the Paris Climate Accord, but also reduce dependence on imports and offer the potential for development of an indigenous renewable energy industry. However, the high population density and importance of tourism to the Sri Lankan economy means that the amount of solar and wind power is likely to be limited; marine renewable energy is a source of energy that could provide a significant contribution, but is currently in the pre-commercial phase of its development.

By making a small investment to encourage the development of marine renewable energy in Sri Lanka the opportunity exists to create an industry that can make a significant contribution to the Sri Lankan GDP of the future. Moreover, it is possible that returns on the investment can be made in the relatively short-term as international companies are attracted to Sri Lanka for testing, which has the twin advantages of inward investment and development of local knowledge and skills in the field. However, this opportunity is time-limited and if it is to be grasped then action

needs to be taken relatively promptly to maximise the potential benefits.

## References

- [1] Permanent Mission of Sri Lanka to the United Nations. Sri Lanka signs the Paris Agreement on Climate Change. Available: <https://www.un.int/srilanka/news/sri-lanka-signs-paris-agreement-climate-change>
- [2] Manpreet Singh et. al., 100% Electricity Generation Through Renewable Energy By 2050 — Assessment Of Sri Lanka's Power Sector. UNDP/ADB Report. Available: <http://www.adb.org>
- [3] C Jones and J Eiser. Understanding 'local' opposition to wind development in the UK: How big is a backyard? *Energy Policy*, 2010, 38(6), 3106-3117
- [4] H.W.K.M. Amarasekara. et.al. A Prefeasibility Study On Ocean Wave Power Generation For The Southern Coast Of Sri Lanka: Electrical Feasibility. *Int. J. Distributed Energy Resources and Smart Grids*. 2014, 10(2), 79-93
- [5] ABPmer. Quantification of Exploitable Tidal Resources in UK Waters. R.1349 Vol 1, 2007
- [6] Tidal Energy Today. Carnegie to harness Sri Lanka waves. Available: <http://tidalenergytoday.com/2016/09/30/carnegie-to-harness-sri-lanka-waves/>
- [7] Tidal Energy Today. WERPO to make waves in Sri Lanka. Available: <http://tidalenergytoday.com/2015/07/14/werpo-to-make-waves-in-sri-lanka/>
- [8] Davide Magagna. JRC Ocean Energy Status Report 2016. Publications Office of the European Union

- [9] US Department of Energy. Marine and Hydrokinetic Energy Projects. Available: [eere.energy.gov](http://eere.energy.gov)
- [10] James McCarthy-Price. Ripples to Swells: Iterative Development in Wave Energy. Available: <https://saltcompass.com/ripples-to-swells-iterative-development-in-wave-energy-d6922dcd4519>
- [11] European Marine Energy Centre. Available: [www.emec.org.uk](http://www.emec.org.uk)
- [12] Northwest National Marine Renewable Energy Center. Available: [nmrec.oregonstate.edu](http://nmrec.oregonstate.edu)
- [13] Biscay Marine Energy Platform (BiMEP). Available: [www.bimep.com](http://www.bimep.com)
- [14] WaveHub. Available: [www.wavehub.co.uk](http://www.wavehub.co.uk)
- [15] Danish Wave Energy Centre. Available: [www.danwec.com](http://www.danwec.com)
- [16] Atlantic Marine Energy Test Site. Available: [oceanenergyireland.ie/TestFacility/AMETS](http://oceanenergyireland.ie/TestFacility/AMETS)
- [17] Ocean Plug. Available: [www.oceanplug.pt](http://www.oceanplug.pt)
- [18] International Electro-technical Committee. TS62600-101 Wave Energy Resource Assessment and Characterisation

# Development of a Small Scale Sea Wave Energy Converter System to Generate Electricity

H.M.A.S. Samarakoon<sup>#</sup>, M.S.M. Safeer<sup>#</sup>, Y.V.L.S. Pushpakumara<sup>#</sup>,  
G. V. C. Rasanga<sup>\*</sup>, H.C.P. Karunasena<sup>#1</sup>

<sup>#</sup> *Department of Mechanical and Manufacturing Engineering, Faculty of Engineering,  
University of Ruhuna, Hapugala, Galle, Sri Lanka.*

<sup>1</sup> *chaminda@mme.ruh.ac.lk*

<sup>\*</sup> *Sri Lanka Ports Authority, Magalle, Galle, Sri Lanka.*

## Abstract

Sea wave is a high-density renewable energy source, which has a promising potential for mass scale power generation, providing a sustainable solution for the prevailing global energy crisis. Compared to conventional renewable energy sources such as solar and wind, sea wave energy is available for tapping throughout the year, irrespective of day and night. However, developments towards robust and efficient wave energy convertors (WECs) have been an ever challenge due to the critical dynamic and corrosive sea conditions. Although there have been many WEC systems developed internationally having their own pros and cons, applicability of those systems in Sri Lankan wave conditions is another challenge. Also, there has not been much research output from local researchers on this, particularly in the practical side. In this background, this research aimed to develop a small scale heave type WEC having theoretical energy extraction capacity of 50 W. The system is composed of a 100 l floater attached to a 2.5 m long oscillating structure hinged to a static base having a mechanical power transmission system having sprockets and chains, eventually producing a rotary motion of two flywheels connected to a common shaft. Both flywheel carry bicycle wheels where total of eight bicycle dynamos of 3 W capacity are attached such that the total installed generation capacity is 24 W (6 V (DC)). The system was tested in the sea in the Galle port and average power generation was observed to be 8.1 W, resulting in 33.9% overall efficiency of electrical power generation and 16.3% of overall efficiency of energy conversion from sea wave to electricity. Future work of this research will focus more on efficiency and reliability improvement of the system while increasing the generation capacity. The insights drawn from this research will be highly useful in generating electricity out of waves around Sri Lanka, providing a sustainable solution to the prevailing energy crisis.

**Keywords :** Sea wave energy extraction; Heave type wave energy converter; Renewable energy; Sea wave based power generation; Wave Energy Convertors (WECs);



## Introduction

With the ever rising global demand for energy, relying only on conventional methods of energy production has become challenge since they tend to be sparse and have already caused serious negative environmental impacts in heterogeneous processes of energy production [1]. In fulfilling this gap, a number of renewable energy sources are being researched, globally. Among them, one of the very attractive renewable energy sources is the ocean, which covers three quarters of the earth surface owning a huge amount of energy in different forms which can mostly be tapped via non-polluting means for generating electricity [2]. Ocean energy can be extracted mainly from the waves, tides, ocean currents, temperature gradients, and salinity gradients. Among them, wave energy conversion has been much researched due to its availability compared to wind and solar, and the high energy density [3].

In Sri Lanka, since from few decades, power generation based on renewable sources such as wind and solar have been researched and there are many commercial scale power generation units in operation all over the country. However, wave energy has just started being a popular topic and yet no significant research output or a commercial scale wave energy based power generation system in operation within the country, even though the country is surrounded by sea having 10–20 kW/m wave energy potential [4]. Wave energy being a varying capacity source by nature, numerous power control and storage techniques are essential in wave energy convertor (WEC) systems, while the adverse weather conditions and the corrosive sea

environment demand advanced mechanical and materials engineering inputs to develop reliable and efficient WECs [2]. At present, more than 40 WEC systems are at least in prototype stages, installed in off-shore, near-shore and on-shore locations, and broadly can be categorized in to three types: oscillatory water column, oscillating bodies and overtopping devices [4-8].

Although such different WEC systems are globally available, a tailor made system to match with local wave conditions is a timely requirement in the process of establishing a technologically sound environment in the country on wave energy to proceed to commercial scale units in time to come. In this background, this research focused to develop a small scale WEC system applicable to Sri Lankan sea conditions in order to directly generate electrical power.

## Materials and Methods

In this research, oscillating body system was selected as the base concept for the WEC, providing advantages over oscillating water column and overtopping technologies since, it can mainly be built at a relatively lower cost and can be installed conveniently as an on-shore system, providing convenience in installation and operation. Also, by considering the frequency and height of the sea waves in the south coast of Sri Lanka, oscillating body system can be justified as a viable technology. Figure 1 presents the basic configuration of the system developed in this research, having 50 W theoretical power extraction capacity at pre-determined average wave conditions in Galle port area of south region Sri Lanka (wave height: 1 m, frequency: 4-6 waves per

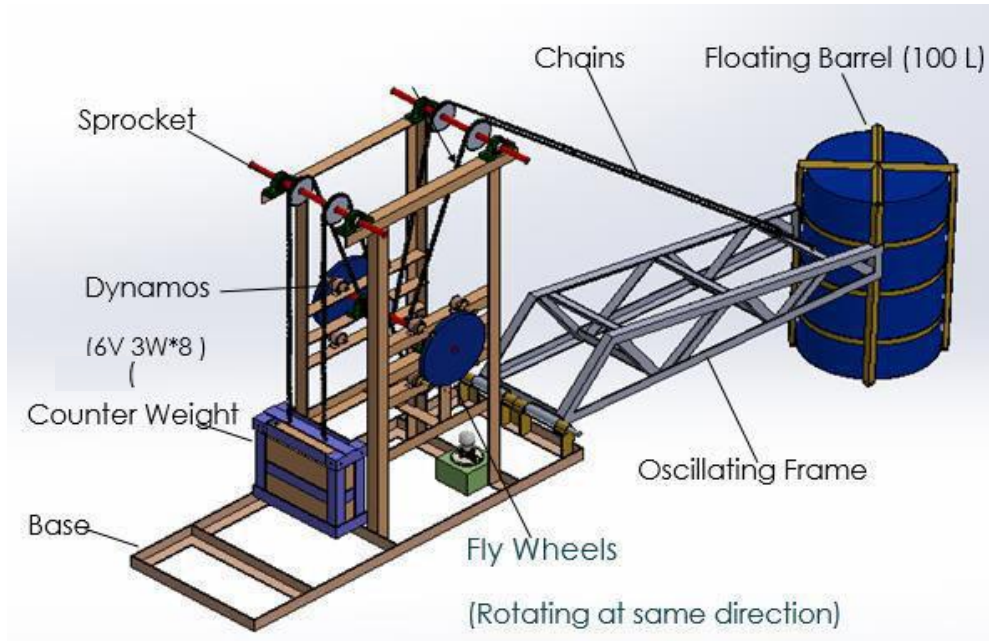


Figure 1: Basic configuration of the system

minute). The system is composed of a 100 l float connected to a reinforced steel frame (approximate length: 2.5 m; weight: 60 kg weight), which is mounted to a ground anchored steel base via a hinge. With the interaction of the sea waves, the float tends to move up and down due to buoyancy forces, causing the steel structure to oscillate around the hinge. Two parallel chains are connected to the steel structure towards the float side and are sent through a series of sprockets (ratcheting bicycle free wheels) though which the oscillatory motion of the structure is converted to a one-direction rotation of a flywheel system composed of two fly wheels (total mass: 20 kg). Other end of the chains are connected to a counter weight (mass: 30 kg) keeping the chains in tension, consistently (see Figure 2).

Based on the absorbed potential energy of the sea waves, the floating structure oscillates and the energy is stored as kinetic energy in the fly wheels.

Alternating current (AC) bicycle dynamos (eight units), each having 3 W (3 V) capacity (total generation capacity: 24 W) were attached to the flywheels in order to convert this kinetic energy in to electrical energy and generated power was regulated to direct current (DC). Here, it should be noted that the eight dynamos were wired as four dynamo sets where in each set, two dynamos are series connected to obtain 6 V DC to drive a LED series while ensuring convenient measurements at 6 V than 3 V using a digital multimeter.

## Results and Discussion

In this research, two sets of trials were conducted in the sea at the Gale port. Firstly, as shown in Figure 3(a), the original dynamo arrangement where the dynamos directly contacting the flywheels were tested and the obtained results are presented in Table 1. Here, the rotational speed of the flywheels



Figure 2: Test apparatus used for the trials at the Galle port area, Sri Lanka

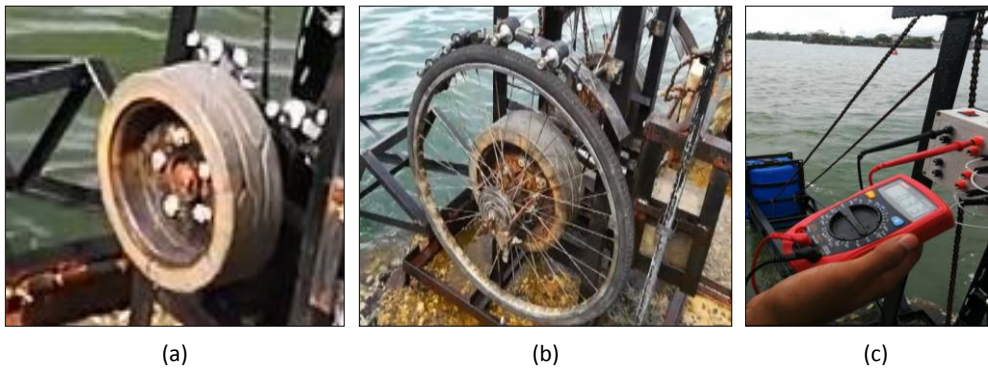


Figure 3: (a) Initial arrangement of the dynamos (directly touching the flywheels) (each fly wheel carries four bicycle dynamos (3 V, 3 W, AC), (b) modified arrangement of dynamos using larger diameter bicycle wheels coupled to the two flywheels in order to increase the rotational speed of the dynamos, and (c) measurements done using a digital multimeter

Table 1: Measurements at the first set of trials having the original arrangement of dynamos, directly contacting the flywheels

Dynamo set number	Voltage output (V)	Current output (A)	Power output (W)
1	4.5	0.08	0.36
2	3.1	0.07	0.22
3	3.4	0.07	0.24
4	3.9	0.08	0.31
<b>Total power generated by dynamo sets (1-4)</b>			<b>1.13</b>

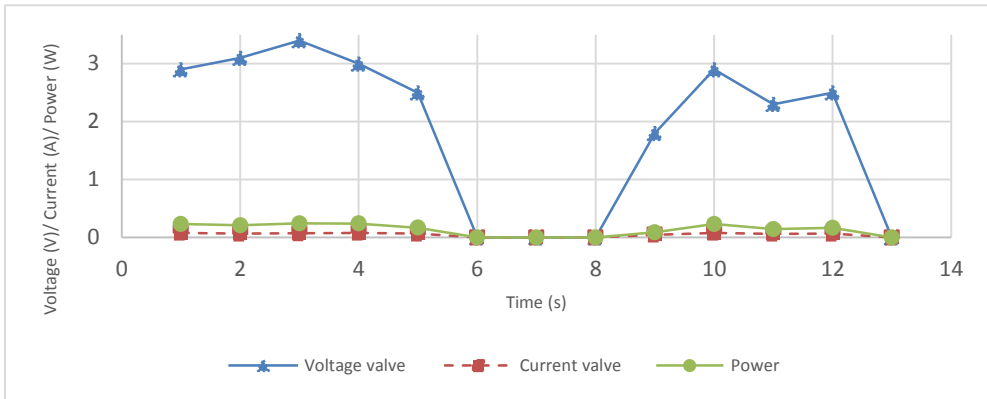


Figure 4: Time variation of the voltage, current, and the total power output measured at the first set of trials having the original arrangement of dynamos, directly contacting the flywheels

Table 2: Measurement done at the second set of trials where the dynamos attached to the larger diameter bicycle wheels connected to the original flywheels

Dynamo set number	Voltage output (V)	Current output (A)	Power output (W)
1	10.4	0.21	2.06
2	10.8	0.22	2.38
3	10.2	0.20	2.04
4	9.2	0.18	1.66
<b>Total power generated by dynamo sets (1-4)</b>			<b>8.14</b>

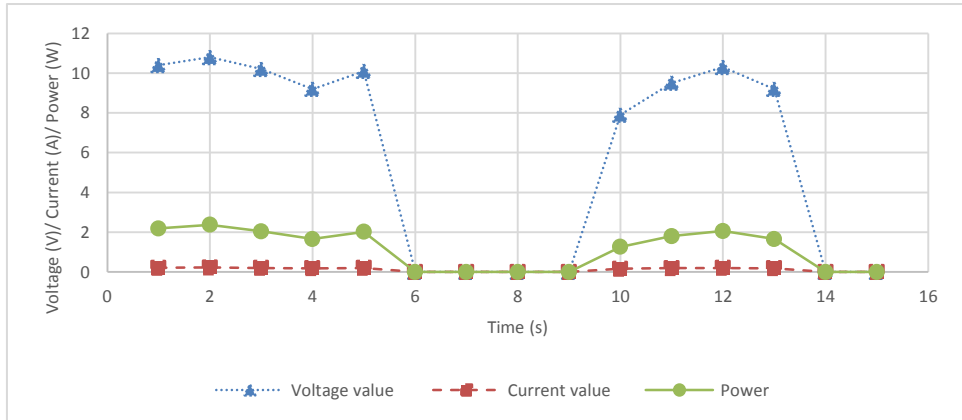


Figure 5: Time variation of the voltage, current, and the total power output measured at the second set of trials where the dynamos attached to the larger diameter bicycle wheels connected to the original flywheels

was in the range of 30 – 35 RPM. From Table 1 and Figure 4, it can be observed that the average power output was far lower (1.13 W) than expected (24 W), resulting an overall electrical power generation efficiency of 5.65% and overall energy conversion efficiency of 2.26% (from sea wave to electricity). The main cause for this lower performance was found to be the lower rotational speed of the dynamos (app. 500 RPM), than their standard rotational speed of 1500 RPM.

Next, in order to increase the speed of rotation of the dynamo heads, two large diameter bicycle wheels were connected to the flywheels, and dynamos were arranged to contact those wheels as shown in Figure 3(b). Here also, the average rotational speed of the flywheel was in the range of 30 – 35 RPM, and the obtained results are presented in Table 2. Here, the total power output was found to be 8.14 W, leading to 33.9% overall efficiency of electrical generation and overall energy conversion efficiency of 16.3%. Furthermore, from Figure 5, it is evident that the magnitude of the generated power fluctuates with time, in

agreement with the sinusoidal form of variation of the sea waves, but with more sustained amplitude (e.g. from 1 to 5 s and 10 to 13s). Furthermore, there is a time interval where no power is generated (e.g. from 6 to 9 s), corresponding to the far most top or bottom position of the float due to the raising and lowering sea waves.

## Conclusion and Future Work

A small scale sea wave based power generation unit has been developed and tested in sea conditions in Galle port of southern coast of Sri Lanka with a total installed generation capacity of 24 W (6 V DC), using eight bicycle dynamos. Two sets of trials were conducted using the setup where the first trials generated less power (1.13 W), mainly due to the lower rotational speed of the dynamos. By incorporating large diameter bicycle wheels, dynamos were arranged to rotate in much higher speeds and the generated power was 8.14 W, with overall electrical generation efficiency of 33.9% and overall energy conversion efficiency of 16.3% (from sea wave to electricity). Due to practical difficulties,

only 24 W capacity generators were used, even though the theoretical generation capacity of the system was estimated to be 50 W.

Although the purpose of having a flywheel system in the WEC was to minimize power output fluctuations, still significant power fluctuations were observed, indicating that a flywheel with larger inertia to be used, better with a geared-up manner, leading to multiple rotations of the flywheel system for a single oscillation of the hinged structure. Furthermore, at the trials, it was clearly observed that the steel structure undergoes corrodes rapidly due to the sea conditions highlighting the necessity to have a marine-grade paint coating to be applied on to the steel structure or using corrosion resistive materials for the structure. With corrosion, the mechanical losses tend to increase and the structural strength can significantly decrease. With suitable modifications addressing such problems, the system can be upgraded to a large scale power generation system or as a modular based electrical power generation system.

### Acknowledgements

Authors wish to acknowledge the support provided by the Sri Lanka Ports Authority and Sri Lanka Customs, Galle branches during trials conducted at the Galle port. Also, the workshop facilities provided by the Department of Mechanical and Manufacturing Engineering, Faculty of Engineering, University of Ruhuna, Hapugala, Galle for the fabrication works of the unit is gratefully acknowledged. This project was funded by the University of Ruhuna, Sri Lanka under the Staff Research Grant

scheme and the Undergraduate Project Grant (total LKR 40,000).

### References

- [1] A. Fischer, "Converting energy from ocean currents," international journal of research in engineering and technology, 2016.
- [2] E. Baddour, "Energy from waves and tidal currents," Institute for Ocean Technology, 2004.
- [3] P. T. J. P. M. V. Roger Bedard, "oceanography," 2010. [Online]. Available: <http://tos.org/oceanography/article/an-overview-of-ocean-renewable-energy-technologies>. [Accessed 26 10 2017].
- [4] M. B. Hosna Titah-Benbouzid, "Ocean wave energy extraction: Up-to-date technologies," November 2014.
- [5] I. Lopez, J. Andreu, S. Ceballos and I. M. De Algria, "Review of wave energy technologies and the necessary power equipment", Renewable and Sustainable Energy Reviews, vol. 27, pp. 413-434, November 2013.
- [6] "Alternative energy tutorials," 2015. [Online]. Available: <http://www.alternative-energy-tutorials.com/wave-energy/wave-energy-devices.html>. [Accessed 10 2017].
- [7] N. J. & E. Olson, "Oscillating Water Column (OWC)," 2010. [Online]. Available: <https://owcwaveenergy.weebly.com/>. [Accessed 26 10 2017].
- [8] L. Margheritini, "Research portal," 2009. [Online]. Available: [http://vbn.aau.dk/en/projects/overtopping-wave-energy-converters-applications-and-optimization-of-power-capture\(aa4f747b-6bf5-44c8-b570-dd28846323e8\).html](http://vbn.aau.dk/en/projects/overtopping-wave-energy-converters-applications-and-optimization-of-power-capture(aa4f747b-6bf5-44c8-b570-dd28846323e8).html). [Accessed 26 10 2017].

# A Correlation Analysis of Factors Influencing Cooling Energy Demand of Condominiums in Sri Lanka

Devindi Geekiyanage<sup>1</sup>, Thanuja Ramachandra<sup>2</sup>

*Department of Building Economics, University of Moratuwa  
Bandaranayake Mawatha, Katubedda, Moratuwa 10400*

<sup>1</sup>d.geekiyanage22@gmail.com

<sup>2</sup>Thanuja03@hotmail.com

## Abstract

Often, energy use for Heating, Ventilation and Air Conditioning is the key contributor to operational energy demand which varies between 50-70% in most of the developed countries. Surprisingly, in Sri Lanka, the energy consumption of space cooling accounts for more than 75% of total electricity used in a typical building. With ever-increasing pace of condominiums in Sri Lanka, the requirement for space cooling has increased significantly which has resulted in enormous energy requirement. On that note, this research investigates the factors influencing cooling energy demand of condominiums in Sri Lankan tropical climate. A questionnaire survey was administered to a sample of 30 professionals employed in condominium operations and maintenance. Analysis of survey findings indicates top five significant determinants of cooling energy demand: building morphology, building technology, environmental factors, physical characteristics, technical factors and human behaviour. Further analyses into building morphology factors which is the key contributor of cooling energy demand indicate that number of floors (0.940), height (0.930), shape (-0.686), grouping of buildings (-0.647), gross internal floor area (0.597), window-to-wall-ratio (0.489) and wall-to-floor-ratio (-0.457) are significantly correlated with cooling energy demand. Therefore, the study recommends designers to consider these design parameters and its impact on cooling energy demand and thereby develop energy efficient condominiums.

**Keywords:** building morphology; condominiums; cooling energy demand; correlations; Sri Lanka

## Introduction

Primary energy consumption of a state can be mainly divided into three sectors such as buildings (i.e. residential and commercial buildings), industrial and transportation. Amongst the primary energy cost sectors, building sector has received a significant place by consuming one-fifth of the world's total energy and consequently accounts for one-third of the global Greenhouse Gas (GHG) emissions [1]. Gradually, residential buildings have become the prime sector of energy consumption superseding the commercial building stock. For example, in the US economy, end-use sector shares of total energy consumption in 2011 indicates that the building sector contributed to 41% of total energy consumption, with the residential sector dominating by consuming 22% [2]. Residential buildings include several sub-sectors such as single-family home, duplex, apartment building, condominium, and townhouse. Each of this residential sub-sector is different from its market structure, energy use, and energy intensity. According to the USDOE [2, 3], single-family homes and multi-family condominium buildings are the two largest energy consuming residential sub-sectors. Amongst all energy end-users in a typical building, Heating, Ventilation and Air Conditioning (HVAC) systems consume a significant share of electricity in developed countries in the range of 50-60% while it could be up to 70% in Australia [4].

Similar to the international context, the sector comprised of household, commercial & others has become the dominant end-user of primary energy consumption in Sri Lanka [5]. This sector consumes 170.6 quads of energy (46% of the total energy consumption), while the

industrial sector and transportation sector consume 94.7 quads (25%) and 107.4 quads (29%) respectively. Further, comparison of the electricity bills and aggregated sub-metering data of buildings for an annual average of electricity end-use breakdown for HVAC system accounts for about 51% in Sri Lanka [6]. However, there is no evidence to show the specific energy consumption of residential building units in Sri Lanka. In another point of view, anecdotal evidences from construction professionals suggest that, both government and private sector investments on condominium buildings have significantly increased in recent past. Consequently, the requirement for space cooling energy demand has increased significantly.

Given this immense increase in energy demand for space cooling of condominiums in Sri Lanka, there is a critical need to design and construct buildings, which are energy efficient. This research therefore analyses factors influencing the cooling energy demand of condominium buildings in Sri Lanka and thereby correlate building morphology factors with the cooling energy consumption. These correlations would enable designers to give due considerations to significant design factors and thereby produce energy efficient buildings.

### **Factors influencing the space cooling energy demand of buildings**

Drivers of energy consumption in buildings are many and different in nature. Accordingly, Table 1 presents the list of factors influencing cooling energy demand of buildings as per the literature findings



Table 1: Factors influencing the cooling energy demand of buildings: A literature review

Major determinant	Causes	Sub-causes	Sources
Physical characteristics	Activity drivers	Attached buildings	[13]
		No. of occupants	[13]
	Use intensity drivers	Floor area per person	[13]
	Energy intensity drivers	Specific energy consumption	[13]
Building morphology	Building geometry	Shape of the building	[7], [8], [12]
		Gross internal floor area	[7], [8], [12]
		Building height	[8], [9], [12]
		No. of floors	[8], [12]
		Building orientation	[7], [8], [12]
		Wall to Floor ratio	[8], [9], [12]
		Window to wall ratio	[8], [9], [12]
		Area of roof	[8], [12]
Building technologies	Construction materials	Insulated building materials	[7], [8], [9]
		U-value: building elements	[8]
		U-value of materials	[8]
		Effects of glazing ratio	[7], [8], [9]
	Typical Air Change Rate (ACH)	[11]	
	Passive strategies	[12]	
Heat gain through building facade			[10]
Economic factors			[12]
Environmental factors	External heat gain (Location)	Climate	[9], [13]
		Local temperature	[7], [10]
		Solar radiation	[7], [10]
		Humidity	[7]
		Wind speed	[7], [10]
Technical factors	Internal heat gain	People design (m <sup>2</sup> /P)	[10]
		Building plant & equipment	[10]
Human behaviour	Biological factors (Thermal stress)	Internal climate	[7], [9], [11]
		Non-meteorological factors	[7]
	Social factors	Socio-demographic factors	[7], [12]

Although the literature review indicated set of factors influencing the cooling energy demand of buildings in different terminologies, most of these factors could be gathered under the term 'Building morphology'. In essence, the content of the building characteristics,

building structure and design, building geometry and use intensity drivers are similar in nature; therefore, referred to building morphology. The next section therefore reviews these building design factors in detail to identify its impact on cooling energy demand.

## **Building morphology and cooling energy demand**

### **Building shape**

Shape of a building refers to the configuration of surfaces and edges of a two or three-dimensional object [14]. Most of the researchers have carried out investigations on the relationship between building shape and energy consumption of buildings in the global context. For example, Catalina, Virgone, and Lordache [15] investigated 12 buildings with varying building forms and glazing percentages and concluded that the impact of building shape is most important in hot climates with higher solar radiation and outdoor temperature values. Further, Alanzi, Seo, and Krarti [16] analysed several building shapes including rectangular, L-shape, U-shape, and H-shape with different building aspect ratios, Window-to-Wall-Ratios (WWR), and glazing types.

The results of a detailed parametric analysis indicate that the effect of building shape on total building energy use depends on primarily three factors: the relative compactness, the WWR and glazing type. For buildings with low WWRs, it is found that the total energy use is inversely proportional to relative compactness and independent of its form in severe cold and scarcely sunny winters. Moreover, Ourghi, Al-Anzi, and Krarti [17] have developed a simplified analysis method to predict the impact of shape on annual energy use for commercial buildings based on detailed simulation. A direct correlation has been established between relative compactness and total building energy use and also with space cooling energy demand.

### **Building orientation**

The orientation of a building means to a particular direction in which the building is placed. According to literature, South-North oriented buildings are the most energy efficient building structures [18]. Further, [16] and [19] stated that the orientation of a building has an impact on its energy performance, especially for the low Window-to-wall-ratio values.

### **Window-to-wall-ratio**

Window area will have an impact on the building's heating, cooling and lighting, as well as relating to the natural environment in terms of access to daylight, ventilation and views. A lower WWR generally indicates better efficiency as windows usually perform less well than the rest of the facade as a thermal barrier [20]. Too high WWR can result in the building being too cold in the winter from the heat loss through windows and too hot in the summer from all the sunlight and heat coming in [21]. Yang et al. [22] carried out a study on variation of annual heating energy demand, annual cooling energy demand and annual total energy consumption in different conditions such as different orientations, patterns of utilization of air conditioning systems, WWR and types of windows. The research findings showed that the total energy consumption increases with increase in WWR.

### **Wall-to-floor-ratio**

The WFR indicates the proportion of external wall required to enclose a given floor area [23]. McKeen and Fung [24] examined the energy consumption of varying WFR in multi-unit residential buildings in Canadian cities. Authors contended that compared to a building

with a less efficient WFR, a reduction of energy consumption by over 15% is possible in many scenarios. Further, authors opined that utilizing the optimum WFR allows buildings to obtain a more solar gain in winter and shading in summer, decreasing the demand for heating and cooling. Moreover, the inclusion of optimum WFR in building design will have a lifelong impact on the future energy demand of buildings. On a similar view, Ayyad [25] contended that the low WFR were found to be reducing energy consumption when compared to offices with high WFR.

### **Roofing and area of the roof**

The heating costs are influenced considerably by the relationship between the area of roof and walls, as roofs are a major element of heat loss [26]. Further, insulating both roof and walls are most effective in cities with cold winters, insulating just the roof is best for temperate climates, and insulating walls is most effective for cities with the year-long warm weather [27].

In addition, Werner and Mahdavi [28] presented a study based on several building morphology factors. Authors simulated the heat consumption of fifty-four (54) morphologically different buildings and concluded that the building shape, RC, orientation, and glazing percentage have a greater influence on the energy intensity of a building.

However, other building morphology factors such as building height, number of floors, Gross Internal Floor Area (GIFA) and grouping of buildings could also influence the cooling energy consumption of buildings. Previous researchers have further focused on the impact of morphology factors on energy consumption in different climates and

seasonal changes with simplified built forms [29]. However, only few studies represent the energy consumption patterns of the built forms in the tropical climates. Moreover, the influence of building morphology factors on the operational cost optimization in the tropics and its impact upon space cooling energy demand have been largely ignored. Thus, the current study investigates the relationship between morphology factors and cooling energy consumption using a correlation analysis.

### **Research Methods**

A quantitative approach followed by a questionnaire survey was administered to collect data related to building morphology factors and annual energy consumption for space cooling. Given the time constraints and limited access to data, a sample of thirty (30) (out of 70) registered luxury residential condominiums with 12 or more floors, constructed after 2010 were selected considering the minimum sample required for a survey design [30]. The participants with over 10 years of experience in condominium operations and maintenance were approached for the data collection.

A descriptive analysis was performed on the collected data to identify the key determinants of cooling energy demand of condominiums in Sri Lanka. Subsequently, the relationship between building morphology factors and cooling energy demand was established using Pearson correlation coefficient statistics. Correlation strength determination followed suggestions by Ricciardy and Buratti [31]. Accordingly, correlation coefficient 'R' is  $0 < |R| < 0.3$  - weak correlation;  $0.3 < |R| < 0.7$  - moderate correlation; and  $|R| > 0.7$  - strong correlation respectively.

## Results and Discussions

### Factors influencing space cooling energy demand of condominiums in Sri Lanka

As shown in Table 1, literature found 07 major determinants (i.e. physical characteristics, building morphological factors, building technologies, economic factors, environmental factors, technical factors, and human behaviour), 12 causes contribute to major determinants, and altogether 27 sub-causes, which

contribute to the rapid growth of energy consumed by space cooling of entire building sector (i.e. both residential and commercial buildings).

Accordingly, participants were asked to select the sub causes influencing cooling energy demand specific to condominiums in Sri Lankan tropical climate and the results are shown in Table 2.

Table 2: Analysis of factors influencing energy demand for space cooling of condominiums in Sri Lanka

Major determinant	Causes	Sub-causes	Frequency	
			No.	%
Physical characteristics	Activity drivers	Attached buildings	17	56
		No. of occupants	26	88
	Use intensity drivers	Floor area per person	26	88
	Energy intensity drivers	Specific energy consumption	30	100
Building morphology	Building geometry	Shape of the building	30	100
		Gross internal floor area	30	100
		Building height	30	100
		No. of floors	30	100
		Building orientation	30	100
		Wall to Floor ratio	14	48
		Window to wall ratio	30	100
		Area of roof	30	100
Building technologies	Construction materials	Insulated building materials	30	100
		U-value: building elements	22	72
		U-value of materials	24	80
		Effects of glazing ratio	30	100
	Typical Air Change Rate (ACH)	26	88	
	Passive strategies	19	64	
	Heat gain through building facade	30	100	
Environmental factors	External heat gain (Location)	Climate	30	100
		Local temperature	30	100
		Solar radiation	30	100
		Humidity	26	88
		Wind speed	11	36
Technical factors	Internal heat gain	People design (m <sup>2</sup> /P)	30	100
		Building plant & equipment	16	52

Human behaviour	Biological factors	Internal climate	30	100
	(Thermal stress)	Non-meteorological factors	26	88
	Social factors	Socio-demographic factors	10	32
Economic factors			0	0
<b>Total no. of respondents</b>			<b>30</b>	<b>100</b>

According to Table 2, all respondents have approved the findings from the literature related to the determinants of space cooling energy demand in the building sector. Nevertheless, none of the respondents have selected economic factors as a determinant of cooling energy demand of condominium facilities.

As shown in Table 2, 16 out of 27 sub-causes, which include specific energy consumption, building shape, GIFA, building height, no. of floors, building orientation, WWR, area of roof, grouping of buildings, insulated building materials, effects of glazing ratio, climate, local temperature, solar radiation, people design, and internal climate have been identified as influential factors of cooling energy consumption in condominiums with response rate of 100%. There are another 08 sub-causes with over 50% rate of selection by respondents as building plant & equipment (52%), attached buildings (56%), U-value of building elements (72%), U-value of building materials (80%), no. of occupants (88%), floor area per person (88%), humidity (88%), and non-meteorological factors (88%). Aforementioned sub-causes have its place under major causes such as activity drivers, use intensity drivers, energy

intensity drivers, building geometry, construction materials, typical air change rate, heat gain through building façade, external heat gain, internal heat gain, and biological factors.

In terms of major determinants, building morphology is most influential for the energy demand for space cooling of condominiums.

Therefore, building morphology factors are analysed in detail with cooling energy demand using a correlation analysis.

### **Relationship between cooling energy demand and building morphology factors**

The data collected for nine building morphology factors from 30 condominium buildings were correlated with the average annual cooling energy demand to identify most influential morphology factors for space cooling of condominiums. The results obtained from correlation analysis are presented in Table 3. The table depicts the Pearson correlation (R) and the significance of building morphology factors with respect to the annual cooling energy demand of condominiums in Sri Lanka.

Table 3: Correlations of average annual cooling energy consumption and building morphology factors

Building design variable		1	2	3	4	5	6	7	8	9	10
<b>1. Shape</b>	R	1	-.082	-	-	-.042	.541**	-.224	.535**	.410*	-
	Sig.		.668	.000	.000	.825	.002	.235	.002	.024	.000
<b>2. GIFA</b>	R	-.082	1	.455*	.415*	.378*	.430*	.391*	-.361	.743**	.489**
	Sig.	.668		.012	.023	.040	.018	.032	.050	.000	.006
<b>3. Height</b>	R	-.677**	.455*	1	.983**	.095	-.431*	.455*	-	-.239	.930**
	Sig.	.000	.012		.000	.616	.017	.011	.000	.204	.000
<b>4. No. of floors</b>	R	-.714**	.415*	.983**	1	.064	-.436*	.458*	-	-.287	.940**
	Sig.	.000	.023	.000		.735	.016	.011	.000	.124	.000
<b>5. Orientation</b>	R	-.042	.378*	.095	.064	1	-.116	.345	-.079	.313	.319
	Sig.	.825	.040	.616	.735		.543	.062	.679	.092	.085
<b>6. WFR</b>	R	.541**	.430*	-.431*	-.436*	-.116	1	-.054	.309	.807**	-.457*
	Sig.	.002	.018	.017	.016	.543		.778	.097	.000	.011
<b>7. WWR</b>	R	-.224	.391*	.455*	.458*	.345	-.054	1	-.365*	.035	.597**
	Sig.	.235	.032	.011	.011	.062	.778		.047	.854	.000
<b>8. Grouping of building</b>	R	.535**	-.361	-	-	-.079	.309	-.365*	1	.143	-
	Sig.	.002	.050	.000	.000	.679	.097	.047		.451	.000
<b>9. Area of roof</b>	R	.410*	.743**	-.239	-.287	.313	.807**	.035	.143	1	-.180
	Sig.	.024	.000	.204	.124	.092	.000	.854	.451		.341
<b>10. Cooling energy demand</b>	R	-.686**	.489**	.930**	.940**	.319	-.457*	.597**	-	-.180	1
	Sig.	.000	.006	.000	.000	.085	.011	.000	.000	.647**	.341

\*\* . Correlation is significant at the 0.01 level (2-tailed).  
 \* . Correlation is significant at the 0.05 level (2-tailed).

As observed from Table 3, seven morphology factors out of nine have significant correlations with the cooling energy demand. A summary of Table 3 is presented in Table 4, indicating the significantly correlated morphology factors with cooling energy demand.

Table 4: Correlations of building morphology factors with cooling energy consumption

Building design variable	Average annual cooling energy consumption		
	R	R <sup>2</sup>	Sig. (2-tailed)
WFR	-0.457*	20%	0.011
WWR	0.489**	24%	0.006
GIFA	0.597**	36%	0.000
Grouping of buildings	-0.647**	42%	0.000
Building shape	-0.686**	47%	0.000
Building height	0.930**	86%	0.000
No. of floors	0.940**	88%	0.000

\*. Correlation is significant at the 0.05 level (2-tailed).  
\*\*. Correlation is significant at the 0.01 level (2-tailed).

According to Table 4, based on Pearson correlation coefficients at 5% and 1% significant levels, seven out of nine factors resulted in significant correlations. The factors include: number of floors, building height, building shape, the grouping of buildings, WWR, GIFA, and WFR. All correlations except WFR are significant at the 0.01 level. Factors having significant correlations are discussed further.

#### Strong correlations with cooling energy demand

As observed from Table 4, the number of floors (0.940; 88%) and building height (0.930; 86%) have strong positive relationships with cooling energy demand. Therefore, the cooling energy demand will increase with increase in the number of floors and height of a building. This could be due to the growing internal heat gain (i.e. by increased occupancy and usage of heat emitting appliances) and external heat gain (i.e. additional heat gain from the building façade). Further, the result shows a very strong relationship between building height and number of floors (0.983). Building height would most definitely increase in proportion with number of floors. Thus, once the number of floors increases, energy demand for space cooling of condominiums increases.

#### Moderate correlation with cooling energy demand

Similar to number of floors and height of a building, WWR (0.597; 36%) and GIFA (0.489; 24%) also have positive correlations but moderate with cooling energy demand. The results show that the energy consumption for space cooling increases with the increase of WWR and GIFA. Furthermore, the correlation analysis shows that the WWR is positively correlated with the height of the building (0.455) and number of floors (0.458). Simply, when building height increases the wall area increases, resulting in high WWR. The coefficient of determination calculated indicates that the WWR determines 36% of the mean cooling energy demand of condominium buildings.

Contrary, correlation of building shape (-0.686; 47%), grouping of buildings (-0.647; 42%) and WFR (-0.457; 20%) with the cooling energy demand of condominiums in Sri Lanka is negative. Here, building shape is considered as irregular and regular shapes with values 0 and 1 respectively. The resulting negative correlation indicates that where the shape is regular, the consumption of cooling energy is reduced. Although building shape is not the only parameter which determines the cooling energy

demand of a condominium in tropical climates, because it has only 47% of coefficient of determination. Further, when grouping of building exits, the energy demand for space cooling may decrease due to covering effects. However, when a building stand alone, there will be an increase in energy consumption for space cooling. Only 42% of the mean value of cooling energy demand could be explained by this parameter. Moreover, when there is a high WFR, the cooling energy demand of that particular condominium would decrease. In order for the higher WFR, the external wall area of a building should be greater than its GIFA. Correlation values obtained for GIFA also indicates that little GIFA consume low energy for space cooling. The coefficient of determination of WFR is 20%, which means 80% of the mean value of cooling energy demand of condominiums in tropics will be determined by other factors.

Unlike previous studies, which revealed altogether five morphology factors influencing the cooling energy demand of buildings in both hot and cold climates, the current study provides an extensive set of nine variables. Findings of the current research are of the similar view of Catalina et al. [15] that building shape has a significant impact on cooling energy demand. Also, results obtained from both initial descriptive analysis and correlation analysis proved that regular building configurations are more energy efficient compared to irregular building forms. In more detail, cooling energy consumption of set of regular building configurations show a positive linear trend line along the increasing GIFA,

similar to irregular shaped buildings but with a less radiant value compared to irregular shapes. Further, this study confirms the findings of Ayeb [18] for hot, and dry climate and Yang et al. [22] for hot summer, and cold winter zones in China, by concluding that buildings, which have long south and north axis result in a reduction in energy consumption compared to east and west oriented buildings. Moreover, similar to [22], authors of the current study found that buildings with high WWR are more likely to experience high-energy demand and that would further increase with having east and west oriented window area. In addition, buildings with high WFR would result in low energy consumption for space cooling of condominium buildings. This result confirms previously held conclusions of Ayyad [25] for office buildings in Dubai, which is a hot and humid climate.

In terms of significance, only seven out of the analysed nine factors, resulted in significant correlation. Building orientation (0.319) and area of roof were the two exceptions. The impact of orientation on cooling energy demand could be offset by the covering effects caused by the grouping of buildings; therefore, the orientation became a non-significant determinant of cooling energy demand. Similarly, the area of roof indicated a minimum correlation (-0.180) as roofs are a major heat gain element, most buildings in hot and tropical climate ensure buildings' thermal comfort through insulation. In line with that consideration, most of the buildings included to the research sample are roof insulated. Thus, the impact of roof area on cooling energy demand is minimum.



## Conclusions

It is concluded that number of floors, building height, building shape, grouping of buildings, GIFA, WWR, and WFR have significant effects upon the cooling energy demand of condominiums. Except for building shape and grouping of buildings, increase of other variables result in increase of cooling energy demand. Results further highlight that regular building configurations (i.e. square, rectangular circle) and having grouping of buildings consume less energy for space cooling of condominiums in a tropical climate.

It is hoped that these findings would provide useful knowledge towards energy efficient building designs. Building morphology factors could then be appropriately varied for condominium buildings in line with passive energy conservation strategies, consequently reducing cooling energy consumption in Sri Lanka.

## Recommendations for further study

The same research methodology adopted for this study can be employed for other types of residential buildings and commercial buildings to develop a model to forecast the annual cooling energy demand. Further, building morphology factors are significant when determining the energy demand for lighting as well. Therefore, it is recommended to explore the relationship between building morphology and lighting of buildings. Further, it can be extending to develop a model to predict energy demand of buildings.

## References

- [1] Independent Evaluation Office, Annual Report 2010, (2010).
- [2] Energy Information Administration (EIA), Commercial Buildings Energy Consumption Survey (CBECS), (2012).  
Available:<http://www.eia.gov/emeu/efficiency/reports.html>.
- [3] U.S. Department of Energy, Energy Efficiency Trends in Residential and Commercial Buildings, Energy. 2008:1–32.
- [4] Australian Greenhouse Office (AGO), Australian Condominium Building Sector Greenhouse Gas Emissions 1990-2010, executive summary, (2010).
- [5] Ministry of Power & Energy, Sri Lanka Energy Sector Development Plan for a Knowledge-based Economy 2015-2025.
- [6] Rajapaksha I, Hyde R, Rajapaksha U. A modelling appraisal of design standards in retrofitting a high-rise office building in Brisbane, (2010).
- [7] Kalma JD, Crossley DJ. Inequities in domestic energy use: Some determinants, Energy Policy. 1982;10:233–243.
- [8] Zangheri P, Armani R, Pietrobon M, Pagliano L, Milano PD, Boneta MF, Müller A. Heating and cooling energy demand and loads for building types in different countries of the EU, (2014).
- [9] London School of Economics and Political Science, Cities and Energy, LSE Cities. 2014:227–249.
- [10] Susorova I, Tabibzadeh M, Rahman A, Clack HL, Elnimeiri M. The effect of geometry factors on fenestration energy performance and energy savings in office buildings, Energy Build. 2013;57:6–13.

- [11] Brown MA, Cox M, Staver B, Baer P. Climate Change and Energy Demand in Buildings Conclusions from the Literature, 2014 ACEEE Summer Study Energy Effic. Build. 2014:26–38.
- [12] Bousquet J, Cremel M, Loper J. Determinants of space heating energy consumption : An analysis of American households Theoretical foundation, (2014).
- [13] Üрге-Vorsatz D, Cabeza LF, Serrano S, Barreneche C, Petrichenko K. Heating and cooling energy trends and drivers in buildings, Renew. Sustain. Energy Rev. 2015;41:85–98.
- [14] Bacon EN. Design of Cities, (1974).
- [15] Catalina T, Virgone J, Iordache V. Study on the impact of the building form on the energy consumption, Building Simu. 2011:14–16.
- [16] AlAnzi A, Seo D, Krarti M. Impact of building shape on thermal performance of office buildings in Kuwait, Energy Convers. Manag. 2009;50:822–828.
- [17] Ourghi R, Al-anzi A, Krarti M. A simplified analysis method to predict the impact of shape on annual energy use for office buildings. 2007;48:300–305.
- [18] M. Ayeb, Building orientation for hot and dry climate, (2016). Available: <https://www.linkedin.com/pulse/building-orientation-hot-dry-climate-majdi-ayeb>.
- [19] Depecker P, Menezes C, Virgone J, Lepers S. Design of buildings shape and energetic consumption. 2001;36:627–629.
- [20] window-to-wall ratio \_ Definition \_ Meaning.
- [21] Sustainable Window Design - Green Garage Detroit.
- [22] Yang Q, Liu M, Shu C, Mmereki D, Uzzal Hossain M, Zhan X. Impact Analysis of Window-Wall Ratio on Heating and Cooling Energy Consumption of Residential Buildings in Hot Summer and Cold Winter Zone in China, J. Eng. (United States) 2015.
- [23] Muhaisen AS. Effect of Building Form on the Thermal Performance of Residential Complexes in the Mediterranean Climate of the Gaza Strip, (2012).
- [24] McKeen P, Fung A. The Effect of Building Aspect Ratio on Energy Efficiency: A Case Study for Multi-Unit Residential Buildings in Canada, Buildings. 2014;4:336–354.
- [25] Ayyad TM. The Impact of Building Orientation, Opening to Wall Ratio, Aspect Ratio and Envelope Materials on Building Energy Consumption in the Tropics, J. Chem. Inf. Model. 2013;53:1689–1699.
- [26] Omari DO. Factors affecting the maintenance cost of commercial buildings, (2015).
- [27] Lucero-álvarez J, Rodríguez-Muñoz NA, Martín-Domínguez IR. The effects of roof and wall insulation on the energy costs of low income housing in Mexico, Sustain. 2016;8:1–19.
- [28] Werner P, Mahdavi A. Building Morphology, Transparency and Energy Performance, Build. Simul. 2003. 2003:1025–1032.
- [29] Hyde R, Rajapaksha U, Rajapaksha I, Riain MO, Silva F. A Design Framework for Achieving Net Zero Energy Commercial Buildings, (2012).
- [30] Altunışık R, Coşkun R, Bayraktaroğlu S, Yildirim E. Sosyal Bilimlerde Araştırma Yöntemleri, (2004).
- [31] Ricciardi P, Buratti C. Thermal comfort in the Fracchini theatre ( Pavia , Italy ): Correlation between data from questionnaires, measurements and mathematical model, Energy Build. 2015;99:243–252.

# Design of a Control System to Optimize Power Consumption in Air Conditioners to Satisfy Human Thermal Comfort

S.Nidershan<sup>\*1</sup>, W.A.D.D.K.Wickramaarachchi<sup>#2</sup>, B.G.D.H.Bopitiya<sup>#3</sup>,  
H.Krishnarajah<sup>#4</sup>

*# Department of Interdisciplinary, Faculty of Engineering, University of Jaffna  
Ariviyal Nagar, Killinochchi, Sri Lanka*

<sup>1</sup>nidershan@gmail.com

<sup>2</sup>dinuwickramaarachchi@gmail.com

<sup>3</sup>dimuthhbopitiya@gmail.com

<sup>4</sup>Hamshie.k@gmail.com

## Abstract

According to the Sustainable Energy Authority, air conditioning accounts for 75% of the energy balance of a building. Therefore, it is obvious that the HVAC systems need optimization in their energy consumption. However, United States Advanced Research Projects Agency for Energy has stopped funding for hardware improvement in the air conditioners reasoning its saturated state. Modern researches are based on advanced control system, thermoelectric solid to absorb heating, cooling with sound waves or magnets. Human motion detection and precooling in a controlled environment are current research focused by many air-conditioner manufacturers. This research is based on how to ensure human thermal comfort without precooling the environment. Methodology is by using two cameras to locate the entering occupant's position of the body and creating a temporary environment to ensure the occupant to feel the thermal comfort in a sudden phase and later gradually cool the environment. This rapid cooling process is achieved through the camera detection and controlling the direction of the fan blade pointing towards a single human motion path. Prior analysis of the controlled environment was developed using a thermal array matrix inside the cabin and the variation in temperature, primary flow parameters were noted. Using MATLAB and CFD analysis the controlled environment was modeled for observations. Later by detecting the human, rapid cooling technique was tested to suddenly satisfy them for achieving their thermal comfort. Even though, thermal comfort varies for different personnel the diversion of cool air suddenly focusing towards them is a satisfactory method in a tropical country like Sri Lanka.

**Keywords:** Rapid Cooling, Air Conditioners, Thermal Comfort

## Introduction

It is clear that the world is stepping towards the concept of 'sustainability'. Definition of sustainability is consuming the resources while saving it to the next generation. When we consider the resources that should be protected for the next generation, energy comes first. After the industrial revolution the life became mechanized and people developed tendency to use electricity for all of their day to day applications. Not only in industrial purposes but also in domestic purposes such as kitchen appliances, fans, air conditioners, washing machines, etc. World Energy Outlook has forecasted that the world's demand for electricity will grow by 85 percent between 2010 and 2040 and this increase is more than today's total use of electricity in the USA, the European Union, China, Russia, Japan, Australia and India [4]. However, generating electricity to satisfy the demand is a major problem. Depletion of water resources affects critically on hydro power generation. Moreover, generating electricity using coal and nuclear power causes environment hazards.

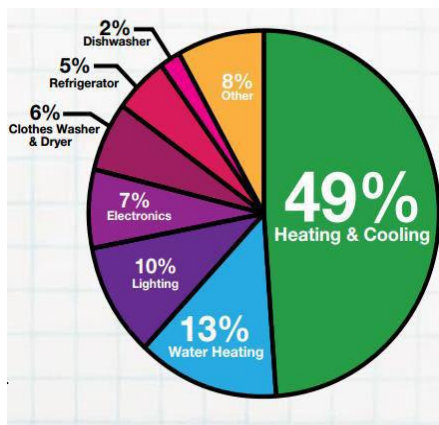


Figure 1. Typical energy consumption of a building

## HVAC systems

HVAC systems are used in buildings to provide thermal comfort and better air quality environment. As shown figure 1, the major energy consumption sources are heating and cooling appliances. In the many types of these systems, considerably split type, centralized HVAC and window type are commonly used in industries and residencies. The centralized systems are used in environments with more occupants and the split and window types are used in individual environments. Therefore, split and window type are the major source of energy consumption and ideal candidate for substantial reductions in energy demand [5]. In this research our focus is to detect a single human path and control a split type air conditioner to work in rapid cooling method for energy saving.

## Thermal Comfort

Thermal comfort is defined as 'that condition of mind which expresses satisfaction with the thermal environment and is assessed by subjective evaluation'. It is also known as human comfort and the thermal comfort is the occupants' satisfaction with the surrounding thermal conditions and it is essential to consider when designing a structure that will be occupied by people. A cold sensation will be pleasing when the body is overheated, but unpleasant when the core is already cold. At the same time, the temperature of the skin is not uniform on all areas of the body. There are variations in different parts of the body which reflect the variations in

blood flow and subcutaneous fat. The insulate quality of clothing also has a marked effect on the level and distribution of skin temperature. Thus, sensation from any particular part of the skin will depend on time, location and clothing, as well as the temperature of the surroundings.

A person's physical characteristics should always be borne in mind when considering their thermal comfort, as the factors such as their size and weight, age, fitness level and sex can all have an impact on how they feel, even if other factors such as air temperature, humidity and air velocity are all constant. In this research aspect the outer environment data is obtained itself from the air conditioner and the rapid cooling effect is adjusted to a temperature which is 5°C lower than the detected temperature. At a stage of very low outdoor the air conditioner would adjust to its lower values of temperatures. However, the accepted level of thermal comfort in Sri Lanka is 27°C and therefore the system is designed to saturate in that temperature [10]. As user defined parameters their comfort values could be selected by personals.

#### **Features of air conditioners**

The air-conditioned room temperature is expected to stay constant or change within a comfortable range. The real-time temperature is measured by the temperature sensor inside the room, and transferred to the controller. After comparing with set point, the control signal will be transmitted to the electric

control valve in Air Handling Unit (AHU). If the value of the deviation signal is zero, the control valve does not act. Otherwise, the opening of the valve will be adjusted according to the signal. Popular control methods are, [6]

- PID (Proportional, Integral, Derivative) control
  - Artificial neural network
  - Fuzzy control
  - Model predictive control
  - VAV (Variable Air Volume)
- VVW (Variable Water Volume) and VRV (Variable Refrigerant Volume) system control
  - Water pump control
  - Compressor control

However, the major air conditioner manufacturing companies try to introduce many energy saving methods to promote their products [8,9]. As a new concept, this project focuses to design a control system in order to decrease the power consumption of air conditioner by rapid cooling method while entering the room.

#### **Methodology**

The methodology for the complete systems is explained here in stages. The system is analyzed in categories of data acquisition, thermal comfort, available technologies and the controller design.

#### **Model**

Initially a fully air-conditioned room was selected for the study of the research and later it was developed as a model for further thermal analysis. The temperature levels in different places of the room were

noted by forming a matrix of temperature sensor array in the room. The room of 15 m<sup>2</sup> area is used and it is compatible for eight persons if it is considered in an aspect of a conference room. However, our analysis is on the basis of the room utilized by a single person.

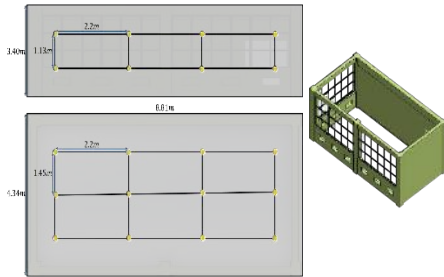


Figure 2. Perspective view of selected room

### Sensor Arrangement

Temperature sensors were arranged in a matrix of as shown in figure 2. Two layers of twelve sensors were fixed inside the cabin to obtain temperature measurements at each position. Room is divided into three segments and the gap between each sensor position is 2.2 m.

### Data logging

Initially twenty four, LM35 temperature sensors were used and Arduino MEGA2560 and SD (Secure Digital) Card module were used to record the temperature data. Arduino MEGA2560 has only 16 pin so it needs at least 2 Arduino to get the whole data. Then the data should be transferred from one Arduino to the other. In order to mitigate this issue one wire technique was used. Further, the resolution of the LM35 is very low with  $\pm 1^{\circ}\text{C}$ , however, the DS18B20 one wire sensor's resolution is  $\pm 0.5^{\circ}\text{C}$  [9].

### One wire

The basis of 1-Wire<sup>®</sup> technology is a serial protocol using a single data line plus ground reference for communication. Each 1-Wire slave device has a unique, unalterable, factory-programmed, 64-bit identification number, which serves as device address on the 1-Wire bus. 1-Wire is the only voltage-based digital system that works with two contacts, data and ground, for half-duplex bidirectional communication.

### One WIRE Temperature sensor

This sealed digital temperature probe lets you precisely measure temperatures in wet environments with a simple 1-Wire interface. The DS18B20 provides 9 to 12-bit (configurable) temperature readings over a 1-Wire interface, only one wire (and ground) needs to be connected from a central microprocessor [7].

### Arduino

It's a simple open source prototyping platform which uses ATmega microcontrollers. Here, Arduino is used as data interpreter. Real temperature is fed as a voltage to Arduino and it sends the data as a temperature value by performing some simple calculation.

### SD card module

The communication between the microcontroller and the SD card uses serial peripheral interface, which takes place on digital pins 50, 51, and 52 (Arduino Mega). Additionally, another pin must be used to select the SD card.

### Coding

Coding for Arduino and Matlab real time recording were written and a graphical user interface is developed for monitoring the initial monitoring values. Arduino microcontroller uses its own graphical language for programming. Matlab graphical interface is developed to monitor the values of temperature sensor data in real time to mitigate technical errors in initial stage.

### Data Acquisition

Finally temperature at each point was recorded in every 10 seconds and 604 measurements were taken until the temperature is stable. Cumulatively it took 1 hour and 41 minutes for complete data. The maximum average temperature was  $29.37^{\circ}\text{C}$  and the minimum average temperature was  $23.31^{\circ}\text{C}$  but the air conditioner was set to  $18^{\circ}\text{C}$ . We can check basic ability of the control system. Average temperature distribution in Celsius is shown in Figure 3.

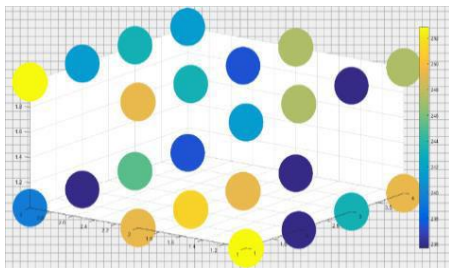


Figure 3: Average temperature distribution

### ANSYS simulation

The entire room was modeled using SolidWorks in same scale and exported

the Model to ANSYS to further analysis. Analysis of the thermal distribution of the sample room using the temperature set points data, cooling pattern was investigated and flow rate is determined according to the distance. SolidWorks 3D model is exported as a .step file and parameters were assigned according to material and complete model has been meshed into 500 000 particles. Imported ANSYS model is given in Figure 4.



Figure 4: ANSYS Model of the room

### Controller

Controller is the main part of this mechanism for rapid cooling. When a person enters the room from a hot environment he/she feels more cool air that should be provided for thermal comfort. In order to achieve this, hardware parts of the air conditioners were modeled using SolidWorks and then exported to the MATLAB as .xml file. PID controller was implemented to the shaft by considering the shaft as the motor. Control unit worked with infra-red sensors and the human position is noted for providing cool air. Figure 05 shows the controller complete block diagram representing all variable data.

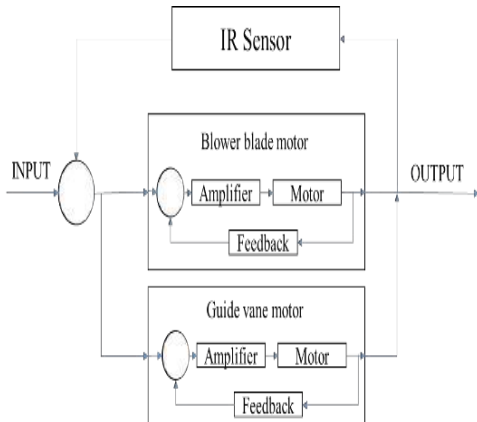


Figure 5: Control block diagram

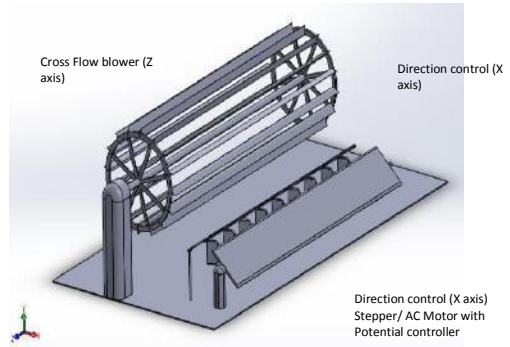


Figure 6: Prototype of fan controller

The fan blade of the controller prototype is shown in figure 6. The cross flow blower is fixed with an AC motor and the directional control blower are with AC motors and servo motors.

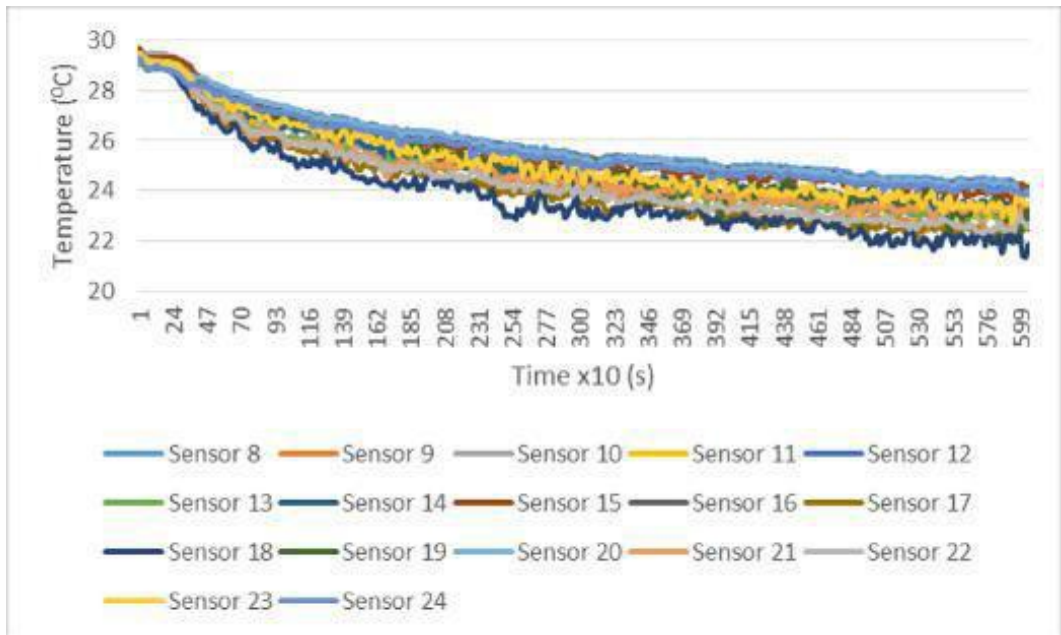


Figure 7: Temperature variance



Control unit worked with infra-red sensors and the complete system with air conditioner has obtained primary data from the sensor matrix array. For the tested conditions the temperature distribution at room entrance level is obtained as primary data. Figure 7 shows sensor temperature distribution for the controller design.

### **Thermal IR sensor**

The D6T-44L-06 from Omron is a Micro-Electro-Mechanical System (MEMS) thermal sensor. It is a small size, high accuracy, low noise, high sensitivity sensor that enables detection of stationary human presence by non-contact temperature measurement with the help of 4 x 4 element type, in the voltage range of 4.5 V – 5.5 V DC and point of view of 44.2° and 45.7°.

### **Stereo Vision**

The 3D camera consists of two cameras of parallel optical axes and separated horizontally from each other by a small distance and these two cameras are combined together in a single frame. The 3D camera is used to produce two stereoscopic pictures for a given object. The distance between the cameras and the object can be measured depending upon the distance between the positions

of the objects in both pictures, the focal lengths of both cameras as well as the distance. Triangulation is used to relate those mentioned dimensions with each other. Image processing is used to determine relations between the pictures of the object in the images formed by left and right camera through the technique of template matching. Template matching is used to find similarity between parts of the two images containing the object picture, which lead to find the amount of disparity in the object position coordinates. The distance of the object varies inversely with disparity and the accuracy of distance measurements depends on resolution of the camera pictures, lens optical properties and separation between the optical axes of both cameras. Throughout this work a 3D webcam is used and a Matlab code was written to find the object distance.

### **PID Controller**

PID is implemented to the directional control and cross flow blower motors. Servomotors and AC motors are controlled using PID tuning to minimize response errors. The complete functional internal unit of an air conditioner integrated with the installed modification is shown in figure 8.

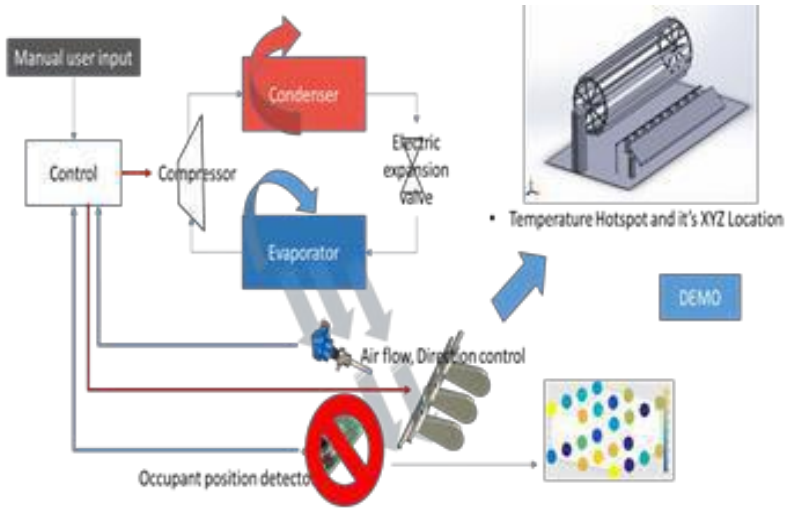


Figure 8: Schematic diagram

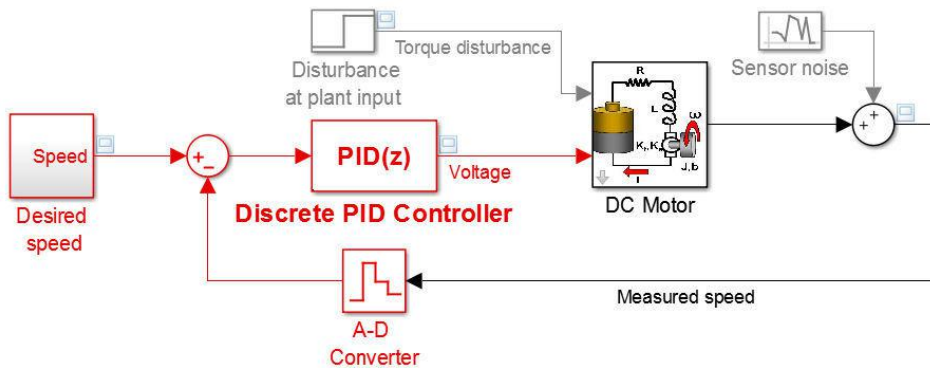


Figure 9: PID Controller diagram

## Results and Discussion

The expected goals of smart control for air conditioner include human comfort and energy conservation. They could be evaluated by:

- Temperature analysis
- CFD model
- Controller
- Image Analysis

Proposed speed controller for the DC Blower motor in the air conditioner is shown below it used to control the drastic speed variation in the blower motor here we have simulated “LG Electronics 4681A20064N Air Conditioner Fan”

## Conclusions

The study showed that the positive effects in reduced level of temperature variations in air conditioner and the long lasting performance of the air conditioner. In the system the major difficulty faced is to fix the fan controller to the existing device. The prior manufacturer's allowed space is not enough for fixing the prototype.

The energy saving concept is achieved through the rapid cooling method which enables person to feel thermal comfort suddenly rather than operating air conditioner in low temperatures for long period. Maintaining a temperature at 26°C is tested through the research after rapid cooling to a lower temperature comparing the outdoor temperature.

In future works the image processing based air condition controller could be developed in manufacturing aspect. The control technology development to fuzzy or neural aspects are available in research arena.

## References

- [1] Mardiana A, Riffat SB, "Building Energy Consumption and Carbon dioxide Emissions: Threat to Climate Change," Earth Science & Climatic Change, 2015.
- [2] U. d. o. Energy, "ARPA-E," USA government, [Online]. Available: [https://arpa-e.energy.gov/?q=site-page/funding-agreements-](https://arpa-e.energy.gov/?q=site-page/funding-agreements-project-guidance)
- [3] D. Biello, "New Technologies Aim to Save Energy--and Lives--with Better Air Conditioning," Scientific American, September 6, 2013.
- [4] I. E. Agency, "World Energy Outlook," 2016. [Online]. Available: <https://www.iea.org/publications/freepublications/publication/WorldEnergyOutlook2016ExecutiveSummaryEnglish.pdf>. [Accessed 31 01 2017].
- [5] M.Muhammad Waseem AhmadE mail author, "Computational intelligence techniques for HVAC systems: A review," Building Simulation, vol. Volume 9, no. Issue 4, August 2016.
- [6] Z. Z. & N. Yu, "The application of advanced control technologies," Advances in Building Energy Research, 23 Dec 2015..
- [7] Dallas, DS 18B20 programmable resolution wire digital thermo meter.
- [8] C.-C. C. a. D. Lee, "Smart Sensors Enable Smart Air Conditioning Control," Sensors, 24 June 2014.
- [9] D.-S. L. Chih-Sheng Chen, "Energy Saving Effects of Wireless Sensor Networks: A Case," Sensors, Published: 10 February 2011.
- [10] E. R. Johansson E, "The influence of urban design on outdoor thermal comfort in the hot, humid city of Colombo, Sri Lanka," International Journal of Biometeorology, p. 51(2):119–33, 2006.

# Thermal Performance Analysis of Walls for Designing Green Buildings

KS Niroshan<sup>1</sup>, AGJP Kumara<sup>2</sup>, MIM Premalal<sup>3</sup>, MMID Manthilake<sup>4</sup>

*Department of Mechanical Engineering, University of Moratuwa  
Katubedda, Sri Lanka*

<sup>1</sup> saliyaniroshan@gmail.com  
<sup>2</sup> pushpaanush19581108@gmail.com  
<sup>3</sup> ishanmadhuranga91@gmail.com  
<sup>4</sup> inoka@mech.mrt.ac.lk

## Abstract

Use of active air conditioning for achieving thermal comfort is becoming extensively popular in the tropical countries in spite of being unsustainable both economically and environmentally. The main contributor of the cooling load of a typical office building is heat gains across the building envelope and a major part of that is through the building walls. Time variation of temperature and resulting heat transfer across the building walls is unsteady or transient and sinusoidal in response to the variation of outdoor temperature. The heat gains can be reduced by choosing wall materials with suitable thermal properties. This will reduce the cooling load on active air conditioning system and may even provide comfort without having to use air conditioners. This paper presents an interactive tool to select thermal properties i.e. the U factor and the thermal mass of walls for a building based on the local climate to ensure thermal comfort in terms of indoor temperature. Further, the users can use this tool as a guide on their preferred wall materials and /or wall thickness to ensure comfortable indoor temperatures. The tool is tested on case studies carried out in buildings in three different climatic locations in Sri Lanka.

**Keywords** : Building envelope, Thermal analysis, Passive cooling, Climate response, Thermal comfort

## Introduction

In general the energy share of comfort conditioning of a country is nearly 40% of its total energy demand, and even without having any severe cold weather the Asian countries also appear to be closely following this trend [1]. The energy demand for active air conditioning systems is over 50% of total energy use of a typical office building in tropical countries [1]. Out of the total cooling load, over 60% is due to the external heat gains from the heat transferred into the building across the envelope by conduction, radiation and convection. Over 35 % of this is due to the heat conducted across the walls [1]. Energy saving opportunities such as measures for mitigating building thermal gains have to be incorporated at the earliest stages of building design for economic benefits [2]. This paper presents three case studies carried out in different locations of the country showing the effect of wall thermal behaviour on indoor climate.

## Literature Review

By acting as a thermal barrier, the building envelope plays an important role in regulating indoor temperatures and helps to reduce the amount of energy required to maintain thermal comfort. Minimizing heat transfer through the building envelope is crucial for reducing the power for heating as well as for cooling [3, 4].

### Purposes and Functions of building envelopes

A building envelope is the primary interface with the outdoor

environment and the physical separator between the conditioned and the unconditioned environment. A good building envelope is climate appropriate, structurally sound and aesthetically pleasing [1].

Being the skin of the building, the appearance and the operation of the envelope has an influence on the interior environment and on factors such as productivity and satisfaction of occupants. It supports most of structural loadings and resist or transfer the loads imposed by the interior and exterior environments. Building walls control and regulate the energy and mass transfer between external and internal environments such as by resisting water penetration and condensation, excessive air or smoke infiltration, noise transmission and heat transfer [2, 3].

### Construction and thermal properties

A variety of building materials are used for building construction including natural substances such as clay, sand, wood and rock, grass and tree leaves and artificial products such as concrete, glass, brick, and plasterboard defines the thermal response of the building envelope [4].

The thermal properties of materials include: thermal conductivity (k), thermal conductance (C), thermal transmittance (U), thermal resistance (R-value = 1/U), thermal mass, density, specific heat capacity, thermal capacity and Thermal Lag [8]. The Figure 1 shows that the peak indoor temperature for a building with a high thermal mass construction occurs after 6 hours of that of the outdoor wall surface. [5, 6].

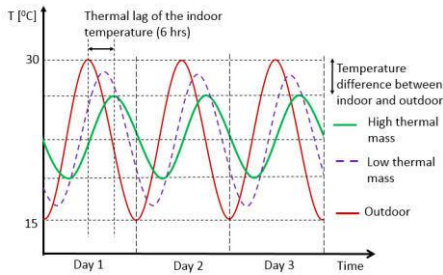


Figure 1: Variation of indoor temperature as a result of wall thermal properties

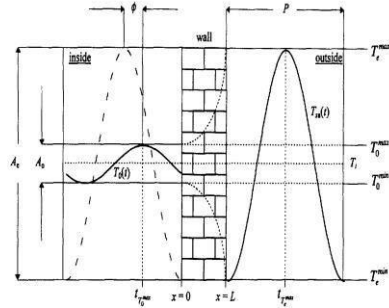


Figure 2: A schematic of time lag and decrement factor [6]

**Effect on indoor temperature from outdoor temperature**

Although the indoor temperature is desired to be maintained at a constant level, the outdoor temperature varies over the day with the temperature of atmospheric air (as shown in the mathematical models 1 and 2) which is a result of several factors: the position of the Sun (time of the day), clouds, wind and the moisture content.

The harmonic response method is widely used to analyse the heat transfer through a building envelope with periodic variation of outdoor and the resulting indoor temperature [5].

The schematic diagram in Figure 2 shows the propagation of heat wave across a building wall. The building wall stores a part of the heat and causes a delay and a reduction in the amplitude of the heat wave. As mentioned before, the time taken for heat wave to propagate from outer surface to the inner surface named as 'time lag' and the decreasing ratio of its amplitude is named as 'decrement factor'[5, 6, 7].

The time lag  $\phi$  is defined as:

$$\phi = \begin{cases} t_{T_o,max} > t_{T_e,max} = t_{T_o,max} - t_{T_e,max} \\ t_{T_o,max} < t_{T_e,max} = t_{T_o,max} - t_{T_e,max} + P \\ t_{T_o,max} = t_{T_e,max} = P \end{cases}$$

Where  $t_{T_o,max}$  and  $t_{T_e,max}$  (h) represents the time in hours when inside and outside surface temperatures are at their maximum respectively and  $P$  (24 h) is the period of the wave. The decrement factor DF is defined as:  $DF = \frac{A_i}{A_e} = \frac{t_{T_i,max} - t_{T_i,min}}{t_{T_e,max} - t_{T_e,min}}$ . Where  $A_i$  and  $A_e$  are the amplitudes of the wave in the inner and in the outer surfaces of the wall respectively.

Assuming, the temperature of indoor surface ( $T_i$ ) and the outdoor surface temperature ( $T_o$ ) are harmonic functions of time with angular frequency  $\omega$  and amplitudes  $A_i$  and  $A_o$ ,  $\bar{T}_i$  and  $\bar{T}_o$  are the average temperatures of the indoor wall surface and the outdoor surface respectively, period of 24 hours giving  $\omega = 2\pi/24 h^{-1}$ , and the phase shift from outdoor surface temperature is  $\phi_i$ . The effect of thermal mass on indoor air temperature for a single room with windows can be modelled as follows [5].

$$T_o = \bar{T}_o + A_o \cos(\omega t) \quad \dots (1)$$

$$T_i = \bar{T}_i + A_i \cos[\omega t - \phi_i] \quad \dots (2)$$

The temperature distribution on the indoor surface of the wall is uniform and can be described by  $T_i$ , with an angular frequency  $\omega$ ,  $\varepsilon_i$  Time lag and amplitude  $A_i$ .

$$T_i = \check{T}_i + A_i \cos(\omega t - \varphi_i) = \check{T}_i + A_i \cos[\omega(t - \varepsilon_i)] \quad \dots (3)$$

The equations above shows that the temperature of any cross section through the wall is varying periodically over 24 hour period giving a sinusoidal relationship. Hence, the indoor air temperature of a building is driven by the outdoor temperatures and the thermal properties of the building envelope. A tool was developed with a GUI, based on above models and was tested on selected three case buildings.

## Case studies

Case studies were conducted in Hambantota, Colombo and Matara districts to investigate the effect of thermal mass on the indoor temperature. Data were collected for solar air temperature, outdoor air temperature, wall outer surface temperature, indoor air temperature and wall inner surface temperature which are required to above mathematical relations. For all case studies, it was assumed there are no internal heat sources in the used buildings and the effect on thermal performance of the wall from the coatings of the wall surfaces is negligible.

Case Building I: A domestic building in Hambantota built in 1985. The walls were constructed with 230 mm thick burnt mud brick layer sandwiched between 125 mm cement plaster on both external surface and internal

surface. South direction external wall was selected for case study. The roof was of roofing tiles with an asbestos ceiling.

Case study II: A room in the 2<sup>nd</sup> floor of a domestic building built in year 2000 in Colombo. As this building has a 3<sup>rd</sup> floor, both floor and roof of the room are concrete slabs. The north facing external wall was selected for study and walls were constructed with a 230mm burnt mud brick layer with 125mm cement plaster on both sides.

Case study III: A room in a domestic building in Matara district built in 2007. The walls were constructed with 15 cm cement brick layer with paint coating on both sides. The room dimensions were 4.07 m x 3.05 m x 2.3 m. East facing external wall was selected for the study. The roof was built with roofing tiles with an asbestos ceiling.

## Analysis of the data

Table 1 gives experimental data on the time lag and decrement factor [5, 6]. For each case building, real and modeled variation of the outside wall surface temperature and inside wall surface temperature were plotted against time.

Further, to show the effect of wall thermal transmittance (U factor), an expanded polystyrene (EPS) layer was added (W3 in Table 1) and modeled for the indoor wall surface temperature. The thermal performance of walls are given in the table below [5, 7]. The abbreviations are CP = Concrete plaster, BW = Brick wall and CB = Cement Brick.

Table 1: Thermal properties of few wall configurations

Wall (in-out)mm	$\frac{U}{W}$ $\frac{m^2K}{W}$	$\frac{R}{m^2K}$ $\frac{W}{W}$	Time lag $\epsilon_i$ (hrs)	DF
<b>W1</b> 12.5 CP, 230 BW, 12.5 CP	2.09	0.478	7.262	0.174
<b>W2</b> 150 CB <b>W3</b> 12.5 CP, 50 EPS, 230 BW, 12.5 CP	3.63	0.275	2.512	0.488
	0.52	1.923	12.275	0.009

#### Case Building I: Hambantota

Consider Figure 3. Comparing the variation of real surface temperatures of outdoor wall and the indoor wall, the peak temperature of indoor wall surface is observed after nearly 7 hours of that of outdoor wall surface. Similar

variation is observed for that of the modeled. The temperature variation on indoor surface varies between 30.5°C and 28°C. The indoor temperature is further reduced down to the average temperature by improving wall thermal properties as shown by the indoor wall temperature curve for modified wall (W3 in Table) with a lower U value.

#### Case Building II: Colombo

Comparing the variation of measured temperatures of outdoor and the indoor wall surfaces (Figure 4), the peak temperature of indoor wall surface is observed after nearly 4 hours of that of outdoor. The temperature variation on indoor surface varies between 30.5°C and 32.5°C while, that of the outdoor wall surface is 28.5°C and 34.8°C. The day time peak indoor temperature is further reduced by using a wall with (W3 in Table 1).

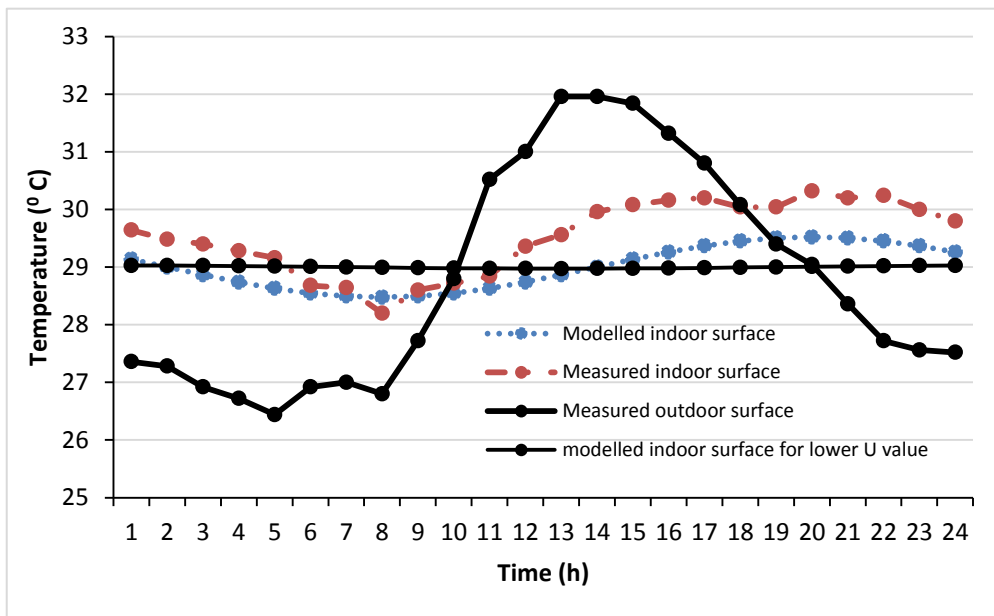


Figure 3: Variation of wall surface temperatures for a domestic building in Hambantota





lower U value as shown by the temperature curve for the modified wall

Case Building III: Matara

Consider Figure 5. The actual temperature profile of the indoor wall surface is observed to be closely following that of outdoor wall surface

ensuring that the wall is constructed using cement bricks. The temperature on indoor surface varies between 30.7°C and 27.3°C while, that of the outdoor wall surface is 32.5°C and 25.6°C. The day time indoor temperature can be reduced to 29°C using a wall with lower U value

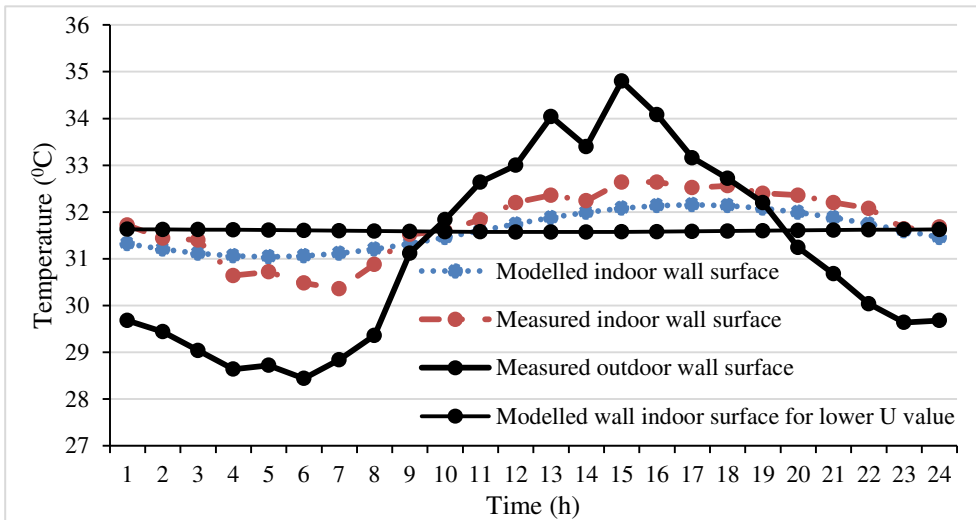


Figure 4: Variation of wall surface temperatures of a domestic building in Colombo

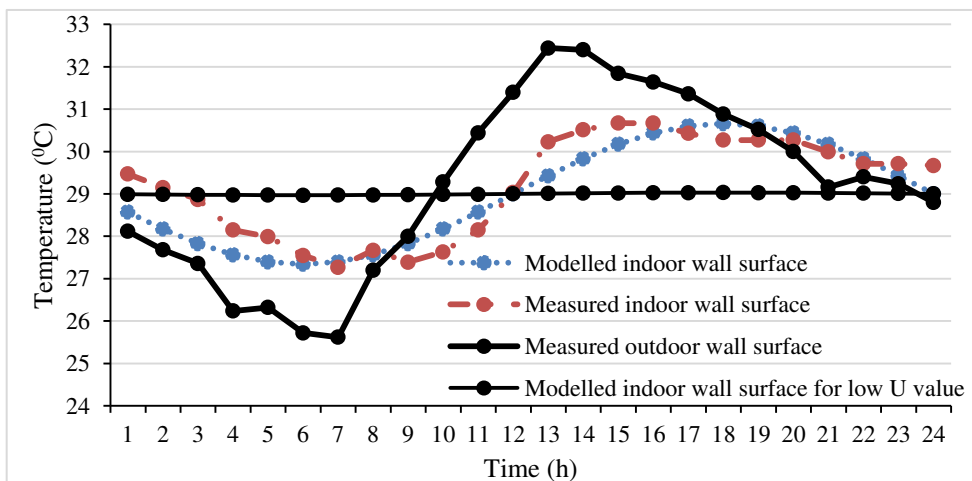


Figure 5: Variation of indoor and outdoor wall surface temperatures of a building in Matara



## Results and Discussion

The results are laid out considering each case building. The effect of wall thermal properties on the thermal response and limitations of improving thermal comfort are also discussed.

### Case Building I: Hambantota

With the existing construction the temperature of the internal wall increases beyond 30°C during the afternoon and continues to be hot over the night time. Using low U value material, the temperature of indoor surface is reduced by, 1.5°C down to 29°C.

### Case Building II: Colombo

The average indoor wall temperature is 31.6°C, which is over 4°C beyond the comfort temperature for Sri Lankans [9]. By using low U value wall material the temperature of indoor surface is reduced down to 31.6°C.

### Case Building III: Matara

The temperature variation of the inside surface of the wall appears to be closely following that of outside in terms of both temperature and time. The maximum temperature of inside

wall surface was 30.67°C, just 1.7°C below that of the outside wall surface with a time lag of 2 (h). When a low U value wall material (i.e. W4 type) is used, the temperature of indoor surface is reduced to almost a constant value of 29°C.

In essence, using a low U value material for wall construction reduces the indoor temperature level and variation. If an active AC system was used, this reduction will result in significant energy and cost savings [10]. In every case study the minimum indoor temperature achievable was the average temperature of the indoor wall surface.

As the comfort temperature for Sri Lankans is  $27 \pm 1^\circ\text{C}$  [9], the indoor temperature needs to be further reduced. This is achievable by using active methods such as, use of fans or AC systems and passive methods such as shading. Considering the actual wall materials of the case buildings, the rate and the magnitude of the heat propagation can be compared using Figure 6.

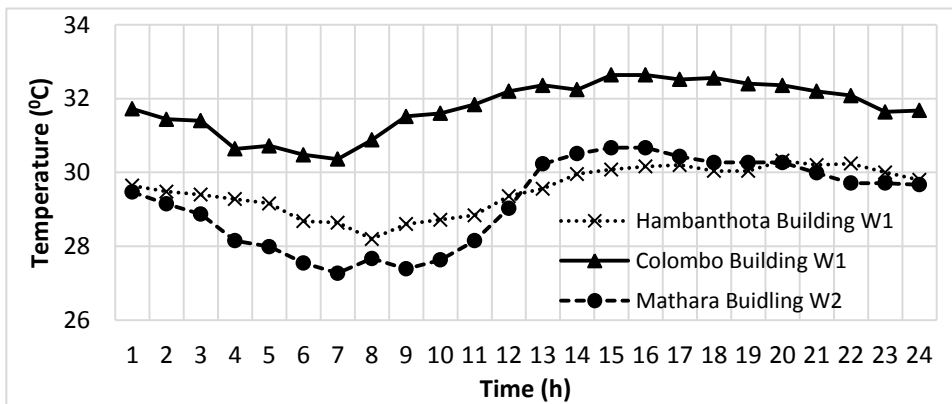


Figure 6: Variation of actual temperature of indoor wall surface based on the wall construction material

The minimum indoor temperature achievable by improving wall thermal properties alone is the mean temperature of outdoor temperature profile as can be clearly seen in the Figure 6. For example, the average temperature of Colombo outdoor environment is greater than 31.6°C and so is the achievable temperature of indoor wall surface.

### Conclusion and Future Work

A thermal response analysis was carried out for walls of three case buildings in Sri Lanka: Hambantota, Colombo and Matara Districts. The Key findings of the studies are as follows,

- Improving the thermal properties of walls reduce the magnitude and fluctuation of the indoor temperature.
- The average outdoor wall surface temperature is the limit for minimum indoor temperature reachable by improving thermal properties alone.
- If the local average outdoor temperature is hot, additional methods of cooling the indoor air has to be integrated to the building design to bring thermal comfort.
- A graphical user interface was developed to select suitable wall thermal properties for a given locality based on its climate.

Future work:

A data base for the thermal properties of local building materials has to be integrated in the developed computer aided tool.

Although all case buildings were situated within 2 km from the coastal area, the outdoor environment in

Colombo was over 4°C hotter than the other two. This may be due to dense city construction or some other reason. However, it is worth investigating the effect of built environment on changing the local climate of a city.

### References

- [1] Waite M., Cohen E., Torbey H., Piccirilli M., Tian Y. and Modi V. 2017, Global trends in urban electricity demands for cooling and heating, Energy ,Volume 127, pp. 786 – 802.
- [2] Feng, S. C. and E. Y. Song. 2000. Information modelling of conceptual design integrated with process planning. In Proceedings of symposia on design For manufacturability. International Mechanical Engineering Congress and Exposition.
- [3] Ng P. K., N. Mithraratne, H. W. Kua. 2013. “Energy analysis of semi-transparent BIPV in Singapore buildings”. Energy and Buildings, Volume 66 pp. 274–281.
- [4] Chwieduk D. A., 2016, “Some aspects of energy efficient building envelope in high latitude countries”, *Solar Energy*, Volume 133, pp 194-206.
- [5] Balaji, NC, M. Mani, B.V. V. Reddy, 2013. Thermal performance of building walls. Proceedings of 1st IBPSA Italy conference, International Building Performance Simulation Analysis Association.
- [6] Asan, H. 1998. “Effects of wall’s insulation thickness and position on time lag and decrement factor”. Energy and Buildings. Volume 28. Pp. 299-305
- [7] Duan Shuangding, 2011 “Indoor temperature Fluctuation and Cooling Load Reduction Using Thermal Mass and Night Ventilation”, International

Conference on Computer Distributed Control and Intelligent Environmental Monitoring, China.

[8] Karlsson, J. 2012. "Possibilities of using thermal mass in buildings to save energy, cut power consumption peaks and increase the thermal comfort Division of Building Materials", LTH, Lund University, 2012.

[9] Emmanuel, R. and Rathnayake, G. 2002. "Indoor thermal comfort in contemporary Sri Lankan urban houses: a simulation study". Built-Environment-Sri Lanka -Volume 02, pp. 22-27.

[10] G. Papadakis, P. Tsamis, S. Kyritsis. 2001. "An experimental investigation of the effects of shading with plants for solar control of buildings". Energy and Buildings, Volume 33, pp. 831-836.

# Introduce 12V/ 24V Direct Current for Lighting Buildings to Save Energy and Reduce Electronic Waste

K.K.L.B. Adikaram

Computer Unit, Faculty of Agriculture, University of Ruhuna, Mapalana 81100, Sri Lanka  
lasantha@agricc.ruh.ac.lk

## Abstract

LED bulbs working with 230V alternative current (AC) has become a popular way of lighting in both residential and commercial buildings. Because LED bulbs need direct current (DC), present system converts 230V AC to DC (6V to 24V) by means of an electronic circuit in each bulb. Energy loss due to rectification, additional cost of electronic parts, and being an electronic waste at the end of life cycle of the bulb are the negative impacts caused due to the present system. Those drawbacks can be easily overcome by replacing 230V AC lighting system with LED bulbs working with 6V to 24V DC. The proposed system improves the efficiency of the bulb (1% - 5%), reduces energy loss due to rectification (1% - 4%), reduces electronic waste, reduces production cost of the bulb ( $\approx 20\%$ ), and reduces electrical hazards. The proposed method supports integration with solar power with less energy loss. Furthermore, proper implementation of the proposed method eliminates the need of extra emergency lighting system. Nevertheless, availability of DC breakers and DC wires are low and implementation cost of the proposed method is relatively high. Thus, especially, residential consumers are reluctant to implement such a system. Therefore, this research proposes to accept the proposed method as standard method and promote it among the society.

**Keywords** :AC to DC conversion; electronic waste; electrical hazards; energy efficiency; energy conservation; LED technology

## Introduction

Energy conservation and impact on environment are two vital facts that are considered when implementing energy related applications. Nevertheless, design and the usage of some electrical devices do not adhere to the above mentioned concept. For example, most of the electronic equipment we use really operate with low direct current (DC) supply (3V to 48V) though those devices connected to 230V or 110V alternative current (AC) power supply. For example, information and communication related equipment such as computers, servers, data switches, wireless devices and IOT devices, and audio visual equipment such as radio, television, and security systems operate with DC supply. Since the standard is 230V or 110V AC supply, each device equipped with AC to DC converter (rectification unit) which includes additional production cost and causes energy loss during conversion. Furthermore, at the end of life cycle those devices, converter electronics in those devices become waste.

When considering the lighting systems, lighting systems based on light emitting diode (LED) technology is consider as efficient approach for lighting systems. Thus, deploying bulbs based on LED technology is currently the most popular method in practice for lighting systems [1, 2]. When compared with ordinary bulbs (Incandescent light bulbs and filament light bulbs), bulbs with LED technology show energy saving of 30%-80% [1]. Therefore, majority of present

day researches are focusing to improve the efficiency of existing LED bulbs [3]–[5].

As the above mentioned electronic devices, LED bulbs are also originally designed for low voltage DC. Nevertheless, to adhere to existing regulations and standards, LED light systems are designed as 230V (or 110V) AC driven units. This conversion is usually done by electronic rectifier unit in each LED bulb unit. Due to this rectification unit there are main three disadvantages: 1. includes additional cost for production cost of the LED unit, 2. energy loss due to rectification and 3. becomes an electronic waste at the end of the life cycle of the LED unit. On the other hand, absence of rectification unit reduces the production cost, eliminate the energy loss at the LED unit, and produces less electronic waste at the end of the lifecycle of the LED unit.

Integrating normal dimmers with LED bulbs driven with 230V AC is not possible and this requires special high cost solutions. Furthermore, integrating remote control switches is also expensive. In contrast, low voltage DC supply system will be a good solution for above mentioned matters and provides easy means of controlling of LED bulb units via simple electronic unit with optional remote control unit.

Eliminating rectification unit in devices such as ICT related devices and audio visual devices is not an easy task. It needs considerable architectural changes as



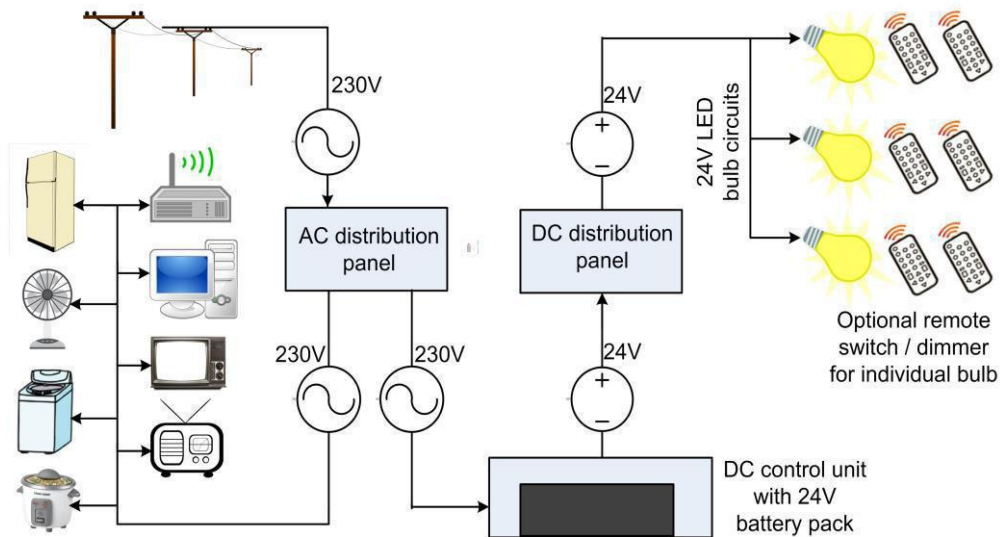


Figure 1: Proposed electrical system for lighting system of residential and commercial buildings. The proposed system equipped with 24V DC supply via inline battery pack. Furthermore, some of the LED bulb units were controlled via remote switch / dimmer.

well as standards changes in international level, or at least in national level. However, eliminating rectification unit in LED unit is very easy. It can be easily done even in home. Therefore, in this paper is focusing only about DC LED bulb units.

In the same time, some different approaches such as replacing total AC systems with 350V to 380V DC system [6], [7] can be found. This approach proposed to use total DC supply with DC equipment (LED bulbs, equipment with DC motors, etc.) and use DC-DC converts depending on the requirement of the driver of the equipment. Furthermore, studies highlighted the importance of using LED lighting units as lightning system. Most importantly, research shows that the usage of DC system has advantages over AC system.

After considering all the factors, this paper shows an electrical system which replaced the 230V AC lighting system

with 12V DC system; LED bulb units driven with 12V DC supply were used as bulbs.

## Material and Methods

This paper proposes to replace 230V AC lightning system of a building with DC system while keeping 230V AC supply for other equipment such as kitchen appliances, ICT related devices, and audio visual devices and other heavy duty devices. After considering the cost of the battery pack, expected voltage drop, cost of the wires, cost of the DC circuit breakers and the structure of the LED bulb unit, 24V was selected as the voltage of the DC system.

To isolate two supply systems (AC system and DC system), it is necessary to maintain two independent channels (conduit lines) wires. This needs to be done when designing the building, especially inside the concrete slabs. Depending on the selected voltage and load, miniature circuit breaker (MCB) and circuit breakers have to be selected. Based upon the selected values,

diameter of the wire was calculated by means of following equation.

$$d = \frac{(L \times I \times 0.04)}{(V/20)}. \quad (\text{Eq. 1})$$

Where

- $d$  = Diameter of the cable in mm.  
 $L$  = Length of the wire in m.  
 $I$  = Current in ampere.  
 $V$  = Voltage in volte.

It was decided to limit load of a circuit to 3A, set the voltage to 24V DC and use LED bulbs driven by 24V DC supply. If the average length of wire (path distance of circuit) is 10m, then from Eq. 1,  $d = 1\text{mm}$ . Figure 1 illustrates the complete overview of the proposed system.

As shown in Figure 1, remote switches and dimmers were connected to some LED bulb units. Furthermore, DC supply is empowered with inline battery pack. The proposed system was implemented on a new domestic building.

## Results and Discussions

When implementing the system, the first barrier was to overcome the social pressure (from family members, friends and colleagues) almost all were against the idea and turned down the idea. The second barrier was to find people who have knowledge and confidence to do the task among the ground level work force. However, some experts mentioned concept is good, feasible but currently applied as industrial solution (with solar systems) because it is not financially beneficial to residential consumers. Of course, the devices such as DC wires and DC circuit breakers are relatively expensive than 230V AC equipment. Cost of such devices are more than 100%

expensive than that of equivalent 230V devices. I think this is because of the less demand for such equipment. However, when the system become popular, I hope that the cost of the equipment would become low. LED bulb units were locally developed and the cost is about 20% less than the medium quality 230V LED bulb unit.

In the proposed system it is necessary to maintain 230V AC supply to drive devices such as rice cooker, iron, washing machine, etc.. To distinguish two different power systems, initial plan was to use conduits with different colors. Unfortunately, it was not possible to find conduits with different colors in same brand. Thus, conduits with different diameters were used to distinguish two power systems.

Ultimately the system was successfully deployed in the building. However, still it has not been fully evaluated. According to the evidences of previous researches, I expect at 1% - 5%, efficiency of the DC LED bulb unit and expect 1% - 4% reduction of energy loss due to rectification [8].

In any good lighting design backup system is required to overcome the influences due to power interruptions. Usually, separate system is maintained to accomplish the said requirement. However, this is another financial overhead. In contrast, the proposed system does not require separate backup power system and save considerable amount of money. Though a 24V DC system is used here, depending on the other factors (e.g.: length and the thickness of the wires) it can be reduced to 12V or increased to 36V or 48V.

Absence of rectification electronics in the proposed LED bulb units, structure of the

LED bulb unit become simpler than AC LED bulb unit. This approach reduces the amount of electronic waste to the nature at the end of the lifecycle of the LED bulb unit. Furthermore, due to the simple structure of the DC LED unit, it can be easily repaired and can be reused in case of failure.

As a result of DC system, integration with dimmers and remote switches was easier and cheaper than with AC LED bulb units. More importantly, usage of remote switches reduces some two way switches and saved the cost of such equipment as well as cost for the labor.

### Conclusions

The low voltage DC system presents in this paper is an energy efficient and environmental friendly lighting system for residential and commercial buildings, which has low electrical hazard possibilities. Proper deployment of the

system provides a system with better control and makes isolated backup system unnecessary.

Since DC is not a standard yet in rules and regulations it is very important to identify standards for DC systems and implement those as accepted standards and regulations. After setting standards, the proposed method can be promoted among the society.

### Future Works

Integration of the proposed system with solar energy will make the system more energy efficient and environmentally friendly system. Figure 2 illustrates diagram of such a system.

Furthermore, because of low voltage DC platform, IOT solutions can be easily intergraded with the proposed lighting system.

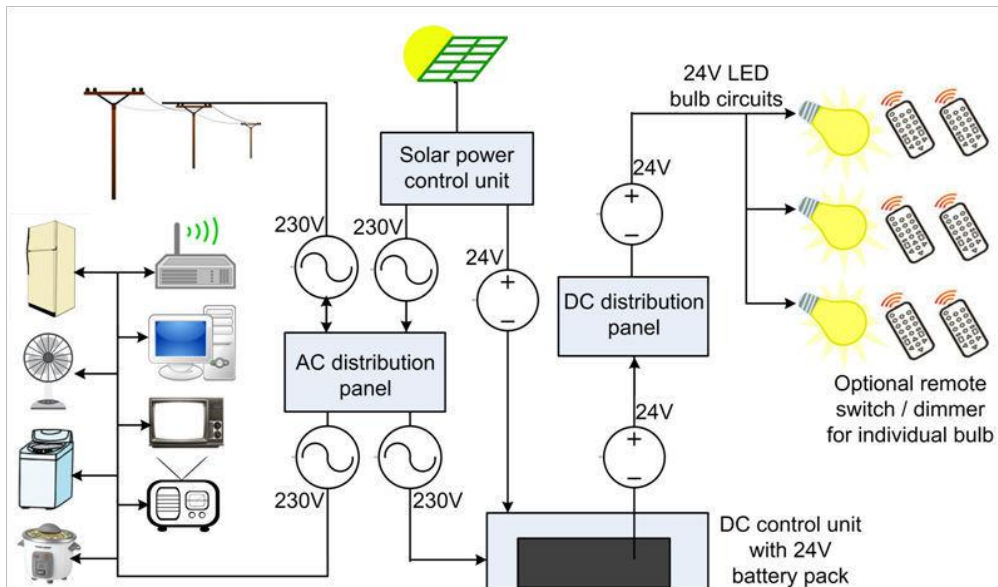


Figure 2: Integration of the proposed system with solar energy.

## References

- [1] M. F. Lee and N. Q. Zulkafli, "A case study on energy saving through lighting system for building: An internal energy review," *2016 IEEE International Conference on Power and Energy (PECon)*. pp. 575–579, 2016.
- [2] A. Jhunjhunwala *et al.*, "Energy efficiency in lighting: AC vs DC LED lights," *2016 First International Conference on Sustainable Green Buildings and Communities (SGBC)*. pp. 1–4, 2016.
- [3] A. Gago Calderón, L. Narvarte Fernández, L. M. Carrasco Moreno, and J. Serón Barba, "LED bulbs technical specification and testing procedure for solar home systems," *Renew. Sustain. Energy Rev.*, vol. 41, no. Supplement C, pp. 506–520, 2015.
- [4] R.-T. Wang and J.-C. Wang, "Analyzing the structural designs and thermal performance of nonmetal lighting devices of LED bulbs," *Int. J. Heat Mass Transf.*, vol. 99, no. Supplement C, pp. 750–761, 2016.
- [5] L. Sun, J. Zhu, and H. Wong, "Simulation and evaluation of the peak temperature in LED light bulb heatsink," *Microelectron. Reliab.*, vol. 61, no. Supplement C, pp. 140–144, 2016.
- [6] Eberhard Waffenschmidt, "Direct Current (DC) Supply Grids for LED Lighting," *LED Prof.*, 2015.
- [7] M. Hulsebosch, P. Willigenburg, J. Woudstra, and B. Groenewald, "Direct current in public lighting for improvement in LED performance and costs," *2014 International Conference on the Eleventh industrial and Commercial Use of Energy*. pp. 1–9, 2014.
- [8] Y. SeokLee, S. U. Choi, and S. A. S. Mohamed, "An energy efficient extremely low voltage DC-LED lighting system," *2015 IEEE 7th International Conference on Cybernetics and Intelligent Systems (CIS) and IEEE Conference on Robotics, Automation and Mechatronics (RAM)*. pp. 25–29, 2015.

# Investigation of Energy Efficiency Improvement by Replacement of Standard Efficiency Motors with Premium Efficiency Motors in Tea Withering Troughs

Delpitiya, C. H. K<sup>1</sup>., Wimalarathna, G. B.<sup>2</sup>

*Energy NAMA Project, United Nations Development Program, Sri Lanka*

<sup>1</sup>chamila.delpitiya@undp.org

<sup>2</sup>gbwimalaratne@yahoo.com

## Abstract

Sri Lanka is the 4<sup>th</sup> largest tea producer in the world and tea sector is one of the main export revenue source of the country. Tea industry is one of the largest energy consumer in the industrial sector. The most energy consuming operation of the tea manufacturing process is withering. Energy NAMA project implemented by the United Nations Development Program, Sri Lanka and Sustainable Energy Authority conducted a study to investigate the feasibility of replacing standard efficiency motors with Premium Efficiency motors for the tea withering process. It is considered that the industry has been using induction motors of standard efficiency class or lower of which some of them are very old motors and/or rewound motors as well as oversized motors.

The study consists of analyzing the replacement of 18 standard efficiency motors at 5 selected tea factories. Electrical and operational parameters of each motor was logged/recorded for a period of 3 days under the normal factory operating conditions. The experiment was repeated after the standard efficiency motors were replaced by IE3 class premium efficiency motors (PEMs) of same or nearly the same capacity. In order to validate the results of the trial, another verification test was conducted under the close supervision and minimum variation of control parameters.

It is observed that the energy saving by replacing standard efficiency motors with premium efficiency motors in withering troughs is insignificant and is not encouraging in most cases. This paper presents the methodology and results of the experiment conducted by the project.

**Keywords:** Tea Sector, Withering, Premium Efficiency Motor, energy

## Introduction

Sri Lanka is the fourth (4<sup>th</sup>) largest tea manufacturer [01] and the second (2<sup>nd</sup>) largest tea exporter [02] in the global tea market. The total foreign income generated from tea exports in year 2016 was US\$ 1.3 billion [02]. The tea export accounts for about 14% of the total exports and about 62% of total agriculture exports of the country [03].

Tea industry is one of the major electrical and thermal energy consuming industry in the country, which consumes approximately 235 GWh of electricity per year, which is around 7% of the total industrial electricity consumption of Sri Lanka [04].

Stages of the orthodox tea manufacturing process are withering, rolling, fermenting, drying, grading and packing while the second stage differs in orthodox-rotorvane and CTC methods to rolling cum rotorvane, cutting respectively.

Electricity is used mainly for running the machineries and a small fraction is used for lighting. In the case of orthodox tea production, the withering and rolling processes consume more energy compared to other process stages [05]. On average, the withering operation contributes to 40 – 50% of the total energy requirement of a tea factory [06].

## Withering

The partial removal of moisture in fresh tea leaves is called withering and is done by spreading green tea leaves on a bed, known as withering trough and blowing air through the leaves. A fan blows air under the layer of tea leaves laid in the trough, and air passes through the tea leaves carrying the moisture. These fans

are driven by electric motors and the motor capacities range from 3 kW to 10 kW. A withering cycle is about 12 – 14 hours and the duration depends on the ambient conditions. The normal practice is to operate the withering fan at full speed throughout the wither and flow regulation is done by inlet damper control.

## IE3 category or Premium Efficiency Motors (PEMs)

According to the efficiency classes defined by IEC 60034-30:2008, IE3 called as premium efficiency motors have an efficiency gain varying from 10% to 2% depending on the motor size 0.75kW to 375kW respectively [07]. High Efficiency motors operate with less slip which yields a slightly higher speed, around 20 rpm compared to a standard efficiency motor.

## Test methodology

### Selection of Tea Factories and PEMs for the Trial

Five tea factories in 3 tea grown regions, up country, mid country and low country engaged with two different tea processing methods, orthodox and CTC, were selected for the test.

The details of selected tea factories are given in table 1.

18 PEMs of 7 different brands compliance to IE3 category were used for the trial. The details of the selected PEMs are given in table 2.

**Test procedure**

Troughs for which motors to be replaced with PEM and reference troughs were selected with consultation of the factory staff.

Following electrical and operational parameters were measured and logged simultaneously for a minimum of 3 days for all the existing standard efficiency motors and for the reference motor before PEM installation.

*Table 0: Selected Tea Factories for the Study*

Region	Tea Factory	Location	Manufacturing method
Low Grown	Factory 1	Rathnapura	Orthodox
	Factory 2	Galle	Orthodox
Mid Grown	Factory 3	Gampola	CTC
High Grown	Factory 4	Talawakelle	Orthodox - Rotorvane
	Factory 5	Hatton	CTC

*Table 2: Details of PEMs Used for the Test*

No.	Product Name	Country of Origin	Quantity
1	Make 1	Brazil	2
2	Make 2	Czech Republic	3
3	Make 3	Czech Republic	3
4	Make 4	India	2
5	Make 5	India	3
6	Make 6	India	2
7	Make 7	Europe	3

*Table 3: Electrical parameters to be monitored/ logged*

Parameter	Unit of Measure	Measuring Interval (min)	Min.	Max.	Avg.	Remarks
Voltage	V	5				Logged continuously using power meters
Current	A	5				
Power	kW	5				
Demand	kVA	5				
Energy	kWh	5				
Power Factor	-	5				

Then standard efficiency motors were replaced with PEMs of same capacity or nearly the same capacity. The trough dimensions, fan and blade angles were kept unchanged. After installation of

PEMs performance of each motor was continuously monitored for a minimum of 3 days keeping the selected reference trough unchanged. Figure 1 illustrates the experimental arrangement.

Table 4: Operational parameters monitored in withering troughs

Parameter	Unit of Measurement	Measuring Interval
Green leaf loading rate	(kg <sub>green tea leaves</sub> / ft <sup>2</sup> )	Once
Withering start time		Once
Weight of green tea leaves	kg	Once
1 <sup>st</sup> Turning over (time)		Once
2 <sup>nd</sup> Turning over (time)		Once
Withering end time		Once
Weight of withered tea leaves	kg	Once
Ambient temperature	°C	30 min
Ambient RH	%	30 min
Motor Speed	rpm	2 hour
Dry bulb temperature	°C	2 hour
Wet bulb temperature	°C	2 hour
Air flow velocity at trough entrance (9 – 12 locations)	ms <sup>-1</sup>	2 hour
Static pressure inside the Trough	Pascal	2 hour

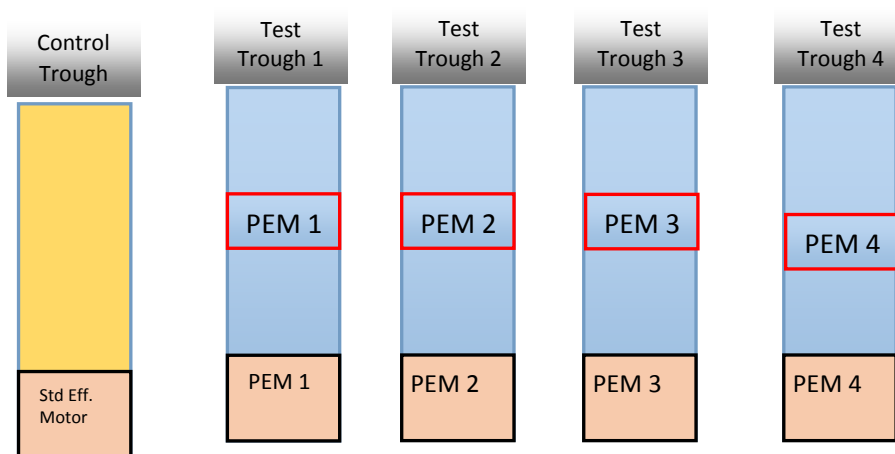


Figure 1: Testing arrangement after PEM installation

(Testing was carried out under normal operating conditions as practiced by factory operators.)



### Verification Test

For further verification of results obtained from 18 premium efficiency motors, another test was performed with tight control of external parameters using trough 3 and 4 of St. Coombs Tea Factory, which are identical in all aspects. Further trough 3 was operating with a standard efficiency motor of similar capacity and age of the motor in trough 4, which was replaced by a PEM.

### Observations and Results

Initially it was intended to compare the total electricity consumption (kWh) or electricity consumption per one kg of moisture removal from green tea leaf. However, due to many variables and uncertainties within the process and difficulty of eliminating them, load profile was considered for comparison for energy consumption of withering trough motors. Since the load on fan motor is nearly constant throughout the withering period, the measured motor power can be taken for the comparison and estimation of energy saving. The following noticeable observations were made during the experiments;

- It was observed from the test results that in two occasions have a saving close to 10%, which is even higher than the theoretically calculated saving. This could have happened due to measurement errors or unusual process variations. There is slight increase or same in power consumption in 10 PEMs while only 4 has a marginal saving percentage.

Special attention was given to maintain external parameters with proper control. The variation of the moisture content of tea leaves in both withering troughs were monitored periodically while all the parameters in Table 4 are being monitored. The idea of the reference trough is to see whether there are significant variations on the process parameters such as ambient conditions, quality of tea leaf etc compared to the previous tests (with standard efficiency motor).

A summary of test Results is given in table 5 below.

- As it was expected the motor rpm of PEMs is slightly higher than that of standard efficiency motors. The observed values are 10 – 20 rpm higher than the replaced motors’.
- The withering process has many external parameters that can affect the actual power consumption.
- It was observed that some factories do not maintain recommended withering conditions (eg. the recommended loading rate, hydrometer deference, etc.) which results in energy wastes apart from the product quality
- Even in the case of replacement of aged, rewounded or oversized motors, a noticeable energy efficiency improvement was not observed.
- The average withering time is 12 – 14 hours. However, there are occasions withering time varies from 4 – 24 hours depending on wither conditions, manufacturing method, factory intake etc.

Table 5: Summary of Test Results for Trough Fan Motors

	Factory	Machine No	Old Motor			New Motor			% Saving	Remarks
			Rated kW	Avg. measured (kW)	Rated rpm	Rated kW	Avg. measured (kW)	Rated rpm		
1	Factory 2 - Elpitiya	Trough No 3	7.5	4.35	955		4.41		Control trough	
2		Trough No 5	7.5	5.46	955	5.5	5.17	975	5.31	Rewound
3		Trough No 6	7.5	5.04	955	5.5	5	965	0.79	Rewound
4		Trough No 7	7.5	4.9	955	5.5	4.88	972	0.41	
5		Trough No 8	7.5	4.94	955	5.5	4.28	966	13.36	
6	Factory 1 - Rathnapura	Trough No 1	4	2.54			2.45			Control trough
7		Trough No 2	4	2.32	970	4	2.48	980	-6.90	
8		Trough No 3	5.5	3.35			3.47			Control trough
9		Trough No 4	5.5	2.64	955	5.5	2.88	955	-9.09	Rewound
10		Trough No 7	4	3.94	960	7.5	4.22	970	-7.11	
11		Trough No 8	7.5	3.29	955	7.5	3.3	980	-0.30	
12	Factory 3 - Gampola	Trough No 4	5.5	2.99	960	5.5	2.92	975	2.34	
13		Trough No 5	4	3.34	965	4	3.2	970	4.19	
14		Trough No 9	4	3.17	960	4	3.19	965	-0.63	
15		Trough No 10		3.1			3.1			Control trough
16		Trough No 11	5.5	4.76	945	5.5	4.29	960	9.87	
17	Factory 4 - Thalawakalle	Trough No 4	3	2.86	970	3	3.06	975	-6.99	
18		Trough No 5	4	3.84	965	4	4	960	-4.17	
19		Trough No 6		4.01			3.9			Control trough
20	Factory 5 - Hatton	Trough No 1		3.25			2.76			Control trough
21		Trough No 3	3.7	2.28	950	3.7	2.1	965	7.89	
22		Trough No 4	3.7	0.75	950	3	2.8	973		Not Considered
23		Trough No 9	7.5	3.43	960	4	3.52	971	-2.62	Oversized
24		Trough No 12	4	2.48	950	3.7	4.16	940		Not Considered

Indicated in red are doubtful. Even theoretically impossible

NOTE:

- I. Since due to measuring errors results of line 22 and 24 of this chart were not considered.
- II. Only motors 2, 3 and 9 are confirmed as rewind motors. Information is not available for others

**Results of the Verification Test**

- Results of the verification test is also in agreement with the results observed in study. Load profiles of 2 motors selected for verification test are shown in figure 2. Test results are shown in Table 6.
- The moisture removal rate of both troughs are similar and the variation with time is shown in figure 3.

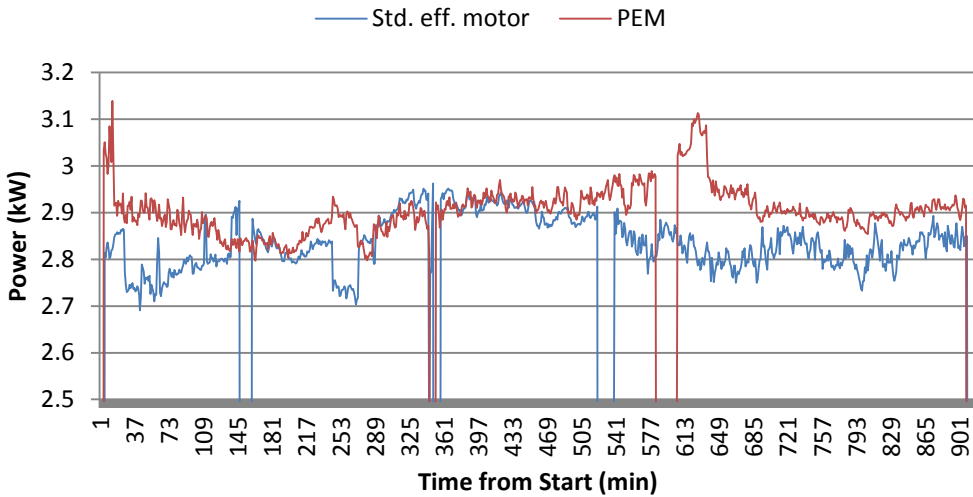


Figure 2: Load profiles of the PEM and the standard Efficiency motors

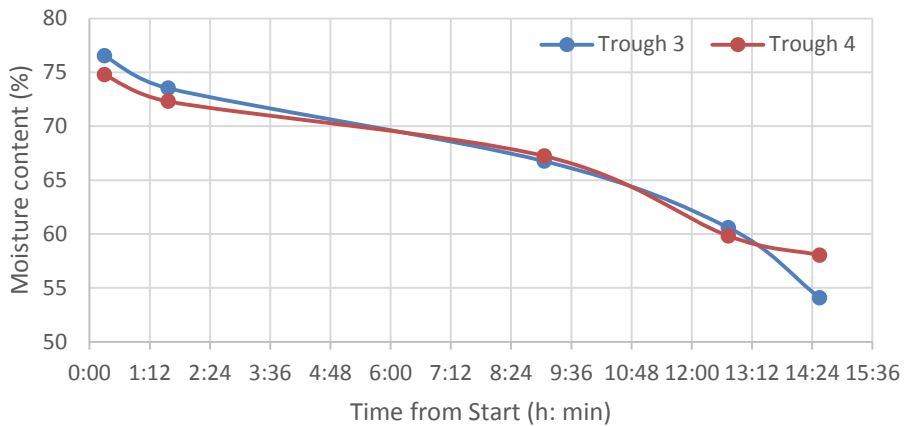


Figure 3: Variation of the moisture content of tea leaves in test

Table 6: Summary of Test Results of the Verification Test

Parameter		Trough 3	Trough 4
1	Motor	Old Motor	PEM
2	Motor rated power (kW)	3	3
3	Motor efficiency (%)		85.6
4	Total energy consumed (kWh)	<b>41.217</b>	<b>42.524</b>
5	Total time for withering (hh:mm)	14:40	14:41
6	Average power of the motor (kW)	2.81	2.90
7	Average Voltage (V)	242	242
8	Motor speed (rpm)	969	984
9	Average Dry - Wet temperature difference	6	5.875
10	Static pressure at starting (Pa)	135	105

**Discussion:**

Deviation of actual results from the predicted results is possible in an application like blower fan where output is not constant unless motor speed remains the same. In general, PEMs have a lower slip and hence higher speed of between 10- 20 rpm compared with the standard efficiency motors. Higher rpm of the PEMs discharges the air with a slightly higher pressure and volume which results in drawing a slightly high power. **Few percentages of efficiency gain by PEM application could be set off by the increased input power due to speed increase.** Since the shaft power is proportional to the cube of speed this incremental power due to increase in speed will be significant compared to the saving expected from efficiency gain. Increase in flow in the trough is not detectable by the method used by the factory to monitor the flow (floating handkerchief method). Even it is detected, flow regulation by dampers (choking) or VFD will not bring any significant energy saving.

This situation is clear from the results obtained at the verification test with close supervision and keeping the uncertainties and uncontrolled variations to a minimum. Test results of other factories also reveals a similar situation.

Trough No. 3 and No.4 of St Coombs Factory are identical in size and dimensions, and fan construction.

Trough No. 4 fan motor was replaced with 3kW PEM of make 3.

Input power to St.Eff motor = 2.81 kW  
 Input power to PEM = 2.90 kW

Speed of old St Eff motor = 969 rpm  
 Speed of New PEM = 984 rpm  
 Efficiency of old motor – 79.7%<sup>1</sup> (standard efficiency motor)  
 Efficiency of new motor – 85.6%

**Calculation of potential power saving**

Assuming output load (shaft power) is constant and works at same load factor (Motor speeds are same)

$$\text{kW saving} = \text{output power} \left( \frac{100}{\eta_1} - \frac{100}{\eta_2} \right)$$

where,  $\eta_1$  and  $\eta_2$  are standard motor efficiency and PEM efficiency.

$$= 2.9 \text{ kW} \left( \frac{100}{79.7} - \frac{100}{85.6} \right)$$

$$= 0.258 \text{ kW}$$

However due to the speed increase, air flow and pressure also increase resulting increase in output and input power.

Accordingly output power increases by a factor of  $\left(\frac{N_2}{N_1}\right)^3$

Where,  $N_1$  and  $N_2$  are standard motor rpm and PEM rpm.

Therefore input power to the PEM

$$= 3 \text{ kW} \times \left(\frac{N_2}{N_1}\right)^3 / \eta_2$$

$$= 3.670 \text{ kW}$$

Input power to the old motor

$$= 3 \text{ kW} / \eta_1$$

$$= 3.764 \text{ kW}$$

Net kW saving = 0.094kW

---

<sup>1</sup> Motor efficiency values are as per the standard IEC60034-30. These values are tally with name plate data given by manufacturer.

In a real situation, the above saving may not be possible due to many variables, measurement accuracies and uncertainties associated with the process. This is the reason for not realizing the expected power saving with the replacement of standard efficiency motors by PEMs, which has lower slip (higher speed) in the pilot trial carried out by the project. Therefore, in this particular application (withering fan blower), replacing an old standard efficiency motor with a PEM will not necessarily reduce energy consumption.

Total energy consumption of withering depends on many factors and some of them are listed as given below.

- a. Quality of green leaf
- b. Initial moisture content (surface and internal)
- c. Ambient conditions (temperature, relative humidity)
- d. Operators behavior
- e. Type of withering fan used
- f. Trough arrangement, size, shape of the mixing chamber and transformation duct
- g. Flow control arrangement
- h. Maintenance of the hydrometer reading
- i. Actual green leaf loading rate
- j. Whether loosening and turning done on time

Some of the factors affect the motor load and some affect the withering time, hence the energy consumption. But for comparison same day test, the impact of some of the parameters have no influence to the final result. However, significant variations of test results obtained in different days can be observed due to one or more of above factors.

The PEM installed in trough no 8 in Factory 2 shows a 13% reduction in energy consumption. The possible efficiency gain of the motor itself is approximately 6% and hence this could be due to a measurement error or other factors involved in the process. Therefore, this result is not considered in the study.

Trough 4 and trough 12 of Factory 5 were not considered in as there were measuring errors. Initial measurement of trough 4 was incorrect. PEM was installed in a different trough instead of originally selected trough and hence No. 12 was omitted.

The accuracy of measuring instruments is also affect the accuracy of results. Since the difference in energy consumption trying to compare in the test is a marginal value, measuring accuracy can affect the result significantly.

## Conclusion

The results of the above tests confirm that the replacing existing withering trough motors does not realize a significant saving for this particular (centrifugal load) application. The few percentage points of efficiency gain by the PEM has been offset by the speed increase due to lower slip compared to a Standard Efficiency motor. Results further lead to the conclusion that it is not a financially viable energy saving measure. Simple payback period of the incremental cost for installing a PEM to replace a burnt/damaged motor is also not justifiable due to high cost of PEMs with no/marginal saving.

## References

- [1]. The whistling kettle, Top 10 Tea Producing Nations. [Online]. Available: <http://www.thewhistlingkettle.com/info/index.php/blog/post/top-10-tea-producing-nations>
- [2]. World's Top Exports, Tea Exports by Country. [Online]. Available: <http://www.worldstopexports.com/tea-exports-by-country/>
- [3]. Sri Lanka Export Development Board, Tea Export Growth. [Online]. Available: <http://www.srilankabusiness.com/tea/tea-export-growth.html>
- [4]. Sri Lanka Sustainable Energy Authority. Energy Management program in tea sector – Summary report.
- [5]. De Silva, W. C. Status review of energy utilization by the tea industry in Sri Lanka. Sri Lanka Journal of Tea Sciences 1994; 46-58.
- [6]. Keegel, E.L. Monographs on tea production in Ceylon No. 4. Thalawakalle: Tea Research Institute; 1983
- [7]. International Electromechanical Commission, International Standard, IEC 60034-30:2008. Edition 1. 2008-10

# Development of Energy Saving Charcoal Based Evaporative Cooling System for Preservation of Perishable

G.T.U. Wickramarathna, C.P. Rupasinghe

*Department of Agricultural Engineering, Faculty of Agriculture, University of Ruhuna,  
Matara, Sri Lanka  
chintha@ageng.ruh.ac.lk*

## Abstract

Most of the post-harvest losses of agricultural products occur due to lack of proper storage facilities. Controlling both temperature and relative humidity is very important for reducing post-harvest losses. Refrigerators fulfill these requirements but there are some issues such as energy intensive appliance, greenhouse gas emission and high initial cost. Low temperature and high relative humidity can be achieved by using less expensive methods of evaporative cooling. In this study, charcoal coolers were constructed with 0.027 m<sup>3</sup> storage capacity. Charcoal produced from coconut and cinnamon sticks was used as the absorbing material. Charcoal was made using pyrolysis process to have increased porosity. High porosity level helped to absorb more water to increase the efficiency of evaporation. Relative humidity (Rh) and temperature difference in inner and outer chambers were measured. Measurements were taken under unload condition and load condition. Data were taken in hour time intervals from 8.00 a.m. to 16.00 p.m. Quality parameters of stored food were measured using titratable acidity and TSS value. Difference was observed and result revealed that significant temperature ( $P<0.05$ ) exist in between cinnamon charcoal and Coconut shell charcoal type structures under the load condition. The shelf life of tomato was extended more than 25 days using both models. The temperature drop of the cooler was about 3-4°C compared to ambient temperature and relative humidity increment was about 8%-10%. Cooling efficiency was significantly ( $P<0.05$ ) higher in coconut shell charcoal cooler compared to cinnamon stick charcoal cooler. The models with coconut shell charcoal showed significantly better results than cinnamon stick charcoal. When compared with control experiment both charcoal coolers were significantly showed better results.

**Keywords :** charcoal; evaporative cooling; temperature; humidity



## Introduction

With the growth of population, demand of food is increasing hence proper management of food is a major requirement. Among those food, fruits and vegetable are vital for supplying human nutrition. They are rich in vitamins and minerals such as provitamin A; carotene, ascorbic acid, riboflavin, iron, iodine, calcium, etc. [1].

The quality of fruits and vegetable depend on the Post-harvest handling process. Most of fruits and vegetables are destroyed due to the improper postharvest handling operations. In 2001, Approximately 270,000 tons of fruits and vegetables are destroyed during post-harvest operations and value of this loss is approximately Rs Million 9,000 [2]. The major problem is changing some physical characteristics such as texture, color and freshness during the storage period. It is very important to control both temperature and relative humidity during the storage period to reduce post-harvest losses.

The cooling process during post-harvest period helps to overcome these problems such as it inhibit and slow growth rate and activity of pathogens, suppress enzymatic degradation and respiration, slow and inhibit water loss, reduce the production of ethylene or minimize a commodity's reaction to ethylene [3].

Therefore it is very important to maintain low temperatures during post-harvest handling and storage to minimize the losses [4]. Reducing temperature of surrounding air of the product can be maintained by forced air

cooling, hydro cooling, vacuum cooling, and adiabatic cooling [5].

Sophisticated techniques such as mechanical refrigeration, controlled atmospheres, hypobaric storage, etc are practiced for reducing post-harvest losses of perishable. These techniques are highly capital and energy intensive for small scale farmers, wholesalers and retailers in developing countries. Moreover, in the existing mechanical refrigerating systems are not often put into consideration as stored perishable products were normally subjected to excessive chilling or freezing due to injuries. As a remedial action for these, evaporative cooling technique has high potential for reducing post harvest losses of fruits and vegetable. Evaporative cooling is dependent on the condition of the air and it is necessary to determine the weather condition. That may be encountered to properly evaluate the possible effectiveness of the evaporative coolers [6]. The amount of water vapor that can be taken up and held by the air is not constant: it depend on two factors: the first is the temperature which determines the energy level of the air to take up and hold water vapor. The second involves the relative humidity which represents the availability of water [7].

The principle of cooling is evaporation. Evaporation efficiency mainly depends on four factors, being wind speed, surface area, temperature of the air and Relative humidity. Sometimes evaporative cooling system is used for preservation; it is used with shade on top [8]. Evaporative cooling is a physical incident that changes the phase liquid to gas, typically into surrounding air, cools an object or a liquid in contact with it. Latent heat, the amount of heat that is

needed to evaporate the liquid, is drawn from the air. When considering water evaporating into air, the wet-bulb temperature, as compared to the air's dry-bulb temperature, is a measure of the potential for evaporative cooling. The greater difference between the two temperatures, the greater the evaporative cooling effect [9].

Evaporative cooling structures are normally prepared with porous material with fed of water. When hot dry air passing through the structure, relative humidity of air increases and at the same time the temperature is decreased. Low temperature helps to reduce respiration rate and reducing growth of spoilage microorganisms. Respiration is very important factor for shelf life of fruits and vegetables [10]. In this study the main consideration is conservation of energy by using alternative cooling systems to minimize the losses.

The research is focused to develop alternative, low cost, environmental and user friendly charcoal based cooling system with keeping good quality of fruits and vegetables.

## Methodology

In this study, models of evaporative coolers were designed with the capacity of  $0.027 \text{ m}^3$  ( $0.3 \times 0.3 \times 0.3 \text{ m}^3$ ). The structure of the charcoal cooler was made using parallel chicken mesh walls in between filled with charcoal Figure 1. The thickness of the wall for filling charcoal was 0.5 m. Top and bottom sides of the cooler were made with solid boards. Plastic tube with drippers was used to wet the charcoal continuously at the rate of 15 ml/min.

Cinnamon stick charcoal and coconut shell charcoal were prepared under pyrolysis condition at elevated temperature of  $300^\circ\text{C}$  [11]. These two types of charcoal were selected as both are generated as byproducts of agricultural industries and available in abundance. Bulk density of prepared charcoal was tested as 0.16 and 0.19  $\text{g/cm}^3$  in Coconut shell and Cinnamon stick charcoal respectively. Low bulk density of charcoal mean high porosity and it is helpful in absorbing more water.

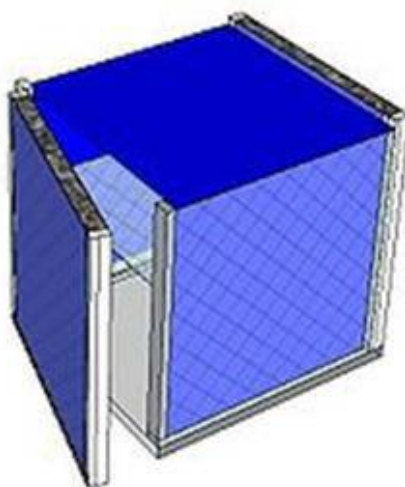


Figure 1: Structure of charcoal coolers

Prepared charcoal was filled in between the chicken mesh. The experimental procedure was designed with three treatments such as charcoal prepared by cinnamon sticks, charcoal prepared by coconut shell and without charcoal as the control. These treatments were replicated three times. Complete randomize design (CRD) was followed as experimental design. The data was analyzed using statistical software Mini tab 16.

The experiments were conducted load and unload condition with agricultural commodity tomato. Dry bulb temperature (Td), Wet bulb temperature (Tw) and RH were measured inside and outside of the chamber. Data was taken on hourly basis from 8.00am to 4.00pm.

One criterion for cooling pad evaluation is cooling efficiency calculated by following equation [12].

$$\eta_{cooling} = \frac{\Delta T}{T_d - T_w} \quad (\text{Eq. 1})$$

Where  $\Delta T$  is the change in actual temperature of ambient air, Td and Tw are the dry bulb and wet bulb temperatures respectively.

Tomato (*Lycopersicon esculentum*) produced in the area of Matara district in Sri Lanka under normal production practices, were harvested in mature green to pink (turning) in color for the experiment. Colorimetric measurements and chemical analysis such as titratable acidity and Total soluble solid (TSS) were measured as parameters of a stored agricultural product, tomato.

According to colorimetric maturity index of tomatoes there are six stages as green, breaker, turning, pink, light red, red. This colour index is visualized regarding the shelf life of the tomatoes.

The titratable acidity was as citric acid content. The 30 g was weighted and it was blended. Then the volume was made up to 100 ml. The prepared

solution (20ml) was taken into a conical flask and it was titrated with 0.1N NaOH using phenolphthalein indicator. End point was taken when the color of the solution turns into pink. Titratable acidity value was calculated using following equation 2 [13].

$$Z = \frac{V \times N \times \text{Meq.wt} \times 1000}{Y} \quad (\text{Eq. 2})$$

Where: Z = g/l of acid in Sample;  
V = Volume in ml on NaOH titrated;  
N = Normality of NaOH (0.1N);  
Meq. Wt. = Millequivalents of acid, 0.064 for citric acid;  
Y = Volume in ml of sample.  
Total Soluble Solid (TSS) was measured using refractometer as Brix value as percentage.

## Results and Discussion

### Temperature variation of models

Highest temperature difference was observed as 5.8 °C in charcoal coolers with coconut shell charcoal at 12.00 am at unload condition (figure 2). Temperature difference with unload condition was significantly difference at  $p > 0.05$  in both type charcoal coolers compare to control. Mean temperature drop of coconut shell charcoal cooler and cinnamon stick charcoal cooler was observed as 3.5°C and 3.2°C respectively. According to that result Coconut shell charcoal cooler was showed better performance.

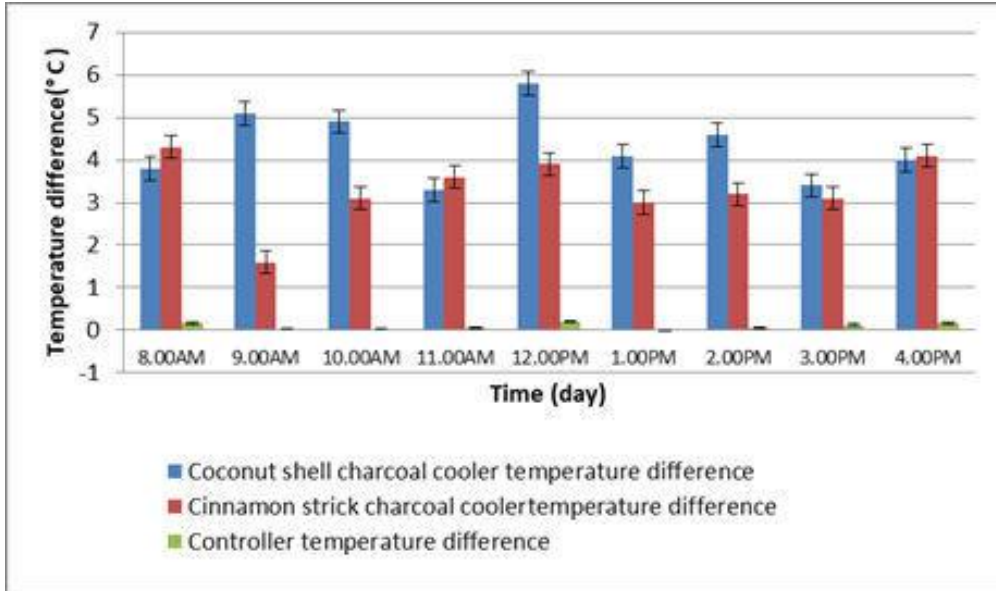


Figure 2: Temperature drop under the unload condition

### Temperature difference under the load condition

Under load condition, highest temperature difference could be seen in coconut shell charcoal cooler as about 6°C (figure 3). The reason is due that coconut shell charcoal has shown higher porosity than Cinnamon stick charcoal. It helps to retain more water. Coconut shell charcoal bulk density and Cinnamon stick charcoal were recorded as 0.16 g/cm<sup>3</sup> and 0.19 g/cm<sup>3</sup> respectively.

### Relative humidity variation of models

Highest difference of Rh of the tested models was observed as 7% at 12.00 am and 2.00 pm in unload condition (figure 4 (a)) and around 9% relative humidity drop was observed at 10.00 am and 2.00 pm in load condition (figure 4(b)). Relative humidity was increased in all

models. High humidity helps to increase the shelf life of tomatoes because less amount of water vapor evaporated from tomato. Relative humidity of inside cooler was higher than outer ambient condition. During the storage and preserving process of fruits and vegetables, the moisture and relative humidity also affect the shelf life, quality and other characteristics because mostly fruits and vegetables has shown better quality aspects at higher relative humidity (80-95%) [14].

### Cooling efficiency

Mean value of cooling efficiency of coconut shell charcoal cooler and cinnamon stick charcoal cooler were observed as 70.9% and 57.2% respectively. According to the mean value of cooling efficiency, Coconut shell charcoal cooler showed better performance when compared the mean value of cooling efficiency (figure 5).

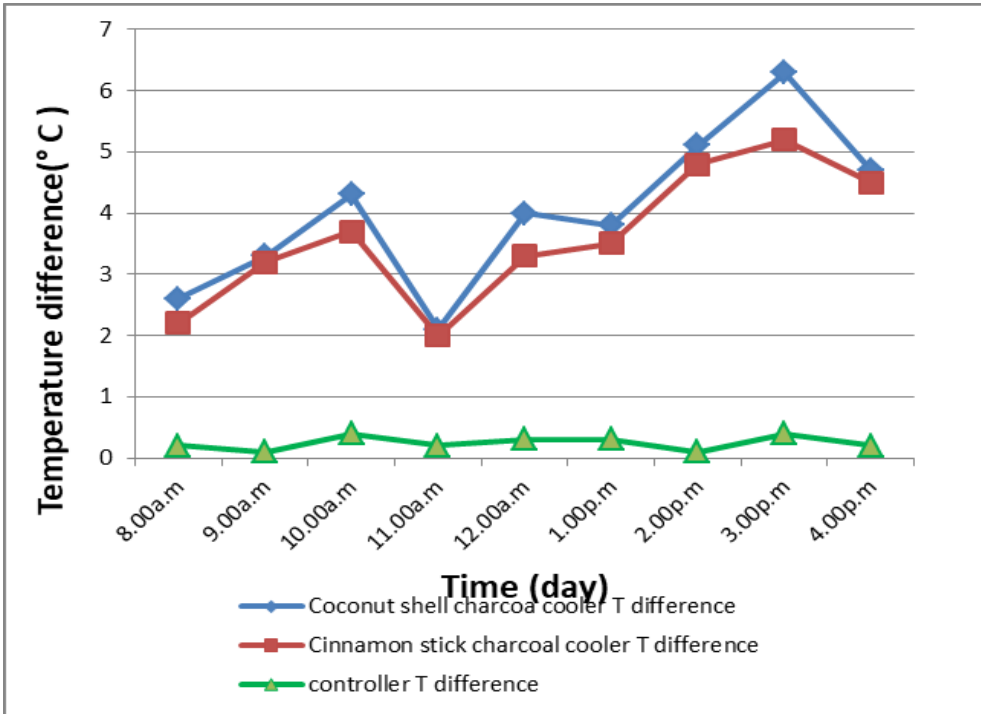


Figure 3: Temperature difference under load condition

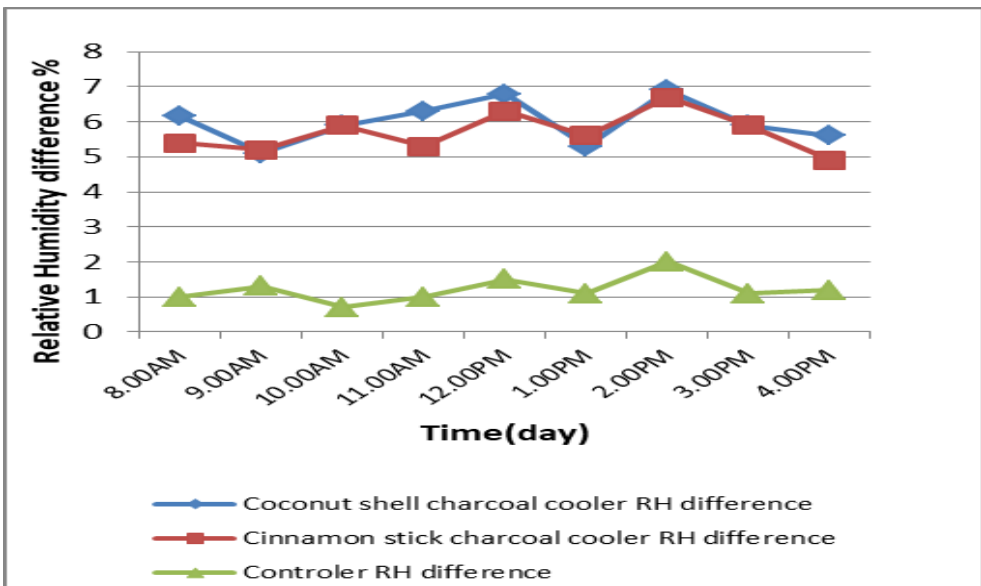


Figure 4 (a): Relative Humidity difference under unload

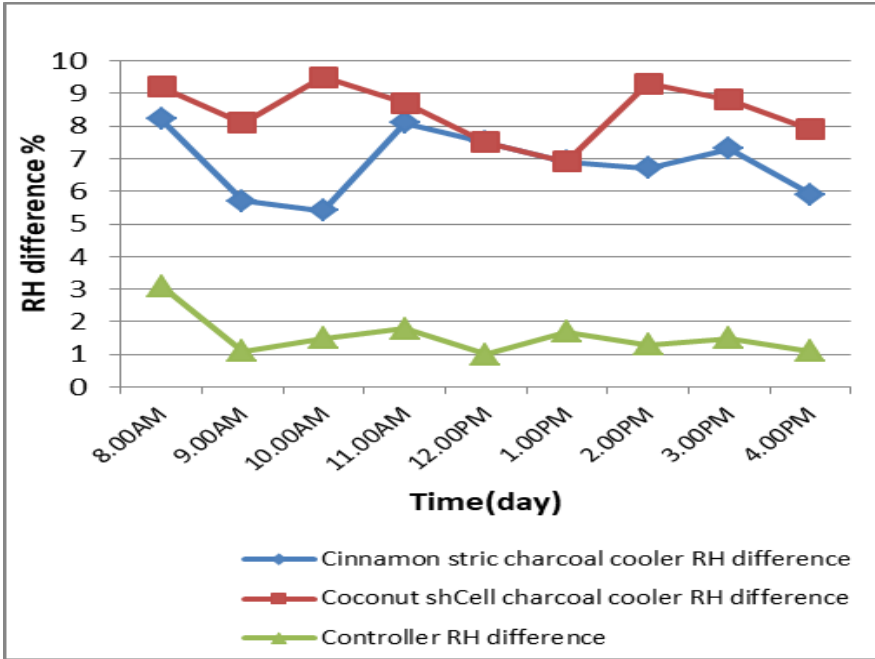


Figure 4 (b): Relative Humidity difference under load condition

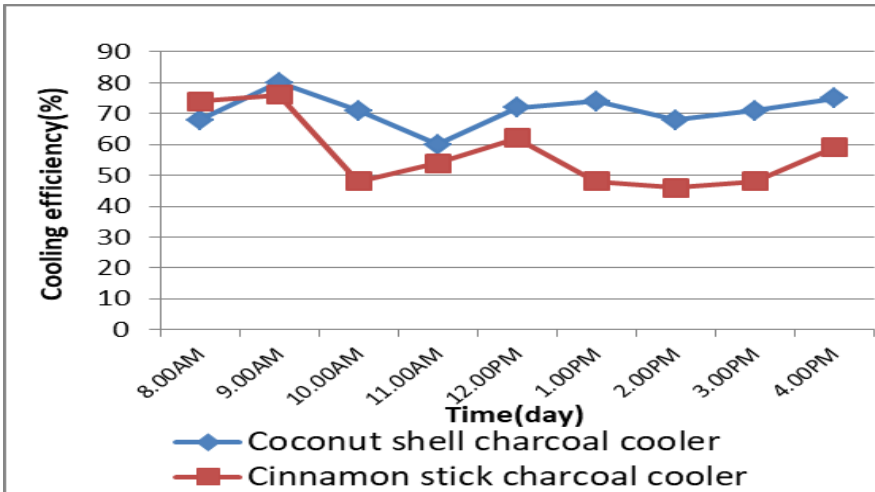


Figure 5: Cooling efficiency of different chambers

Low cooling efficiency is happens due to high relative humidity. One of the main factor affect for the cooling efficiency is relative humidity. High relative humidity means the amount of water vapor in the air as a percentage of the maximum

quantity that the air is capable of holding at a specific temperature. Evaporation rate was decreasing due to that reason. According to the observed result highest cooling efficiency was recorded at 9.00 a.m. [15].

**Variation of total soluble solid and titratable acidity**

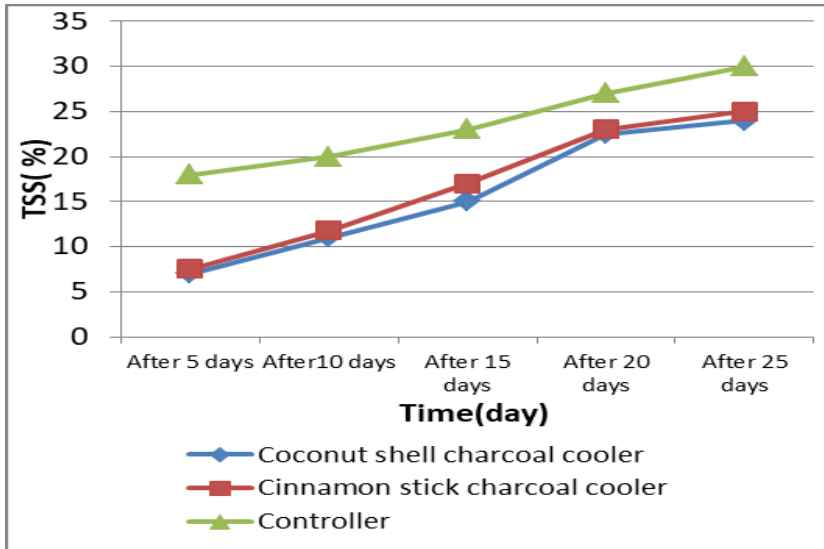


Figure 6: Variation of TSS

The figure 6 showed the variation of TSS content of tested models. The highest TSS (%) value was observed in tomato which kept in controller after 25 days. TSS was increased with the maturity and reported that by [16]. This result may

have been related to the persistent consumption of sugars and organic acids for fruit tissue metabolism, rather than the solute concentration effects, during storage.

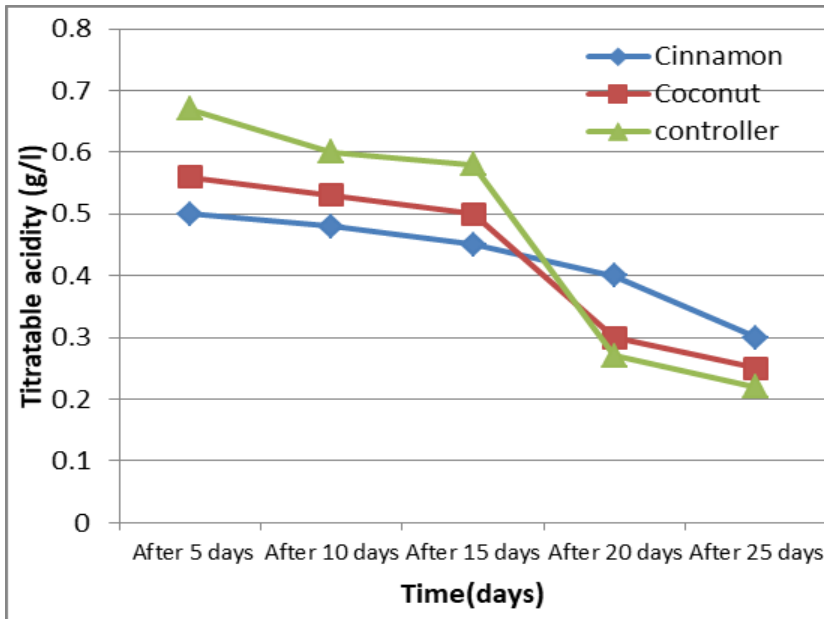


Figure 7: Variation of titratable acidity

The titratable acidity content was gradually decreased in all samples during storage period (figure 7) and it confirms the earlier findings by [13]. The most abundant acid in tomatoes are citric acid. Citric acid begins to reduce the step-wise by chemical reactions that synthesize energy as a result of ripening.

### Physical parameters

Physical parameters of tomato were evaluated by the color index. It helped to get an idea about shelf life of tomatoes. Tomatoes have six ripening stages. More tomatoes which were kept in controller reached to light red stage after 25 days. About 16% of stored tomatoes in coconut shell charcoal cooler were still in color turning stage after 25 days while 83% of stored tomatoes were in pink stage in cinnamon stick charcoal cooler. Evaporative cooling is not only lowering the air temperature surrounding the produce, it also increases the moisture content of the air. This helps prevent the drying out of the produce, and therefore extends its shelf life [17].

### Conclusion

The performance of coconut shell charcoal cooler is significantly better when compared with other models. The maximum drop of temperature was 5.8°C and maximum Rh increment was 8.7%. Both charcoal cooler was shown better performance compare to control condition. This type of alternative low cost charcoal cooler can be easily made with locally available materials and no need to special skill or knowledge to operate. According to the required capacity, sizing can be done easily.

### Reference

- [1] Ihekoronye, A.I. and P.O. Ngoddy (1985): Tropical Fruits and Vegetables. In: Integrated Food Science and Technology for the Tropics, Macmillan Publ. Ltd.; London and Basingstoke; 293 – 311.
- [2] IPHT Technical Note (2001),“ Fresh chain to reduce postharvest losses of fruits and vegetables”, Institute of Post-Harvest Technology , Research and Development Center, JayanthiMawatha, Anuradhapura.
- [3] Narayanasamy P. 2006. Postharvest Pathogens and Disease Management. Hoboken (NJ): John Wiley & Sons
- [4] Seyoum TW, Woldetsadik K (2004). Forced ventilation evaporative cooling of fruits: A case study on Banana, Papaya, and Orange. Lemon and Mandarin. Trop. Agric. J., 81(3): 179-185.
- [5] Thompson F, Mitchell FG, Runsey TR, Kasmire RF, Crisosto CH (1998). Commercial cooling of fruits, vegetables, and flowers. UC Davis DANR Publications, 21: 56-61
- [6] Mentzer, J.E. and Dale, A.C. 1960. “Evaporative Cooling of Animal Shelters”. Journal of American Society of Agricultural Engineers. 816-819, 821.
- [7] Mogaji, Taye S. and Fapetu, Olorunisola P., 2011. Development of an evaporative cooling system for the preservation of fresh vegetables, African Journal of Food Science Vol. 5(4), pp. 255 – 266.



- [8] Kittas, C., Bartzan, T. and Jaffrin, A., 2003. Temperature Gradients in a Partially Shaded Large Greenhouse equipped with Evaporative Cooling Pads, *Biosystems Engineering*, Volume 85, (1), pp 87-94
- [9] Marikar, F.M.M.T. and Wijerathnam, R.S.W. 2010, Post-harvest storage of lime fruits (*Citrus aurantifolia*) following high humidity and low temperature in a modified brick wall cooler, *International Journal of Agriculture & Biological Engineering*, Vol. 3 (3) pp. 80-86
- [10] Ryall, A.L. and Pentzer, W.T. (1982). *Handling, Transportation and Storage of Fruits and Vegetables Vol. 2. Fruits and Tree Nuts*. 2nd ed. AVI Publishing. Westport. CT
- [11] Singh M, Naranyahgkeda KG. Investigation and development of indirect evaporative cooling using plastic heat exchanger. *Mech Eng Bull*. 1999;14(7):61–65.
- [12] Al-Sulaiman, F. (2002), Evaluation of the performance of local fibers in evaporative cooling. *Energy Conversion and Management*, vol. 42, pp. 2267-2273.
- [13] Tapare A.R. and Jain R.K. (2012). "Study of advance maturity stage of banana" *International journal of Advanced Engineering Reseach and Studies.*, vol 1(3),pp272:274
- [14] Bachmann, J. and Earles, R. 2000. Postharvest handling of fruits and vegetables. *Appropriate Technology Transfer for Rural Areas*. NCAT Agriculture Specialists. pp. 1-19.
- [15] Libertya, J.T., Ugwuishiwua, B.O., Pukumab S.A and Odoc, C.E., 2013 *Principles and Application of Evaporative Cooling Systems for Fruits and Vegetables Preservation*, *International Journal of Current Engineering and Technology*, Vol.3, (3) pp 1000-1006.
- [16] Singh, Z., Lalel, H.L.D., Nair, S. 2002. A review of mango fruit aroma volatile compounds - state of the art research, *ISHS Acta Horticulturae 645: VII International Mango Symposium*,
- [17] AP-Tech. 1980. "A Village Food Cooler". *AP-Tech Newsletter*. 1:10-11.

# Criticality of Building Morphology on End Use Energy Demand: Evidence based assessment of urban office stock in Colombo Metropolitan Region

I. Rajapaksha<sup>1</sup> and U. Rajapaksha<sup>2</sup>

*Department of Architecture, Faculty of Architecture, University of Moratuwa*

## Abstract

City of Colombo is evident for an Urban Heat Island which is expanding its boundaries due to increasing built-up area. Present urban development strategy for city of Colombo as a megapolis extends the magnitude of urban building stock. Thus it's important to explore end use energy demand of national building stock and this study investigated the morphology of the office building stock in Colombo Metropolitan Region and appraises its relationship with energy indices.

Office building stock of CMR is primarily distributed in 6 GN divisions and predominantly composed of air-conditioned office spaces with basic plan forms of linear and square shapes. Facades are predominantly detailed with glass and Aluminium cladding. Buildings with East-West oriented front facades demonstrate the highest annual mean BEI of 212kWhm<sup>-2</sup>. Thus the overarching character of national urban office building stock in CMR is energy obsolete with 'road side sealed offices'.

Further an onsite thermal investigation of critical office building morphologies of Deep plan and shallow plan office interiors inform a clear difference in indoor air temperature profiles among two plan shapes. Deep plan form has a greater potential to control external heat gain and reduce the end use energy demand in comparison to shallow plan form. Thus the findings of this study represent the criticality of building morphology based on plan shape, orientation and interior planning which demonstrate a significant impact on end use energy demand due to external heat loads.

**Key words:** Morphology; building stock; urban offices; Building energy intensity; interior; thermal behaviour

## Introduction

With the concentration of 70% of the global urbanization in developing countries of Asia and Africa by the year 2030 tropical urbanization promotes a significant trend in Global GHG emissions (UNFPA, 2007). Urbanization inflates the urban building stock in cities and enhances the formations of Urban Heat Islands (UHI). There is no exception for the existence of Surface Urban Heat Island (SUHI) in Colombo Metropolitan Region (CMR) which indicates intensifying effects from 2007 to 2017 due to rapid urbanization (Ranagalage et al., 2017). In 2005 the extent of UHI was 42% of the total land area of CMR. This UHI is growing and predicted for an annual increase of 1.75%. Moreover, an increasing trend is apparent in the extent of built-up area from 74% in the year 2005 to 97.3% by the year 2013 (Ukkwatta et al., 2012). Thus proves at present City of Colombo is enclosed within the boundaries of a UHI. Scientific disclosure of the influence of UHI on increasing energy demand is well established.

Literature informs many developed countries have prioritised the surveys on national building stocks. These stocks were evaluated for the relationship between energy consumption and the characteristics of the existing building stock (Dascalaki, et al. 2010, Ifigeneia et al., 2011, Mortimer et al., 1999, Choudhary et al., 2014). Moreover the building stock was further investigated to identify the effect of building morphology such as shape, composition, orientation, fenestration details for assessment of building performance and the end user energy demand (Depecker et al., 2001, Bekkouche et al., 2015,

Catalina et al., 2011, Tsikaloudaki et al., 2012, Gasparella et al., 2011).

However the studies on building stocks in Sri Lanka are less prioritised. The available few studies on energy consumption of buildings have focused on energy efficiency measures of lighting and simulations to assess indoor environmental quality of buildings (Wijayathunga et al., 2004, Ratnaweera et al. 2002). Furthermore these studies are based on secondary data and evident for lack of a comprehensive national database which integrates the characteristics of the building stock and the energy utility intensities.

This study explores the office building stock of Colombo Municipal Council region to evaluate the impact of building morphology on end use energy demand by formulating Building Energy Indices (BEI). The Colombo Municipal Council region which is composed of the highest office building density of the country justifies the appropriateness of the study location as the critical urban area to explore the national urban building stock for end use energy demand.

## Methodology of the Study

This study is consists of a walk through survey and an onsite experimental investigation. A walkthrough field investigation was performed in 35 Grama Niladhari (GN) divisions in Colombo Municipal Council region. Data collection protocol was structured with the use of geographical information system (GIS) data and activity zone maps of the CMC region. This office building stock excludes mixed administration buildings and contains buildings exclusively use for administration activities of private and government

organizations including banks and other financial offices. Data on Building morphology is focused on building design parameters such as orientation, shape, composition, construction materials and fenestration details. Moreover operational characteristics were recorded as working hours, space conditioning systems and use of office equipment. Critical building morphologies were further assessed through onsite experimental investigations. Thermal variables of indoor air and surface temperatures were recorded using data loggers and monitoring was performed continuously for a week in the hottest month of March 2017.

## Results and Discussion

The results explicitly prove the urban Office building stock is predominantly composed of air-conditioned office spaces. Use of natural ventilation is limited to common spaces and mixed mode is apparent for 78% of buildings of this stock. Clear diversity in end user demand is evident through variations in Building energy indices. The average Building Energy Intensity of CMC is  $211.59 \text{ kWhm}^{-2}\text{annum}$  and the average building height is 6 floors. This paper focuses on dispersion of office building stock in GN divisions of CMR and characterizes critical GN divisions for end use energy demand.

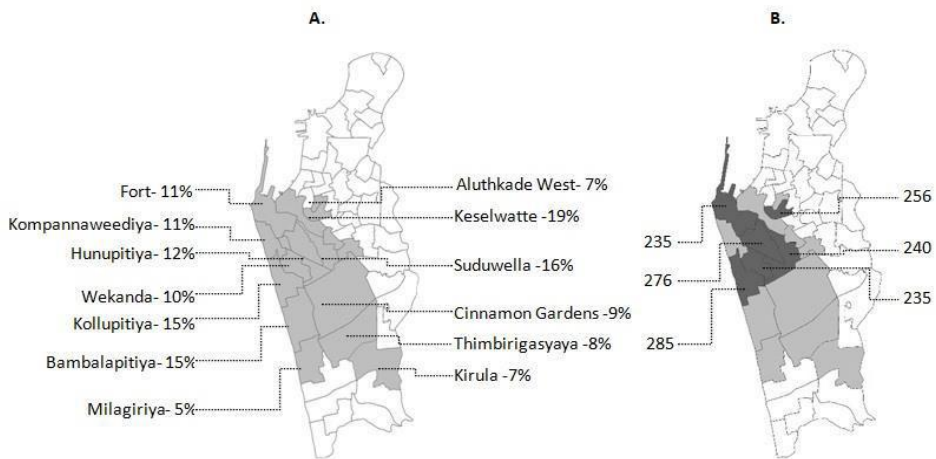


Figure 1: Characterizing the office building stock in CMR, A. Dispersion of office building stock, B. End Use Energy Demand for critical GN divisions with the highest concentration of office buildings

### Dispersion of office building stock

Office building stock is concentrated towards Northwest and West locations of the Colombo district. Figure 1 shows the distribution of office building stock and end use energy demand of the critical GN divisions in CMR. As shown in Figure 1A, among the 35 GN divisions a substantial number of office buildings are distributed in 13 GN divisions. The percentage of office buildings to the total buildings of these GN divisions vary from 5% to 19%. Thus the highest building stock of offices is in Keselwatte and the lowest is in Milagriya with a percentage of 19 and 5 respectively. Descending order of GN divisions from the 2nd highest percentage of 16 up to 10% of the office stock are Suduwella, Kollupitiya, Bambalapitiya, Hunupitiya, Kompannaweediya, Fort and Wekanda. Positioning of offices along high density traffic arteries is common in these zones and the corresponding roads are Galle road, Dharmapala Mawatha, Sangharaja Mawatha, Sir James Peiris Mawatha and D.R Wijewardana Mawatha. Thus the road side sealed offices is the overarching character of national urban office building stock in CMR.

### Characterizing end user energy demand of critical office building stock

End Use Energy Demand (EUED) of the office building stock was assessed for 06 critical GN divisions. These GN divisions represent the considerable number of office buildings and correspond to a range of 19 to 10 percent of office buildings in each division. End use energy demand for office buildings of each division is presented as the mean Building Energy Index (BEI). BEI of each office building in these zones was calculated by collecting annual electricity bills of each building and corresponding physical data of the usable floor area. Figure 1B presents the EUED of six of critical GN divisions. The results show the annual EUED varies from 235 to 285 kWhm<sup>-2</sup>. The highest demand is apparent in Kollupitiya and followed by Hunupitiya GN division with an office building stock of 15% and 12% respectively. Results prove there is no relationship between the percentage of the building stock and EUED. Thus prioritize the importance of investigating morphology of office buildings in critical GN divisions.

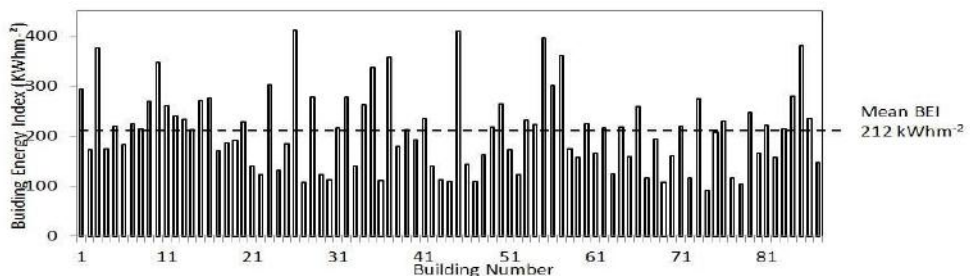


Figure 2: Variations in Building Energy Index of each office building in 06 critical GN divisions of CMR

**Dispersion of Building Energy Indices in the critical office building stock**

Annual BEI of 86 office buildings with an approximate floor area of 73000m<sup>2</sup> distributed among 6 GN divisions were assessed and shown in Figure 2 (above). The annual BEI in these office buildings varies within the range of 412 to 91 kWhm<sup>-2</sup> and 95% of the buildings are above 110kWhm<sup>-2</sup>, which represents the accepted standard for energy efficient building codes (ECG19). Within this building stock 56% of the buildings shows an annual BEI above 200kWhm<sup>-2</sup> of which almost half of the buildings are above 250 kWhm<sup>-2</sup>. Mean BEI for critical office building stock in CMR is 212 kWhm<sup>-2</sup> and assures an energy obsolete building stock which is beyond the standards specified in majority of the building codes worldwide. Thus informs further investigation of the characteristics of the building stock which has an effect in increasing the end use energy demand of this stock.

**Characteristics of the Building morphology**

**a. Plan Forms**

Office building stock of CMC is predominantly composed of six types of office building plan forms. These plan forms can be generalized as basic plan forms and composite plan forms. Basic plan forms consist of square, linear, and circular plan forms. Composite plan forms derived from a combination of basic plan forms and demonstrate the shapes of L, U and trapezium. Table 1 shows the classification of office building plan forms and its percentage distribution within the stock. Basic plan forms are commonly used in the office building designs and 85% of the buildings demonstrate a combination of linear and square plan forms. In these basic plan forms 62% and 23% are with linear and square plan forms respectively.

Among the composite plan forms L shape is prominent with a percentage distribution of 8.1%. Although there are office buildings with circular, trapezium and U shape plan forms they are not been used widely.

*Table 1. Classification of plan forms of office building stock*

Basic plan forms		Composite plan forms	
Linear Plan 62%  	L shape Plan 8.1%  		
Square Plan 23%  	U shape plan 2.3%  		
Circular plan 2.3%  	Trapezium plan 2.3%  		

Table 2. Fenestration details of the front facades and percentage distribution within the stock




Composite facades	Aluminium facades	cladding	Glazed facades
 57%	 26%	 17%	

Table 3. Relationship between orientation of front facades and mean Building Energy Index (BEI)

Orientation	Percentage	Mean BEI (kWh/m <sup>2</sup> /annum)
East-West	41.4%	211.6
North-South	13.8%	200.2
North East-South West	25.6%	200.1
North West-South East	19.2%	205.7

#### b. Building facade detailing and Orientation

Building facade detailing demonstrates a significant impact on the thermal behavior of a building corresponding to the proportion of glazed to wall area and facade orientation. Increased glazing propositions of the facades facing critical orientation of hot climates promotes higher gain in solar radiation and the overheated interiors increase the cooling load of air-conditioned offices. Table 2 presents material compositions of front facades and percentage distribution of each facade type within the office building stock.

In this office building stock facades are predominantly composed of glass and Aluminium cladding. The percentage distribution of these materials in front facades such as glazed, Aluminium cladding and composites are 17, 26 and 57 respectively. Glazed facades are primarily curtain walls and composed of fixed and few operable panels with

blinds to control the heat gain. These facades are orientated in different directions within the building stock. Table 3 represents the details of the facade orientations, its percentage distribution and relationship between the orientation and mean BEI. Office buildings in this stock represent 4 main orientations such as East-West (EW), North-South (NS), Northeast-Southwest (NE-SW) and Northwest-Southeast (NW-SE). As shown in Table 3 the percentage distribution of office buildings for EW, NS, NE-SW and NE-SW orientations are 41%, 14%, 26% and 19% respectively. The major characteristic of the building morphology of this stock is the orientation of the front facade towards East or West direction. Solar geometry for tropics informs the highest solar radiation is incidence on East and West facades of the buildings. Thus this building stock is evident for less attention on climate responsive design strategies which has affected the end use energy demand. Buildings with EW oriented front facades demonstrate the

highest annual mean BEI of 212kWhm<sup>-2</sup>. These findings confirm the criticality of the building morphology of this office building stock due to inappropriate

orientation and material usage irrespective to climatic forces of the locality.

Table 4: Morphological characteristics and operation details of critical offices with deep and shallow plan forms





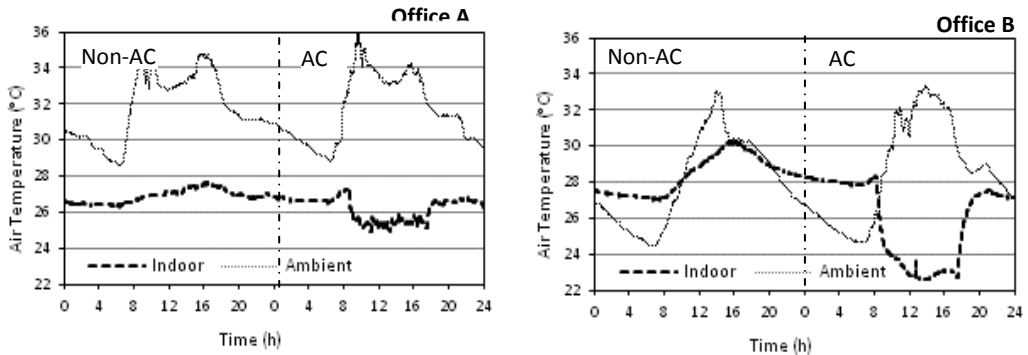
Morphology	Office A - Deep plan	Office B- Shallow plan																
																		
Orientation	East-West Orientation (long axis)	North-South Orientation (long axis)																
Composition	Detached Building	Detached Building																
A/C Area	Office areas mechanically ventilated Lift lobbies, service areas and corridors are natural ventilated	Office areas mechanically ventilated Lift lobbies, service areas and corridors are natural ventilated																
AC set point	24°C	24°C																
Building envelop	Sealed – Airtight	Sealed – Air tight																
Number of occupants	110	150																
Working hours	8.30 am to 5.00pm Extended working hours	8.30 am to 5.00pm Extended working hours																
Wall to window ratio (WWR)	<table border="1"> <tr> <td>East</td> <td>West</td> <td>North</td> <td>South</td> </tr> <tr> <td>0.62</td> <td>0.53</td> <td>0.47</td> <td>0.51</td> </tr> </table>	East	West	North	South	0.62	0.53	0.47	0.51	<table border="1"> <tr> <td>East</td> <td>West</td> <td>North</td> <td>South</td> </tr> <tr> <td>0.58</td> <td>0.71</td> <td>0.35</td> <td>0.64</td> </tr> </table>	East	West	North	South	0.58	0.71	0.35	0.64
East	West	North	South															
0.62	0.53	0.47	0.51															
East	West	North	South															
0.58	0.71	0.35	0.64															
Material composition of Front facade																		



Figure 3: Average Indoor temperature behavior in deep and shallow plan form with and without air-conditioning



### c. Composition

Buildings within an urban block represent two types of compositions of its positioning in respect to other buildings such as attached and detached. This office building stock consists of a mix of both compositions with 63% and 37% of detached and attached buildings respectively. The attached buildings represent variations such as attached from single and both facades. Variation in composition shows marginal differences in annual BEI in the stock with 211 and 210 kWhm<sup>-2</sup> for detached and attached buildings respectively. However, the buildings with both sides attached to another structure control the interaction with solar radiation and are beneficial in controlling the overheated office interiors. But on the other hand, this will increase the use of artificial lighting due to daylighting restrictions and thus demands for strategies to promote natural lighting towards interiors. Thus, the lack of difference in annual BEI through various compositions highlights the energy demand for lighting has affected the BEI of attached office buildings. Furthermore, it informs the importance of a comprehensive study to calculate the tenancy energy demand of this stock, but one of the limitations is less regulatory mechanisms to initiate

sub-metering of the national building stock.

### Onsite thermal investigations of critical office buildings

With an intention on generalizing the findings through the stock, two representative office building morphologies were considered for an evidence-based study. These critical office building morphologies were selected based on high annual BEI and its physical and operational characteristics. Both cases are similar with their composition as detached and annual BEI is above 250 kWhm<sup>-2</sup>. Office A represents a Deep plan office with the long axis positioned along East-West direction. Office B represents a Shallow plan office with the long axis positioned along North-South direction. Front facade with the entrance is towards West and East of Office A and B respectively. Long facades of Office A are oriented towards North and South directions and vice versa for Office B. These building morphologies are widely distributed in the city of Colombo due to the pattern of land subdivision and road network. Table 4 demonstrates the operational and morphological details of the critical offices. High annual

building energy index informs the criticality of these building morphologies on end user energy demand of the office building stock.

The impact of building morphology on indoor air temperature behaviour of these offices was investigated for a typical working day with air conditioning and a typical non-working day in the weekend without air conditioning. This study assumes the day without air conditioning demonstrates the effect of environmental load on indoor thermal behaviour. Internal and ambient temperature readings were recorded in HOBO data loggers and surface temperature was recorded using thermocouples. Immediate microclimatic data were recorded onsite. This paper presents the indoor temperature profiles of the critical case office buildings.

### Indoor temperature profile with and without Air-conditioning

Indoor temperature variations in the core of office interior with and without air-conditioning are shown in Figure 3. Each office interior was monitored for a typical weekday and weekend with the Air-conditioner switch on and off mode respectively.

Results explicitly prove a clear difference in indoor air temperature profiles of office spaces. Although office A is evident for less differences in interior temperature during air-conditioned and non-air conditioned days a clear difference demonstrates in shallow plan offices. Shallow plan of the Office B makes the indoor temperature closely follows the pattern of ambient temperature during the non-air conditioned period. There is no difference between indoor and outdoor temperature from 16h to 20h. Deep plan Office A with and without air conditioning represents a mean indoor temperature of 26.9°C and 26.2°C respectively. Mean indoor temperature difference of 2.4°C with and without air-conditioning is apparent in shallow plan Office B. Thus informs the deep plan Office A has a greater potential to control external heat gain and reduce the end use energy demand in comparison to shallow plan Office B.

Difference between outdoor ( $T_o$ ) and indoor ( $T_i$ ) temperature ( $\Delta T$ ) for AC and non AC days of both offices are shown in Figure 4. Positive and Negative value of  $\Delta T$  represents lower and higher indoor temperature levels than the immediate outdoors respectively.

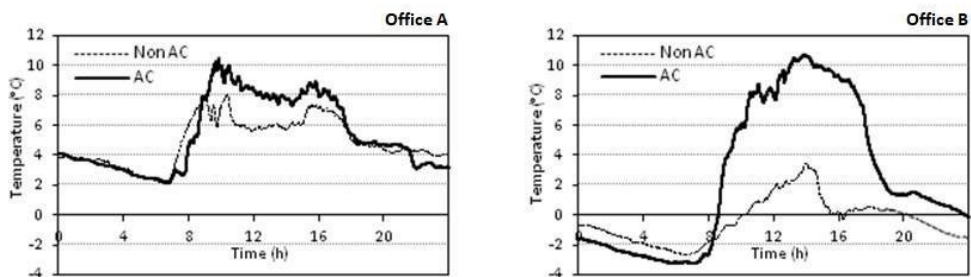


Figure 4: Temperature difference profile with and without Air conditioning for Office A and B

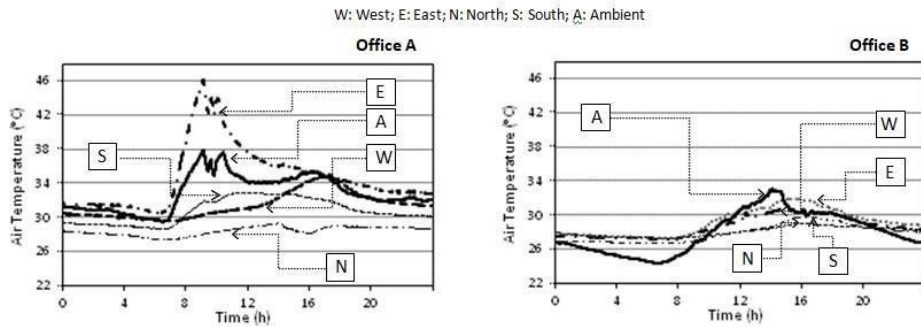


Figure 5. Indoor temperature profiles of perimeter zones without air conditioning for Office A and Office B

Results highlight office A maintains lower indoor temperature in Non AC day and less difference is evident for indoor temperatures on the day with AC. Mean  $\Delta T$  during 8 hours of working period (9-17h) of Non AC and AC period is  $6.4^{\circ}\text{C}$  and  $8.4^{\circ}\text{C}$  respectively. Thus demonstrates building morphology has lessened the cooling energy demand of this building by controlling the external heat gain.

However the  $\Delta T$  profile of shallow plan office B represents predominantly a warm office interior on non AC day. In this office almost for 18 hours of the day from 4pm in the evening to 10am in the morning indoor temperature remains above outdoors. Mean  $\Delta T$  during 8 hours of working period (9-17h) of Non AC and AC period is  $1^{\circ}\text{C}$  and  $8.5^{\circ}\text{C}$  respectively.

Considerably high temperature difference of  $7.5^{\circ}\text{C}$  between Non AC and AC interior of Office B demonstrate the increased demand on cooling energy due to high external gains of the building envelope. Furthermore from 5.30pm indoor temperatures begins to exceed the AC set point of  $24^{\circ}\text{C}$  and continues until 9.30 am. Thus demonstrates although the AC system is switched on in the morning by 8am the set point temperature is achievable almost after

one and half hours of its operation. Thus the findings highlight shallow plan shapes makes the office interiors warmer than deep plan shapes and interiors of these forms closely follows its immediate hot microclimates. These building morphologies are unable to act as barriers to reduce environmental loads which influences in the energy demand.

### Indoor temperature profile in perimeter zones of critical case offices

#### a. Non air-conditioned interiors

Indoor temperature profiles of the perimeter zones of interiors close to East, West, North and South facades are assessed for the effect of thermal behaviour of each façade on cooling energy demand. Figure 5 shows the relationship of the indoor temperature profiles of four perimeters zones with the ambient temperature for Deep and shallow plan offices without Air conditioning.

It is evident that the East perimeter zone of the deep plan Office A is over heated and the maximum temperature has reached to  $46^{\circ}\text{C}$  by 9am and gradually decreases while remaining above ambient temperature throughout the day. However all other perimeter zones

demonstrate a lower temperature profile except for West facade getting warmer than the ambient from 4pm until 7am. The lowest indoor temperature profile is apparent in the zone of North perimeter followed by the perimeter of South. Therefore North and South perimeter zones are comparatively less uncomfortable than East and West facades of Deep plan buildings.

However shallow plan interior of Office B is evident for less variation in indoor temperature behaviour of all perimeter zones. Except for very marginal lower temperature levels in North and South perimeter zones East and West facades are almost equal to ambient temperature profiles. Thus shallow plans restrict the use of perimeter zones for office activities due to warm interiors.

#### b. Air conditioned interiors

Figure 6 shows the thermal profiles of perimeter zones with air conditioning for two office interiors. Results show in deep plan office A except for perimeter zone of East all the facades are with lower temperature than the ambient temperature. However it is apparent that the indoor temperature close to AC set point temperature of 24°C is remained only in the West perimeter zone with a mean temperature of 24.4°C all through the working hours.

Mean temperature during the working period of 9h-17h of the perimeter zones of North and South are 28.2°C and 28.8°C respectively. Perimeter zones of East and North are evident for similar thermal profile for both days with and without air conditioning. Lack of consistency in indoor temperature distribution with air conditioning informs the variations in the levels of heat gain from different facades have affected the optimum performance of air-conditioning system. Thus the thermal comfort levels of the office workers vary in relation to the variations in heat gain from facades and also the internal heat gains. These findings inform the importance of interior planning of the working spaces to minimize the impact of external heat on occupants.

As shown in Figure 6 of Office B the Indoor air temperature levels of all four zones of the air conditioned office B are below the ambient temperature with the lowest temperature levels are apparent in the perimeter zones of North and South. Mean indoor temperature during the working period (9-17h) of the perimeter zones in North, South, East, West are 20.5°C, 21.7°C, 26°C and 24.4°C respectively.

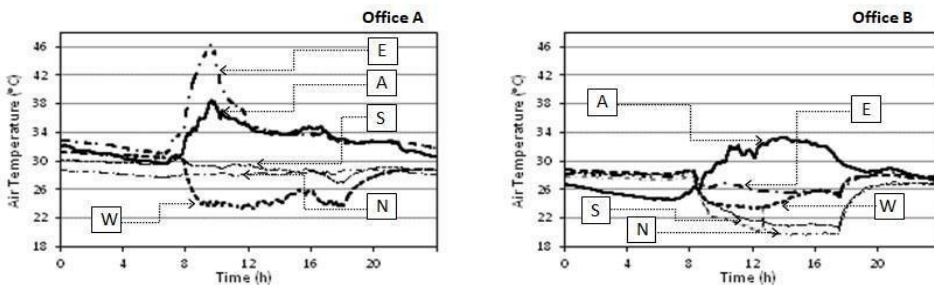


Figure 6. Indoor temperature profiles of perimeter zones with air conditioning for Office A and Office B

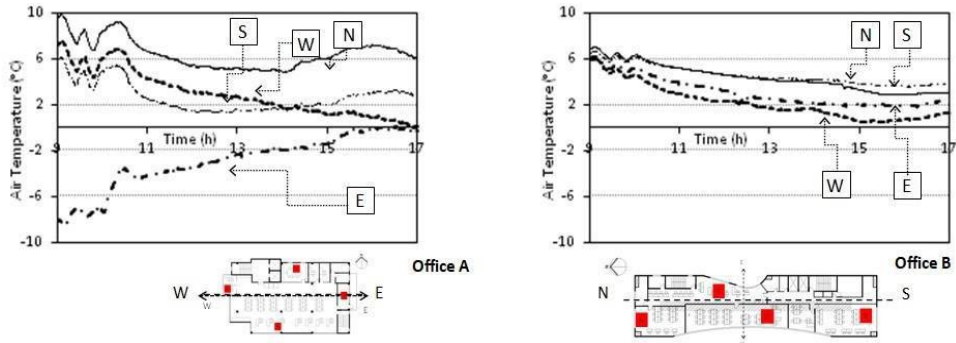


Figure 7. Indoor temperature differences of perimeter zones without air conditioning for Office A and Office B

Cooling energy demand from all four zones is depended on the magnitude of indoor overheating. Effect of building facades in overheating of each zone was assessed from the temperature differences ( $\Delta T$ ) of indoor and outdoor temperature of non air conditioned offices. Figure 7 shows the temperature difference of all zones during the working hours of non air conditioned interiors of Office A and B. Except for the East zone of deep plan interior of Office A all the other facades are evident for a lower temperature zones than ambient. Mean  $\Delta T$  of South, West, North and East zones for 8h period are 2.6°C, 3.0°C, 6.5°C and -2.9°C respectively. North zone represent the lowest temperature followed by West and South zones. Interior arrangement of working spaces with an open plan office in the North zone highlights the most occupied zone of this office is not affected from indoor overheating. Thus shows the highest  $\Delta T$  minimizes the demand on cooling energy. Moreover the overheated East zone is composed of service core and less occupied. Thus the interior planning of the deep plan office is favorable in reducing the end use energy demand of this office.

In contrary a lesser variation among zones is evident for shallow plan office B. All zones represent lower indoor temperature than ambient and the mean  $\Delta T$  of North, South, East and West zones during 8h working period are 4.4°C, 4.6°C, 3.1°C and 2.2°C respectively. Office A represents a warm East and West zones than the North and South zones. Interior arrangement shows the office areas are mostly integrated with the West zone. All service spaces are positioned along East zone with few cellular offices towards North and South zones. The most unfavorable zone of this office is with high occupancy highlights the impact of internal and external heat loads on end use energy demand.

The findings of this study represent the criticality of building morphology based on plan shape, orientation and interior planning has a significant impact of end use energy demand due to external heat loads. Thus the designing of East facades with less use of glass and heat resistant materials are crucial for tropics. Moreover it is common that the East facades of this building stock represent the front face of the office building thus the aesthetic appearance has been the governing design principle than

prioritizing its impact on building performance.

## Conclusion

This study explores the office building stock of Colombo Municipal Council region to evaluate the impact of building morphology on end use energy demand (EUED). A walkthrough field investigation was performed in 35 Grama Niladhari (GN) divisions of CMR to formulate a database on Building Energy Intensity of urban office building stock. Office building stock is primarily distributed in 6 GN divisions and predominantly composed of air-conditioned office spaces. Use of natural ventilation is limited to common spaces and mixed mode is apparent for 78% of buildings of this stock. Thus the overarching character of national urban office building stock in CMR is “road side sealed offices”. Annual BEI varies within the range of 412 to 91 kWhm<sup>-2</sup> and 95% of the buildings are above the accepted standards of energy efficient building codes worldwide. Mean annual BEI of 212 kWhm<sup>-2</sup> assures an energy obsolete building stock.

Office building designs are with basic plan forms and 85% of the buildings demonstrate a combination of linear and square plan forms. Facades are predominantly composed of glass and Aluminium cladding with four primary orientations such as East-West (EW), North-South (NS), Northeast-Southwest (NE-SW) and Northwest-Southeast (NW-SE). The major characteristic of the building morphology of this stock is the orientation of the front façade towards East or West. Buildings with EW oriented front facades demonstrate the highest annual mean BEI of 212kWhm<sup>-2</sup>.

Further an onsite thermal investigation was performed in two representative building morphologies of this stock.

Office A represents a Deep plan office with the long axis positioned along East-West direction. Office B represents a Shallow plan office with the long axis positioned along North-South direction. Long facades of Office A are oriented towards North and South directions and vice versa for Office B. These building morphologies are widely distributed in city of Colombo due to the pattern of land sub division and road network. Each office interior was monitored for a typical weekday and weekend with the Air-conditioner switch on and off mode respectively.

Results explicitly prove a clear difference in indoor air temperature profiles of office spaces. Deep plan Office A with and without air conditioning represents a mean indoor temperature of 26.9°C and 26.2°C respectively. Mean indoor temperature difference of 2.4°C with and without air-conditioning is apparent in shallow plan Office B. Thus informs the deep plan Office A has a greater potential to control external heat gain and reduce the end use energy demand in comparison to shallow plan Office B.

Findings of this study represent the criticality of building morphology based on plan shape, orientation and interior planning has a significant impact of end use energy demand due to external heat loads. Designing of buildings should not only prioritize the aesthetic appearance. Thus it is paramount important to formulate design guidelines to improve building performance of the obsolete and ageing national office building stock.

## Acknowledgement

Authors acknowledge the National Research Council Grant 13-109 for

funding of this research and Ms. W.S. Jayasinghe for conducting onsite field investigations.

## References

- [1] UNFPA, 2007, UNFPA report on 'State of the World's Population 2007' NY
- [2] Ranagalage, M., Estoque, R., Murayama, Y., 2017, An urban heat island study of the Colombo metropolitan area, Sri Lanka based on Landsat data (2007-2017), *International Journal of Geo Information*, 6, 189, pp.1-17
- [3] Ukkwatta, N.L., Dayawansa, N.D.K., 2012, . Urban Heat Islands and the Energy Deamn: An Analysis for Colombo City of Sri Lanka Using Thermal Remote sensing data, *Society for social management*, 1(2) pp. 124-131.
- [4] Dascalaki, E.G., Droutsas, K., Gaglia, A.G., Kontoyiannidis, S., Balaras, C.A., 2010, Data collection and analysis of the building stock and its energy consumption, *Energy and Building*, 42(8), pp.1231-7
- [5] Choudhary and R., Tiran, W. 2014, , Influence of district features on energy consumption in non-domestic buildings, *Building Research and information* 42, pp. 32-46.
- [6] Ifigeneia, T., Papadopoulos, A.M., Hegger, M, 2011, A Typological classification of the Greek residential building stock, *Energy and Buildings* 43(10), , pp. 2779-2787
- [7] Mortimer, N.D., Ashley, A., Elsayed, M., Kelly, M.D., Rix, J.H.R., 1999, Developing a database of energy use in the UK non-domestic building stock, *Energy Policy*, 27(8), pp.451-468
- [8] Depecker, P., Menezo, C., Virgone, J., Lepers, S., 2001, Design of building shapes and energetic consumption, *Building and Environment*, 36, pp. 627-635
- [9] Catalina, T., Virgone, J., Lordach, V., 2011, Study on the impact of building form on the energy consumption, *Proceedings of Building Simulation*, Sydney, pp.1726-29
- [10] Bekkouche, S.M.A, Benouza, T., Hamdani, M, Cherier, M.K., Yaiche, M.R., Benamrane, N., 2015, Diagnosis and comprehensive quantification of energy needs for existing residential buildings under Sahara weather conditions, *Advances in Building Energy Research*, pp.37-51
- [11] Tsikaloudaki, K., Laskos, K., Bikas, D., 2012, On the establishment of climatic zones in Europe with regard to the energy performance of buildings, *Energies*, 5(1) pp. 32-44
- [12] Gasparella, A., Pernigotto, G., Cappelletti, F., Romagnoni, P., Baggio, P., 2011. Analysis and modelling of window and glazing systems energy performance for a well insulated residential building. *Energy Build.* 43 (4), 1030–1037
- [13] Wijayatunga, P., Attalage, R., 2003, Analysis of rural households energy supplies in Sri Lanka: Energy efficiency, fuel switching and barriers to expansion, *Energy conversion and management*, 44(7), pp. 1123-30
- [14] Ratnaweera, C., Hestnes, A.G., 1996, Enhanced cooling in typical Srilankan dwellings, *Energy and Buildings*, 23(3), pp.183-90
- [15] ECG19, 2003, Energy Consumption Guide: Energy Use in Offices, <http://www.cibse.or>

# Numerical Modelling of Thermally Thick Biomass Particle Pyrolysis

W.A.M.K.P.Wickramaarachchi<sup>#1</sup>, M.Narayana<sup>#2</sup>

<sup>#</sup>*Department of Chemical and Process Engineering, University of Moratuwa  
Katubedda, Moratuwa, Sri Lanka*

<sup>1</sup>kethakiuom@gmail.com  
<sup>2</sup>mahinsasa@uom.lk

## Abstract

The main objective of the research work is to evaluate the parameters of biomass pyrolysis process. Variations in the heat of series and parallel reactions with temperature are needed to be account for the formulation of energy conversion in pyrolysis of a biomass particle. In this study, the complex chemical and physical processes such as drying, gas formation and heterogeneous char reactions of a typical woody biomass particle associated with phase changes, heat and mass transfer phenomena inside the particle are investigated. A mathematical model is developed to determine the spatial variation of temperature and mass loss with time domain. The model is validated using the experimental results gained from pyrolysis of a thermally thick, cylindrical wood particle. A particle of 9.5 mm diameter and 9.5 mm height and 6% moisture content is subjected for the analysis. A good agreement of the model with experimental data is accurately proven. The difference between particle surface and center temperatures confirm the necessity for deliberation of intra-particle gradients which is incorporated in the study. To acquire knowledge and to predict the performance of biomass pyrolysis, the model is numerically simulated by Computational Fluid Dynamics (CFD) framework with open source CFD codes in OpenFOAM. The three dimensional transient single wood particle CFD model is also sufficient to apply in biomass packed bed pyrolysis and combustion.

**Keywords :** biomass pyrolysis, CFD, mathematical model, single wood particle



## Introduction

During the past years biomass has gained an utmost importance in energy field not only because of renewable and environmentally friendly energy source but also it is a better alternative to fossil fuel. The naturally occurring incident of Photosynthesis is the major process of producing biomass, which converts sunlight into plant material. All biomass resources hold the energy of sunlight being stored in chemical bonds. This energy is again converted to useful forms of solid, liquid and gaseous products by breaking bonds using number of technologies. However, the one leading factor when considering the use of biomass as an energy source is mitigation of global warming. Since biomass absorbs almost the same amount of CO<sub>2</sub> released during burning, for its natural regrowing, it does not contribute for enhancing the CO<sub>2</sub> in atmosphere[1].

The history of biomass energy begins with burning wood for domestic heating purposes, which is as old as the history of humanity. Present day, the same method could not be followed as it is essential to fulfil other crucial factors such as minimizing environmental effects and improving efficiency. Therefore raw biomass fuel cannot be burnt as they are[2]. Production of bioenergy is done by a number of processes among the major types are thermo-chemical conversion and bio-chemical conversion. Thermochemical conversion includes three main processes; combustion, pyrolysis and gasification.

In pyrolysis it burns biomass in the absence of air to produce liquid, solid and gaseous fractions. Gasification uses

partial oxidation method to convert biomass into combustible gas mixture at elevated temperatures. If the biomass is burnt in the presence of air the process is known as combustion [3]. Mostly available combustion systems in the industry are fixed beds (packed beds) and fluidized beds. Development of these combustion systems are always impeded by the complexity of understanding the mechanisms of combustion of wood particles [4].

Researching about the energy generation of biomass from different technologies is not an easy task with large number of available biomass feedstocks and the use of separate reactors and reaction paths. Therefore, modelling methods can be used to analyze the systems in the real world safely and cost effectively. The models consist of simple heat and mass balance models, to advanced numerical models which utilize tools such as Computational Fluid Dynamics (CFD) [5].

Mathematical modelling can assist for a deep understanding of combustion systems by giving an approximate overview of the real system. Troubleshooting, fine-tuning, assisting with new designs can also be done using the model. As a fuel at its mature level, numerical models for coal combustion, gasification and pyrolysis has been developed in large number. Since there is a huge difference of characteristics between coal and biomass, the same models are not applicable in finding solutions of biomass processes [6]. Presently, only several studies have been conducted on biomass combustion to improve numerical models incorporating detailed models for both bed and gas phases [7].

The present work is focused on investigating drying coupled with pyrolysis of a single wood particle associated with phase changes, heat and mass transfer phenomena inside and outside the particle. Acquiring knowledge and predicting the performance in terms of conversion rates and transportation of species of further improved combustion process is the ultimate goal of the research. To achieve these objectives, a model is developed and simulated in Computational Fluid Dynamics (CFD) framework with open source CFD codes and OpenFOAM. The transport equations are applied to describe the changes of wood particle and to understand what is happening in its environment considering it as a porous media. The icoFoam solver has been modified to make it suitable for modelling thermally dense biomass particle. The simulation results are validated by using experimental data from previous research work.

### Material and Methods

A cylindrical shaped wood particle hovers in the reactor. A schematic diagram of the particle with all dimensions is shown in Figure 1. Inert nitrogen gas at 1276K is sent as the carrier gas at the bottom part of the reactor. The particle exchanges heat through conduction, radiation and chemical reactions and mass with the surrounding. The conservation equations for heat and mass transfer applied with appropriate initial and boundary conditions.

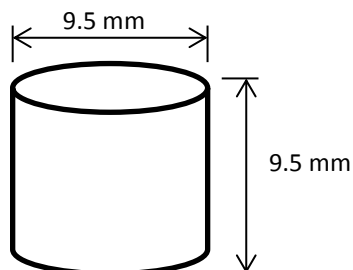


Figure 1: Schematic diagram of the particle

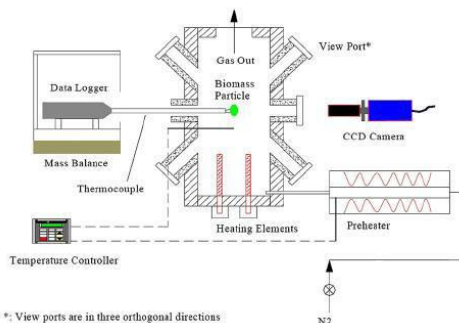


Figure 2: Schematic diagram of the single particle reactor

Drying, devolatilization, char conversion are the main processes taken place in the reactor. The processes occur both sequentially and simultaneously according to particle and reactor conditions. The particle is divided into three dimensional finite particles to obtain a fine-tuned analysis.

### Drying

Among the three different models, the equilibrium model, thermal model and kinetic rate model encountered in literature for drying, the kinetic rate model is used in this study. It is presumed that drying rate is completely depending on heat transfer, the shrinkage during drying is negligible and only the density is varying. The rate of drying described by Eq. 1[8].

$$R_{drying} = M_{H_2O} \times A_w \times \exp\left(\frac{-E_w}{RT}\right) \quad (\text{Eq. 1})$$

Where,

$M_{H_2O}$  = Amount of moisture in wood particle ( $kg/m^3$ )

$A_w$  = Pre exponential factor ( $s^{-1}$ )

$E_w$  = Activation energy (J/mol)

$R$  = Universal gas constant (J/mol.K)

$T$  = Temperature (K)

Moisture content in wood is divided to two types; free water and bound water.

Free water exists as liquid and vapor in cell cavities while bound water exists in cell walls. The wood particle has 6% moisture content which is totally the bound water. Moisture content above fiber saturation point (FSP) is categorized as free water. Below FSP, it is bound water. General value of FSP is 30%. The heat of evaporations of free water and bound water are given by Eq. 2 and Eq. 3[9].

$$\Delta h_{fw} = 3179.0 - 2.5T \quad (\text{Eq. 2})$$

$$\Delta h_{bw} = 3179.0 - 2.5T + 1176.2 \exp(-15.0Y_b) \quad (\text{Eq. 3})$$

Where,

$Y_b$  = bound water content

The total heat released during drying is calculated by following Eq. 4.

$$Q_{drying} = R_{drying} \cdot \Delta h_{bw} \quad (\text{Eq. 4})$$

### Pyrolysis

The improved version of single step mechanism of pyrolysis is selected for the study. Where, the major components that form the biomass are decomposed separately and produce gas and char. This model highly consider the composition of components; cellulose,

hemicellulose and lignin. The devolatilization of cellulose and hemicellulose is quick compared to lignin[10]. The flatter temperature ranges for independent devolatilization of cellulose, hemicellulose and lignin are 315-400 °C, 220-315 °C, and 160-900 °C respectively[11]. The pyrolysis of each component is explained by Arrhenius equation in Eq. 5. The rate of pyrolysis is given by Eq. 6. The kinetic parameters are obtained as reported by R. Mehrabian et al. by fitting experimental data from thermo gravimetric analysis (TGA) concerning mass loss rate versus temperature.

$$R_i = M_i \times A_i \times \exp\left(\frac{-E_i}{RT}\right) \quad (\text{Eq. 5})$$

$$R_{pyrolysis} = -\sum_{i=1}^3 R_i \quad (\text{Eq. 6})$$

Decomposition generates a complex mixture of volatile gasses consists with CO, CO<sub>2</sub>, H<sub>2</sub>O, H<sub>2</sub>, light and heavy (tar) hydrocarbons. For the simplicity light and heavy hydrocarbons are lumped together. The physical and chemical properties of Methane are postulated for this. The gases cross the char layer where heterogeneous reactions take place. The heat absorption rate of pyrolysis is as follows.

$$Q_{pyrolysis} = R_{pyrolysis} \cdot \Delta h_{pyrolysis} \quad (\text{Eq. 7})$$

Where,

$a_i$  = mass fraction of component

$\rho_{df}$  = mass of wood in dry basis

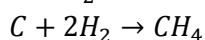
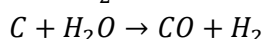
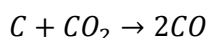
$\Delta h_{pyrolysis}$  = heat of pyrolysis

Table 1: Properties of Wood [14],[15]

	Property	Units	Value
1	Dry wood density	Kg/m <sup>3</sup>	545
2	Char density	Kg/m <sup>3</sup>	200
3	Ash density	Kg/m <sup>3</sup>	300
4	Y <sub>b</sub>	-	6%
5	a <sub>cellulose</sub>	-	0.64
6	a <sub>hemicellulose</sub>	-	0.26
7	a <sub>lignin</sub>	-	0.10
8	A <sub>cellulose</sub>	1/s	1.379×10 <sup>14</sup>
9	A <sub>hemicellulose</sub>	1/s	2.527×10 <sup>11</sup>
10	A <sub>lignin</sub>	1/s	2.202×10 <sup>12</sup>
11	E <sub>cellulose</sub>	J/mol	193000
12	E <sub>hemicellulose</sub>	J/mol	147000
13	E <sub>lignin</sub>	J/mol	181000

### Char conversion

Char conversion occurs with CO<sub>2</sub>, H<sub>2</sub>O and H<sub>2</sub> gases released during pyrolysis. The reactions of char conversion are represented by following three reactions. In comparison with oxidation, gasification reaction rates are rather lower. In the absence of oxygen these reactions become important. Since these reactions are heterogeneous between solid and gaseous phases, some key steps followed by participating agents. First gas components should reach the solid surface and adsorb to the surface. After the chemical reactions desorption occurs then the products diffuse to the surrounding[12].



There are two factors that affect the rate of char reactions. Kinetic rates are much higher than the mass transfer rate

therefore the reaction is limited by the mass transfer reaction. The kinetic rate of the process can be explained as follows[8].

$$R_{char,k,i} = A_{spc} A_i T \exp\left(\frac{E_i}{RT}\right) \left(\frac{M_{char}}{v_i M_i}\right) \rho_i \text{ (Eq. 8)}$$

Where,

A<sub>spc</sub> = Specific area of char (m<sup>-1</sup>)

M<sub>char</sub> = Molecular weight of char (kg/mol)

M<sub>i</sub> = Molecular weight of reacting species (kg/mol)

v<sub>i</sub> = Stoichiometric coefficient of reacting species

ρ<sub>i</sub> = Density of reacting species (kg/m<sup>3</sup>)

Until the pyrolysis process is finished the weight of solid phase continues to decrease since the release of volatile components. Solid phase consists with three components which are unreacted biomass, char and ash. Due to the fact, the specific area of char is also varying with the weight of solid components. Mass transfer rate equation for reactant gas towards char particle is as follows.

$$R_{char,m,i} = k_{m,i} A_d (\rho_i - \rho_{is}) \text{ (Eq. 9)}$$

Where,

k<sub>m,i</sub> = Mass transfer coefficient (m/s)

A<sub>d</sub> = Specific surface area for gas diffusion (1/m)

ρ<sub>is</sub> = Density of reacting speice at the surface of the particle (kg/m<sup>3</sup>)

### Radiation model

The term  $Q_{\text{radiation}}$  is the amount of heat due to radiation inside the solid wood. P-1 model has been applied for radiation calculation since it has several advantages over other models. This model is easy to solve with little CPU demand, and can be applied to complicated geometries[13]. The equations governing the radiation throughout the particle are as follows.

$$-\nabla Q_{\text{radiation}} = aG - 4an^2\sigma T^4 \quad (\text{Eq. 9})$$

Where,

- G = Incident radiation ( $\text{W}/\text{m}^2$ )
- a = Absorption coefficient of gas phase ( $\text{m}^{-1}$ )
- $\sigma$  = Stefan constant ( $\text{W}/\text{m}^2 \cdot \text{K}^4$ )
- n = Refractive index of gas phase
- T = Temperature (K)

Except the chemical reactions in drying, pyrolysis and gasification, there are remaining energy and mass transport reactions. The governing equations should be inputted in CFD modeling in which the parameters are solved by the programme.

The species equation given by Eq. 10 and Eq. 11 are applied for the conservation of wood components; moisture and wood in solid phase.

$$\frac{\partial \rho_{\text{moisture}}}{\partial t} = -R_{\text{drying}} \quad (\text{Eq. 10})$$

$$\frac{\partial \rho_{\text{drywood}}}{\partial t} = R_{\text{pyrolysis}} + R_{\text{char}} + R_{\text{ash}} \quad (\text{Eq. 11})$$

For the gas phase species reactions,

$$\frac{\partial \varepsilon \rho_g Y_i}{\partial t} + \nabla \varepsilon \rho_g Y_i = \nabla (\varepsilon \rho_g D_i) \nabla (Y_i) + Y_i \cdot R_{s,i} \quad (\text{Eq. 12})$$

Eq. 13 describes the gas phase momentum equation,

$$\frac{\partial \varepsilon \rho_g u}{\partial t} + \nabla \varepsilon \rho_g u u = -\nabla \varepsilon p + \nabla (\varepsilon \mu) \nabla (u) \quad (\text{Eq. 13})$$

The energy equation given by Eq. 14 is built based on the presumption that liquid water and the water vapour in the gas phase are in thermodynamic equilibrium.

$$\frac{\partial \varepsilon \rho_s C_{\text{eff}} T}{\partial t} + \nabla \varepsilon \rho_s u C_{\text{eff}} T = +\nabla \varepsilon k_s \nabla T + Q_{\text{drying}} + Q_{\text{radiation}} - Q_{\text{pyrolysis}} + Q_{\text{charconversion}} \quad (\text{Eq. 14})$$

### Numerical Model

For computational Fluid Dynamics (CFD) modelling, the cylindrical geometry of the wood particle is constructed by an available mesh development tools. Numerical simulations were performed using open source CFD software OpenFOAM. The domain is discretized into a grid with 3000 cells. Finally mesh refinement is done by increasing number of cells into 7800. The domain consists with both solid phase and gas phase. In this study, a transient solver, which is based on PISO algorithm (Pressure implicit with splitting of operator), was developed by considering all chemical kinetics and thermal-mass transport in gas and solid phases. Dynamic simulations were performed by OpenFOAM to obtain present results.

## Results and Discussion

The single particle pyrolysis model was validated by utilizing the experimental data published by Lu et al. Mass loss data as a function of time was obtained by the experiment of a single particle reactor. The data measured during non-oxidizing condition were incorporated in model validation in this study. Diameter of the particle is 9.5mm, length 9.5mm and cylindrical in shape. In non-oxidizing

condition, nitrogen gas enters the reactor at the bottom then leaves at the top. The average wall temperature is 1276K which is used in the model as reactor wall temperature. A relationship of time and surface temperature according to surface temperature data was built up from experimental data and used as the boundary temperature. Pressure in the particle boundary is considered as 1atm and velocity gradient is zero.

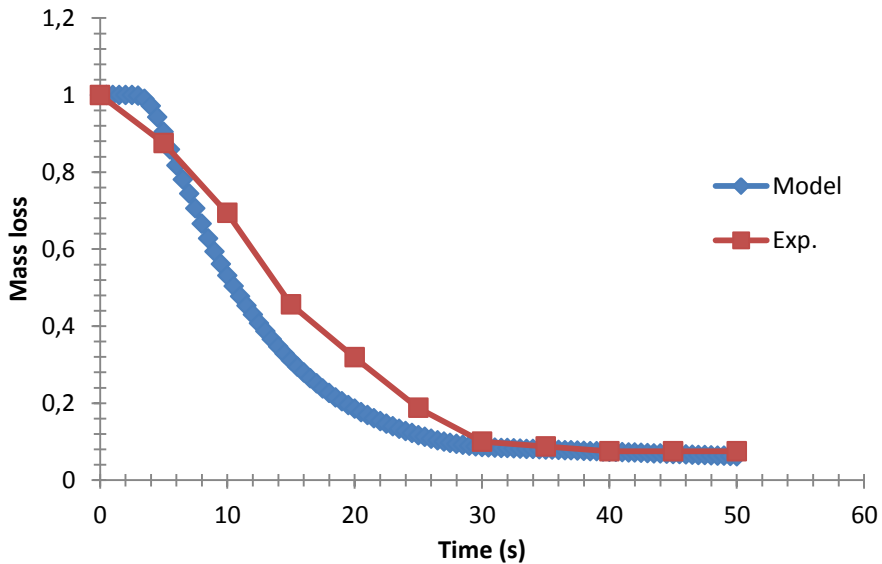


Figure 2: Comparison between modelled and measured mass loss rate of the particle

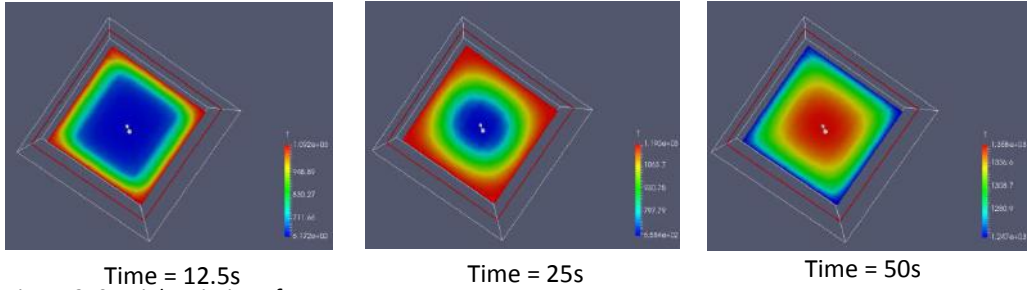


Figure 3: Spatial variation of temperature

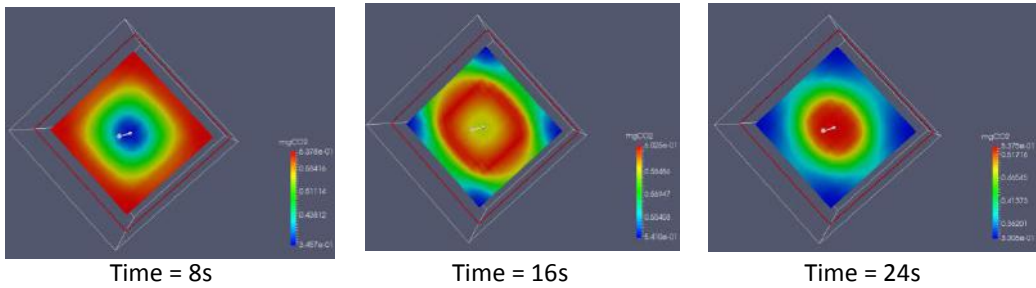


Figure 4: Spatial variation of CO<sub>2</sub> gas inside the particle

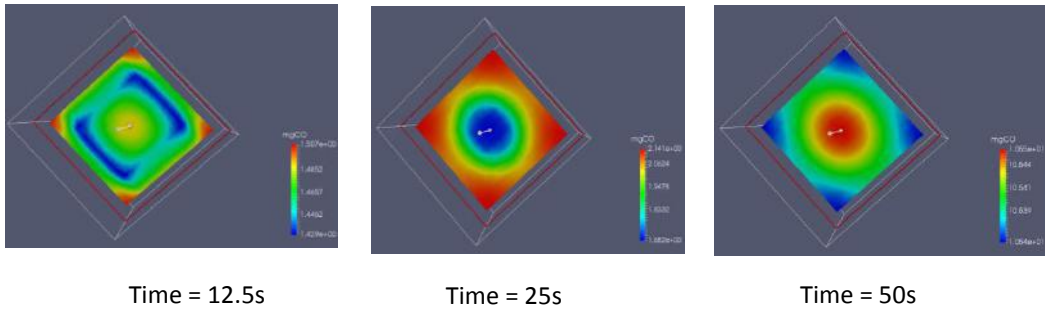


Figure 5: Spatial variation of CO gas inside the particle

It can be seen that the mass loss is well predicted by the model and in consistence with measurements as in Figure 2. According to Figure 2, decrease of mass by the predicted by the model is little slower at the beginning though it becomes faster than the experimental data after few seconds. This is believed to be happened due to simultaneous occurrence of drying, pyrolysis and char

reaction processes. Within last 20s there is no significant variation of mass due to small amount of char is left at the center of the particle to react with gas. However, at this time almost all gas produced have streamed out of the particle.

In addition, the spatial variations of temperature, CO<sub>2</sub> and CO are shown in Figure 3, Figure 4 and Figure 5.

## **Conclusion**

A three dimensional single wood particle model is developed to investigate the thermal conversion of thermally thick biomass particle. Intra particle temperature gradients are considered since the particle is thermally thick. Kinetic rate model is assumed for the moisture evaporation. Three parallel reactions of decomposing of three major components in wood particle are considered in pyrolysis. Char reactions are calculated using both kinetics and diffusion. Mass loss results are analysed compared to experimental data. The discrepancy between graphs can be occurred due to model parameters taken from empirical values. The results show a

good agreement between model and experimental data indicating higher accuracy of the model. Further, the model can be modified to apply for processes such as torrefaction and to examine packed bed performance with woody biomass which are extremely important in modern energy field.

## **Acknowledgement**

The authors would like to thank University of Moratuwa senate research grant: SRC/ST/2017/06 for funding and the Department of chemical and process engineering, University of Moratuwa for resources and support provided to make this research project a success.



## References

- [1] M. Peter. Energy production from biomass (part 1): overview of biomass. *Bioresource Technology* 2002; 37–46.
- [2] C. Bruch, B. Peters, and T. Nussbaumer. Modeling Wood Combustion Under Fixed Bed Conditions. *Fuel* 2003; 729–738.
- [3] P. McKendry. Energy production from biomass (part 2): Conversion technologies,” *Bioresource Technology*. 2002; 47–54.
- [4] J. Porteiro, J. L. Míguez, E. Granada, and J. C. Moran. Mathematical modelling of the combustion of a single wood particle. *Fuel Process. Technol.* 2006; 169–175, 2006.
- [5] T. JUŘENA. Brno University of Technology Numerical Modelling of Grate Combustion. 2012; 1–109.
- [6] Y. Haseli. Modeling Combustion of Single Biomass Particle. 2012; 1-113.
- [7] J. Collazo, J. Porteiro, D. Patiño, and E. Granada. Numerical modeling of the combustion of densified wood under fixed-bed conditions. *Fuel*. 2012; 149–159.
- [8] N. Fernando and M. Narayana. A comprehensive two dimensional Computational Fluid Dynamics model for an updraft biomass gasifier. *Renew. Energy*. 2016; 698–710.
- [9] U. Sand, J. Sandberg, J. Larfeldt, and R. Bel Fdhila. Numerical prediction of the transport and pyrolysis in the interior and surrounding of dry and wet wood log. *Appl. Energy*. 2008; 1208–1224.
- [10] K. U. C. Perera, M. Narayana, and A. Drying, “Finite Volume Analysis of Biomass Particle Pyrolysis,” *MERCon* 2017, Colombo, 2017, no. 2, pp. 379–384.
- [11] H. Yang, R. Yan, H. Chen, D. H. Lee, and C. Zheng. Characteristics of hemicellulose, cellulose and lignin pyrolysis. *Fuel* 2007; 1781–1788.
- [12] C. A. Kovfopoulos, G. Maschio, and A. Lucchesi. Kinetic Modelling of the Pyrolysis of Biomass and Biomass Components. *Can. J. Chem. Eng.* 1989; 75–84.
- [13] Ansys Fluent, User Guide (Release 15.0), Multiphase Flows. ANSYS Inc. 2012; p.189-238.
- [14] R. Mehrabian et al. A CFD model for thermal conversion of thermally thick biomass particles. *Fuel Process. Technol.* 2012; 96–108.
- [15] H. Lu, W. Robert, G. Peirce, B. Ripa, and L. L. Baxter. Comprehensive study of biomass particle combustion. *Energy and Fuels*. 2008; 2826–2839.

# Eulerian-Lagrangian Approach for Modeling of Biomass Fluidized Bed Combustion

D. G. C. Wickramasinghe<sup>1</sup>, M. Narayana<sup>2</sup>, A. D. U. S. Amarasinghe<sup>3</sup>

*Department of Chemical and Process Engineering, University of Moratuwa  
Bandaranayake Mawatha, Katubedda, Moratuwa 10400, Sri Lanka*

<sup>1</sup> chathurangawi@gmail.com

<sup>2</sup> mahinsasa@uom.lk

<sup>3</sup> adusa2@uom.lk

## Abstract

Nowadays, many more attention has been made by the biomass due to its zero carbon emission and renewability. However, its optimum conversion is utmost necessary for clean and sustainable consumption. The gasification and direct combustion are the promising energy conversion technologies for biomass. The fluidized bed combustor among various other combustors is a better candidate due to its almost perfect mixing, high heat and mass transfer rates and very good controllability. However, because of complex reaction schemes and various characteristics properties of biomass, it is much challenging to use conventional fluidized bed combustor without optimization. To overcome these difficulties, a numerical model was developed in this study to analyze the transport phenomena in the freeboard. Rather than building and testing with a complex and expensive experimental unit, modeling and simulating with computational fluid dynamics (CFD) is the most efficient and productive way. The CFD modeling is based on Eulerian-Lagrangian concept, which tracks each biomass particle individually with association of multiple physics, particle collision and thermo-chemical properties.

**Keywords:** Computational Fluid Dynamics, Eulerian-Lagrangian, Biomass, Fluidized Bed,

## Introduction

With the depletion of fossil fuels, renewable and clean energy sources are promoted as remaining and possible ways of satisfying the world's energy demand. Due to zero carbon emission and its renewability, biomass is a most promising energy source among other renewable energy sources. Furthermore, among various available biomass to energy conversion technologies, fluidized bed combustion is a better energy conversion technology due to many reasons including (i) better temperature distribution due to almost perfect mixing, (ii) high freeboard temperature, (iii) complete combustion, (iv) less flue gas loss, and (v) very good controllability [1]. However, because of complex reaction schemes and various characteristics properties of biomass, it is much challenging to use conventional fluidized bed combustor without optimization.

Modelling with CFD is the most efficient and productive way to perform a characteristic analyse of dense solid-gas flow, like a fluidized bed combustor. Generally, there are two approaches for model a multiphase flow, namely Eulerian-Eulerian and Eulerian-Lagrangian. The Eulerian-Eulerian approach which, treats all phases as continuum, has dominated the fluidized bed modeling due to relatively low computational cost [2] [3]. However, it can only predict the macroscopic characteristics, but not the discrete characteristics of particle cloud. These difficulties can be overcomes by Eulerian-Lagrangian based CFD approach, due to it tracks each biomass particle individually in continuous gas phase with association of particle collision (4-way coupling) and thermo-chemical properties.

The objective of this present study is to model fluidized bed combustion. With helps of simulation results, we can optimize system parameters for mixing and entrainment, gas production as well as emission, freeboard temperature and carbon conversion, with efficient utilization of biomass.

## Mathematical Modelling

The CFD model is based on the transient Eulerian-Lagrangian approach. The fundamental spray equation is based on a Lagrangian description of the spray droplets [4] using the droplet distribution function. The Analytical approach for interface between gas phase and particle cloud is obtained by reduction of a Liouville-like equation to a one-particle distribution function, which have been developed for particle-laden suspensions [5], and bubbly flows [6]. In this study, the interaction between the gas phase and the discrete particle cloud is taken into account by treating the exchange of mass, momentum and energy.

## Discrete particle phase

The discrete particle phase consists of biomass particles. The governing equations are default mathematical models described by the Lagrangian particle tracking of OpenFOAM, an open source C++ CFD toolbox [7].

Due to the complexity, only one-step drying, pyrolysis model and char oxidation are used as the chemical conversion. The products of pyrolysis mainly consist of  $H_2$ ,  $CO$ ,  $CO_2$ ,  $H_2O$ , hydrocarbon mixture, char and ash. For the calculation simplicity, this hydrocarbon mixture is lumped and assumed as  $CH_4$ . The volatile gas composition is tabulated in Table 1.

Table 1: Volatile Gas Composition [8]

Component	Mass Fraction
H <sub>2</sub>	0.109
CO	0.396
H <sub>2</sub> O	0.249
CO <sub>2</sub>	0.209
CH <sub>4</sub>	0.127

### Continuous gas phase

For continuum gas phase, general governing equations have been modified in order to include the effect of volume fraction of gas as well as the transfer of mass, momentum and energy from the discrete particle phase.

$$\frac{\partial}{\partial t}(\varepsilon_g \rho_g) + \nabla \cdot (\varepsilon_g \rho_g \mathbf{u}_g) = S_{p,m} \quad (\text{Eq. 1})$$

$$\frac{\partial}{\partial t}(\varepsilon_g \rho_g \mathbf{u}_g) + \nabla \cdot (\varepsilon_g \rho_g \mathbf{u}_g \mathbf{u}_g) = -\nabla p + \nabla \cdot (\varepsilon_g \boldsymbol{\tau}_{eff}) + \varepsilon_g \rho_g \mathbf{g} + S_{p,mom} \quad (\text{Eq. 2})$$

$$\begin{aligned} \frac{\partial}{\partial t}(\varepsilon_g \rho_g E) + \nabla \cdot (\varepsilon_g \mathbf{u}_g (\rho_g E + p)) \\ = \nabla \cdot (\varepsilon_g \alpha_{eff} \nabla h_s) + S_h + S_{p,h} + S_{rad} \end{aligned} \quad (\text{Eq. 3})$$

$$E = h_s - \frac{p}{\rho_g} + \frac{u_g^2}{2} \quad (\text{Eq. 4})$$

$$\begin{aligned} \frac{\partial}{\partial t}(\varepsilon_g \rho_g Y_i) + \nabla \cdot (\varepsilon_g \mathbf{u}_g \rho_g Y_i) \\ = \nabla \cdot (\varepsilon_g \rho_g D_{eff} \nabla Y_i) + S_{Y_i} + S_{p,Y_i} \end{aligned} \quad (\text{Eq. 5})$$

Where,

- $\varepsilon_g$  = Volume fraction of gas
- $\rho_g$  = Gas density (kg/m<sup>3</sup>)
- $\mathbf{u}_g$  = Gas velocity (m/s)
- $S_{p,m}$  = Mass source term (kg/m<sup>3</sup>s)
- $p$  = Pressure (Pa)
- $\boldsymbol{\tau}_{eff}$  = Effective stress tensor (Pa)

- $S_{p,mom}$  = Momentum source term (N/m<sup>3</sup>)
- $\alpha_{eff}$  = Effective thermal diffusivity (kg/ms)
- $h_s$  = Sensible enthalpy of gas phase (J/kg)
- $S_h$  = Enthalpy source term due to homogeneous reaction (W/m<sup>3</sup>)
- $S_{p,h}$  = Enthalpy source term from particle phase (W/m<sup>3</sup>)
- $S_{rad}$  = Radiation source term (W/m<sup>3</sup>)
- $Y_i$  = Mass fraction of species  $i$
- $D_{eff}$  = Effective mass diffusion coefficient for gas (m<sup>2</sup>/s)
- $S_{Y_i}$  = Species source term due to gas phase reactions (kg/m<sup>3</sup>s)
- $S_{p,Y_i}$  = Species source term from particle phase (kg/m<sup>3</sup>s)

As shown by Eq. 5, the transport equation is solved for each gas species and gas phase properties are updated accordingly. After that mass (Eq. 1), momentum (Eq. 2) and enthalpy (Eq. 3) equations are solved along with laminar turbulence model [9].

There are so many homogeneous reactions in biomass combustor. For the sake of simplicity, three global reactions are used here.

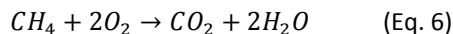


Table 2: Kinetic Data for Reactions [10]

Reaction	Frequency Factor	Activation Energy (kJ/mol)
Eq. 6	$5.2 \times 10^{13}$	130
Eq. 7	$2.32 \times 10^{12}$	167
Eq. 8	$1.08 \times 10^{13}$	125

## Results and Discussions

The mathematical model is simulated in a computational domain, which is a rectangular container of 0.15 m (width) x 0.45 m (height) x 0.015 m (thickness). Initially, the combustor is filled with packed biomass bed that is composed of 6250 spherical particles with a diameter of 2.5 mm. These biomass particles are allowed to fall down under gravity with the absence of airflow to prepare the initial bed, because it capture both initial particle coordinates and forces and torques which related to the packing process [11]. After that, biomass bed is fluidized by the airflow from the bottom of the container. The following results are taken after 1-day running time on a 32 processors that is equal to 1 s real time simulation.

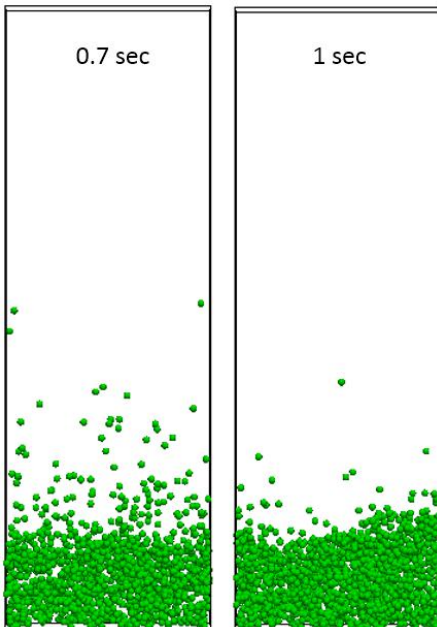


Figure 1: Particle flow patterns at the end of simulation

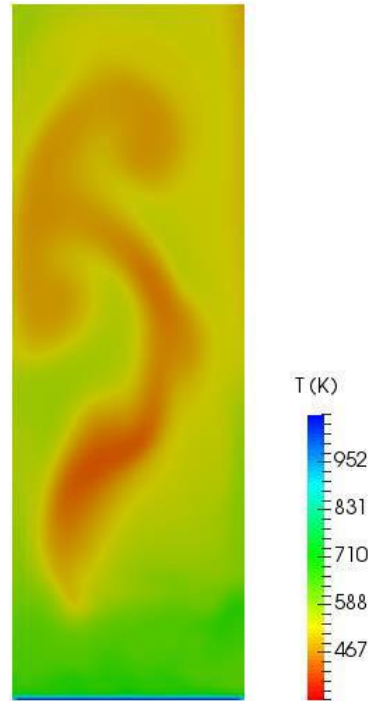


Figure 2: Combustor temperature profile at the end of simulation

Fig. 1 presents the particle flow patterns at the end of the simulation. Generally, fluidized bed is not symmetrical due to biomass pyrolysis and gas phase turbulence. Fig. 2 depicts the combustor temperature profile. It easily observed that particle cloud at the near bottom has the maximum temperature. At the same time, strong mixing of gas phase due to turbulence can be observed.

## Conclusions

The Eulerian-Lagrangian approach for modeling of fluidized bed combustion of biomass has been succeeded with the help of open source C++ CFD toolbox OpenFOAM. The developed model in this study accounts for one-step drying, basic pyrolysis, char oxidation reactions and gas phase combustion. All three modes of heat transfer were included since

radiation is the main mode of heat transfer and critically important. The simulation results are acceptable with data of similar studies from literature. In future, extend of presented mathematical model can be used as a numerical tool to optimize fluidized bed combustion processes.

### Future Works

The model consists of many runtime variable inputs such as airflow rate (primary and secondary) and physical and chemical properties of biomass feedstock. The model can be used to perform parameter studies to find the process parameters for efficient combustion and minimized emission. The model is to be further improved by implementing an advanced pyrolysis scheme, char conversion reactions, GRI-Mech reaction scheme [12] for homogeneous reaction and advanced turbulence modelling.

### Acknowledgements

This research work was supported by University of Moratuwa Senate Research Grant Number SRC/ST/2017/06.

### References

- [1] Oka SN. *Fluidized Bed Combustion*, 1st ed. New York: Marcel Dekker, 2004.
- [2] Gerber S, Oevermann M, Behrendt F. "An Euler-Lagrange modeling approach for the simulation of wood gasification in fluidized beds."
- [3] Wang X, Jin B, Zhong W. "Three-dimensional simulation of fluidized bed coal gasification," *Chem. Eng. Process. Process Intensif.*, vol. 48, no. 2, pp. 695–705, 2009.
- [4] Williams FA. "Spray Combustion and Atomization," *Phys. Fluids*, vol. 1, no. 6, p. 541, 1958.
- [5] Koch DL. "Kinetic theory for a monodisperse gas–solid suspension," *Phys. Fluids A Fluid Dyn.*, vol. 2, no. 10, pp. 1711–1723, 1990.
- [6] Zhang DZ, Prosperetti A. "Ensemble phase-averaged equations for bubbly flows," *Phys. Fluids*, vol. 6, no. 9, pp. 2956–2970, 1994.
- [7] OpenFOAM dev: The OpenFOAM Foundation, 2017. [Online]. Available: <https://cpp.openfoam.org/dev/>.
- [8] Lu H, Robert W, Peirce G, Ripa B, Baxter LL. "Comprehensive study of biomass particle combustion," *Energy and Fuels*, vol. 22, no. 4, pp. 2826–2839, 2008.
- [9] Ku X, Li T, Løvås T. "CFD-DEM simulation of biomass gasification with steam in a fluidized bed reactor," *Chem. Eng. Sci.*, vol. 122, pp. 270–283, 2015.
- [10] Liu H. "CFD Modeling of Biomass Gasification Using a Circulating Fluidized Bed Reactor," p. 129, 2014.
- [11] Xu BH, Yu AB. "Numerical simulation of the gas-solid flow in a fluidized bed by combining discrete particle method with computational fluid dynamics," *Chem. Eng. Sci.*, vol. 52, no. 16, pp. 2785–2809, 1997.
- [12] M. Frenklach, T. Bowman, G. Smith. "GRI-Mech," *Gas Technology Institute (GTI)*. [Online]. Available: <http://combustion.berkeley.edu/gri-mech/index.htm>.

# Assessment of performance and development of biomass fired cabinet dryers for improved energy efficiency

Neethan Ratnakumar<sup>1</sup>, Asiri Roshan Wijethilaka<sup>2</sup>, Rohini Ramachandran<sup>3</sup>

*Department of Interdisciplinary Studies, University of Jaffna*

*Ariviyal Nagar, Kilinochchi, Sri Lanka*

<sup>1</sup> neethanwz4681@gmail.com

<sup>2</sup> asirirosahan00@gmail.com

<sup>3</sup> roh.rama@eng.jfn.ac.lk

## Abstract

Biomass operated small scale cabinet dryers are used as a cheap alternative for electric dryers in many small and medium size enterprises in Sri Lanka. But problems encountered such as low product quality due to non-uniform drying and high energy consumption has made the effective use of them questionable. This research project targets on finding possible ways to eliminate the non-uniformity in drying by doing an experimentally validated Computational Fluid Dynamic (CFD) analysis on the existing Biomass Cabinet Dryer with new dryer configurations and indirectly reducing the energy consumption by doing so. Experiments were carried out using winter melons and the hypothesis that uneven temperature and airflow distribution is the reason for non-uniform drying was proven true. Four hours of drying resulted in only a maximum of 50 degree Celsius and temperature ranges at steady state were non-uniform with a minimum of 44 degree Celsius near the vertices of the dryer. Six different types of geometrical configurations were numerically analyzed under 5, 10 and 15 m/s inlet flow rates and the most uniform set of configuration was identified. Future work planned to be carried out includes incorporation of thermal solar heating as energy source and precise measurement of flow parameters using sophisticated air flow systems for experimental validation.

**Keywords :** Biomass dryer, CFD, turbulence model, uniformity

## Introduction

Drying is retaining physico-chemical properties of materials, to ensure the preservation of materials over prolonged periods and plays a great significance in food preservation and is often the final operation in many manufacturing operations. Industrial applications of drying other than food preservation are numerous such as in paper making and in the seasoning of timber. Drying methods have evolved through history with the introduction of new technology and various devices are used and patented yearly. However, the struggle of the farmers and small and medium enterprises to achieve proper drying in an economical way in developing countries such as in Sri Lanka is conspicuous. Moreover, Drying is a highly energy-intensive process, accounting for 10–20% of total industrial energy use [1].

The usage of locally designed and fabricated tray type cabinet biomass sourced batch dryers is noticeable in small and medium food processing plants in Northern Sri Lanka, while farmers and villagers still prefer traditional open sun drying. But these available local dryers tend to disrupt the final product due to non-uniform drying in the trays and have high energy consumption. The problems with the traditional open sun drying include contamination of the product by dust and insects, it is labor intensive and important nutrients are unable to be preserved.

Computational Fluid Dynamics (CFD) has been found to be a very effective tool in predicting the drying process in industrial dryers [2].

Identifying ideal drying chamber configurations and airflow rates for uniform drying and low energy consumption is the main objective of this study. This will be attained by experimentally validated CFD analysis on a locally available biomass fired tray dryer. The outcomes of this study will benefit the small scale village based farmers and enterprises. Moreover, the newly developing Palmyra based food processing industry of Northern Sri Lanka will be stabilized by the findings of this research.

Uniformity and efficiency issues of tray dryers have been addressed by various researchers starting from the 80s. In 1985 Adams and Thompson studied the airflow inside of an air drying chamber. This study proofed through experiments the significant variation of velocities in the tunnel air dryer analysed and it was found that adding baffles reduces this variation of velocities significantly. The drying rate in a dryer is strongly related to airflow velocity [3]. It has been found that the drying rate increases with air velocity up to a velocity of 1.5 m/s [3] or 1.2 m/s [4]. An algorithm of loading developed proofs that to obtain homogenous drying in a batch tray dryer loading of trays plays a vital role; as the air gets cooler and more saturated with moisture when moving upwards, the tray loading should be reduced [5]. Further researches have also proven that reduction in air mass flow rate in the tray dryer will reduce non-uniformity in drying and reduce the fuel consumption at the same time [6].

In 1998 [4] the air movement inside a batch dryer was simulated, the PHOENICS code was used which is based on the finite volume method, as developed by Patankar and Spalding in



1972. Here, comparison of data obtained by the CFD and data obtained from the drying tests showed a strong correlation between the drying rate and the air velocity. A study by Margaris and Ghiaus [7] confirmed the ability of CFD methods in predicting the air flow patterns inside the tray dryer and in improving the design of these dryers. Y. Amanlou [8] used CFD to design a new fruit dryer. Seven different geometries of cabinet dryer were envisaged theoretically by CFD. Experiments were conducted on the most appropriate sketch with acceptable uniform air flow and temperature distribution. The experimental results showed that the new cabinet dryer illustrated an even distribution of air velocity and temperature throughout the dryer. Similarly S. Misha (2013) [9], Waseem Amjad [10] and P. S. Mirade [11] use CFD analysis in their designs for tray dryers for prediction of uniformity.

## Material and Methods

### Drying uniformity and Temperature

A tray type biomass cabinet dryer as shown in Figure 1 available at Faculty of Engineering, University of Jaffna was utilized for the conduction of a set of experiments where equal pieces of winter melons were evenly distributed at equal weight on all the trays of the dryer and were allowed to dry for 4 hours.

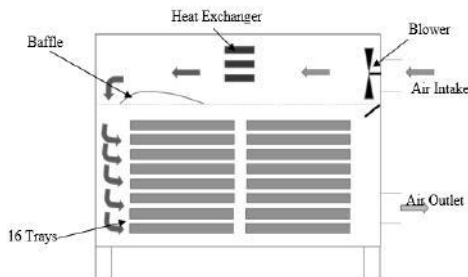


Figure 1: Illustration of the biomass dryer

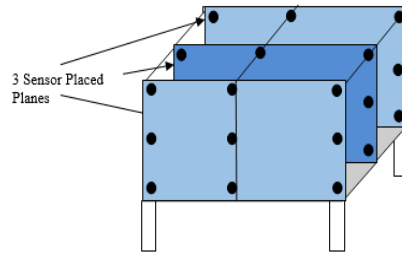


Figure 2: Sensor placement

The evaporation from each tray was calculated by measuring the weight loss and the temperature readings at 27 positions in the 3D chamber was collected by DS18B20 onewire sensors for throughout the drying process. Sensor positions are shown in Figure 2.

### Numerical Simulation

A CFD analysis was performed on a simplified 2D model of the available tray biomass dryer, airflow and temperature distributions were observed. Six different geometrical configuration changes were brought on to the model and the analysis has been repeated with similar boundary conditions for each situation to find the best uniformity. The geometrical changes brought in are as following: change in heat exchanger position, addition of guiding vanes to the trays, removal of air baffle, step type staking of tray, allowing air recirculation and a simplification in design by direct exposure of trays to hot air flow.

Ansys Fluent was utilized for the simulations with mesh refinements near to named selection surfaces, walls and where possibilities for flow separation or high turbulence were anticipated. The following conditions, models and methods were used for the setup of the simulations in Ansys Fluent: the two equation  $k - \epsilon$  turbulence model with a turbulence intensity of 5% was

used for all simulations, turbulence viscosity ratio was set at 10, the simulations were run 3 times with inlet air velocity conditions of 5 m/s, 10 m/s and 15 m/s.

## Results and Discussions

### Drying uniformity and Temperature

The bar chart given in Figure 3 illustrates the evaporation in grams of each winter melon tray in the chamber. As it can be observed from this the drying pattern shows an increase towards the bottom of the chamber and it is observable that the left side shows higher evaporation rates than the right hand side of the chamber.

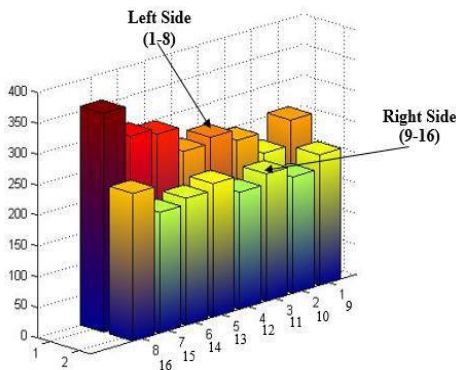


Figure 3: Evaporation of each tray in grams

Temperature distribution on the front (1) mid (2) and rear (3) planes of the drying chamber at steady state are shown in Figure 4. The temperature is higher where air flow is possible to pass over the trays. A maximum temperature of near to 50 degree Celsius was registered.

### Numerical Simulation

The velocity (left) and temperature (right) distributions obtained for the available dryer by the numerical solving in CFD for 10 m/s inlet velocity is presented in Figure 5 in m/s and Kelvin

respectively. Here, high degree of non-uniformity is observable.

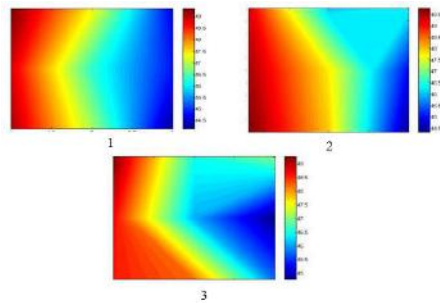


Figure 4: Temperature distribution Celsius

Figure 6 illustrates the velocity (left) and temperature (right) (in m/s and Kelvin respectively) obtained by CFD for the direct airflow design simplification at 5 m/s inlet air velocity. This configuration was giving the best uniformity for temperature and air velocity within the drying chamber.

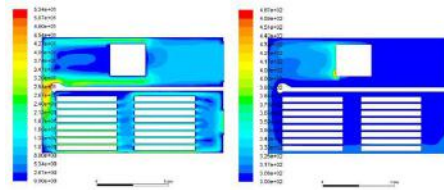


Figure 5: Velocity and Temperature for available dryer at 10 m/s inlet flow

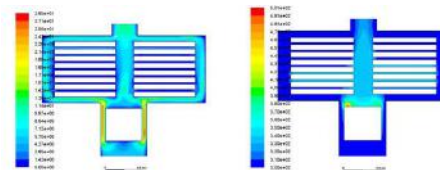


Figure 6: Velocity and temperature for direct air flow at 5 m/s inlet flow

## Conclusions

From the set of experiments carried out to find the temperature values and the amount of dehydration at given points within the drying chamber of the available biomass cabinet dryer, the

cause has been identified as weak temperature distributions as hypothesized. The six geometrical configuration changes made up on the model, based on the observed drying pattern in the chamber (i.e. as observed from the results the drying pattern shows an increase towards the bottom of the chamber and it is observable that the left side shows higher dehydration rates than the right hand side of the chamber) show better uniformity for the 5 m/s air flow condition. Furthermore, numerical analysis conducted on these six modifications clearly show improvement in flow and temperature uniformity for the direct flow simplification of the biomass dryer. Therefore it can be concluded based on the analysis that reduction in airflow rates and direct flow design simplifications can increase drying uniformity and product quality, whereas experimental validation of numerical analysis is required for further certainty.

### Future Works

The findings of the current study are limited due to no validations have been done on the model. The implementation of experimental validation on the computational model can be completed in future studies. Specific products exhibit distinctive drying properties and follow different drying curves. Product specific studies have also to be conducted in future studies.

### Acknowledgements

This research project was supported by the Faculty of Engineering, University of Jaffna.

### References

- [1] Kemp, I. C. (1996). Unpublished survey on energy use in industrial drying for ETSU, UK. Department of Energy, UK.
- [2] Tarek J. Jamaledine, M. B. (2010). Application of computational fluid dynamics for simulation of drying processes: A Review. *Drying Technology* 28, 120-154.
- [3] Mulet, A. B. (1987). Effect of air flow rate on carrot drying. *Drying Technology* 5 (2), 245-258.
- [4] E. Mathioulakis, V. T. (1998). Simulation of air movement in a dryer by computational fluid dynamics: Application for the drying of fruits. *Journal of Food Engineering* 36, 183-200.
- [5] Khattab, N. M. (1996). Toward a Homogeneous and Efficient Batch-Tray Dryer. *Energy Sources* 18 (4), 447-459.
- [6] Marcelo Precoppe, S. J. (2015). Batch uniformity and energy efficiency improvements on a cabinet dryer suitable for smallholder farmers. *Journal of Food Science Technology* 52 (8), 4819-4829.
- [7] Margaris, D. & Ghiaus, A. (2006). Dried product quality improvement by airflow manipulation in tray dryers. *Journal of Food Engineering*.
- [8] Amanlou, Y. (2010). Applying CFD for designing a new fruit cabinet dryer. *Journal of Food Engineering*.
- [9] S. Misha, S. M. (2013). Review on the application of a tray dryer system for agricultural products. *World Applied Sciences Journal* 22 (3), 424-433.
- [10] Waseem Amjad, A. M. (2015). Spatial homogeneity of drying in a batch type food dryer with diagonal

- air flow design. *Journal of Food Engineering* 144, 148-155.
- [11] Mirade, P. S. (2003). Prediction of the air velocity field in modern meat dryers using unsteady computational fluid dynamics (CFD) models. *Journal of Food Engineering* 60, 41-48.

## Sri Lanka Sustainable Energy Authority

1<sup>st</sup> Floor, Block 05, BMICH, Bauddhaloka Mawatha, Colombo 07  
**Email:** [symposium@energy.gov.lk](mailto:symposium@energy.gov.lk) | **Telephone:** 011-2677445  
**Web:** [www.energy.gov.lk](http://www.energy.gov.lk) | **Facsimile:** 011 - 2682534

